

POLITECNICO DI TORINO

Master of Science in Automotive Engineering

Master Thesis

**Niobium-Alloyed Stainless Steel for Automotive  
Exhaust Systems**



**Supervisors:**

Prof. Paolo MATTEIS

**Candidate:**

Bachar FATFAT

March 2021

# **Niobium-Alloyed Stainless Steel for Automotive Exhaust Systems**

Dissertation presented to Politecnico di Torino to obtain the title of Master of Science.

Concentration Area:

Automotive Engineering.

Advisor: Prof. Paolo MATTEIS.

Torino

2021

# Acknowledgements

I would like to express my appreciation and gratitude to my advisor Pr. Paolo Matteis for giving me the opportunity to complete this thesis at **CBMM- *Companhia Brasileira de Metalurgia e Mineração***, and for all his guidance along the way.

Special thanks to Mr. Eng. Caio De Paula Camargo Pisano, the technical market development manager at CBMM, for following up and for his help during the development of this thesis. He has been always available for help whenever needed, and for taking time to review the thesis, without hesitation, in a very timely manner. Without his help the thesis work would have been a much more difficult task, and for that I am very grateful.

I would like to thank also my home university, the Lebanese University, for providing this opportunity to me as a double degree student. A special thanks go to Dr. Adel al-Hallak, Dr. Clovis Franciss, and Dr. Bassam Al-Etter, whom did their best to facilitate my academic exchange process.

Gratitude also expressed to **DCL-Lebanon (Development, Culture and Leadership)** association for providing the support whenever needed, a special thanks to its founder, Dr. Mounzer Fatfat, for his continuous support, although he has been in a different country, he has been always my role model and mentor throughout the years.

# Abstract

## Niobium-Alloyed Stainless Steels for Automotive Exhaust Systems

Bachar Fatfat, M.Sc.

Politecnico di Torino

Niobium, previously known as Columbium (Cb), is a ductile grey transition metal that has been reported in 1801 by the English chemist Charles Hatchet as Columbium, then in 1809 it was reported again by the English chemist William Wollaston who named it Niobium without figuring out that it is the same as columbium. Later in 1864-1865 they were stated as a single element by the German chemist Heinrich Rose, and it took its identity as Niobium.

Niobium has a large domain of applications, among which his role as an alloying element in stainless steels is one of the most important. It is added in the melt shop during the steel making process in the form of ferrous niobium in order to produce Niobium-Alloyed stainless steels. It is a well-known ferrite stabilizing element that expands the  $\alpha$ -field and closes the  $\gamma$ -field of the Carbon-Iron biphasic diagram.

In accordance to the stringent emission regulations associated with the ecological and economic competition in the automotive sector, OEMs adopted a continuous improvement approach in optimizing the energy efficiency of the vehicle, which demanded a faster reach of the light-off temperature of the catalytic converter (to be able to decrease the emissions), and the usage of a lighter material. The result of the increased efficiency is a higher exhaust gas temperatures up to 1000-1050°C. Due to these high temperature, the conventional cast iron exhaust system components in the hot end are not effective anymore, and finding a new material that is able to withstand these high temperature while keeping a good mechanical properties is a must, as well as the increase in the warranty period up to 10 years demanded a material that has superior corrosion resistance. Henceforth, cast iron has evolved to thin sheets of Stainless steels, in particular, ferritic stainless steel grades are the most promising as they are found to be lighter, cheaper, and more resistant to service conditions of the automotive exhaust systems.

Although stainless steels were able to perform at a higher temperature than that withstood by cast iron, however up to 1050°C in the hot end was a challenge which required a further improvement in stainless steels grades themselves, and even the invention of new grades, which are found to be Niobium alloyed. For the hot end components, the Niobium-alloyed ferritic stainless steels EN 1.4521 and EN 1.4622 has proven to fulfill the needs, providing superior oxidation and creep resistance while maintaining the good corrosion resistance, however, the Niobium-alloyed ferritic grades UNS S43932 (Ti and Nb) and DIN. 1.4509 showed exceptional performance in the cold end, providing the needed corrosion resistance.

In addition, Niobium as an alloying element has proven to be effective in mitigating all the problems that the automotive exhaust components suffer from. In particular, it provided a high temperature strength, creep and oxidation resistance in the hot end through the solid solution hardening, precipitate hardening, grain refinement, and laves forming mechanisms. It

has also been effective in increasing the pitting resistance equivalent number (PREN) that proves the higher pitting corrosion resistance required mainly in the cold end. On the other hand, Niobium as an individual alloying element, has also been effective in improving the manufacturing mechanisms that are carried out to fabricate the complex shapes. Niobium has increased the average anisotropic coefficients that corresponds to the better deep drawing performance by improving the texture, as well as it hindered the intergranular corrosion that is so common in the welded zones, mainly the heat affected zone, by forming Niobium carbides, thus keep the chromium in the matrix instead of its depleting it. It is also important to mention the economic benefits associated with the usage of niobium, where the recommended ferritic grades were able to replace the austenitic grades such as 304, 309, and 316 and their improved versions, thereby eliminating the additional cost associated with the expensive addition of Nickel, making it also a cost-effective invention.

**Keywords:** Niobium, Stainless Steel, Automotive Exhaust System, Intergranular corrosion, High temperature strength, Dual Stabilization.

# Table of Contents

ACKNOWLEDGEMENTS.....	II
ABSTRACT.....	III
LIST OF FIGURES.....	IX
LIST OF TABLES.....	XIV
ABBREVIATIONS .....	XV
SYMBOLS.....	XVI
OBJECTIVE .....	XVII
CHAPTER 1: STEEL MAKING PROCESS.....	1
1. INTRODUCTION TO STEEL MAKING PROCESS.....	1
1.1. STEEL MAKING PROCESS .....	1
1.1.1 REDUCTION .....	2
1.1.1.1. <i>Blast furnace Process:</i> .....	2
1.1.1.2. <i>Electric Arc Furnace:</i> .....	4
1.1.2. MELT SHOP.....	5
1.1.2.1. <i>Steel Making Process</i> .....	5
1.1.2.2. <i>Addition of Niobium as an Alloying Element</i> .....	7
1.1.2.3. <i>What is Niobium</i> .....	7
1.1.2.4. <i>Niobium Addition Process</i> .....	7
1.1.2.5. <i>Continuous Casting</i> .....	9
1.1.2. HOT ROLLING .....	10
1.1.3. COLD ROLLING .....	11
1.1.4. ANNEALING.....	12
1.1.5. PICKLING .....	12
1.1.6. FINISHING .....	13
1.1.7. NIOBIUM IN IMPROVING THE PRODUCTION EFFICIENCY .....	14
1.2. PHASE DIAGRAM.....	15
1.2.1. IRON-CARBON PHASE DIAGRAM.....	15
1.2.2. IRON-CHROME PHASE DIAGRAM .....	16
1.2.3. ELEMENTS EXPANDING THE A-PHASE .....	16
1.2.4. ELEMENTS EXPANDING THE $\Gamma$ PHASE .....	17
1.2.5. SCHAEFFLER DIAGRAMS AND DE LONG DIAGRAMS .....	18
1.3. STAINLESS STEELS.....	20
1.3.1. STAINLESS STEEL PASSIVATION .....	21
1.3.2. FERRITIC STAINLESS STEELS .....	24
1.3.2.1. . METALLURGY.....	24
1.3.2.2. PHYSICAL AND MECHANICAL PROPERTIES.....	25
1.3.2.3. ROLE OF NIOBIUM IN THE FERRITIC STAINLESS STEEL FAMILY .....	27
1.3.2.4. FIELDS OF APPLICATIONS .....	28

1.3.3.	AUSTENITIC STAINLESS STEELS .....	29
1.3.3.1.	METALLURGY .....	29
1.3.3.2.	MARTENSITE FORMATION IN AUSTENITE .....	30
1.3.3.3.	PHYSICAL AND MECHANICAL PROPERTIES .....	31
1.3.3.4.	ROLE OF NIOBIUM IN AUSTENITIC STEELS .....	32
1.3.3.5.	FIELD OF APPLICATIONS .....	35
CHAPTER 2: AUTOMOTIVE REVISION .....		36
2.1.	HISTORY OF EXHAUST SYSTEMS .....	37
2.1.1.	EXHAUST SYSTEM COMPONENTS .....	38
2.1.1.1.	EXHAUST MANIFOLD .....	39
2.1.1.2.	THE CATALYTIC CONVERTER .....	40
2.1.1.3.	MUFFLER .....	43
2.1.1.4.	PIPES: .....	44
2.1.2.	EUROPEAN REGULATIONS FOR EMISSION LIMITS .....	45
2.2.	EXHAUST SYSTEM PROBLEMS .....	47
2.2.1.	FATIGUE .....	47
2.2.1.1.	THERMO-MECHANICAL FATIGUE .....	48
2.2.1.2.	MECHANICAL FATIGUE .....	50
2.2.1.3.	CREEP .....	50
2.2.1.4.	OXIDATION .....	52
2.2.1.4.1.	<i>High Temperature Oxidation of Stainless Steels</i> .....	53
2.2.2.	CORROSION .....	55
2.2.2.1.	INTERGRANULAR CORROSION .....	56
2.2.2.2.	PITTING CORROSION .....	58
2.2.2.3.	STRESS CRACKING CORROSION .....	60
2.2.3.	VIBRATION AND NOISE .....	61
2.2.3.1.	MATERIAL EFFECT ON NATURAL FREQUENCIES .....	62
2.2.4.	CONCLUSION .....	64
CHAPTER 3: STAINLESS STEEL IN EXHAUST SYSTEMS .....		65
3.1.	MATERIALS TREND: FROM CAST IRON TO STAINLESS STEEL .....	66
3.1.1.	STAINLESS STEEL ADVANTAGES IN TERMS OF OXIDATION RESISTANCE .....	66
3.1.2.	STAINLESS STEEL ADVANTAGES IN TERMS OF FATIGUE STRENGTH .....	70
3.1.3.	STAINLESS STEEL ADVANTAGES IN TERMS OF CREEP RESISTANCE .....	71
3.1.4.	STAINLESS STEEL ADVANTAGES IN TERMS OF DENSITY .....	71
3.1.5.	FERRITIC VS. AUSTENITIC STAINLESS STEEL .....	73
3.1.5.1.	<i>Ferritic Stainless Steels</i> .....	73
3.1.5.2.	<i>Austenitic Stainless Steels</i> .....	73
3.2.	BENEFITS OF NIOBIUM ALLOYED STAINLESS STEEL INTO THE APPLICATION OF EXHAUST SYSTEM COMPONENTS .....	75
3.2.1.	HOT END COMPONENTS .....	75

3.2.1.1.	EXHAUST MANIFOLD .....	75
3.2.1.2.	NIOBIUM ALLOYED STAINLESS STEEL FOR EXHAUST MANIFOLD .....	76
3.2.1.2.1.	<i>The New Ferritic Grade 1.4521 (AISI 444)</i> .....	76
3.2.1.2.2.	<i>The New High Nb Ferritic Grade 1.4622</i> .....	79
3.2.1.2.	CATALYTIC CONVERTER .....	82
3.2.1.3.	FLEXIBLE JOINT .....	82
3.2.2.	EFFECT OF NIOBIUM ON HIGH TEMPERATURE STRENGTH .....	82
3.2.2.1.	NIOBIUM ROLE AS A STABILIZING ELEMENT .....	83
3.2.2.2.	NIOBIUM ROLE IN IMPROVING HIGH TEMPERATURE STRENGTH .....	84
3.2.2.3.	NIOBIUM IN INCREASING CREEP RESISTANCE .....	85
3.2.2.4.	NIOBIUM ROLE IN MITIGATING LUNDERS DEFORMATION AT HIGH TEMPERATURE .....	87
3.2.3.	COLD END COMPONENTS .....	89
3.2.3.1.	MUFFLER .....	89
3.2.3.1.1.	<i>Niobium Addition for Muffler's Stainless Steel</i> .....	90
3.2.3.2.	TAIL END PIPE .....	91
3.2.4.	NIOBIUM AGAINST CORROSION .....	92
3.2.4.1.	NIOBIUM AGAINST PITTING CORROSION .....	92
3.2.4.2.	NIOBIUM ROLE IN REFINING INCLUSIONS .....	94
CHAPTER 4:	MANUFACTURING PROCESSES .....	96
4.1.	FORMABILITY .....	96
4.1.1.	DEEP DRAWING PROCESS .....	98
4.1.2.	ANISOTROPIC COEFFICIENTS .....	99
4.1.3.	CRYSTALLOGRAPHIC TEXTURE .....	99
4.2.	NIOBIUM ROLE IN IMPROVING FORMABILITY AND DEEP DRAWING .....	101
4.2.1.	EFFECT ON FORMABILITY AND DEEP DRAWING .....	101
4.2.1.1.	<i>Niobium Role in promoting <math>\gamma</math>-fibers</i> .....	101
4.2.2.2.	<i>Effect of Niobium on Improving Formability</i> .....	102
4.2.2.	FORMABILITY OF THE FERRITIC GRADES 1.4622 AND 1.4521 .....	105
4.2.3.	FORMABILITY OF THE FERRITIC GRADE AISI 409 .....	106
4.3.	WELDABILITY .....	108
4.3.1	WELDABILITY OF FERRITIC AND AUSTENITIC GRADES .....	110
4.3.1.1.	FERRITIC GRADES .....	110
4.3.1.2.	AUSTENITIC GRADES .....	110
4.3.2.	STAINLESS STEEL WELDING TECHNIQUES .....	112
4.3.2.1.	<i>TIG – GTAW Electric Arc Welding Technique</i> .....	113
4.3.2.2.	<i>MIG-GMAW Electric Arc Welding Process</i> .....	114
4.3.3.	CHOOSING THE FILLER MATERIAL .....	115
4.3.4.	NIOBIUM AGAINST INTERGRANULAR CORROSION .....	117
4.3.5.	NIOBIUM ROLE IN IMPROVING WELDABILITY .....	119
4.3.6.	WELDABILITY OF THE GRADES 1.4622 .....	119
4.3.7.	WELDABILITY OF THE GRADE AISI 444 .....	119
4.3.8.	WELDABILITY OF THE DUAL STABILIZED AISI 409 .....	121

<b>4.4. POST-WELDING CLEANING .....</b>	<b>121</b>
<b>CHAPTER 5: METALLURGICAL MECHANISM IN INCREASING THE PERFORMANCE .....</b>	<b>122</b>
<b>5.1. ALLOYING.....</b>	<b>122</b>
<b>5.1.1. MOLYBDENUM (Mo).....</b>	<b>122</b>
<b>5.1.2. TUNGSTEN (W).....</b>	<b>122</b>
<b>5.1.3. VANADIUM (V).....</b>	<b>124</b>
<b>5.1.4. NITROGEN (N).....</b>	<b>124</b>
<b>5.1.5. SILICON (Si).....</b>	<b>126</b>
<b>5.2. TWO STEP REDUCTION.....</b>	<b>127</b>
<b>EFFECT OF TWO STEP COLD ROLLING ON HARDNESS.....</b>	<b>127</b>
<b>5.3. WARM ROLLING.....</b>	<b>128</b>
<b>5.4. SHEAR BANDS .....</b>	<b>129</b>
<b>5.5. PRECIPITATIONS IN INCREASING CREEP RESISTANCE .....</b>	<b>130</b>
<b>5.5.1. MX CARBIDES .....</b>	<b>130</b>
<b>5.5.2. Z-PHASE .....</b>	<b>130</b>
<b>5.6. SHOT PEENING .....</b>	<b>130</b>
<b>5.7. POST WELD HEAT TREATMENT (PWHT).....</b>	<b>130</b>
<b>5.8. TITANIUM FOR A FINER GRAIN IN THE WELDING ZONE .....</b>	<b>131</b>
<b>CONCLUSION.....</b>	<b>132</b>
<b>FUTURE TRENDS .....</b>	<b>133</b>
<b>REFERENCES.....</b>	<b>134</b>

# List of Figures

Figure 1 Possible steel making routes [1] .....	2
Figure 2 Simplified scheme of Blast furnace [1] .....	3
Figure 3 Schematic representation of Electric Arc furnace .....	4
Figure 4 Steel Melt shop [3] .....	5
Figure 5 LD converter [1] .....	6
Figure 6 OBM (Q-BOP) converter [1].....	7
Figure 7 Ferroniobium Particles [5].....	8
Figure 8 FeNb delivery into the ladle [5].....	9
Figure 9 Continuous Casting [1].....	9
Figure 10 rolling process scheme [16].....	10
Figure 11 Microstructure of steel in hot rolled condition [7] .....	10
Figure 12 Effect of cold rolling on AISI 304N specimen [8] .....	11
Figure 13 the effect of annealing on the microstructure of cold worked metals. (a) Cold worked, (b) after recovery, (c) after recrystallization, (d) after grain growth [6].....	12
Figure 14 Surfaces generated by different abrasive methods [13] .....	13
Figure 15 Niobium in improving the production efficiency [15] .....	14
Figure 16 Carbon-Iron phase diagram [6] .....	15
Figure 17 Iron-Chrome phase diagram [17] .....	16
Figure 18 Effects of different alloys on the Fe-C diagram in expanding the $\alpha$ -phase [16] .....	17
Figure 19 Effects of adding (a) nickel (b) Nitrogen and (c) Carbon [17].....	17
Figure 20 Schaeffler Structural Diagram [17] .....	18
Figure 21 De Long Diagram [17] .....	19
Figure 22 Chromium role-Passive layer [17].....	21
Figure 23 Re-passivation phenomenon [17] .....	21
Figure 24 Passivation curve of a generic Stainless steel [17].....	22
Figure 25 Effect of alloying elements on the active-passive characteristics of a generic stainless steel [17].....	23
Figure 26 Body centered cubic lattice [6, 34].....	24
Figure 27 main ferritic stainless steels from AISI 430 .....	24
Figure 28 Fe-Cr binary section of Fe-C-Cr ternary diagram [17] .....	27
Figure 29 Face centered cubic crystalline structure [6,34] .....	29
Figure 30 Fe-Ni-Cr ternary phase diagram.....	29
Figure 31 Strain induced Martensite formation as a function of strain at various temperatures [21].....	31
Figure 32 HV, YS, TS and EL% as function of Niobium in cast steels [22] .....	33
Figure 33 a sample with 2 wt% Nb under electron Microscopy [22].....	34
Figure 34 Niobium effect on solidification [22].....	34
Figure 35 Four stroke internal combustion engine .....	36
Figure 36 Typical view of an Automotive Exhaust System [39].....	38
Figure 37 schematic representation of a typical Exhaust Manifold [25].....	39

Figure 38 Catalytic converter efficiency as a function of Air to fuel ratio of a spark ignition engine [27] .....	40
Figure 39 Three way Catalytic Converter [26 ,27] .....	41
Figure 40 Metallic/Ceramic Monolithic converter [26].....	41
Figure 41 Close coupled configuration [26] .....	42
Figure 42 Pre catalyst + Underfloor Catalyst configuration [26] .....	42
Figure 43 pathway of the exhaust gas in a muffler [80] .....	43
Figure 44 Reactive Muffler.....	43
Figure 45 Chambers of typical muffler [80].....	43
Figure 46 Helmholtz resonator [80].....	44
Figure 47 Absorptive Muffler [28] .....	44
Figure 48 development of European regulations through the years [29].....	45
Figure 49 CO <sub>2</sub> limits from 2000 to 2030 [29].....	45
Figure 50 Limits on toxic emissions through the years [29] .....	46
Figure 51 The three stages of fatigue [32] .....	47
Figure 52 Basquin-Manson-Coffin Curve [30].....	49
Figure 53 In-phase and Out of Phase TMF cycles [30] .....	49
Figure 54 the three stages of creep [32].....	50
Figure 55 Effect of temperature and stress on the creep behavior [32] .....	51
Figure 56 Schematic representation of Sag test [45] .....	51
Figure 57 Metal oxidation phenomenon [32] .....	52
Figure 58 Oxidation of Iron [32] .....	52
Figure 59 Oxidation: the diffusion mechanisms [6] .....	53
Figure 60 porous Fe <sub>2</sub> O <sub>3</sub> layer (900 C, Air, Hk30) [17] .....	54
Figure 61 Different form of cracks [30] .....	54
Figure 62 Electrochemical corrosion in a homogeneous metal [17] .....	55
Figure 63 Chromium depletion at grain boundaries [32].....	56
Figure 64 Sensitization curves for ferritic and austenitic stainless steels with the same amount of chromium [17] .....	57
Figure 65 Grooves at sensitized areas due to Integranular corrosion [32] .....	57
Figure 66 pitting corrosion phenomenon and pits or holes morphologies [17].....	58
Figure 67 Corrosion under deposit in a pipe [17].....	59
Figure 68 Mass loss as function of cycles for different stainless steel grades [33].....	59
Figure 69 Pitting corrosion on 304 stainless steel plate [32].....	59
Figure 70 Stress Cracking Corrosion for a 18-20% Cr stainless steel [17] .....	60
Figure 71 bellow type joint used in exhaust systems.....	61
Figure 72 trend of natural frequencies as a function of Poisson ratio for fixed Elastic modulus (a), and fixed shear modulus (b) [38].....	62
Figure 73 trend of Natural Frequency as a function of Elastic modulus [38].....	63
Figure 74 trend of natural frequencies as a function [38].....	63
Figure 75 Material Properties for a durable exhaust manifold .....	64
Figure 76 Benefits of Stainless Steels.....	65
Figure 77 oxidation data at 750°C in air with 10% H <sub>2</sub> O [41].....	66

Figure 78 Backscatter SEM cross-section images of D5S cast iron after 1,000 h and 5,000 h in air with 10 % H <sub>2</sub> O. a–c 650 °C/1,000 h; d 650 °C/5,000 h; e, f 700 °C/1,000 h; g 700 °C/5,000 h [41] .....	68
Figure 79 Backscatter SEM cross-section images of austenitic stainless steels after 5,000 h at 800 °C in air with 10 % H <sub>2</sub> O. a, b TMA 4705; c, d HK; e, f TMA 6301; g, h HP; i, j CAFA 4 [41] .....	69
Figure 80 Prices of Stainless steels and Ni based alloys [39].....	70
Figure 81 Fatigue life against thermal expansion coefficient for Stainless Steels and Ni based super alloys [39].....	70
Figure 82 Creep stress versus the Larson Miller for cast iron and CF8C stainless steels [42].....	71
Figure 83 Young modulus Vs. Density for Stainless steels and Ni based super alloys [39].....	72
Figure 84 Material Trend evolution for exhaust manifold.....	75
Figure 85 the higher tensile strength of AISI 444 between 750 and 1000 °C [44] .....	76
Figure 86 Fatigue limit of AISI 444 at 2 million cycles as function of Temperature [44].....	77
Figure 87 Cyclic oxidation at 1000 °C of AISI 444 and 1.4509 [44].....	77
Figure 88 deflection of different Stainless steel grades at different temperatures [44] .....	78
Figure 89 Lifetime of different stainless steel grades up to 1000°C [44].....	78
Figure 90 Corrosion resistance of AISI 444 compared to other Ferritic and Austenitic Grades [60].....	79
Figure 91 η-phase solvus temperature as function of Nb content [45].....	79
Figure 92 creep resistance of hot end candidate steels [45].....	81
Figure 93 Pitting corrosion resistance of the grades 1.4622 and 1.4521 compared to other stainless steels [46] .....	81
Figure 94 comparison between the effect of Mo and Nb on high temperature strength at 900 and 1000°C [48].....	82
Figure 95 Niobium effect in Stabilization of T409 stainless steels [49].....	83
Figure 96 Tensile strength as function of temperature of AISI 439, 441, and 444 .....	84
Figure 97 Effect of different alloying elements on yield strength [49] .....	85
Figure 98 Bright field images of the precipitates in fractured specimens for (a) 15CrNbTi and (b) 15Cr0.5MoNbTi in simulated exhaust gas [50].....	85
Figure 99 Stress-strain diagrams of non-stabilized and stabilized grades at different temperatures [51].....	86
Figure 100 Laves phase Transformation at (a) 1000°C, (b) 1050°C, and (c) 1100°C [53].....	87
Figure 101 Effect of Niobium and annealing temperature on the proof stress [48] .....	88
Figure 102 resistance to pitting corrosion of different stainless steels [57] .....	89
Figure 103 Life prediction of 409Ti-Nb and 409 Ti [52] .....	90
Figure 104 Yield and Tensile strength of 409Ti and 409 Ti-Nb at different functions.[52] .....	90
Figure 105 fatigue life comparison for 0.31%, 0.15% and 0% Nb [52] .....	91
Figure 106 pitting depth trend as function of Niobium content in Ferritic stainless steel.....	92
Figure 107 Niobium effect in improving lifetime [52].....	93
Figure 108 Effect of Niobium in increasing the resistance to pitting corrosion in Austenitic stainless steel.....	93
Figure 109 Niobium effect on inclusion shapes [52].....	94
Figure 110 Effect of Nb on inclusion average size.....	95

Figure 111 Niobium effect in increasing fatigue life [52] .....	95
Figure 112 different stamped automotive exhaust components [60].....	96
Figure 113 Forming Limit Diagram zones [59].....	97
Figure 114 FLD of different stainless steel grades [60] .....	97
Figure 115 scheme of the deep drawing operation [60] .....	98
Figure 116 LDR comparison between different stainless steel grades [60] .....	98
Figure 117 Euler representation of fibers orientation in the lattice .....	99
Figure 118 effect of Niobium in improving the crystalline structure [15] .....	100
Figure 119 Niobium effect on Homogeneity and recrystallization [55].....	101
Figure 120 $\alpha$ and $\gamma$ fibers in cold rolled sheets with single (a) and (b) and double stabilization (c) and (d) [55] .....	102
Figure 121 ODF sections of hot rolled sheets (a) Ti stabilized, (b) Ti-Nb stabilized [55].....	102
Figure 122 Anisotropy coefficients of single and dual stabilized grades .....	103
Figure 123 Swift test comparison for single (a) and dual (b) stabilized grades [55].....	103
Figure 124 LDR improvement by the addition of Niobium [49].....	104
Figure 125 Effect of Niobium on the mean anisotropic coefficient [48].....	104
Figure 126 optimized microstructure of 1.4622 with high $\gamma$ -fiber intensity [61] .....	105
Figure 127 Anisotropic coefficients of EN 1.4622 and EN 1.4509.....	105
Figure 128 Effect of Dual Stabilization on the LDR of AISI 409 [49] .....	106
Figure 129 Effect of Ti addition on Nb stabilized Stainless steel.....	107
Figure 130 Welded automotive exhaust component [60] .....	108
Figure 131 Stabilization effect on increasing weldability .....	110
Figure 132 Welding different zones [32].....	111
Figure 133 Stainless Steel Welding Techniques.....	112
Figure 134 Schematic Representation of TIG welding process [67].....	113
Figure 135 Schematic representation of MIG welding process [67] .....	114
Figure 136 filler material compatibility check by Schaeffler diagram [68] .....	116
Figure 137 Microstructure of (a) AISI 441 Ti-Nb and (b) AISI 409 Ti [70].....	117
Figure 138 HAZ in (a) Nb-Ti stabilized AISI 441, and (b) Ti alloyed AISI 409 [70] .....	117
Figure 139 Effect of Nb stabilization at the grain boundaries at the HAZ at macro-structural level [70].....	118
Figure 140 Effect of Niobium on microstructural level at HAZ [70].....	118
Figure 141 Hardness distribution in the welded zone [70].....	119
Figure 142 Grain structure of fusion zone obtained with the filler metals 1, 6, and 7 in the pulsed mode [73].....	120
Figure 143 Tungsten in increasing the offset yield strength [54] .....	123
Figure 144 Effect of W on the laves phase size (a) with Nb (b) with W and Nb [71] .....	123
Figure 145 Improvement in the deep drawing performance of AISI 444 by the addition of tungsten .....	124
Figure 146 Pitting resistance increase with the addition of Vanadium .....	124
Figure 147 Creep curve flattering by increasing the nitrogen content [76].....	125
Figure 148 Nitrogen influence on steady state creep[76] .....	125
Figure 149 Effect of increasing nitrogen content on rupture [76] .....	126

Figure 150 Life Influence of nitrogen on surface cracks [76] .....	126
Figure 151 Microstructure after 2 step cold rolling [64] .....	127
Figure 152 two-step cold rolling effect on hardness.....	127
Figure 153 Texture of conventional (a and c) and warm rolled (b and d) specimens [77].....	128
Figure 154 Roughness and Formability improvements by warm rolling .....	129
Figure 155 Stress-Strain diagrams of TIG weldments after different PWHT temperatures [69]	131
Figure 156 Molten zone macro and micrographs showing the effect of Ti in refining the grain size [72].....	131
Figure 157 evolution of car share from 2017 to 2040 [29].....	133

# List of Tables

Table 1 Main reactions taking place during the oxidation process.....	6
Table 2 Properties of Niobium and Ferroniobium.....	7
Table 3 Chemical specification of standard FeNb, CBMM spec. 111 .....	8
Table 4 Chemical composition of some main types of Ferritic stainless steel [from EN 10088].	25
Table 5 High performance stabilized stainless steels containing Nb.....	26
Table 6 Mechanical Properties of some of the main ferritic stainless steels .....	26
Table 7 Physical Properties of some of the main ferritic stainless steels [From EN 10088].....	27
Table 8 Chemical Composition of some Austenitic Stainless Steels [from EN 10088].....	30
Table 9 Physical properties of some Austenitic grades [from EN 10088] .....	31
Table 10 Mechanical Characteristics of some Austenitic Stainless Steel.....	32
Table 11 comparison between developed ferritic grades and the basic austenitic grade 304.....	74
Table 12 Chemical composition of the new ferritic Stainless steel AISI 444 .....	76
Table 13 Chemical composition -by mass%- of 1.4622 and High Nb Stainless steels .....	80
Table 14 Chemical composition in wt.% of the tested filler wires for the AISI 444.....	120
Table 15 Comparison between hot and warm rolled results in terms of formability, grain size and roughness .....	129

# Abbreviations

AISI	American Iron and Steel Institute
AOD:	Argon-Oxygen Decarburization
BOF:	Basic oxygen Furnace
BCC	Body Centered Cubic
EAF:	Electric arc furnace
FCC	Face Centered Cubic
HB	Hardness Brinell
HCF	High Cycle Fatigue
HR	Hot Rolling
HV	Hardness Vicker
IP	In-Phase
LCF	Low Cycle Fatigue
LD	Linz-Donawitz
LDR	Limiting Diagram Ratio
MIG	Metallic Inert Gas
OBM	Oxygen Bottom Maxheutte
OP	Out of Phase
OSC	Oxygen Storage Capacity
PREN	Pitting Resistance Equivalent Number
SUH	Stainless Steel Heat Resistance
SUS	Steel Use Stainless
TIG	Tungsten Inert Gas
TMF	Thermo-Mechanical Fatigue
TWC	Three way Catalyst
VOD:	Vacuum-oxygen Decarburization

## Symbols

wt.%	Weight percent
$\varepsilon$	Strain
$\sigma$	Stress
N	number of cycles
$R_m$	Tensile strength
$\bar{r}$	Average Anisotropic coefficient
$\Delta r$	planar anisotropic coefficient
$R_{p0.2}$	Yield strength

*\*Some symbols which are used less frequently, are defined directly in the text.*

# Objective

This work is aimed at providing a bibliographic research for Stainless Steels Applications in Exhaust Systems, with shedding the light on the added value corresponding to the addition of Niobium in terms of mechanical and metallurgical mechanisms in the application considering the main trends of the future in what concerns the higher exhaust temperatures and the stringent emission regulations.

# CHAPTER 1

## Steel Making Process

### 1. Introduction to Steel Making Process

Over the years, Iron and Steel have played a major role in human civilization development, they have been employed in different life sectors such as automotive, agriculture, construction, power distribution, machinery and equipment, and many others in order to solve everyday problems, and facilitate our daily life.

Steel, as a definition, belongs to the iron carbon system that has the unique feature of being alloyed with elements such as Chromium (Cr), Magnesium (Mg), Titanium (Ti), Niobium (Nb), and many others depending on the desired chemical composition and manufacturing process, the steels can be categorized in different families in which each one of these families will be employed in different applications. The alloying elements are added into the melt shop during the steel making process.

Steels could be classified according to their carbon content, these categories are the low carbon steels (lower than 0.25 wt.% carbon), medium carbon (between 0.25 and 0.6 wt.%) and high carbon content (0.6 to 1.4 wt.%) [1]. Each of these categories has its own application according to its mechanical and physical properties. Carbon is considered the main and most important element because it increases the strength and allows the heat treatment procedure, so that improved and enhanced physical and mechanical properties are obtained.

### 1.1. Steel Making Process

The Steel making process consists of several consecutive steps, starting from the iron oxides' reduction and ending with the finished (or semi-finished) steel products available at the market. The steps are the following:

- 1- Reduction
- 2- Melt shop
- 3- Hot rolling
- 4- Cold rolling
- 5- Annealing
- 6- Pickling
- 7- Finishing

Technically, different routes could be followed in order to obtain the iron melt, such as Classical Blast furnace/Basic Oxygen furnace (BOF), Electric Arc Furnace (EAF), smelting reduction, and direct reduction [1].

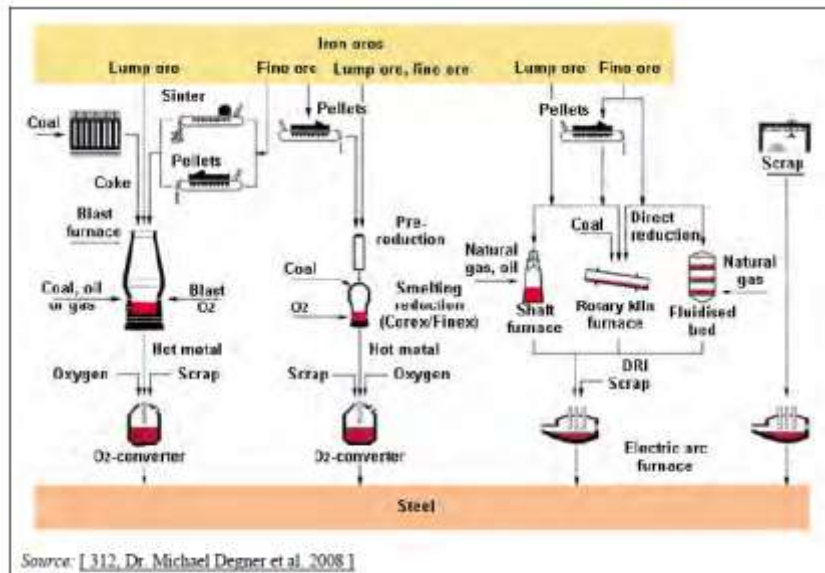


Figure 1 Possible steel making routes [1]

### 1.1.1 Reduction

The reduction of oxide ores i.e. Iron making leads to the formation of liquid metallic iron, thus it is considered as the first operation in this process. It is important to define some terms used in this process such as:

**Coke:** produced from coal by means of distillation in the coke oven where additional reducing agents such as oil, natural gas, or fuels are injected (and in some cases plastics), it is the main reducing agent in the blast furnace, it also acts as fuel.

**Charcoal:** commonly used reducing agent made up of amorphous form of carbon, considered more sustainable than other reducing agents.

**Fluxes:** commonly used lime/limestone/dolomite, added to lower the melting point and improve the sulfur uptake by slag, and reduce the viscosity of the slag.

**Pellets:** small crystallized balls of iron ore with a size ranging from 9 to 16 mm.

**Sinter:** produced from a pre-designed mixtures of fine ores, residuals and additives, used as agglomerating material.

**Slag:** solution of oxides with small amount of sulphides, phosphides, silicates, and other undesired elements, it is formed during hot metal refining where Si, Mn, Fe, P, Ca, and Mg are oxidized.

#### 1.1.1.1. Blast furnace Process:

The burden is made up of coke, a mixture of sinter and/or pellets, fluxes and lump ore and is fed into the furnace top. As the burden moves down in the blast furnace, its temperature increases as shown in figure 2, and its composition varies accordingly [1]. Iron is obtained from Iron oxides by the reduction using coal. Iron ores used contain hematite ( $Fe_2O_3$ ) and small amounts of magnetite ( $Fe_3O_4$ ) [2], these compounds are strongly reduced in the blast furnace resulting in Iron Oxide ( $FeO$ ) which, in turn, is partially reduced and carburized form of solid

iron, at the end, iron charge melts allowing liquid iron and slag to be collected at the bottom. The reducing agents react to form CO and CO<sub>2</sub>. In other words, the chemical reactions that represent the iron making process are [2]:

- $C + O_2 \rightarrow CO_2$  Eq. 1.1
- $C + O_2 \rightarrow 2CO$  Eq. 1.2
- $Fe_2O_3 + 3CO \rightarrow 2Fe + 3CO_2$  Eq. 1.3
- $Fe_3O_4 + 4CO \rightarrow 3Fe + 4CO_2$  Eq. 1.4

For sure, many other elements present within the final charge, these elements are distributed between the hot metal and the slag, for instance, elements like Phosphorus, Sulphur, Manganese, and Silicon. While Titanium, Aluminum, Calcium, Magnesium, and the bulk of silicon and sulphur passes into the slag as oxides.

The Iron passing through the blast furnace absorbs carbon that lowers its melting temperature to 1150°C, however the liquid iron must be maintained at approximately 1500°C to obtain sufficient fluidity [2]

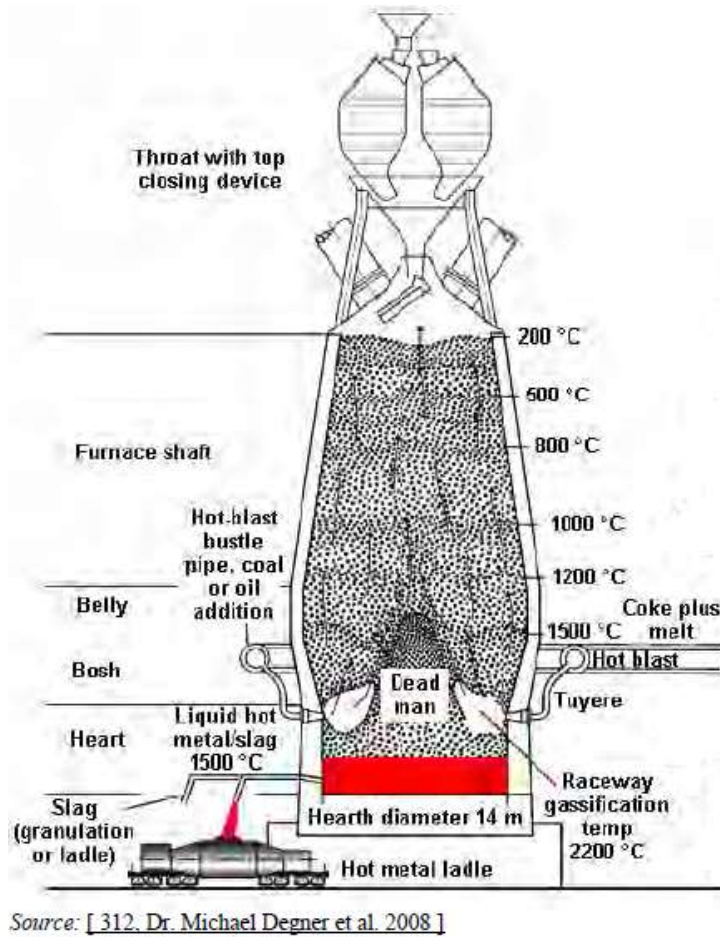


Figure 2 Simplified scheme of Blast furnace [1]

#### 1.1.1.2. Electric Arc Furnace:

The loaded scarp is preheated in the charging basket or the shaft by the off-gas up to 800°C before melting as a step of recovering energy. In this process, the burden consists of scrap with lime for the slag formation, carbon bearing materials are also added, and lump coal is added in some plants in order to adjust the carbon content. Firstly, up to 60% of the scrap is loaded [1], then as soon as the roof closes, the electrodes approach and strike an electric arc above the scrap. The rest of the charge is loaded after the melting of this initial quantity. The power of the arc is kept low during the initial stages to avoid the damage of the furnace by radiation, however it is increased as soon as the arc is shielded by the surrounding scrap. Oxygen lances and/or fuels such as oil or natural gas are used to assist the early stages, as well as oxygen is brought to liquid steel by side or bottom nozzles. The purpose of injecting oxygen is the generation of foaming slag by the CO bubbles that acts as a shield protecting the furnace walls, and decarburization of the melt with removing the undesired existing elements.

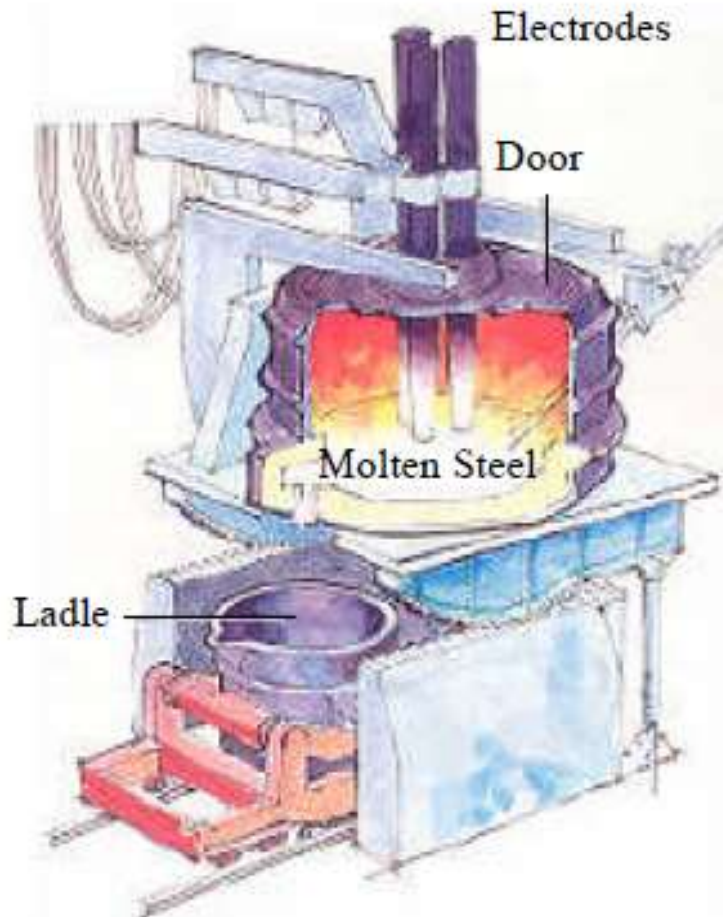


Figure 3 Schematic representation of Electric Arc furnace

### 1.1.2. Melt Shop

Steel Melting shop is the step in which the hot metal obtained from the iron making units is turned into various grades of steel, and casted into slabs, blooms, billets, beam blanks, or rounds, during this step many other processes are involved such as: hot metal pretreatment, primary steel making, secondary steel making, and finally casting [3].

#### 1.1.2.1. Steel Making Process

The collected liquid iron (containing almost 4% C, 0.6% to 1% Si, 0.6% to 0.8% Mn, and 0.1% to 0.2% P) [1] is transported from the blast furnace to the steel making plant by torpedo that is a hot metal mixer travelling on rails. Even though preventive steps have been taken, such as reduction of sulphur by coke or other agents, the pretreatment of hot metal remains an important step in order to remove phosphorus and silicone and other impurities shown in table 1, then it is transported to a basic oxygen furnace where the carbon content being almost 4%, is lowered to less than 1%, thereby resulting in Steel, this is also known as the primary steel making process. However steel metallurgy is controlled downstream the ladle in order to produce steel with the required specifications, and this step is known as the secondary steel making process. During this step oxygen is blown in the ladle in order to achieve the desired composition, as well as this is the step where alloying elements are added. Hence, the main idea of employing ladles and tundishes is to produce steels closer to the desired final chemistry.

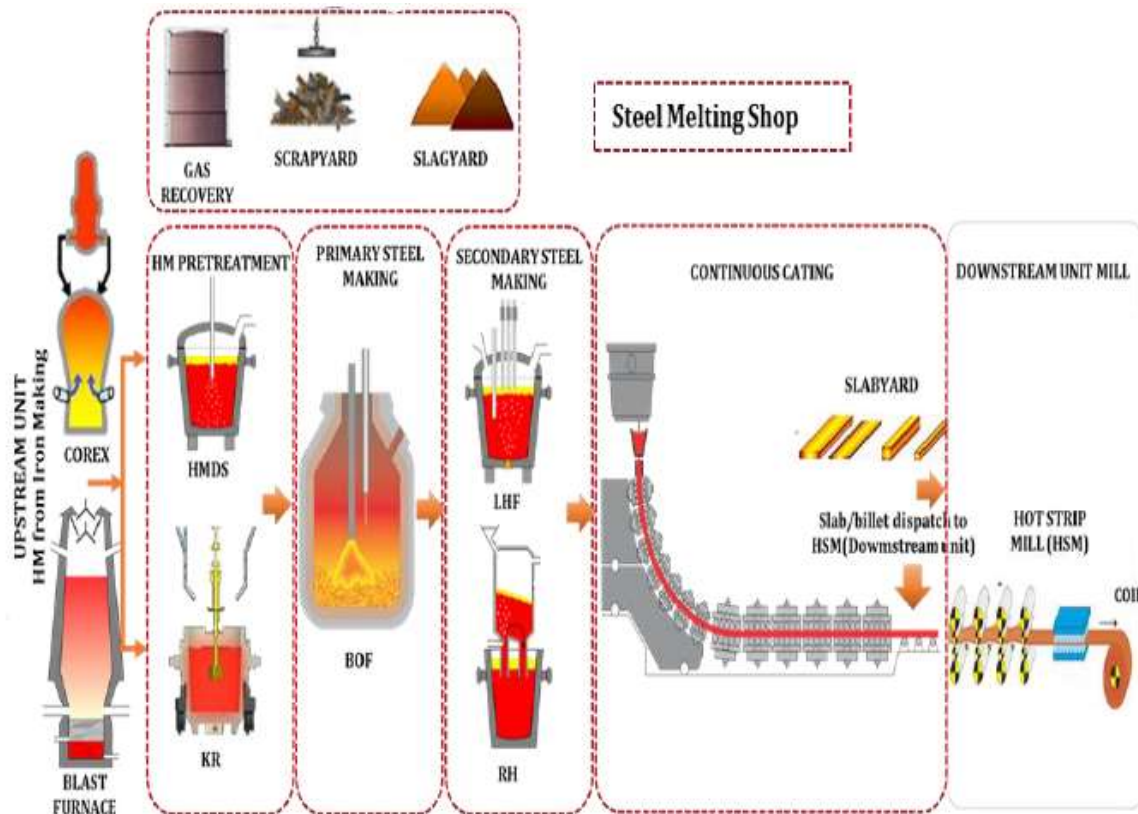


Figure 4 Steel Melt shop [3]

After pretreatment, the stage of oxidation in the basic oxygen furnace starts. The main chemical reactions taking place are shown in table 1, where the undesirable impurities such as Si, Mn, P, and others.

Oxidation process	Chemical reaction
Carbon elimination	$[41]+[O] \rightleftharpoons CO \text{ (off-gas)}$
	$[CO]+[O] \rightleftharpoons CO_2 \text{ (Off-gas)}$
<b>Oxidation of accompanying and tramp elements</b>	
- Desiliconisation	$[Si]+2[O] +2[CaO] \rightleftharpoons (2CaO \cdot SiO_2)$
- Manganese reaction	$(Mn) +[O] \rightleftharpoons (MnO)$
- Dephosphorisation	$2[P]+5[O] +3[CaO] \rightleftharpoons 3CaO \cdot P_2O_5$
<b>Deoxidation</b>	
Removal of residual oxygen through ferro-silicon	$[Si]+2[O] \rightleftharpoons (SiO_2)$
Aluminum reaction	$[Al]+3[O] \rightleftharpoons (Al_2O_3)$
NB: --[ ]= Dissolved in the hot metal --( )= Contained in the slag Source: [200, Commission 2001][363, Eurofer2007]	

Table 1 Main reactions taking place during the oxidation process

There are many types of Basic Oxygen reactors, figure 5 represents the so called LD converter (Linz-Donawitz) used for hot metal with low phosphorus content. Other existing steel making oxygen furnaces types include Oxygen Bottom Maxhutte (OBM) known also as Q-BOP [1] is shown in figure 6.

Furthermore, the LD converter could be enhanced by bottom stirring using a noble gas such as Nitrogen (N<sub>2</sub>) or Argon (Ar) being injected at the bottom through bricks' holes. This technique is used to ensure the homogenization of the steel in terms of composition and temperature, in addition to producing a more intensive circulation of molten steel and improving oxidation reactions.

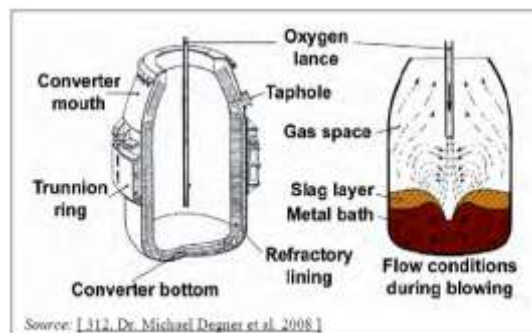


Figure 5 LD converter [1]

In what concerns the secondary metallurgy, by definition, it is a post-treatment employed in order to meet the increasing quality requirements. The main objectives of this secondary step is to mix and homogenize, adjust the chemical composition within close tolerances, temperature adjustment, de-oxidation, further removal of impurities and gases such as hydrogen and nitrogen, and separating the non-metallic inclusions.

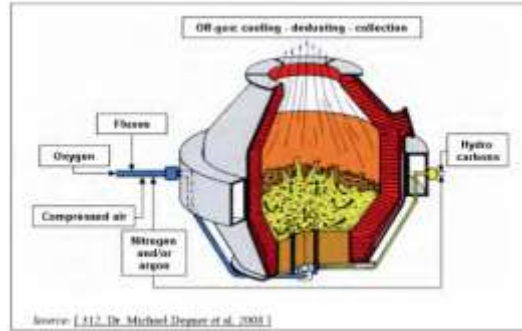


Figure 6 OBM (Q-BOP) converter [1]

Secondary metallurgy is carried out under vacuum, known as “VOD” process (Vacuum Oxygen Decarburization), or in a separate vessel called “AOD” (Argon Oxygen Decarburization), followed by ladle treatments depending on the grade to be produced. Some other secondary metallurgy used techniques include vacuum degassing, Vacuum arc degassing, and ladle heating furnace [4].

#### 1.1.2.2. Addition of Niobium as an Alloying Element

#### 1.1.2.3. What is Niobium

Niobium is a naturally available element whose chemical information are found in table 2, described by ductility, malleability and highly resistance to corrosion. It is used in a wide range of materials and applications due to its consequences in terms of better performance, cleaner environment, improved safety, advanced technologies, and increased value. It is found to be effective in improving the strength, weldability, and toughness, as well as the high temperature properties when added to stainless steels as we will see in chapter 3, which makes it an ideal element to be exploited in the automotive exhaust systems.

#### 1.1.2.4. Niobium Addition Process

During Ladle steelmaking process, Niobium is added during the secondary steel making phase as an alloying element in the form of Ferroniobium FeNb [5] shown in figure 7 (a standard Ferroniobium produced by CBMM spec. 111 has the chemical composition shown in table 3),

Niobium	Density [g/cm <sup>3</sup> ]	Melting point [°C]	Atomic Number	Atomic radius [nm]	Atomic weight
Nb	8.57	2477	41	2.08	92.906
FeNb (min. 63.5% wt Nb)	8.1	1370			

Table 2 Properties of Niobium and Ferroniobium, [Source CBMM.com]



Figure 7 Ferroniobium Particles [5]

The reason behind this delay with respect to the addition of deoxidizers is the low affinity of Niobium that will react with oxygen as according to equation 1.5 and form Niobium oxides (2NbO) which will escape the ladle if added while oxygen is blown.



Another way that Niobium could be wasted is when it is dissolved in the slag. Thus the interaction between Niobium and the slag should be kept to minimum, and this is achieved by ensuring the proper penetration of Nb through the slag so it reaches the liquid steel. The fact that the density of FeNb is higher than that of the liquid steel will play an important role in serving this purpose, but even though, it is much more beneficial to add the FeNb by the chute through a hole in the slag with sufficient velocity [5], then the Argon down injection will ensure the mixing with liquid steel as shown in figure 8.

Ferroniobium Standard Chemical Specifications, wt.%							
Nb	Si	Al	P	C	S	Ta	Fe
63.5 <sub>min</sub>	3.0 <sub>max</sub>	2.0 <sub>max</sub>	0.22 <sub>max</sub>	0.2 <sub>max</sub>	0.04 <sub>max</sub>	0.20 <sub>max</sub>	balance

Table 3 Chemical specification of standard FeNb, CBMM spec. 111

For sure, the melting of the introduced particles depend on their size that ranges from 5 to 50mm for an optimum result [5], in addition to the temperature of the molten steel which is around 1600°C. The dissolution could be described by three steps: firstly, the FeNb particle makes a solidified steel shell around it at the first moments, then it achieves a maximum thickness before it melts again, lately, dissolution occurs, and is enhanced by stirring.

FeNb addition could follow another method when used with Vacuum processes, where the very fine (diameter < 2mm) FeNb particles are introduced via cored wire [5].

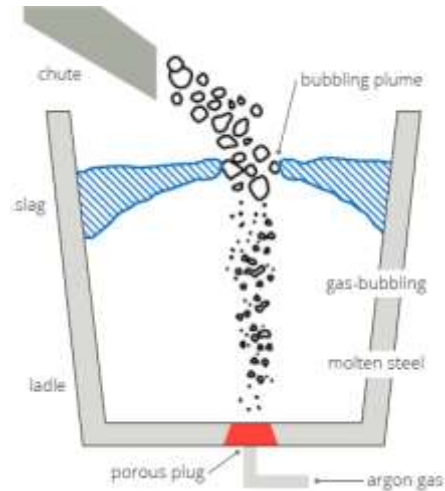
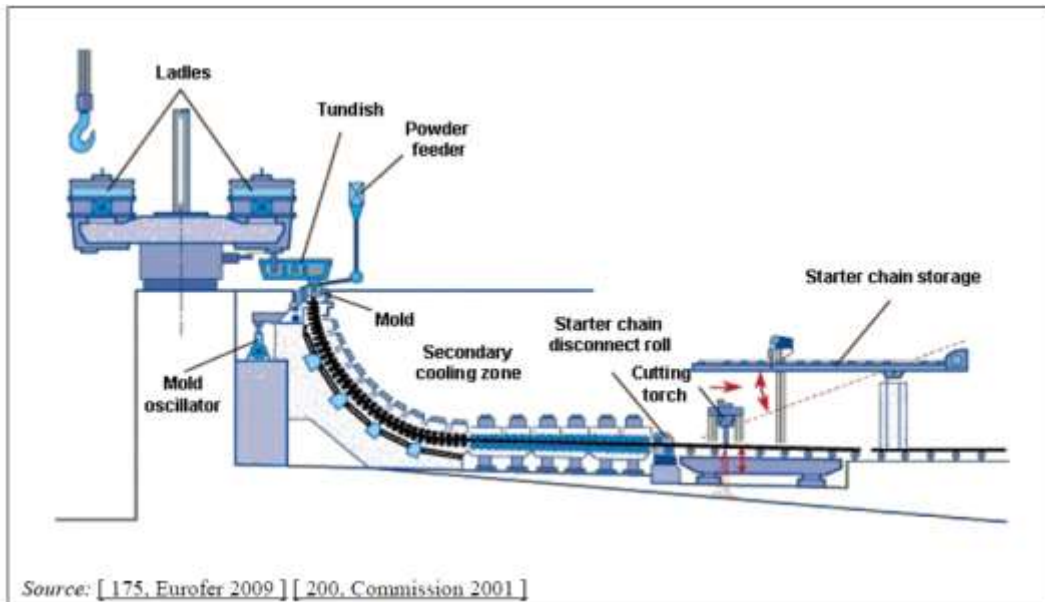


Figure 8 Fe/Nb delivery into the ladle [5]

### 1.1.2.5. Continuous Casting

When the liquid steel has reached the required temperature, it is poured into the tundish (see fig 9), it passes by a water cooled copper mold lubricated by powder or vegetable that oscillates to avoid steel sticking, giving it the desired shape at the same time, so that when the steel leaves the mold it would have a solidified skin. The continuous strand could be billet, bloom, slab, beam blank or strip depending on the application and the market demands.

The direct casting method has replaced the ingots casting due to its advantages in terms of low cost, higher yield, flexibility of operation and ability to achieve high product quality [4]. It includes pouring the liquid steel into then Tundish, then on a water cooled oscillating copper mold, then it passes by a secondary water cooling, containment section and finally withdrawal mills. The products of continuous casting are semi-finished shapes like slabs, blooms or billets which are to be rolled into the desired shapes.



Source: [ 175. Eurofer 2009 ] [ 200. Commission 2001 ]

Figure 9 Continuous Casting [1]

### 1.1.2. Hot Rolling

During the rolling process the steel is plastically deformed by forcing it to pass between two opposite sense revolving rolls which has a lower thickness than the processed part as shown in figure 10, the steel undergoes thickness reduction and lengthening at the same time. Steel may pass through a number of rolls, or back and forth until it reaches the required thickness [6]. Rolling is employed in order to enhance the mechanical and physical properties by modifying the grain structure, making it finer, resulting in greater toughness and strength.

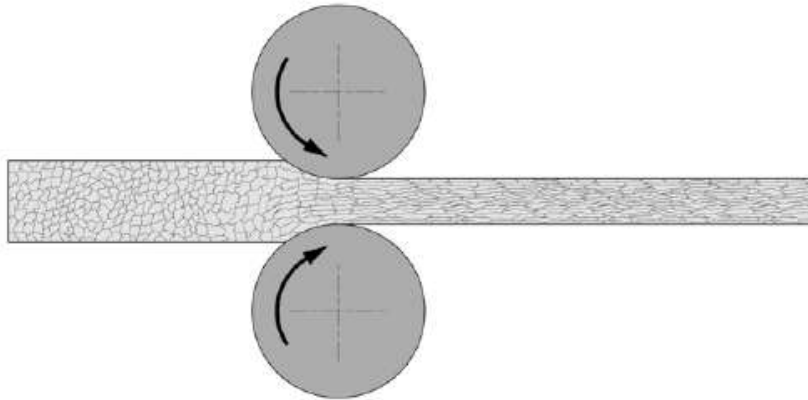


Figure 10 rolling process scheme [16]

No strengthening occur during hot rolling, thus, a very thick plate could be transformed into thin sheet due to the unlimited plastic deformation. It is suitable for large parts due to the lack of strength and high ductility at elevated temperatures.

Hot rolling is useful to obtain the desired shape of the product. The first steps in this process are carried out above the crystallization temperature in order to exploit the lower strength of the material [6], however the last step is carried just above the crystallization temperature, therefore, the material is in continuous recrystallization. The more the steel is rolled, the denser and tougher it becomes but no strengthening occurs. Figure 11 shows the effect of hot rolling on a high nitrogen steel specimen with different hot rolling deformation %, and it is clear that the highest rolling % results in a dominant elongated refined grains [7]. Hot rolling also has advantages in terms of eliminating imperfections such as gas pores, and composition differences. On the other hand, the obtained surface finish is poor and oxides are formed at the surface (known as scales) that require further pickling process (further discussed in this chapter).

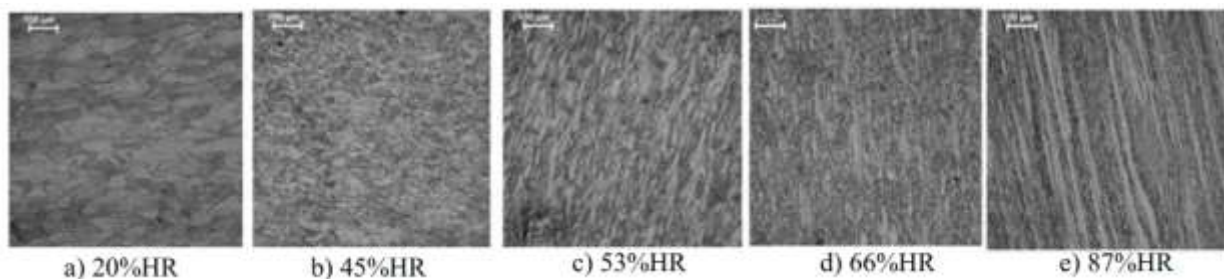


Figure 11 Microstructure of steel in hot rolled condition [7]

### 1.1.3. Cold Rolling

After the hot rolled products are cleaned from scale (the thin oxide layer resulting from the high temperatures of hot rolling), cold rolling is carried out at room temperature in order to increase the strength and hardness, obtain the desired shape with excellent precision. But it causes the loss of ductility [8]. The main difference between hot and cold rolling is that during the later, the grains do not recrystallize automatically, which justify the need of a further heat treatment.

During the rolling process, the grains are oriented in the preferred crystallographic direction giving the sheet texture and enhancing the strength of the rolled part, this is known as the texture strengthening. Considering the direction is important because it is strictly related to the some properties such as young's modulus and the yield strength. However, some of the applied stress is stored in the part in the form of undesirable residual stresses that demands a further annealing known as self-relief annealing.

A study was carried out on the AISI 304N stainless steel [8] showing the effect of cold work on the microstructure and the mechanical properties. The results shows that cold working increases the yield strength, hardness and tensile strength , while ductility decreases as shown in figure 12.

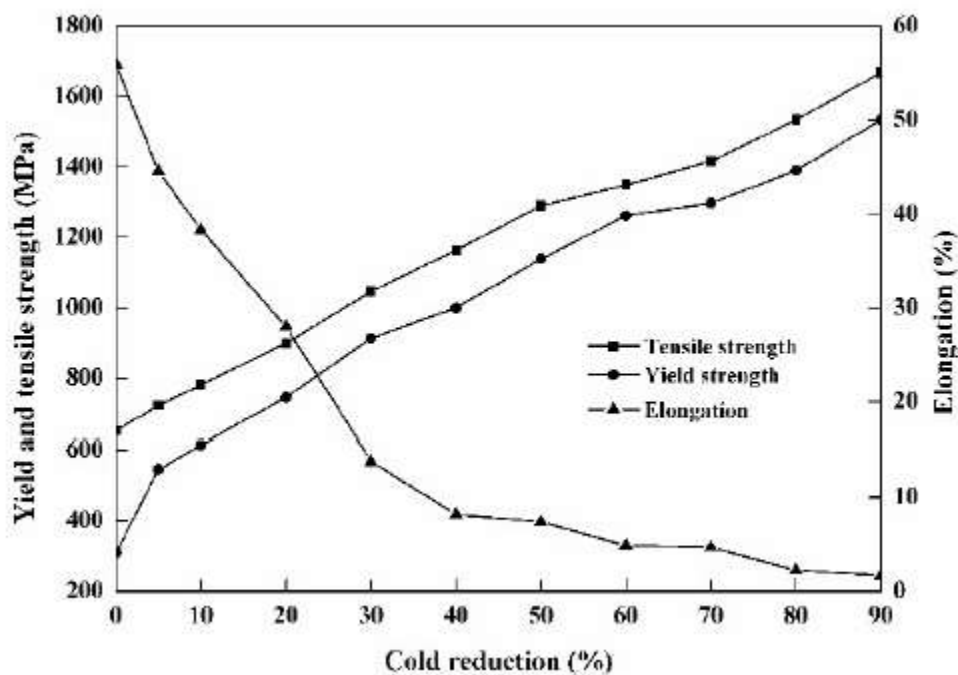


Figure 12 Effect of cold rolling on AISI 304N specimen [8]

#### 1.1.4. Annealing

Heat treatment is a technique used to improve the mechanical properties of the steels such as hardness, ductility, strength, toughness and internal stresses [9]. There are many types of heat treatments that mainly differ in the temperature held and the cooling rate. Annealing process is carried out in a tunnel furnace of tens meter long in which the steel is heated up to high temperatures above the critical range (typically between 900°C and 1100°C for steels [10]) holding at that temperature for specified time (1-2 hours) then cooled at a slow controlled rate. It is important because it eliminates the drawbacks of cold working as it enables the steel to be subjected to further forming operations without the risk of breaking after it has lost its ductility and became thermodynamically unstable during the cold working [10], thus the result is a softer steel with relieved internal stress.

Annealing consists of 3 phases [6]: recovery, recrystallization, and growth rate as shown in figure 13. In the first phase, rearrangement of dislocations takes place with a significant reduction in the residual stress, while the strength and ductility are unaffected. The second step is characterized by the nucleation and growth of strain free grains, hence the badly deformed grains by cold working are replaced by new grains, strength decreases and ductility increases during this step. Finally, even though grain growth of some grains on the expense of other is undesirable, but it results in the best strength-ductility combination.

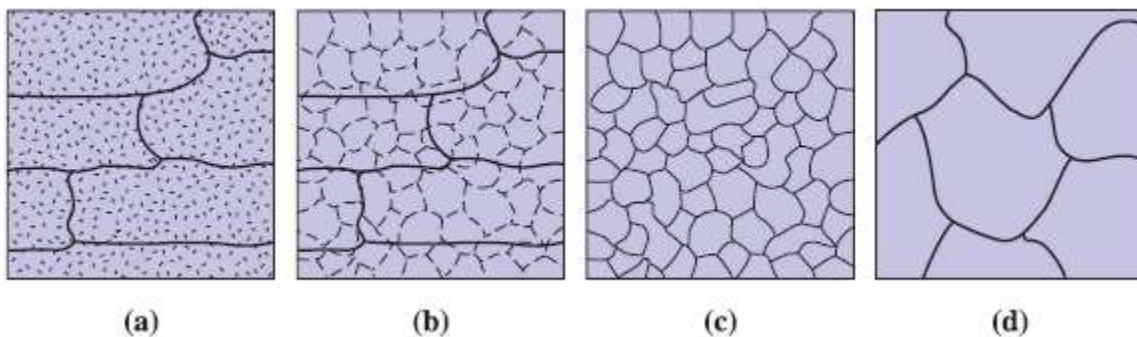


Figure 13 the effect of annealing on the microstructure of cold worked metals. (a) Cold worked, (b) after recovery, (c) after recrystallization, (d) after grain growth [6]

#### 1.1.5. Pickling

The surface finish resulting from the hot worked parts is poor, because oxygen reacts with the metal forming oxides that are forced into the surface during forming. The term “de-scaling” mentioned before stands for the removal of the thick visible grey oxide scale and iron contamination from the surface with inferior protective properties due to the hot working and heat treatments. However, Pickling is a chemical method used for the removal of the thin metal layer that is found directly beneath the scale on the surface of the steel. For this purpose a mixture of 8-20% by volume nitric acid and 0.5-5% by volume hydrofluoric acid is used [11], it is important to avoid hydrochloric agents to prevent pitting corrosion.

Pickling could be carried out in different methods such as: pickling in a bath (known as tank immersion pickling), pickling with the pickling paste, and pickling with pickling solution (in spray form) [12]. Each of these methods is employed according to the application, for instance the bath pickling requires an off-site plant, however spray pickling could be done on site.

### 1.1.6. Finishing

Finishing is a final added value process obtain a high surface quality and accuracy it removes a very small amount of material in the order of micrometers [13]. Finishing process could be mechanical [14] (by applying abrasives) such as polishing and grinding, and non-mechanical such as chemical, photo-chemical, electro-chemical, electrical and optical processes.

Grinding and polishing involve the removal of layer by abrading action by hard particles called abrasives. Grinding signifies the removal of layers resulting from welds or oxide layers, however polishing stands for decorative actions. Brushing is also an abrasive based finishing process, where the abrasive effect on the surface is minimal, mainly this method is used to blend



Figure 14 Surfaces generated by different abrasive methods [13]

the wed in the surrounding metal, for this purpose brushing flap wheels made of Scotch-Brite [13] are employed. Buffing does not involve the removal of material, but it makes the surface brighter and reflective, hence pastes and liquids are used resulting in smoother, high glossy effect surface.

Finishing also include the process in which patterns or etches are implemented on steel's surfaces.

### 1.1.7. Niobium in Improving the Production efficiency

Apart from being an alloying element, Niobium has showed improvements in the production process as a whole. While in the melt shop, Niobium result in less oxidation, where the efficiency of FeNb is about 95%, compared to that of FeTi that ranges from 80 to 85%. Niobium also avoid clogging during casting, and results in less sticking during rolling, it may replaces the higher amounts of Ti that results in surface defects, thus it also improves the surface state. [15]

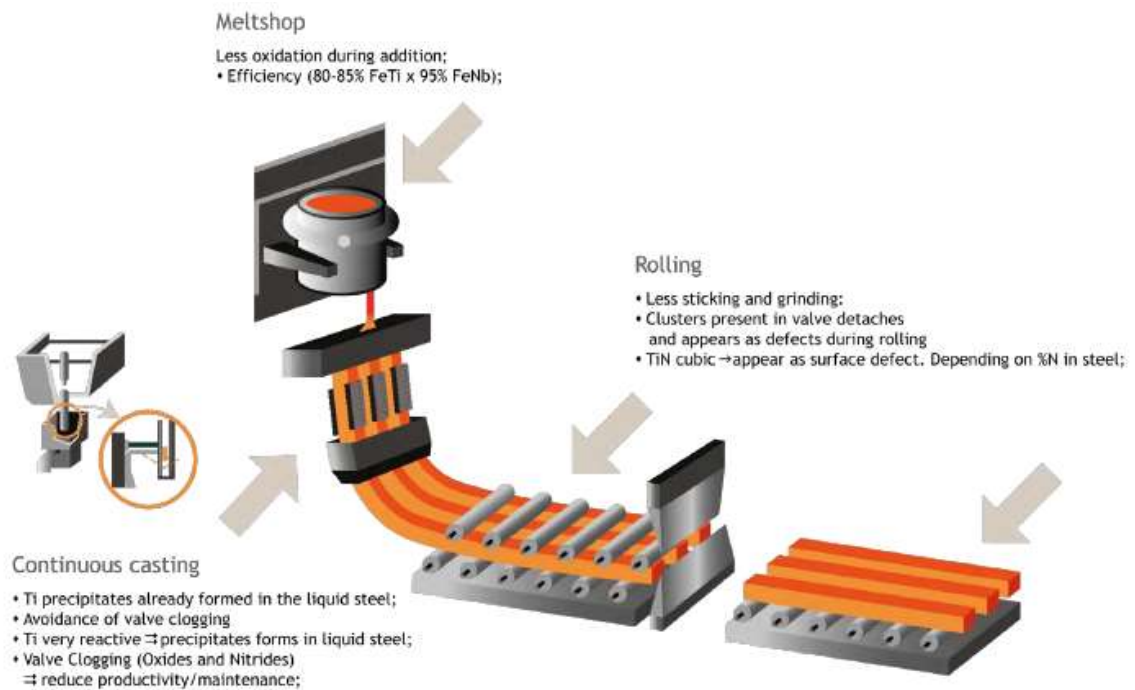


Figure 15 Niobium in improving the production efficiency [15]

## 1.2. Phase Diagram

### 1.2.1. Iron-Carbon Phase Diagram

The Iron-Carbon diagram is a starting point that enables us to understand the phases of the alloy under thermodynamic equilibrium by plotting the different states as function of the carbon content. The “L” region shown in figure 16 represents the liquid phase field limited by the so called “liquidus”. Liquidus line defines the initial solidification point for a well-defined carbon content simply by drawing a vertical line from carbon content value and finding the intersection. The allotropic property of iron is well defined in this structure, where iron may exist in several crystal form depending on the temperature. Other regions are called the “one-phase” fields, such as ferritic field known as  ***$\alpha$  phase***, due to the limited interstitial available sites [16], it has a maximum carbon solubility equals to 0.02% as demonstrated in figure 16, the Austenitic phase known as  ***$\gamma$  phase***, having a higher solubility of carbon that reaches 2.11%, and as shown it is widely spread [16]. On the other hand, we can say that the Fe-C diagram could be divided into two parties, Steels when the carbon content is less than 2.11%, and cast iron above that threshold. It is important to mark that the carbon starts to separate from iron in the form of graphite after 5% according to  $\text{Fe}_3\text{C} \rightarrow 3\text{Fe} + \text{C}$ , the reason why the diagram is truncated at 6.69% of carbon where no further changes are noted beyond.

In order to further clarify the phases and the microstructure of steel, we will refer to Austenite as a homogeneous grains of  ***$\gamma$  phase***, Ferrite as a homogeneous grains of  ***$\alpha$  phase***, Pearlite as a lamellar grains composed of layers of  ***$\alpha$  phase*** and  $\text{Fe}_3\text{C}$ , and Cementite as plates of  $\text{Fe}_3\text{C}$  at the grain boundary of homogeneous crystals.

Another very important application of the Fe-C diagram is its utilization as a base for all the heat treatments as it defines the composition of the stable phases as function of temperature.

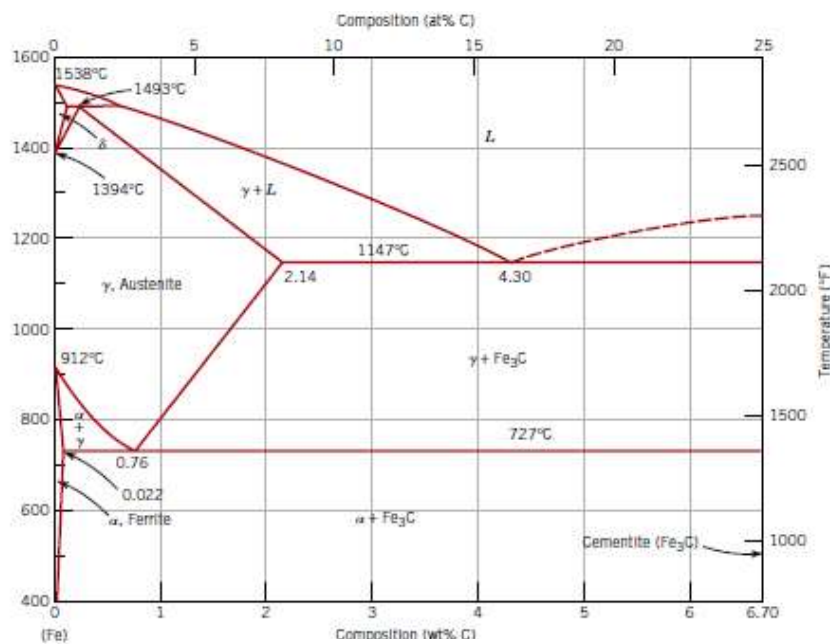
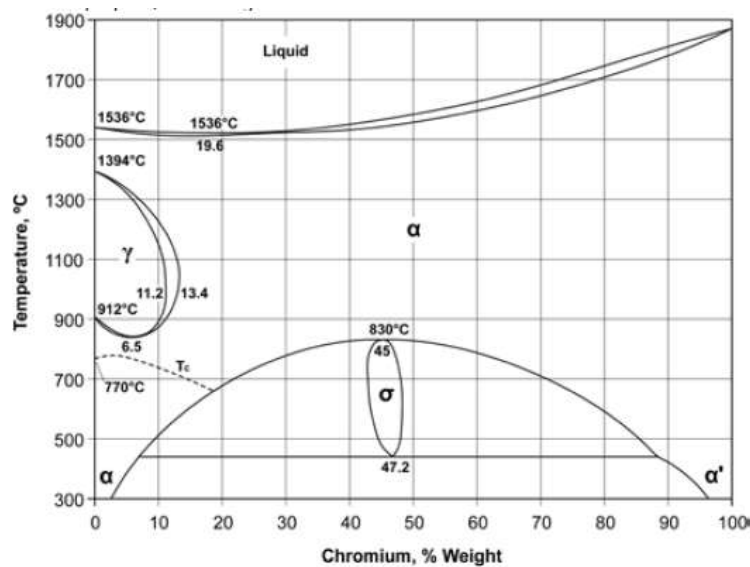


Figure 16 Carbon-Iron phase diagram [6]

### 1.2.2. Iron-Chrome Phase Diagram

As a ferrite forming element, Chromium further expands the  $\alpha$  phase and closes the  $\gamma$  phase between a lower and upper limits 11.2% and 13.4% respectively as shown in figure 17, thus obtaining a stable Ferritic structure when exceeding 13.4% and standard  $\gamma$  to  $\alpha$  transformation occurring below this limit. However, the addition of other Austenitic forming elements such as Ni, C, or N will expand the  $\gamma$  phase (see figure 19) and stabilize it at high temperatures (900-1000 °C) even if 13.4% Cr content is exceeded. On the other hand, if the Chromium content is about 16-17 % and the carbon content is very low (<0.1%) the structure will be always Ferritic with no considerable transformations [17].

$\alpha'$  phase is a rich iron-chromium phase that forms within the ferrite grains and it has a BCC lattice.



- Fe-Cr phase diagram [from ASM-H.3 1992].

Figure 17 Iron-Chrome phase diagram [17]

### 1.2.3. Elements Expanding the $\alpha$ -Phase

Nevertheless, the Fe-C is only a guide because the addition of alloying elements will obviously modify the Fe-C diagram, mainly in two families: the austenitizing elements such as Ni, N, C, etc... that widens the  $\gamma$  **field** and compresses the  $\alpha$  **field**, and the ferritizing elements such as Cr, Ti, Nb, V, Al, etc... that widens the  $\alpha$  **field** and compresses the  $\gamma$  **field**. The graphs in figure 18 [16] show the effect of adding some different ferritizing elements (also called alpha-genic) on the Fe-C diagram.

According to these figures 18, different alloys belonging to the same category does not have the same effect when added in same amounts, for instance, Ti is a higher ferritizing element than Cr [16], as we obtain a closed  $\gamma$  field with 0.8% of Ti compared to a slightly narrowing effect with 5% Cr.

As shown in Figure 18, Niobium is a ferrite forming element that expands the  $\alpha$ -phase, and closes the  $\gamma$ -phase. This is the so called stabilizing effect of Niobium on the ferrite phase, keeping the structure of ferritic stainless steels ferritic at all the temperatures.

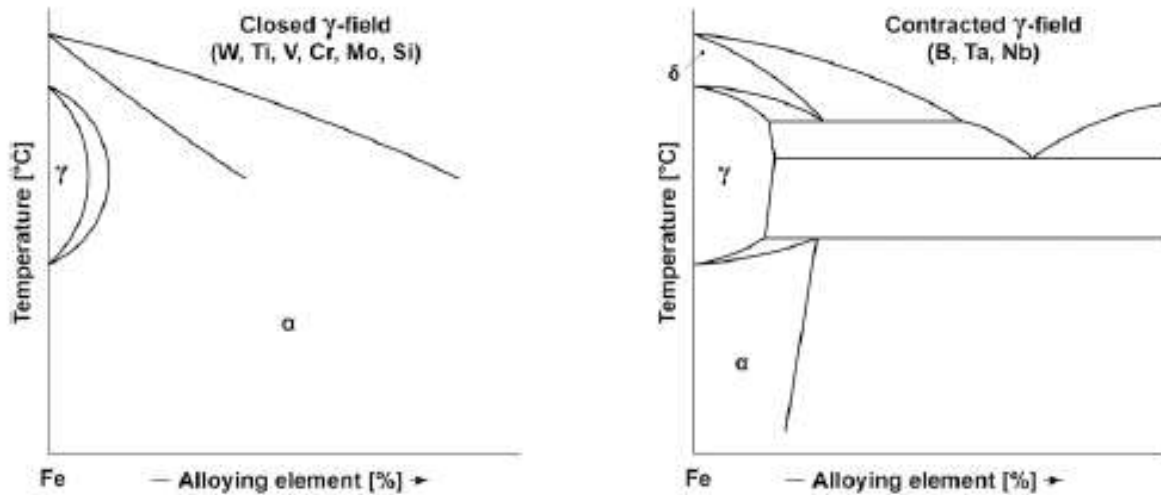


Figure 18 Effects of different alloys on the Fe-C diagram in expanding the  $\alpha$ -phase [16]

#### 1.2.4. Elements expanding the $\gamma$ Phase

In figure 19, the expansion of the  $\gamma$  Phase is shown upon adding different Austenite forming elements in different quantities [16], where Nickel is tested in fig. 19 (a), Nitrogen (with carbon) in fig. 19 (b) and Carbon in figure 19 (c). As the figure reveals, the higher is the added amount of each of the elements, the wider is the  $\gamma$  Phase.

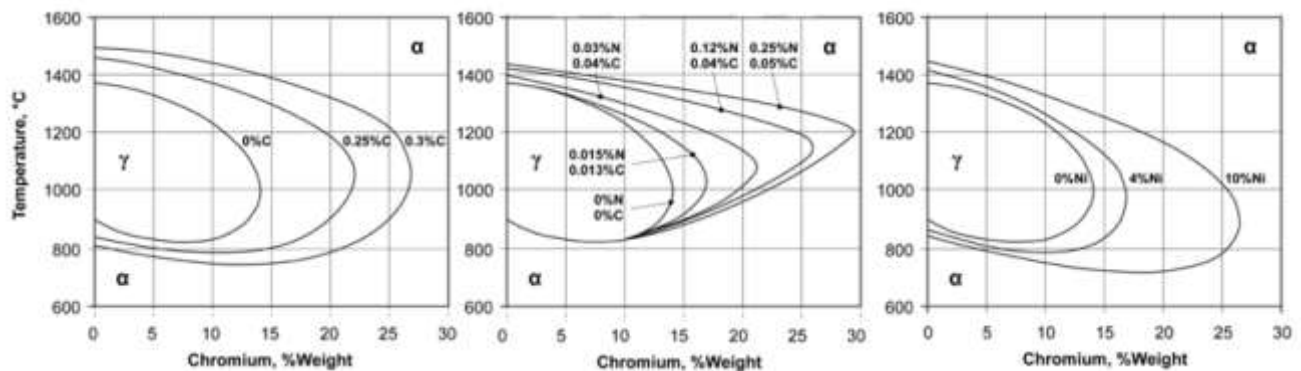


Figure 19 Effects of adding (a) nickel (b) Nitrogen and (c) Carbon [17]

### 1.2.5. Schaeffler Diagrams and De Long Diagrams

In order to define to which of the pre-mentioned families a specific stainless steel belong, Schaeffler Diagram [17], shown in figure 20, is developed considering the great variety of the alloying elements and their percentage, as it plots the limits of each category under the condition of rapid solidification. It is useful in case of welded structures as well, as it defines the areas where the microstructure of the stainless steel is stable.

The percentage of the ferritizing elements is taken as abscissa and that of Austenitic elements as ordinate, known as Chrome equivalent and Nickel equivalent respectively where each other alloy is weighted in the total sum according to its effect (setting 1 for Ni in Austenitic equivalent, and 1 for Cr in Ferritic equivalent [17]).

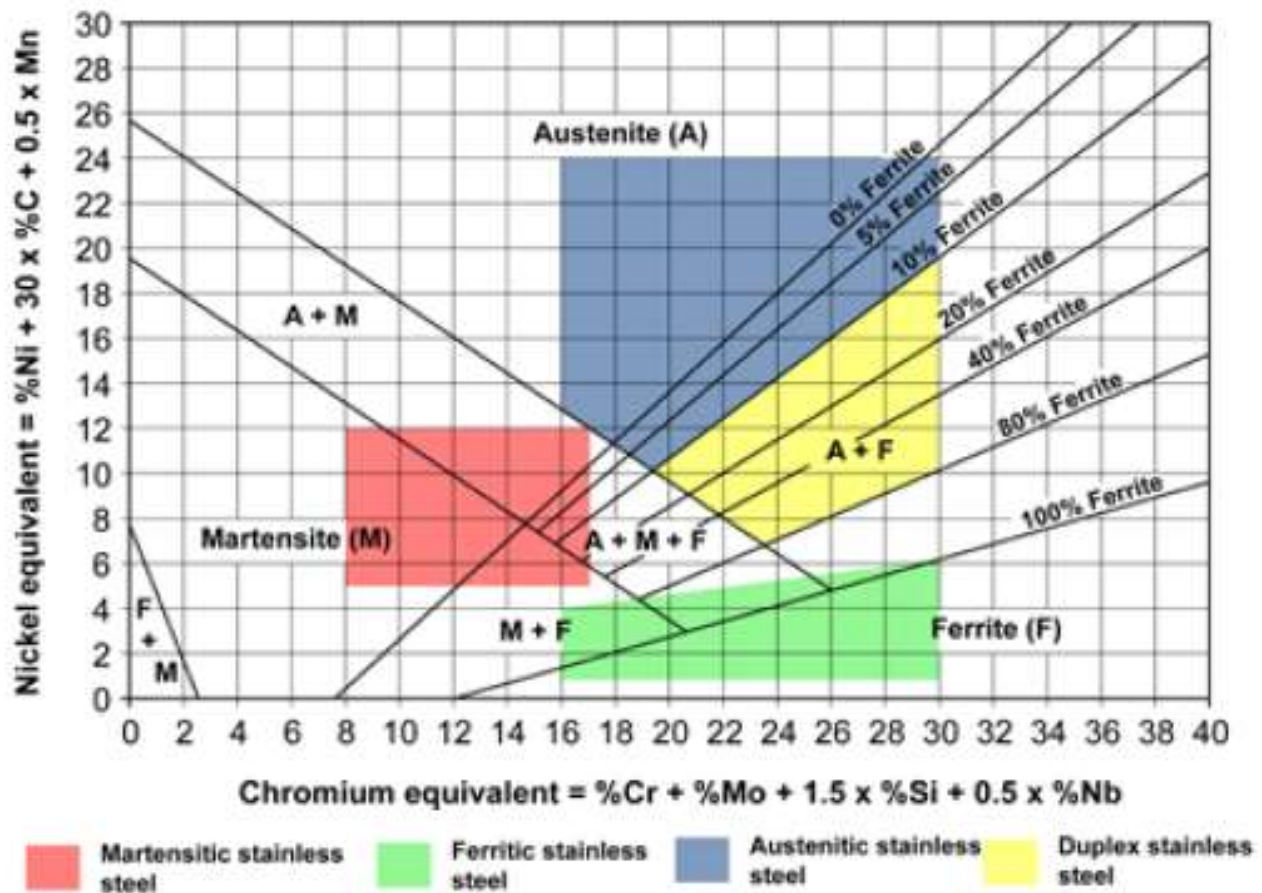


Figure 20 Schaeffler Structural Diagram [17]

De Long [17] in figure 21 is a developed version of Schaeffler that takes Nitrogen into account as alloying element, thus solving a limitation of Schaeffler diagram. Note that Nitrogen is added only to some grades of steel for the purpose of increasing hardness and resistance.

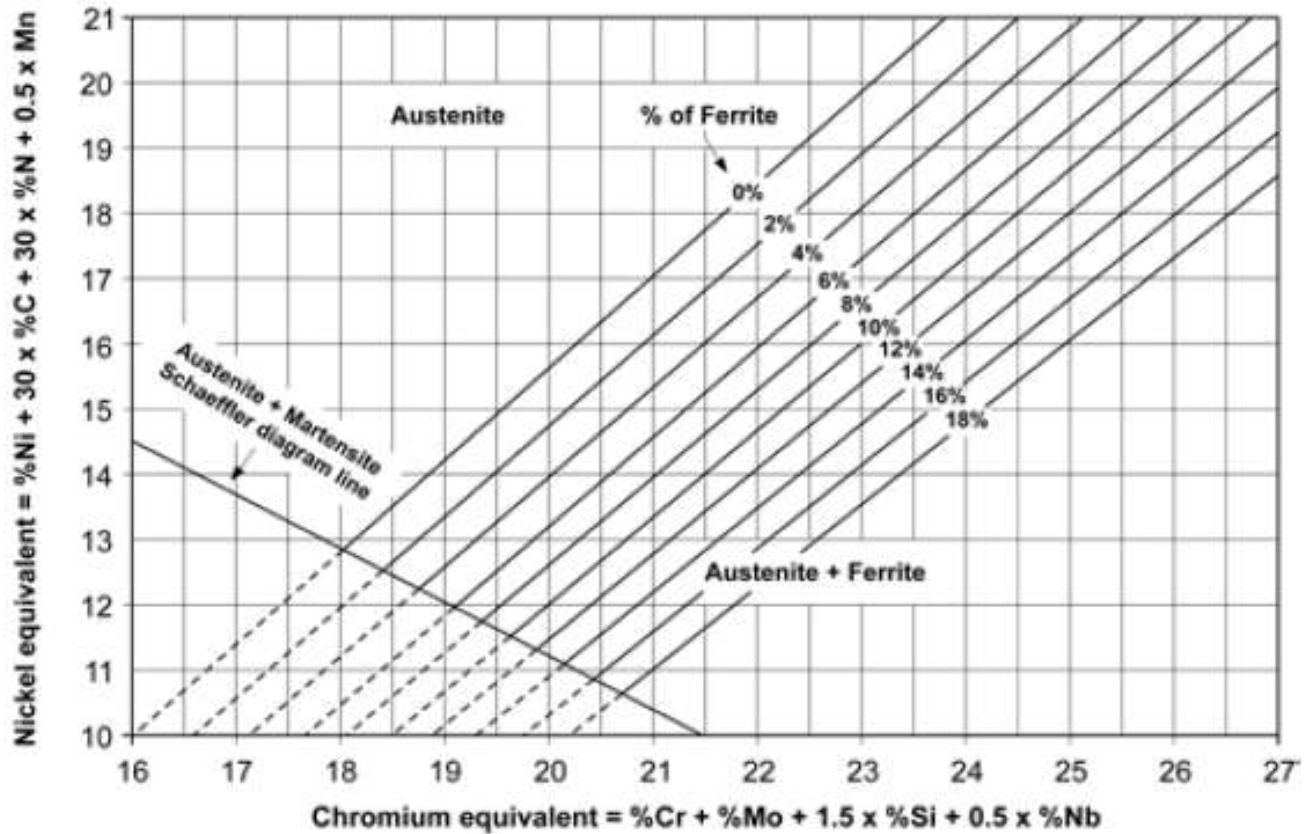


Figure 21 De Long Diagram [17]

## 1.3. Stainless Steels

### Introduction

Stainless steel is a unique grade of Iron-based alloy that features the property of resisting different types of corrosion such as wet corrosion (also known as electrochemical corrosion) in aggressive environments such as fresh water, sea water, etc... as well as dry corrosion (this would be explained in details later), and pitting corrosion. Thus, it was the solution for the major steel's drawback i.e. rust formation due to oxidation under moisture. For this purpose it has been alloyed with a chromium content (Cr) ranging from 10.5% (according to the EU standard EN 10088) up to 30% that creates a very thin layer protecting against corrosion, in addition to other diversity of alloying elements with varying amounts such as Ni, Mo, V, Ti, Nb, etc... enhancing different characteristics such as high temperature resistance, toughness, and formability. Hence, different families of stainless steels could be obtained according to the alloying elements and their percentage, here are the main classification of stainless steel families [17] with their main contents, with the possible addition of other alloying elements.

**Austenitic Stainless Steel:** contains at least 17% Cr, 8 to 13% Ni, and a varying carbon content between 0.02 to 0.15%.

**Ferritic Stainless Steel:** contains 12 to 30% Cr, and a varying carbon content from very low levels such as 0.01% to levels above 0.15%. Grades with added Niobium and/or Titanium are said to be "Stabilized Ferritic Grades"

**Martensitic Stainless Steel:** contains 11.5% to 18% Cr, 8% Ni, and a varying carbon content between 0.1 to 1%.

**Duplex Stainless Steel:** contains 22 to 25% Cr and 4 to 7% Ni.

**Precipitation hardening Stainless Steel:** contains 18-20% Cr, 8-10% Ni, Co, Ti, Al, and Nb.

Henceforth, the main condition in producing stainless steel is controlling the chrome and carbon contents, noting that Chromium content gives satisfactory results starting from 12% [17], and corrosion resistance increases as the chromium content increases and carbon content decreases.

Each of the pre-mentioned families has a wide field of applications, for example, Martensitic Stainless steel's products are employed in the industrial sector, petroleum and organic acids environments, table and cutting knives, surgical instruments, etc... As well as it is employed in the automotive sectors in brake disks, power drive shafts, con rods, and bushings for pumps and compressors, ferritics are applied in the industrial environment as pipes, and in highly corrosive environments, household's appliance, oil sectors and decorative elements. Austenitics are widely employed in various applications such as boilers, elevators, domestic utensils, sinks, chemical, petrochemical, and nuclear industries, canned food. Duplex are used when chloride environments exist or aqueous solutions with chlorides, they are also employed in nitric acids and organic acids plants. Furthermore, they are used in marine sectors, petrochemical fields, and distillation plants (more details about ferritic and austenitic are discussed later in this chapter).

### 1.3.1. Stainless Steel Passivation

The phenomenon of passivity is defined as the loss of the chemical reactivity of the metal/alloy making it extremely inert under specific conditions. Chromium, the main alloying element in stainless steels is the reason behind the corrosion resistance of this category. The formation of a chromium adherent oxide film made up of  $\text{Cr}_2\text{O}_3$  and  $\text{Cr}(\text{OH})_3$  [17] forms naturally on the surface of the metal (the substrate) protecting it against any type of contact that may cause corrosion as shown in figure 22, this layer is known as the passive layer, or passive condition [12], it is just a few nanometers and transparent to the luminous radiation, giving the steel its grey-silver metal finish. One of the most impressive properties of this layer is its ability to reform whenever new substrate material is exposed to an environment that has sufficient oxygen, this property is shown in figure 23. The exposure of the material could be due to any type of damage such as scratching, rubbing, damaging or attacking, hence stainless steels do not require corrosion protecting systems due to this self-healing property. It is revealed that the addition of other elements such as Nickel (Ni), Molybdenum (Mo), Titanium (Ti), Niobium (Nb) and others may also enhance the corrosion resistance of the stainless steel on a wider range.



Figure 22 Chromium role-Passive layer [17]

Despite the fact that the formation of the passive layer is natural, sometimes it is necessary to assist the phenomenon with oxidizing acid treatments [12]. For this, it is found that nitric acid is highly effective, however weaker acids such as citric acid can also help. It is also important to make sure that the surface to be treated is free of scales, pickled and clean of any organic contaminations, oils, or grease.

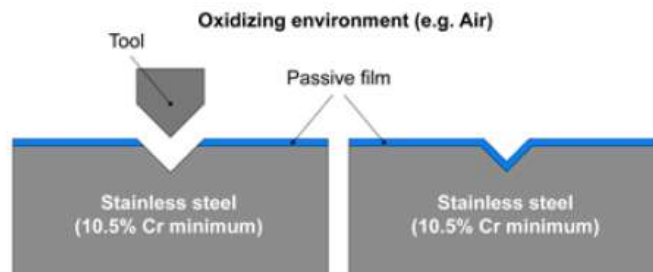


Figure 23 Re-passivation phenomenon [17]

Nevertheless, we cannot consider that stainless steels are always protected against corrosion, there are some conditions where the passive layer is breakable resulting in material's de-passivation in other words, it will be subjected to corrosion. This is better explained in figure 24 that uses the electrical analogy [17] where  $E$  represents the oxidation power and  $i$  represents the corrosion rate. Below  $E_{eq}$  the stainless steel is stable, no oxidation can take place, thus it is immune against corrosion, then from  $E_{eq}$  to  $E_{pp}$  it acts as a common carbon steel with gradually increasing corrosion. At the point  $E_{pp}$  the passivation starts and the protective film starts forming. At point  $E_p$ , Corrosion rate is extremely slow and it could be considered zero due to the stabilized thin chromium oxide protective layer. When the point  $E_t$  is reached, dissolution of the chromium oxide takes place and the stainless steel is subjected to corrosion again. Hence, the high resistance to corrosion is the field extended between  $E_p$  and  $E_t$ .

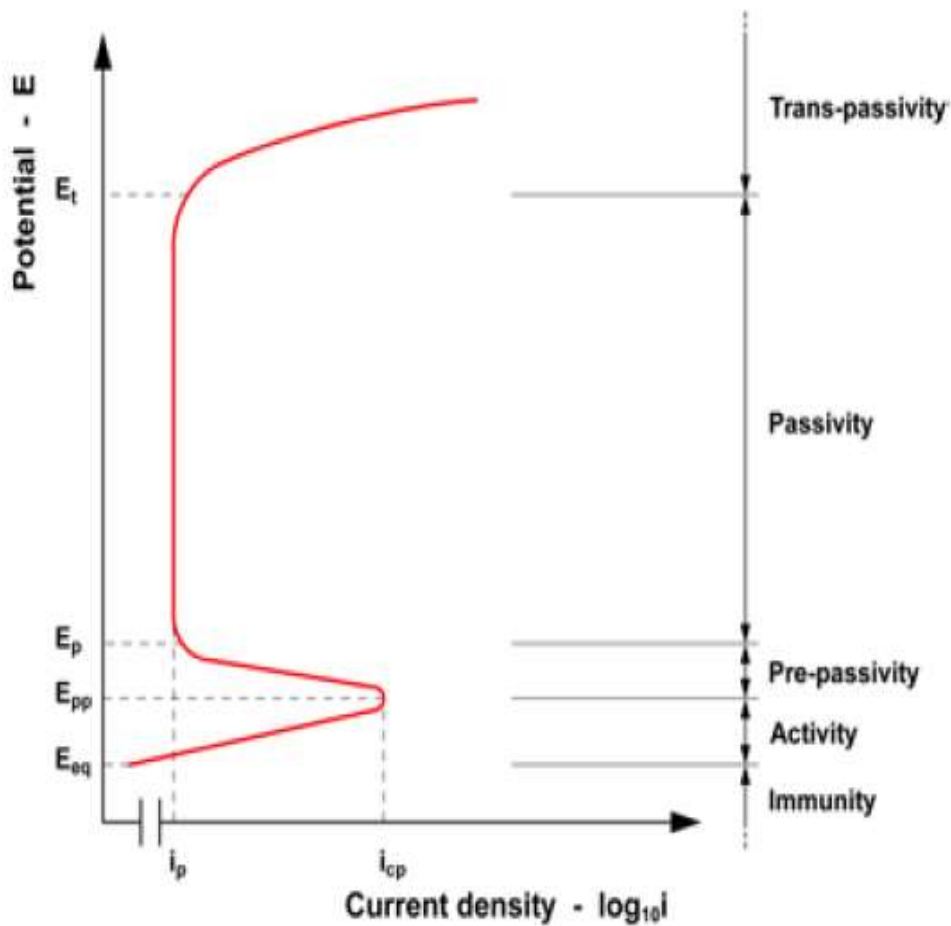


Figure 24 Passivation curve of a generic Stainless steel [17]

The effect of addition of some alloying elements on corrosion resistance could be better explained using this curve. Figure 25 shows the effect of Cr, Mo, Ni, Cu, and N on the de-passivation curve. It is clear that Cr helps extending the corrosion resistance field by increasing the  $E_t$  value and lowering the  $E_p$  value, it also compresses the first part, in other words, the pre-passivation is reached earlier.

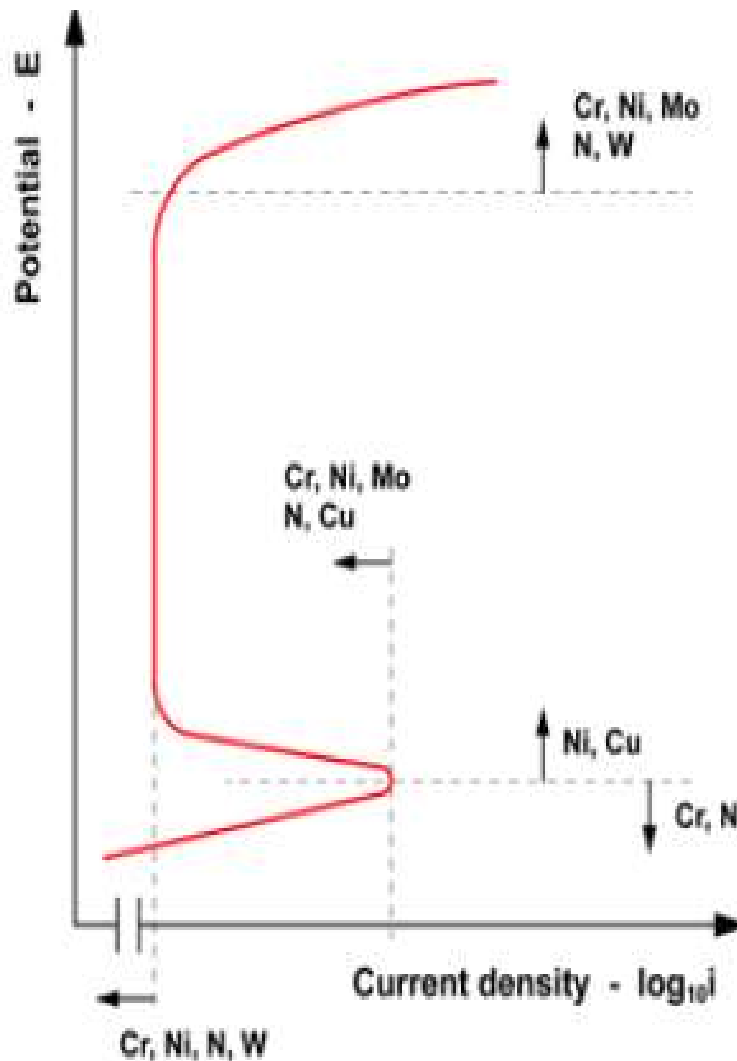


Figure 25 Effect of alloying elements on the active-passive characteristics of a generic stainless steel [17]

## 1.3.2. Ferritic Stainless steels

### 1.3.2.1. Metallurgy

The Crystalline structure of ferrite is described by a unit body centered cubic (BCC) lattice with a total of two atoms per cube as shown in figure 26 (1 atom in the middle, and 1/8 atom at each corner), thus it is a more opened and less dense structure compared to Austenitic cube. In this family, the carbon content is reduced down to below 0.1% keeping the chromium content high (17% up to 30%), the ferritizing effect dominates the austenitic thus resulting in a Ferritic structure at ambient temperature. Different Ferritic grades could be characterized according to their alloying elements and their chromium content, figure 27 shows the main ferritic stainless steel grades starting from AISI 430 as a reference.

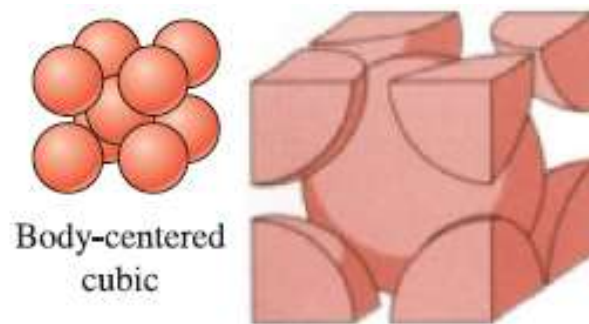


Figure 26 Body centered cubic lattice [6, 34]

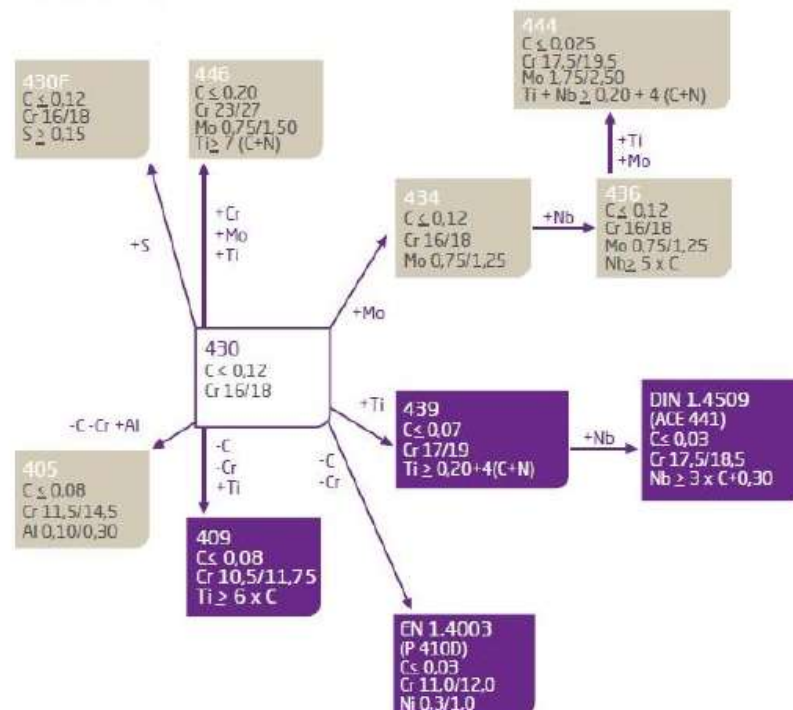


Figure 27 main ferritic stainless steels from AISI 430

Increasing the chromium content, the corrosion resistance is improved, and some other elements enhance other properties such as Oxidation resistance, and weldability. A special importance would be given for the alloys containing Niobium (Nb) in this study, highlighting its major effects on improving several properties of the Ferritic stainless steels, hence widening their field of application.

Nonetheless, many other elements could also be added forming highly alloyed ferritic stainless steels, obtaining the properties that better suits a specific application, making it a cost saving material since it does not have any expensive nickel addition. Among the numerous grades and compositions, table 4 represents the chemical composition of the main types, and table 5 [17] represents the chemical composition of some stabilized ferritic grades.

EN Designation	AISI Approximate	%C	%Cr	%Si	%Mn	%P	%S	%Mo	other
X2CrTi12 (1.4512)	AISI 409	≤0.03	10.5-12.5	≤1.00	≤1.00	≤0.040	≤0.015	--	1
X6Cr17 (1.4016)	AISI 430	≤0.08	16.0-18.0	≤1.00	≤1.00	≤0.040	≤0.015	--	--
X6CrMoS17(1.4105)	AISI 430F	≤0.08	16.0-18.0	≤1.5	≤1.50	≤0.040	0.15-0.35	0.20-0.60	--
X3CrTi17 (1.4510)	AISI 439 (430Ti*)	≤0.05	16.0-18.0	≤1.00	≤1.00	≤0.040	≤0.015	--	2
X6CrMo17-1 (1.4113)	AISI 434	≤0.08	16.0-18.0	≤1.00	≤1.00	≤0.040	≤0.015	0.90-1.40	--
X2CrMoTi17-1 (1.4513)	AISI 436	≤0.025	16.0-18.0	≤1.00	≤1.00	≤0.040	≤0.015	0.80-1.40	3
X2CrMoTi18-2 (1.4521)	AISI 444	≤0.025	17.0-20.0	≤1.00	≤1.00	≤0.040	≤0.015	1.80-2.50	4
X2CrTiNb18 (1.4509)	441*	≤0.03	17.5-18.5	≤1.00	≤1.00	≤0.040	≤0.015	--	5
X10CrAlSi25 (1.4762)	AISI 446	≤0.12	23.0-26.0	0.70-1.04	≤1.00	≤0.040	≤0.015	--	6
X2CrMoTi29-4 (1.4592)	29-4C*	≤0.025	28.0-30.0	≤1.00	≤1.00	≤0.030	≤0.010	3.50-4.20	7

Table 4 Chemical composition of some main types of Ferritic stainless steel [From EN 10088] [17]

### 1.3.2.2. Physical and Mechanical Properties

Heat treatments are carried out to improve the properties of the steels by modifying their crystalline structure, in other words, re-crystallize or reform new grains. In the particular case of the ferritic family, chromium could be uniformly distributed in the crystalline structure by annealing, optimizing the material's resistance to corrosion, noting that this is the only applicable heat treatment [17]. So, a special importance should be considered when choosing the temperature and the holding time for their effect on crystalline grain enlargement phenomenon.

<b>Chemical composition of wrought high-performance ferritic stainless steels (wt. pct.)</b>									
Name	UNS Number	Sub Group	C	N	Cr	Ni	Mo	Cu	Other
Type 444	S44400		0.025	0.035	17.5-19.5	1.00	1.75-2.50	–	Ti, Nb
26-1S	S44626	F - 1	0.060	0.040	25.0-27.0	0.50	0.75-1.50	–	Ti
E-BRITE 26-1	S44627		0.010	0.015	25.0-27.0	0.50	0.75-1.50	–	Nb
MONIT	S44635		0.025	0.035	24.5-26.0	3.5-4.5	3.5-4.5	–	Ti, Nb
SEA-CURE	S44660	F - 2	0.030	0.040	25.0-28.0	1.0-3.5	3.0-4.0	–	Ti, Nb
AL 29-4C	S44735		0.030	0.045	28.0-30.0	1.00	3.6-4.2	–	Ti, Nb
AL 29-4-2	S44800	F-3	0.010	0.020	28.0-30.0	2.0-2.5	3.5-4.2	–	–

source: High performance stainless steel, by Curtis W. Kovach, Technical marketing resources, Inc, Pittsburgh, PA

Table 5 High performance stabilized stainless steels containing Nb

Annealing is also beneficial in enhancing the physical properties, for instance, it enhances the magnetic behavior when annealed with prolonged hold intervals, as well as reaching tensile strength  $R_m$  up to 600 Mpa, and hardness up to 220 HB measured in Brinell Hardness (obviously these values are composition dependent). As mentioned before, no other heat treatments are applicable, making it possible to increase the mechanical resistance up to 1000 MPa [17] by the means of cold drawing or rolling only. In annealed state, Ferritic stainless steel's stress/strain curve shows a yield point followed by a drop due to the breakaway of pinned dislocations thus enabling the true yield stress to be defined.

Table 6 and table 7 [17] represent the mechanical and the physical properties of the previously mentioned grades in table 4.

EN Designation	AISI approximate correspondence	Metallurgic condition	$R_{p0.2}$ [MPa]	$R_m$ [MPa]	A [%]	Hardness
X2CrTi12 (1.4512)	AISI 409	A	250-350	400-500	27-32	140-180 HB
X6Cr17 (1.4016)	AISI 430	A A + CD**	300-400 550-850	450-550 650-950	25-30 5-18	150-200 HB ---
X6CrMoS17 (1.4105)	AISI 430F	A A + CD**	250-350 400-700	450-550 600-850	20-25 5-15	150-200 HB ---
X3CrTi17 (1.4510)	AISI 439 (430Ti*)	A A + CD**	250-350 500-800	450-550 600-900	25-30 5-20	150-200 HB ---
X6CrMo17-1 (1.4113)	AISI 434	A	300-400	480-580	22-28	150-200 HB
X2CrMoTi17-1 (1.4513)	AISI 436	A	250-350	420-520	25-30	140-180 HB
X2CrMoTi18-2 (1.4521)	AISI 444	A	350-450	480-580	25-30	160-220 HB
X2CrTiNb18 (1.4509)	441*	A	250-350	450-550	20-25	150-200 HB
X10CrAlSi25 (1.4762)	AISI 446	A	350-450	550-650	12-18	170-230 HB
X2CrMoTi29-4 (1.4592)	29-4C*	A	450-550	560-660	22-27	150-200 HB

Table 6 Mechanical Properties of some of the main ferritic stainless steels [17]

Even though Ferritic stainless steel can afford a competitive corrosion resistance level at a lower cost, some of their drawbacks are to be stated. These steels are not so useful at sub-ambient temperatures due to their low toughness that could be also an obstacle when thickness above 1.5 mm is needed, their ductility is also an issue when higher elongations (above 30%) are requested [18]. However, their high temperature embrittlement could match the requested level if and only if they are well alloyed.

EN Designation	AISI approximate correspondence	Mass volume [kg/dm <sup>3</sup> ]	Specific heat at 20°C [J·kg <sup>-1</sup> ·K <sup>-1</sup> ]	Electrical resistance at 20°C [W·mm <sup>2</sup> ·m <sup>-1</sup> ]	Thermal conductivity [W·m <sup>-1</sup> ·K <sup>-1</sup> ]	Linear thermal expansion [10 <sup>-6</sup> ·K <sup>-1</sup> ]		Modulus of elasticity [GPa]	
						from 20°C to 100°C	from 20°C to 200°C	to 20°C	to 200°C
X2CrTi12 (1.4512)	AISI 409	7,7	460	0,60	25	10,5	11,0	220	210
X6Cr17 (1.4016)	AISI 430	7,7	460	0,60	25	10,0	10,0	220	210
X6CrMoS17 (1.4105)	AISI 430F	7,7	460	0,70	25	10,0	10,5	220	210
X3CrTi17 (1.4510)	AISI 439 (430Ti*)	7,7	460	0,60	25	10,0	10,0	220	210
X6CrMo17-1 (1.4113)	AISI 434	7,7	460	0,70	25	10,0	10,5	220	210
X2CrMoTi17-1 (1.4513)	AISI 436	7,7	460	0,70	25	10,0	10,5	220	210
X2CrMoTi18-2 (1.4521)	AISI 444	7,7	430	0,80	23	10,4	10,8	220	210
X2CrTiNb18 (1.4509)	441*	7,7	460	0,60	26	10,0	10,0	220	210
X10CrAlSi25 (1.4762)	AISI 446	7,7	500	1,10	17	---	10,5	220	210
X2CrMoTi29-4 (1.4592)	29-4C*	7,7	440	0,67	17	11,5	---	220	210

Table 7 Physical Properties of some of the main ferritic stainless steels [From EN 10088] [17]

### 1.3.2.3. Role of Niobium in the Ferritic Stainless Steel Family

The Fe-Cr equilibrium diagram is the starting point to an important discussion about the phase stabilization and transformation along the manufacturing and application process of stainless steels. The first point that needs to be observed is that for materials with low level of Cr (< 13%) (for example: AISI 409), the gamma loop (austenitic range) is active from the temperatures between 912°C and 1394°C, so if a material is welded or exposed to high this range of temperature in these conditions it can become brittle due to the Martensite formation in the grain boundaries. Working with materials with high levels of Cr, such as DIN 1.4509 (AISI 441),

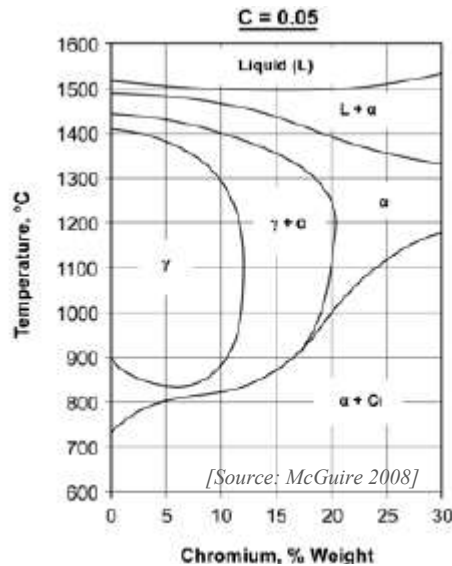


Figure 28 Fe-Cr binary section of Fe-C-Cr ternary diagram [17]

working with low levels of Carbon and Nitrogen and also adding stabilizing elements such as Niobium and Titanium is mandatory for today's quality assurance.

Thus, for applications where high temperatures are of primer importance, such as modern exhaust manifolds, this particular issue is to be considered and solved by the addition of stabilizing elements, such as Niobium that will keep the structure completely ferritic in the entire temperature range from melting to ambient. The phenomenon of carbide precipitation is known

as “sensitization” that would be explained in details in the next chapter, highlighting the positive impact of Nb on preventing the intergranular corrosion and chromium depletion especially in the welded areas.

The grade DIN 1.4509 (AISI 441) alloyed with niobium is of special importance in the Exhaust system applications as it meets wider range of requirements, in particular, it could be formed into complex shapes and joined using the most conventional techniques such as welding, and now it is considered as a competitive of the Austenitic grade 304 showing cost saving due to the absence of nickel [19].

The amount of Niobium to be added depends mainly on the carbon and nitrogen contents due to the formation of carbides (NbC) that will provide the creep resistance at high temperature in addition to the pitting corrosion resistance and the stabilizing effect for which the formation of chromium carbides is totally inhibited. Hence, when the contents of Nitrogen and carbon are optimized for a specific application, the amount of niobium is found to be 6 to 8 times the total amount of C+N [20].

The stabilization offered by Niobium has also a positive impact on the deep drawing, as it eliminates the “stretch strains” which is a small undulations elongated in the tensile directions (also known as worms) [19], as well as it decreases the sensitivity of the steels against roping (known also as ridging). In other words, the deep drawing performance is determined by the LDR “limit drawing ratio” that is correlated to the mean strain ratio that is, in turn, well improved by Niobium, making the ferritic grades show higher LDR than Austenitic, thus more suitable for deep drawing applications.

#### 1.3.2.4. Fields of Applications

Unlike martensitic stainless steels, Ferritic stainless steels are mainly available as steel sheets and strips that could be cold deformed (formed or pressed), and limited in the form of rods and bars. They are applied in the industrial environment as pipes, extruded parts, and in highly corrosive environments such as nitric acids, as well as household’s appliance, oil sectors and decorative elements.

Other grades could have further fields of application such as X2CrTi12 (AISI 409) used in the Automotive sector in manufacturing of exhaust manifold (due to their low thermal expansion and higher conductivity), catalytic converters, and exhaust pipes due to its increased plastic deformability and weldability on the cost of corrosion resistance. Hence, later in this study we will examine the presence of Niobium exactly in this field, and mark its superior advantages in meeting the demands of high temperatures and emission’s quality, for example considering the stabilized version X2CrTiNb18 (AISI 441).

X6CrMoS17 (AISI 430F) is used in the sector of solenoid valves and metal hardware obtained by metal cutting, X3CrTi17 is employed for parts requiring welding such as washing machine drums. It is also important to note that X10CrAlSi25 shows superior resistance to high temperatures up to 1100 °C, and the ability of employment in sulphurous environments [17].

### 1.3.3. Austenitic Stainless Steels

#### 1.3.3.1. Metallurgy

Austenitic Structure at ambient temperature is obtained when nickel content is added in a sufficient quantity (up to 8-9 %) that dominates the ferritic effect of the -at least 17%- chromium content in a relatively low carbon steel. The phase diagram is described by the ternary phase diagram shown in figure 30, it shows the absence of the  $\gamma$  to  $\alpha$  transformation resulting in an exclusive Austenitic structure with a chromium content 17-18% and nickel content 10-12% (or duplex if chromium content is increased up to 25% and nickel is lowered to 4-8%).

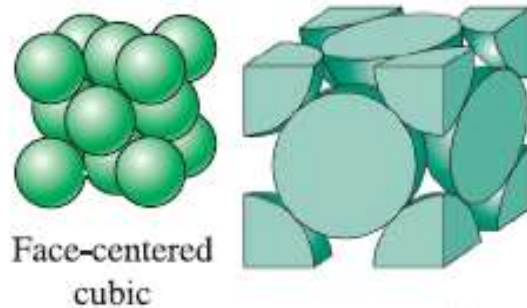
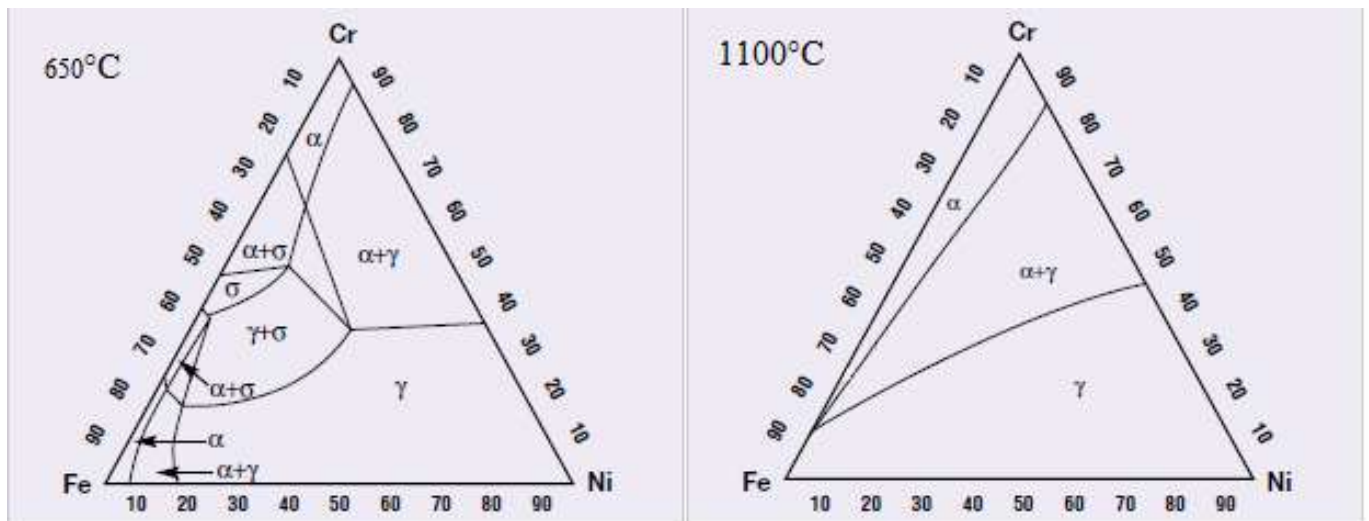


Figure 29 Face centered cubic crystalline structure [6,34]

The combination of Cr and Ni results in a Face-centered cubic lattice (FCC) having a total of four atoms per unit cube shown in figure 29, which makes it a more packed lattice compared to ferrite signifying the higher density. Such steels are highly resistive to corrosion and further



Source: High performance stainless steel by Curtis W. Kovach Technical marketing resources, Inc. Pittsburgh, PA.

Figure 30 Fe-Ni-Cr ternary phase diagram

Increasing this resistance could be achieved by further increasing the nickel content up to 11-12%, or 2-3% of Molybdenum [17] to compensate the relative high cost of nickel, keeping in mind that Carbon and other elements such as nitrogen or manganese also play the role of austenitic formers. In a similar manner to other families, various grades of desired properties could be obtained by varying the alloying elements and their percentage, table 8 shows some

examples of the chemical compositions of some Austenitic Steels. It is important to note that the addition of Molybdenum (Mo, a Chromium equivalent) helps in increasing the corrosion resistance, but has no impact on oxidation resistance, in order to improve the later issue, Silicon (Si) could be added.

EN symbolic designation	AISI approximate correspondence	%C	%Si	%Mn	%P	%S	%Cr	%Ni	%Mo	Other
X10CrNi18-8 (1.4310)	AISI 301	0,05-0,15	≤2,00	≤2,00	≤0,045	≤0,015	16,0-19,0	6,0-9,5	≤0,80	1
X8CrNiS18-9 (1.4305)	AISI 303	≤0,10	≤1,00	≤2,00	≤0,045	0,15-0,35	17,0-19,0	8,0-10,0	---	1, 2
X5CrNi18-10 (1.4301)	AISI 304	≤0,07	≤1,00	≤2,00	≤0,045	≤0,015	17,5-19,5	8,0-10,5	---	1
X2CrNi18-9 (1.4307)	AISI 304L	≤0,03	≤1,00	≤2,00	≤0,045	≤0,015	17,5-19,5	8,0-10,5	---	1
X6CrNiTi18-10 (1.4541)	AISI 321	≤0,08	≤1,00	≤2,00	≤0,045	≤0,015	17,0-19,0	9,0-12,0	---	3
X6CrNiNb18-10 (1.4550)	AISI 347	≤0,08	≤1,00	≤2,00	≤0,045	≤0,015	17,0-19,0	9,0-12,0	---	4
X8CrNi25-21 (1.4845)	AISI 310S	≤0,10	≤1,50	≤2,00	≤0,045	≤0,015	24,0-26,0	19,0-22,0	---	1
X5CrNiMo17-12-2 (1.4401)	AISI 316	≤0,07	≤1,00	≤2,00	≤0,045	≤0,015	16,5-18,5	10,0-13,0	2,00-2,50	1
X2CrNiMo17-12-2 (1.4404)	AISI 316L	≤0,03	≤1,00	≤2,00	≤0,045	≤0,015	16,5-18,5	10,0-13,0	2,00-2,50	1
X2CrNiMoN17-13-3 (1.4429)	AISI 316LN	≤0,03	≤1,00	≤2,00	≤0,045	≤0,015	16,5-18,5	11,0-14,0	2,50-3,00	5
X6CrNiMoTi17-12-2 (1.4571)	316Ti*	≤0,08	≤1,00	≤2,00	≤0,045	≤0,015	16,5-18,5	10,5-13,5	2,00-2,50	3
X1NiCrMoCu25-20-5 (1.4539)	904 L*	≤0,02	≤0,70	≤2,00	≤0,030	≤0,010	19,0-21,0	24,0-26,0	4,00-5,00	6
X1CrNiMoCuN20-18-7 (1.4547)	254 SMO*	≤0,02	≤0,70	≤1,00	≤0,030	≤0,010	19,5-20,5	17,5-18,5	6,00-7,00	7

Table 8 Chemical Composition of some Austenitic Stainless Steels [from EN 10088] [17]

The limited solubility of carbon in the  $\gamma$  phase is of special importance as it explains the certain existence of chromium carbide at ambient temperature that is a major issue to be avoided, it is marked that it occurs within the interval 450-900 °C being 700°C [21] as the most severe.

Other alloying elements could be added for other purposes, such as Sulphur to improve machinability by forming sulphides, Nitrogen improves resistance to corrosion and increase the mechanical strength as it is a strong austenitic element, and copper that improves the cold plastic deformability. For the grades that require enhanced machinability, a high level of controlled inclusions such as sulfides or oxy-sulfides should be kept, but this should be compromised with the corrosion resistance, as the pre-mentioned inclusions deteriorate the corrosion resistance.

### 1.3.3.2. Martensite Formation in Austenite

Martensite may form while Austenitic Stainless steel being cooled below room temperature, or as a result of cold working, this later is known as “strain induced” or “deformation induced” Martensite [21] and is formed at higher temperatures than the first one. Deformation induced Martensite further increases the strength resulting from cold working. Figure 31 shows the strain induced Martensite formation as a function of strain at various temperatures on the steel 304, it is clear that the lower is the temperature, the steeper is the curve even at low strain. Hence, Martensite formation is favored at low strains during low temperature working.

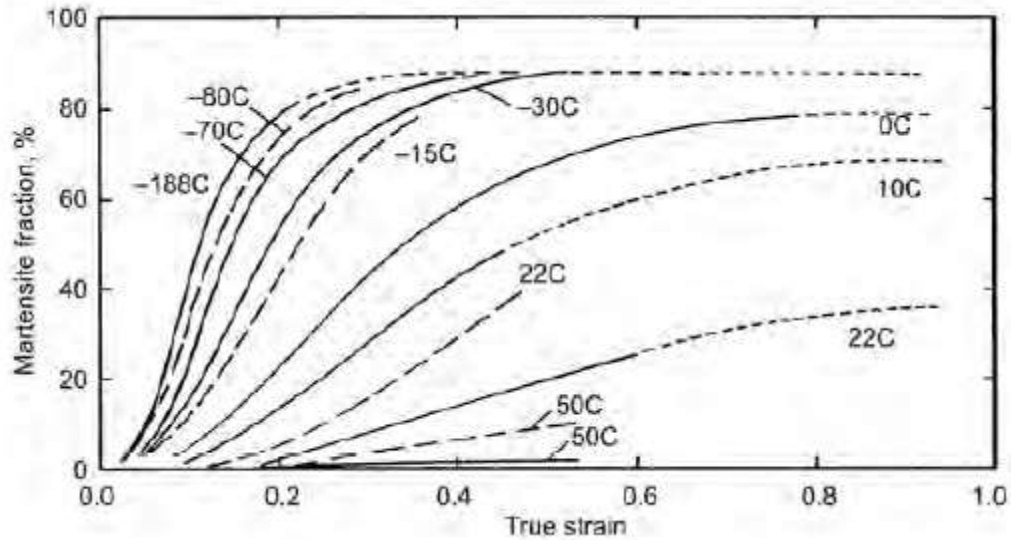


Figure 31 Strain induced Martensite formation as a function of strain at various temperatures [21]

### 1.3.3.3. Physical and Mechanical Properties

The physical properties of the austenitic stainless steels are particular and strongly related to its face-centered cubic lattice. In general terms, compared to ferritic stainless steels, it is found that the later has lower heat expansion, and higher thermal conductivity, thus upon exposure to temperatures, austenitic stainless steels expand more with limited heat transfer. Unlike ferritic stainless steel, the Austenitic category is characterized by the lack of magnetic behavior. Table 9 [17] shows the order of magnitude of the physical properties of some Austenitic grades. Austenitic Stainless steels do not have a clear yield point, but it is found that they start to deform at almost 40% of their yield, it can be said that the behavior is elastic below 50% of the yield, and a negligible plastic deformation occurs below 66% of the yield.

EN Designation	AISI approximate correspondence	Mass volume [kg/dm <sup>3</sup> ]	Specific heat at 20°C [J·kg <sup>-1</sup> ·K <sup>-1</sup> ]	Electrical resistance at 20°C [W·mm <sup>2</sup> ·m <sup>-1</sup> ]	Thermal conductivity [W·m <sup>-1</sup> ·K <sup>-1</sup> ]	Linear thermal expansion [10 <sup>-6</sup> ·K <sup>-1</sup> ]		Modulus of elasticity [GPa]	
						from 20°C to 100°C	from 20°C to 200°C	to 20°C	to 200°C
X10CrNi18-8 (1.4310)	AISI 301	7,9	500	0,73	15	16,0	17,0	200	186
X8CrNiS18-9 (1.4305)	AISI 303	7,9	500	0,73	15	16,0	16,5	200	186
X5CrNi18-10 (1.4301)	AISI 304	7,9	500	0,73	15	16,0	16,5	200	186
X2CrNi18-9 (1.4307)	AISI 304L	7,9	500	0,73	15	16,0	16,5	200	186
X6CrNiTi18-10 (1.4541)	AISI 321	7,9	500	0,73	15	16,0	16,5	200	186
X6CrNiNb18-10 (1.4550)	AISI 347	7,9	500	0,73	15	16,0	16,5	200	186
X8CrNi25-21 (1.4845)	AISI 310S	7,9	500	0,85	15	---	15,5	---	---
X5CrNiMo17-12-2 (1.4401)	AISI 316	8,0	500	0,75	15	16,0	16,5	200	186
X2CrNiMo17-12-2 (1.4404)	AISI 316L	8,0	500	0,75	15	16,0	16,5	200	186
X2CrNiMoN17-13-3 (1.4429)	AISI 316LN	8,0	500	0,75	15	16,0	16,5	200	186
X6CrNiMoTi17-12-2 (1.4571)	316Ti*	8,0	500	0,75	15	16,5	17,5	200	186
X1NiCrMoCu25-20-5 (1.4539)	904 L*	8,0	450	1,00	12	15,8	16,1	195	182
X1CrNiMoCuN20-18-7 (1.4547)	254 SMO*	8,0	500	0,85	14	16,5	17,0	195	182

Table 9 Physical properties of some Austenitic grades [from EN 10088] [17]

In what concerns the mechanical characteristics, the austenitic matrix of such family is characterized by high deformability, resulting in tensile strength  $R_m$  up to 550-650 MPa and yield stress  $R_{p0.2}$  up to 280 MPa, in contrast, it is a high ductile, in which elongation at breakage may reach 50%, and a hardness number between 160-200 HB [21]. The order of magnitude of the mechanical properties is show in table 10. Further hardening is possible and tensile strength  $R_m$  values may exceed 1500 MPa, as well as yield strength  $R_{p0.2}$  may reach 1600 MPa if the product is cold worked such as rolling or drawing. It is also important to mark that this category is highly resistant to brittle fracture, as its matrix keeps it tough even at very low temperatures.

Compared to ferritic stainless steels, Austenitic are less resistant to cyclic oxidation, the reason behind this drawback is their higher thermal expansion coefficient that leads to spall the passive layer, they are more sensitive to stress corrosion cracking (this issue will be further discussed later), and they have lower fatigue endurance limit (30% of their tensile strength, on the other hand it is up to 60% in ferritic), consequently their thermal fatigue behavior degrades.

EN Designation	AISI approximate correspondence	Metallurgic condition	$R_{p0.2}$ [MPa]	$R_m$ [MPa]	A [%]	Hardness
X10CrNi18-8 (1.4310)	AISI 301	Solubilised	250-300	600-750	40-50	170-220
X5CrNi18-10 (1.4301)	AISI 304	Solubilised	220-270	550-650	45-55	160-210
X8CrNiS18-9 (1.4305)	AISI 303	Solubilised	200-250	520-630	35-45	170-220
X2CrNi18-9 (1.4307)	AISI 304L	Solubilised	200-250	520-630	45-55	160-210
X6CrNiTi18-10 (1.4541) X6CrNiNb18-10 (1.4550)	AISI 321 AISI 347	Solubilised + Stabilized	230-280	550-650	40-50	170-220
X8CrNi25-21 (1.4845)	AISI 310S	Solubilised	250-300	550-650	40-50	150-200
X5CrNiMo17-12-2 (1.4401) X2CrNiMo17-12-2 (1.4404)	AISI 316 AISI 316L	Solubilised	250-300	550-650	40-50	160-210
X6CrNiMoTi17-12-2 (1.4571)	316Ti*	Solubilised + Stabilized	250-300	550-650	40-50	160-210
X2CrNiMoN17-13-3 (1.4429)	AISI 316LN	Solubilised	290-340	600-700	40-50	190-240
X1NiCrMoCu25-20-5 (1.4539)	904 L*	Solubilised	230-280	550-650	35-45	170-220
X1CrNiMoCuN20-18-7 (1.4547)	254 SMO*	Solubilised	300-350	700-800	35-45	200-250

Table 10 Mechanical Characteristics of some Austenitic Stainless Steel [17]

#### 1.3.3.4. Role of Niobium in Austenitic Steels

In correspondence to the phenomenon of sensitization due to the limited solubility of carbon in the  $\gamma$  phase, Niobium is added, followed by a stabilization heat treatment, consequently Nb is considered as a stabilizing element that will hinder the formation of chromium carbides solving by that the chromium depletion problem. It form carbides with solubility that follows the following equation [21]:

$$\bullet \quad \text{Log [Nb] [C]} = + 4.55 - 9350/T \quad \text{Eq. 1.6}$$

where T is in Kelvin.

However, Nitrogen also seeks for the available Niobium, thus the amount of niobium to be added depends mainly on the amount of Carbon and Nitrogen contents, so that it combines in a stoichiometric manner. For this purpose, it is found that the amount of Niobium should exceed eight times the carbon plus nitrogen content.

The precipitation that results from the addition of niobium, in other words the dissolved Niobium in the matrix leads in to an increase in the hardness, a study were carried out comparing 4 samples (with 0%, 0.5%, 1, and 1.89% Nb content respectively) and the result is shown in figure 32. The increase in hardness can be explained by the fine grains, high vacancy super-saturation, and Niobium solid solution hardening. In the same figure, the effect on different properties is shown. Note that yield strength (YS) and tensile strength (TS) are measured in N/mm<sup>2</sup>, while elongation is measured in % [22].

Another studied effect of Niobium on the microstructure is shown in the figure 33, where it is found that niobium addition creates a continuous intermetallic phase called “the Laves phase” that is proportional to the amount of Nb added [22]. This Laves phase precipitates first at the grain boundary, then at incoherent twin boundaries, coherent twin boundaries and grain interior respectively, these laves explain the mitigation of crack propagation in the Nb alloyed Stainless steels. Although these Laves are desired and beneficial, they have drawbacks in terms of ductility, and the deterioration in ductility is due to the solid state of these laves.

In addition, Niobium has a considerable effect on the pitting corrosion, due to the increase of Nb content in the matrix which causes “beneficial disorders” increasing corrosion resistance by the formation of Niobium Oxides, which in comparison to Chromium oxides, offer a higher protection [22].

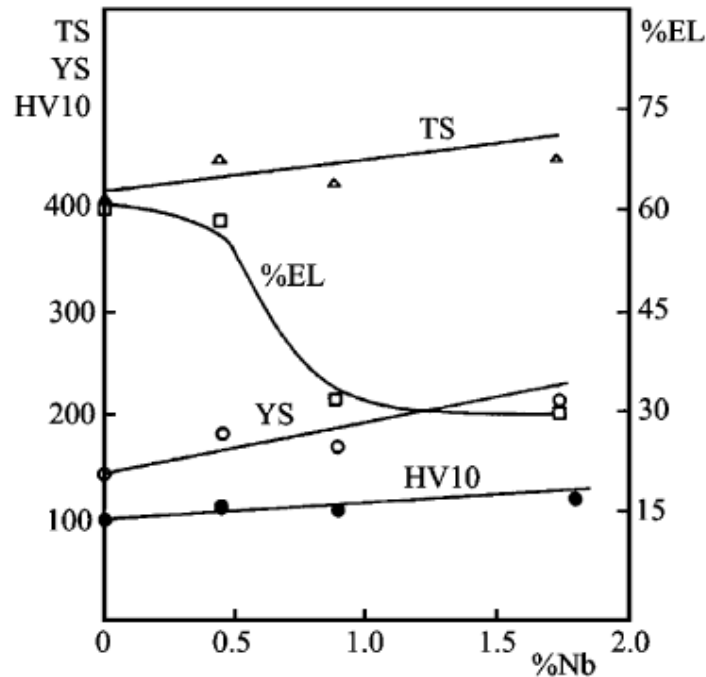


Figure 32 HV, YS, TS and EL% as function of Niobium in cast steels [22]

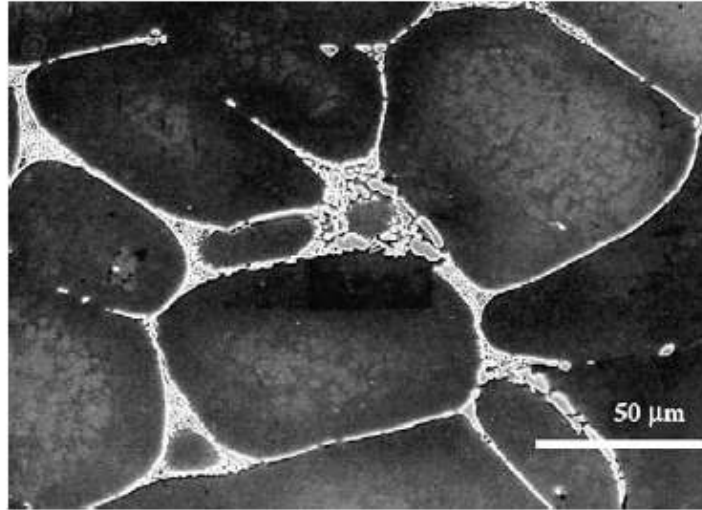


Figure 33 a sample with 2 wt% Nb under electron Microscopy [22]

From metallurgical point of view, a study is carried to figure out the effect of niobium on Austenitic stainless steels [22], the used samples contain 0.5%, 1% and 2% Nb by weight. The effect on the solidification is showed in figure 34 where the liquidus and solidus lines are depressed, enlarging the solidification interval.

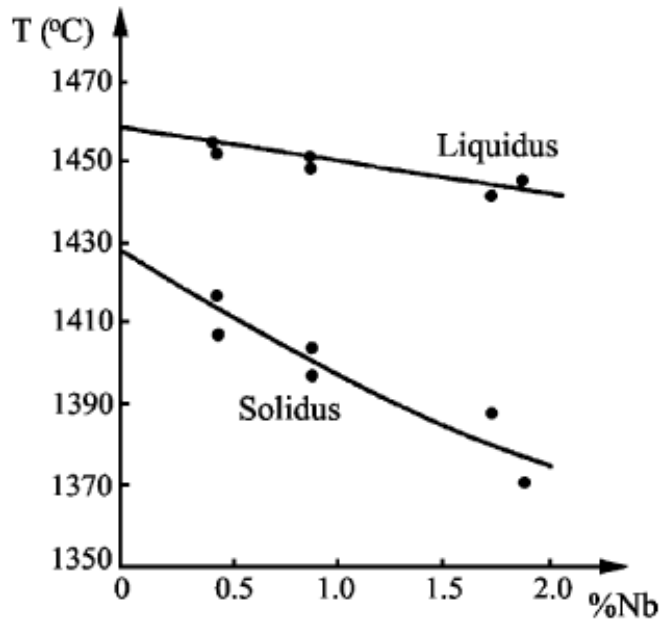


Figure 34 Niobium effect on solidification [22]

#### 1.3.3.5. Field of Applications

Starting with the most popular grade known as AISI 304, it is used in many fields such as industrial, civil, military, etc... due to its superior corrosion resistance that exceeds that of other competitive families of martensitic and austenitic. However Austenitic grades in general are widely employed in various applications such as boilers, elevators, domestic utensils, sinks, chemical, petrochemical, and nuclear industries, as well as in the production of canned food. The lack of magnetism in Austenitic stainless steels makes them an ideal material for military weapons, and their high toughness at temperatures close to absolute zeros implies their employment in the cryogenic field and liquefied gas transport fields.

On the other hand, considering the stabilized versions of the grades, such as AISI 321 and AISI 347 where Titanium and Niobium are introduced, to be of special importance due to their higher corrosion resistance and greater mechanical properties compared to the ordinary Austenitic stainless steel grades, in which they are used in applications where welding is necessary and the part is subjected to high temperatures, consequently making them a highly competitive material for exhaust manifold manufacturing.

Other grades are also employed in the automotive field for the manufacturing of conveyor belts, springs, and load bearing structures such as AISI 301, and the grade X8CrNiS18-9 from which small parts are manufactured (screws, nuts, pins, bushings, etc...).

# CHAPTER 2

## AUTOMOTIVE REVISION

### Introduction

Consider the cycle of a 4 stroke internal combustion engine starting by the intake of the fuel and air mixture (or only air, depending on the injection type), then the compression stroke followed by the combustion of the fuel and air mixture resulting in hot combustion gases that include carbon dioxide, water vapor and some other pollutants, then the expansion stroke pushing the piston downwards causing the crankshaft to rotate, and finally the exhaust stroke during which these hot gases are expelled outside the combustion chamber to the atmosphere passing by exhaust system. Hence, the exhaust system is defined as a system that carries the exhaust gases from the cylinder through the exhaust manifold, treating them to reduce the toxic emissions employing a catalytic converter for this purpose, and expelling them to the ambient atmosphere through the tail pipe. In this chapter we will recall the history of the exhaust systems, the way they developed, and we will go deeper in stating and explaining their main problems.

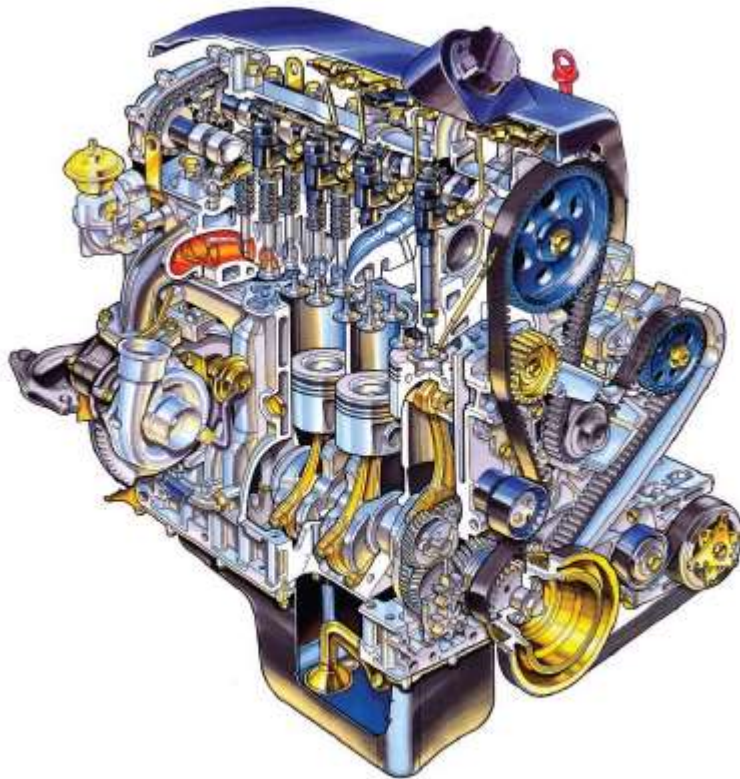


*Figure 35 Four stroke internal combustion engine*

## 2.1. History of Exhaust Systems

Over the years, the Exhaust System's job has grown and it has been given more responsibility, it started from guiding the toxic exhaust away from passenger's compartment, to damped the noise [23], and finally to reduce the toxic emissions.

*In 1881* the United States realized that an excessive amount of smoke is expelled in Chicago and Cincinnati and they issued a law stating that this is an unacceptable situation, and gradually, all the other states started to follow the laws. After the World War II, the automotive sector was considered as a major contributor to the smog and it started to be questioned, not only in the United States, but all over the world.

*In 1962* the Frenchman Eugene Houdry patented his innovation, "The catalytic muffler" which is a silencer mounted in the exhaust system in order to reduce noise, making noise reduction as the exhaust system's main function by that time.

*In 1963* the crankcase forced ventilation device was launched as the first exhaust purifying device used in passenger cars, it was based on re-introducing the leaking exhaust gas into the intake manifold and burning it again hindering by this action its escape to the atmosphere.

*In 1968* the first regulations was published restricting the liner exhaust, the reason that pushed the car makers to take actions for the sake of decreasing the emitted hydrocarbons and carbon monoxide such as reducing the compression ratio, increasing idle speed, preheating the intake, and injecting air in the exhaust manifold to complete the combustion of such gases. Unfortunately, the downside of these actions where the increase in both fuel consumption and the nitrogen oxides (known as Nox) emissions.

*In 1970* the Environmental Protection Agency in the USA had set rules as an action to clean the air, and the available equipment were not sufficient to meet the congress regulations by that time, the reason why car manufacturers started investing in new technologies. During this year, a catalytic process invented by a Frenchman Eugene Houdry was able to double the amount of useable oil produced from crude oil. Using his invention's technology he introduced a catalytic converter for automobile mufflers that was able to reduce the CO<sub>2</sub> and HCs emissions known as catalytic muffler patented in 1962.

*In 1973* the Exhaust Gas Recirculation (EGR) valves was introduced as a response to the regulations that considered the emissions of the nitrogen oxides NO<sub>x</sub>.

*In 1975* the limits on the CO<sub>2</sub> and HC emissions where further lowered, making it obligatory to include an oxidizing converter, with noise regulations came into effect.

*In 1981* more stringent limits were set for the NO<sub>x</sub> emissions. These limits were met by the introduction of a ternary catalytic converters. Oxygen sensors and closed circuit controls were also introduced to maintain a normal operation.

Henceforth, the Exhaust system by now has included the exhaust manifold, the catalytic converter and the muffler. However, to meet the increasingly tightened restrictions, more

attention is made to improve this system such as relocating the catalytic converter closer to the engine and choosing a higher heat conductive material for a faster light-off, or even using two converters using various layouts and catalysts.

### 2.1.1. Exhaust System Components

As mentioned before, the exhaust system is made up of several consecutive components in which the exhaust gases and the sound waves (pressure waves), escaping from the cylinders through the exhaust valves, pass through before they are expelled into the environment. During their passage, 4 main roles are covered [24]:

- 1- Collection of exhaust gases
- 2- Purification of exhaust gases
- 3- Silencing of exhaust noise
- 4- Getting rid of the exhaust gases

In order to execute these operations, the following components are employed [25]: Exhaust manifold, header pipe, Catalytic converter, intermediate pipe, muffler, and tailpipe, and they are divided into two ends: the hot end characterized by temperatures above 600°C including the manifold and the catalytic converter, this section suffers from thermal fatigue and oxidation mainly and salt corrosion at high temperatures, and the cold end where temperatures are below 600°C such as the muffler and the tail pipe which mainly suffer from corrosion due to condensation, and vibration..

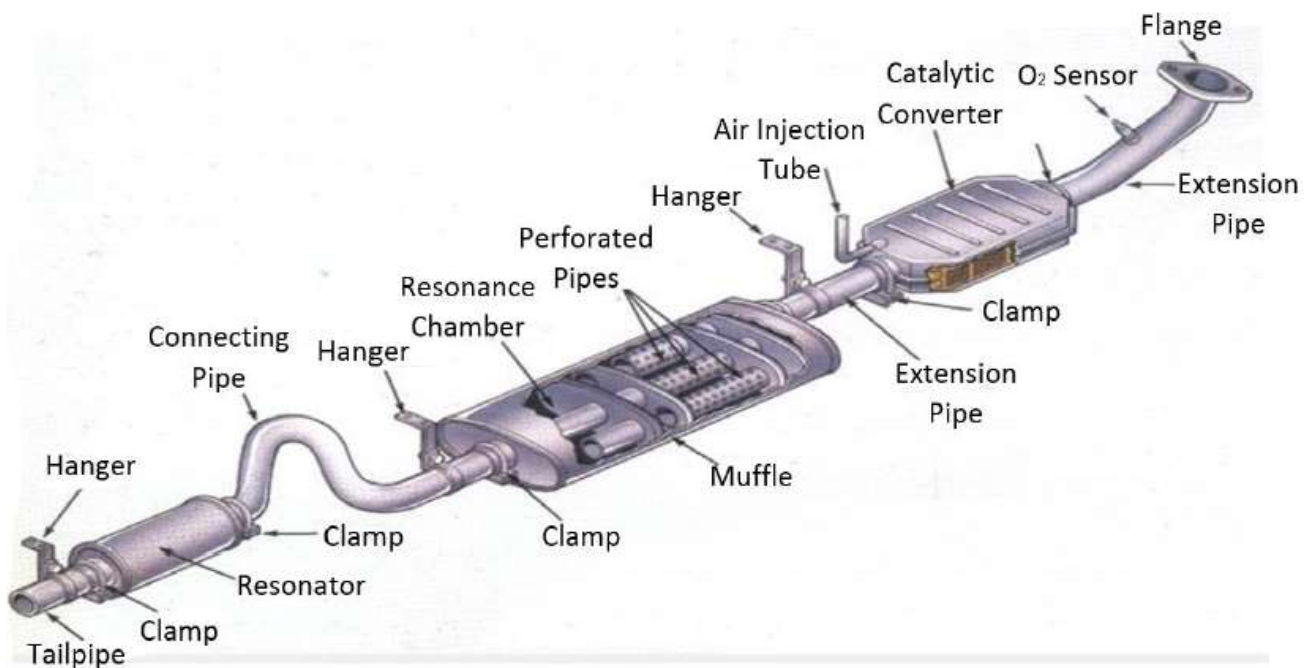


Figure 36 Typical view of an Automotive Exhaust System [39]

### 2.1.1.1. Exhaust Manifold

The exhaust manifold is the part of the engine that connects the cylinder head to the rest of the exhaust system, its main role is to receive the combustion gases and deliver them to the exhaust system to be expelled in naturally aspirated engines, or to the turbocharger in turbocharged engines. Hence, it is in a direct contact with the post-combustion hot gases that signifies the employment of a material which is able to resist this high temperature and its severe consequences such as oxidation resistance, and thermo-mechanical fatigue, this material was chosen to be cast iron. However, nowadays Ferritic and Austenitic Stainless steels are replacing cast iron in order to meet the trending requirements, this would be further discussed in this chapter. Different manifold layouts could be realized considering several factors such that the number of cylinders and their firing order, Turbochargers, front/back exhaust, back pressure, and packaging within the engine compartment which requires a material that has good formability such as press forming and weldability.

In addition, the composition of the exhaust gases should be taken into consideration to avoid the possible chemical reactions between the gases and the component. Even though the products of combustion are carbon dioxide, water vapor, and other pollutants, however the composition of such pollutants differs as it could be the product of diesel, petrol, or natural gas.

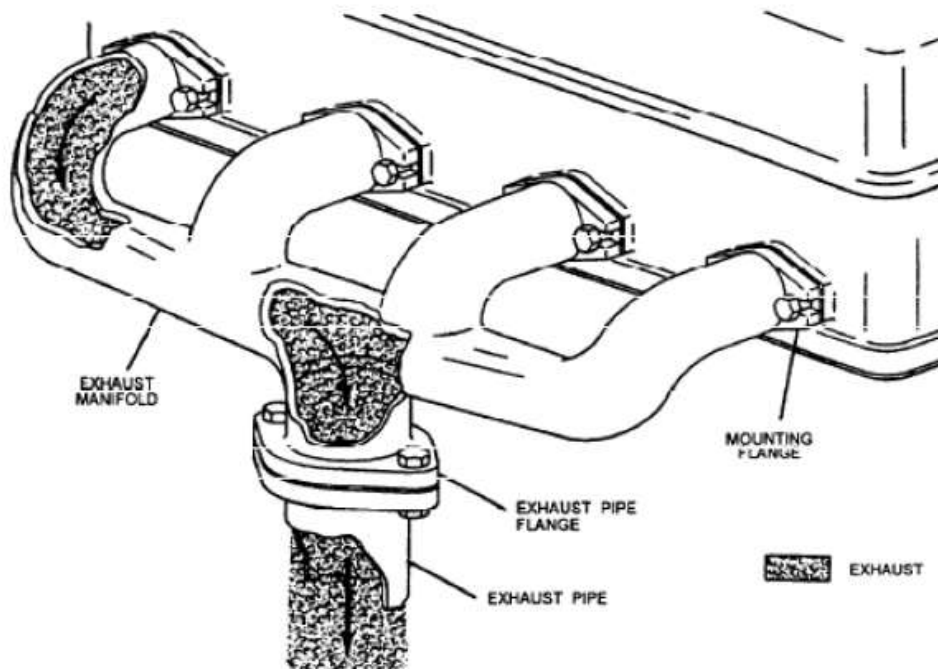


Figure 37 schematic representation of a typical Exhaust Manifold [25]

### 2.1.1.2. The Catalytic Converter

Even though the theoretical products of the combustion are water vapor and carbon dioxide, in fact the combustion in the Internal Combustion Engine (ICE) is incomplete, hence many factors lead to the formation of other toxic gases such as Carbon monoxide (CO), Hydrocarbons (HC), Nitrogen oxides (NO and NO<sub>2</sub>) known as NO<sub>x</sub>, and particulate matter [26]. Considering the dangerous effects of these emissions on humans and the environment, regulations has been growing and becoming tighter with time, requiring the invention of a component that helps these gases to further oxidize into CO<sub>2</sub>, H<sub>2</sub>O and N<sub>2</sub>. Different technologies have been developed for such purpose such as the three way catalyst, adsorption, traps and filtration [26p]. However, the three way Catalytic Converter (TWC) comes to be the most effective solution, as when it reaches the light-off temperature 300°C-400°C, its optimum performance is achieved in a narrow window where the fuel to air ratio (known as  $\alpha$  in most of the books) is almost stoichiometric. Figure 38 shows the efficiency of the catalytic converter as function of Air to fuel ratio in reducing the toxic emissions [26] for spark ignition engine\*.

The CO and HC are oxidized to CO<sub>2</sub> and H<sub>2</sub>O, however NO has to be reduced using CO or H<sub>2</sub>. Some possible NO reactions are [26]:

- $\text{NO} + \text{CO} \rightarrow \frac{1}{2} \text{N}_2 + \text{CO}_2$  **Eq.2.1**
- $2\text{NO} + 5\text{CO} + 3\text{H}_2\text{O} \rightarrow 2\text{NH}_3 + 5\text{CO}_2$  **Eq.2.2**
- $\text{NO} + \text{H}_2 \rightarrow \frac{1}{2} \text{N}_2 + \text{H}_2\text{O}$  **Eq.2.3**
- $2\text{NO} + 5\text{H}_2 \rightarrow 2\text{NH}_3 + 2\text{H}_2$  **Eq.2.4**

*\*Spark Ignition engine and compression ignition engine use different fuels having different chemical composition, thus we have to differentiate them considering that the entire combustion process and consequently, temperatures and chemical composition of the gases are different, for further details about each, please refer to reference 25.*

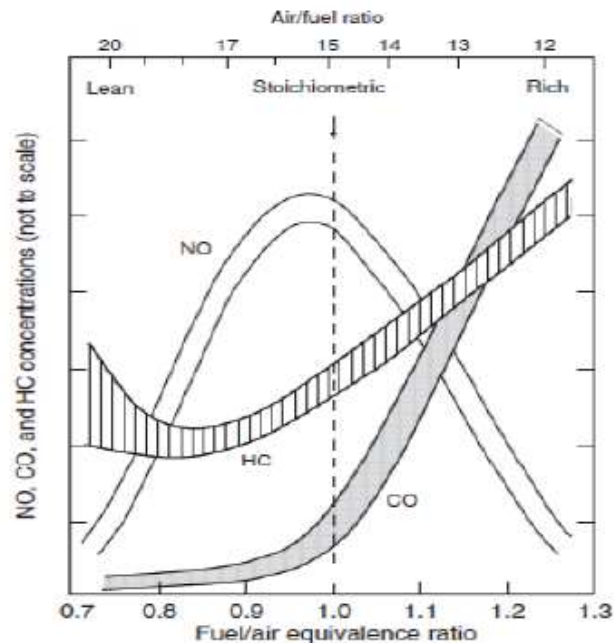


Figure 38 Catalytic converter efficiency as a function of Air to fuel ratio of a spark ignition engine [27]

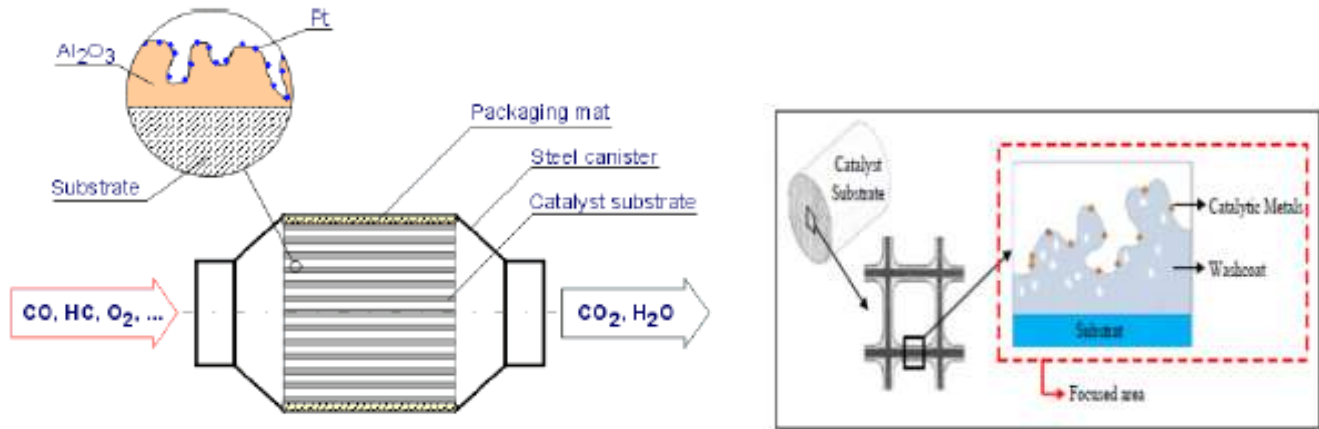
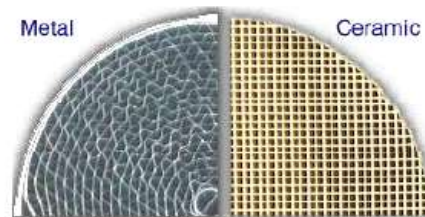


Figure 39 Three way Catalytic Converter [26 ,27]

Catalytic converters are made up of the shell, substrate with monolith or honeycomb structure. The main function of the shell is to hold the catalytic converter internal parts, hence it must be strong and able to resist vibration, high temperatures and their consequences. The washcoat is about 90%  $\gamma$ - $\text{Al}_2\text{O}_3$ . The substrate could be metallic or ceramic as shown in figure 40, however, metallic is preferred for high temperature applications such as FeCrAl [27]. Inner and outer cone are mainly to regulate the flow keeping their uniformity index [27].



Monolithic catalyst

Figure 40 Metallic/Ceramic Monolithic converter [26]

Catalytic converters uses precious metals such as Platinum (Pt), Palladium (Pd), and Rhodium (Rh) to play the role of catalyst, thus speeding up the oxidation of the emissions without being consumed. They could be combined in different quantities depending of the application and the chemical composition of the emissions [27]. It is also important to mention that the metallic substrate of the catalytic converter could be made up of Fe-Cr alloys that shows advantages in terms lower backpressure, thin walls and ability to resist high temperature if close coupled.

Talking about the emissions, it is very important to highlight the periods during which the engines emits the most, apart from abnormality, the cold start is the first major emission contributor because it runs with rich condition (more fuel than air) to increase the temperature of the engine, as well as the catalytic converter is not working during the cold start because the

light-off temperature has not been reached yet. For such reasons, the material of the exhaust manifold and its location are game changing points in order to meet the stringent regulations.

Figures 41 and 42 show some possible locations of the catalyst in different layouts.

In addition, Oxygen storage materials are used, such as Cerium and Zirconium. These elements help in keeping a stoichiometric ratio achieved chemically, i.e. trapping oxygen when then reaction is fuel-lean, and releasing it when operating in fuel-rich conditions, hence minimizing the fluctuations associated with the lag of the closed loop feedback by the oxygen sensor. Taking Cerium as example:

- Fuel rich condition, Oxygen releasing:  $2\text{CeO}_2 + \text{CO} \rightarrow \text{Ce}_2\text{O}_3 + \text{CO}_2$
- Fuel-lean condition, Oxygen capturing:  $\text{Ce}_2\text{O}_3 + \text{O}_2 \rightarrow 2\text{CeO}_2$

Hence, Ceria  $\text{CeO}_2/\text{Ce}_2\text{O}_3$  stabilizes the partial pressure of oxygen at the surface of the catalyst, it was used before the benefits of Zirconium addition was found in  $\text{CeZrO}$  that showed better thermal stability and reducibility, and Yttrium added for its benefits in increasing the oxygen vacancy concentration. As to be shown in Chapter 3, Niobium has proven as an element that increases the Oxygen Storage Capacity (OSC) when added to Cerium and Zirconium, and it performed better than other elements such as Nd and Pr.

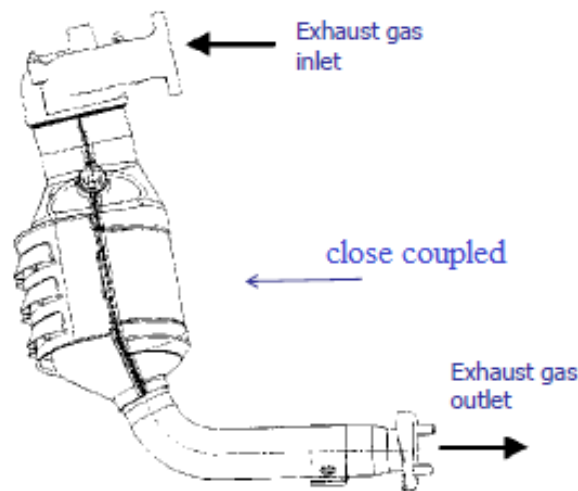


Figure 41 Close coupled configuration [26]

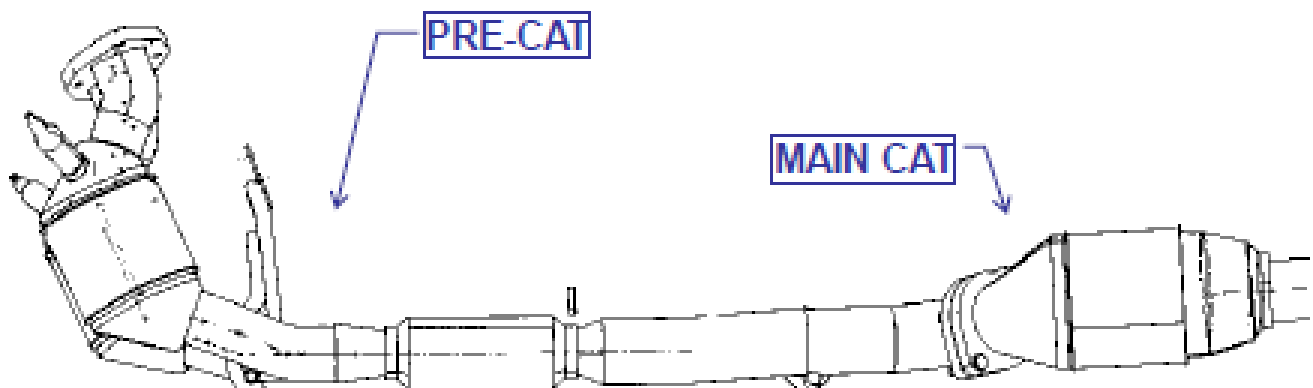


Figure 42 Pre catalyst + Underfloor Catalyst configuration [26]

### 2.1.1.3. Muffler

The main role of the muffler is to reduce the exhaust noise emission, defined as unwanted sound, by breaking the sound waves before expelling the gas to the environment. By definition, sound is a pressure wave formed from pulses of alternating high and low pressure air generated by the exhaust valves operation. In general, the pressure waves are broken by forcing the gas to pass by a series of chambers as shown in figure 43. There are two types of mufflers, known as reactive and absorptive. The objective is to choose the muffler that does its job effectively maintaining low back pressure, adequate insertion loss, and durability [28].

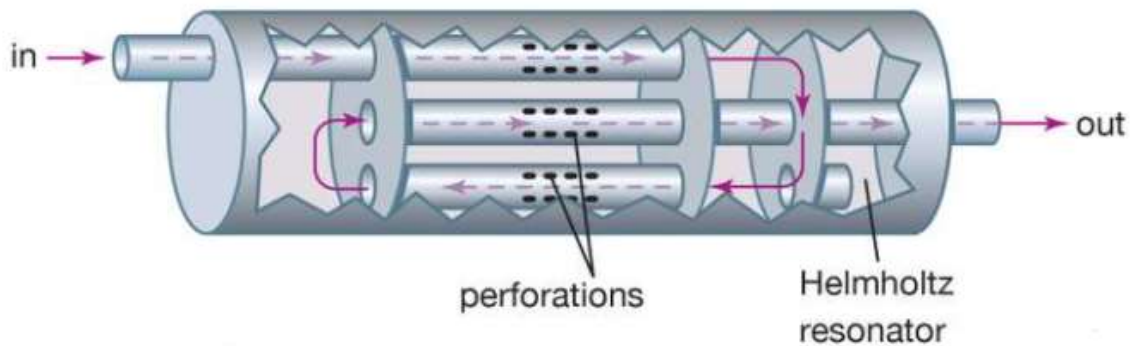


Figure 43 pathway of the exhaust gas in a muffler [80]

*NB: the purple arrows in figure 43 indicate the pathway of the exhaust gas. This type of mufflers is called reverse muffler due to the reverse flow of the exhaust gas before being expelled. Other types such as chamber mufflers features lower back pressure but less effective in noise cancellation.*

In reactive mufflers, are based on the phenomenon of destructive interference. The gas flows into the first expansion chamber as shown in figure 45 where the pressure waves are forced to scatter through the drilled surface, hence cancelling out themselves by destructive interference which occurs when a reflected wave of equal amplitude and 180 degree phase collide with the

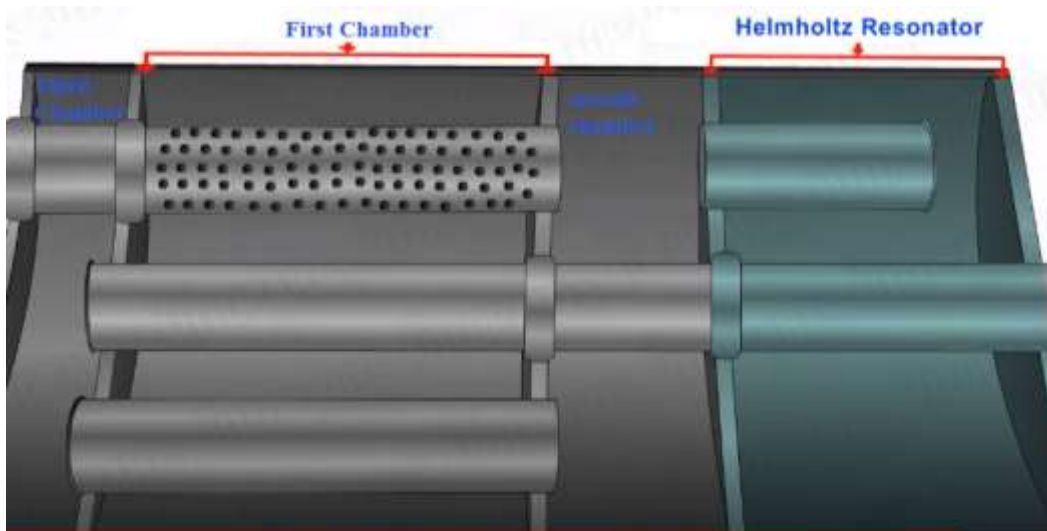


Figure 45 Chambers of typical muffler [80]

transmitted wave. Hence, the discontinuities and geometrical changes are realized so that accomplish the desired reflection. More intense waves reach the second chamber where they are destroyed due to friction upon hitting the wall. The strongest waves are able to pass both chambers and arrive to the resonator addressed as “Helmholtz Resonator” where the wave hits the wall and bounce back generating an opposite sound wave having the same frequency as shown in figure 46. This phenomenon causes the sound waves to be cancelled by mitigating their peaks. The only drawback of such mufflers is their higher back pressure compared to the absorptive one.

Before flowing out through the tail pipe, the gas with the sound waves are directed to flow through the third chamber.

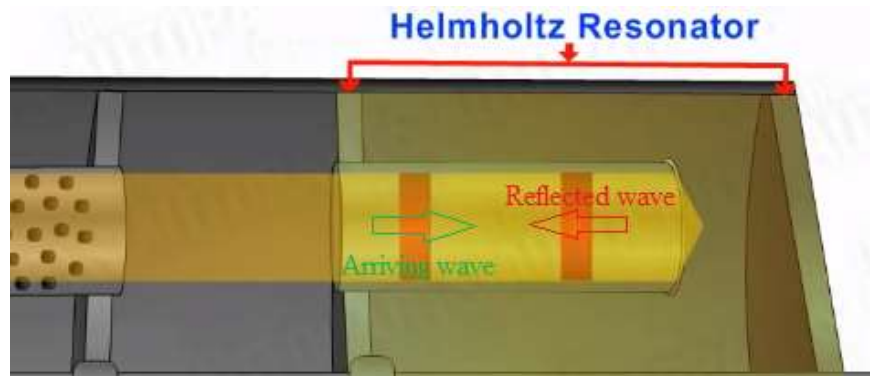


Figure 46 Helmholtz resonator [80]

Absorptive mufflers are based on dissipation phenomenon, where absorptive material is used so that the energy of the sound waves is converted into heat. A typical absorptive muffler is shown in figure 47, the perforated pipe is separated from the steel case by the absorptive material. They are better from back pressure point of view, however they are less effective in reducing noise [28].

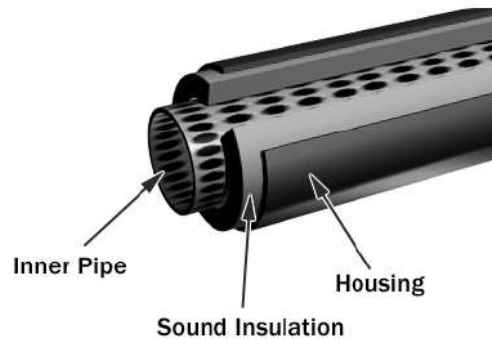


Figure 47 Absorptive Muffler [28]

#### 2.1.1.4. Pipes:

Two different pipes are used, the intermediate pipe settling in the hot end and connecting the components there, these pipes should show good ductility, weld ability, good thermal properties and corrosion resistance, and the second type, i.e. the tail pipe which is in the cold end and it is mainly to let the gases out.

## 2.1.2. European Regulations for Emission Limits

The stringent demands on lowering emissions has not been set only on toxic emissions such as HC and CO, however it also set limits on the greenhouse gases such as CO<sub>2</sub>. Through the years, Europe has updated its regulation making them more and more stringent as shown in figures 58.

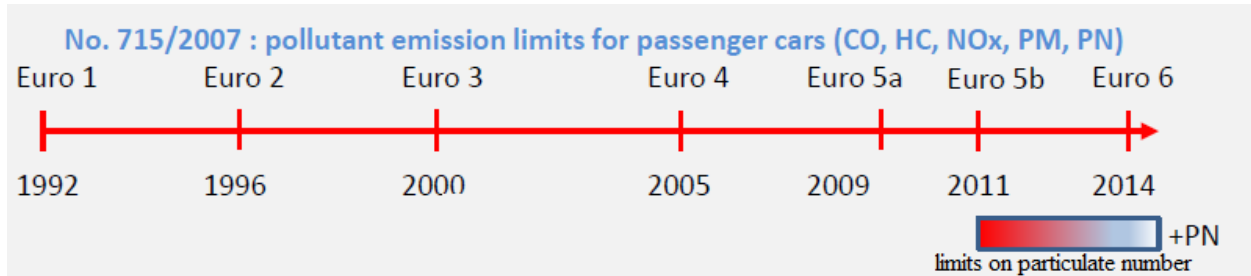


Figure 48 development of European regulations through the years [29]

With each new regulation, the limits are becoming more stringent, demanding new technologies, materials, and layouts. Figure 49 shows the trend of CO<sub>2</sub> from the year 2000 up to present, with the future vision in Europe and across the world, as well as figure 50 shows the trend of limits of toxic emissions.

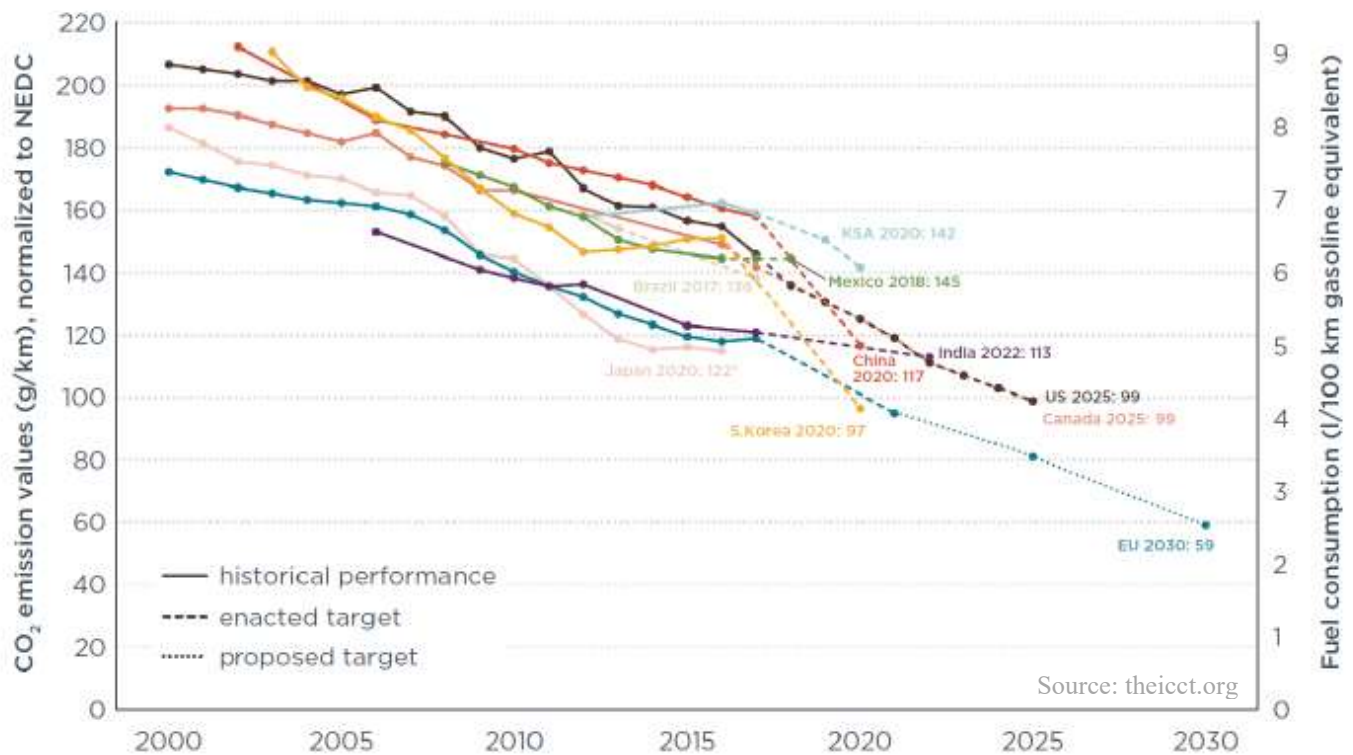


Figure 49 CO<sub>2</sub> limits from 2000 to 2030 [29]

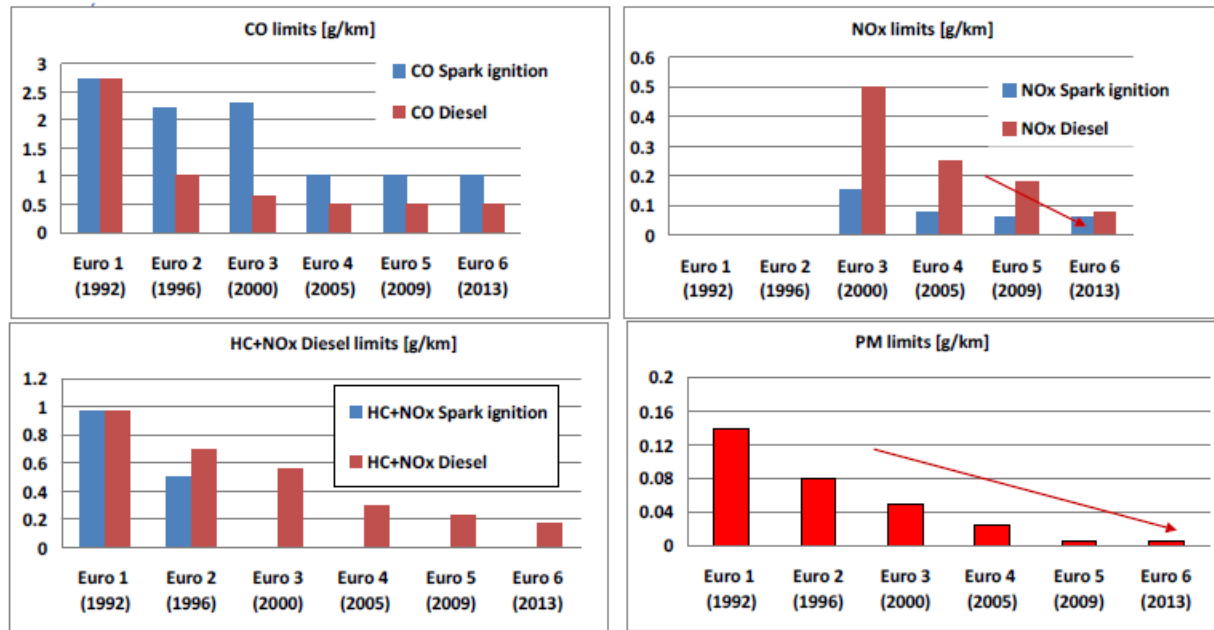


Figure 50 Limits on toxic emissions through the years [29]

Many different techniques has been used to reduce the emissions concerning Exhaust gas recirculation known as EGR, Port injection, Variable Valve timing, injector types and holes, etc... However these was beneficial in terms of reducing toxic emissions, keeping the CO<sub>2</sub> levels unchanged because the amount of CO<sub>2</sub> could be reduced only by decreasing the amount of fuel burnt [29]. For this purpose some effective techniques were turbocharging, and hybridization. In addition, the amount of fuel burnt is proportional to the mass of the vehicle, hence reducing the mass in any possible part/component nowadays is a target.

Therefore, it is clear now that in order to reduce the emissions it is mandatory to reach a faster light-off temperature of the catalytic converter and reduce the total mass of the vehicle, consequently the amount of fuel burnt, and the corresponding amount of CO<sub>2</sub> produced. So, using a material of higher conductivity will serve as will spread faster from the exhaust manifold to the converter, as well as a lighter material is always preferred. So, the first two requirements on the material to be concluded for the realization of an exhaust system are:

- 1- High thermal conductivity in order to allow faster and even spread of heat.
- 2- Lower density material to reduce the amount of fuel burnt.

Later in this study, we will show the effect of Niobium in these fields, with many others benefits in solving the problems in the exhaust manifold that will be addressed in this chapter.

## 2.2. Exhaust System Problems

### Introduction

During its operation, the exhaust system experiences different damaging phenomena due to the high temperature of the exhaust gases, their toxic composition, road salt, vibration, and mechanical loads. These thermal cycles and loadings are combined in thermo-mechanical fatigue (TMF) [30] shortening the life of the components, in addition to the different types of corrosion occurring in different mediums such as dry corrosion in the exhaust manifold, wet corrosion in the muffler and on the outside due to road salt, as well as pitting corrosion resulting in cracks that terminate the life of the component.

Different thermo-mechanical models have been used to evaluate the residual life of the components, mainly, the exhaust manifold. These models take into consideration the mechanical properties of the material as a function of temperature, hence choosing the best material is the starting point for a reliable system. In what follows, we will shed the light on the different problems that are to be taken into account for a reliable component. These problems are in terms of corrosion (wet, dry, intergranular, pitting), thermo-mechanical fatigue, and vibration.

### 2.2.1. Fatigue

By definition, Fatigue is lowering the strength or failure of the material due to the repetitive stress which could be above or below the yield strength. It is a common damage in many fields such as turbine blades, crankshafts, and many other car components such as the exhaust manifold which is subjected to repetitive forms of compression, expansion, bending and vibration. However, in order to occur, at least part of the stress should be tensile [32]. Even though these stresses are below the yield limit, their occurrence in a repetitive manner for a sufficient number of cycles will result in fatigue.

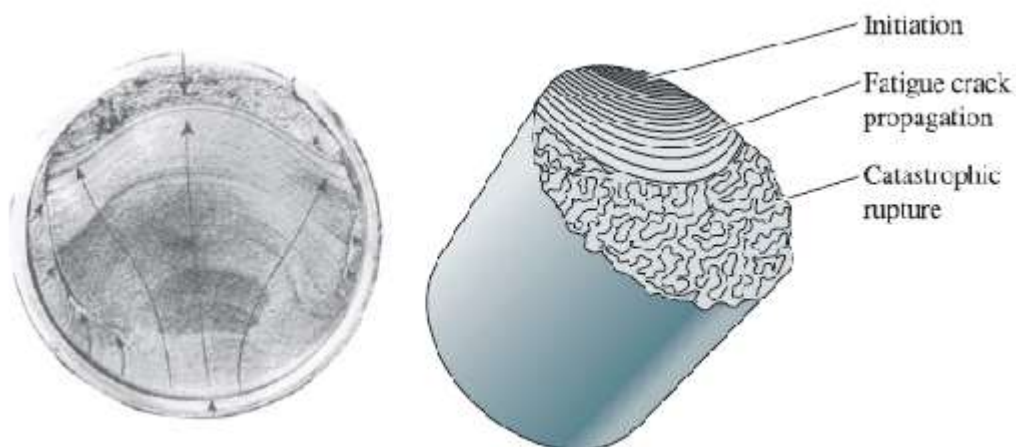


Figure 51 The three stages of fatigue [32]

Fatigue has three stages that make it easy to be detected as shown in figure 51. First it starts with the nucleation of tiny crack mainly at the maximum stress section, or an already existing crack due to pitting or scratch, then this crack propagates in a smooth manner along until the section is not able to resist the load, the moment at which fracture occurs.

Fatigue analysis can indicate the life of the component [31]. Temperature has also a significant effect on fatigue due to the stresses it introduces when the material is subjected to a non-uniform expansion and compression, a typical case that occurs in the automotive exhaust system, mainly the exhaust manifold that experiences crucial thermo-mechanical fatigue.

### 2.2.1.1. Thermo-Mechanical Fatigue

Due to the increasing demands for performance and emissions as discussed before, the phenomenon of Thermo-Mechanical Fatigue (TMF) is becoming more and more common especially for the corresponding high exhaust temperatures up to 1000°C.

Distinguishing between two different fatigue forms, mechanical fatigue is analyzed at constant temperature, it could be high cycle fatigue (HCF) if the maximum applied load does not exceed the yield limit, or low cycle fatigue (LCF) when it does, However, thermal fatigue is the degradation of the material's physical and mechanical properties as a consequence of the temperature variation. Hence, it is important to note that the used constitutive law in determining the component's life has to consider the mechanical properties as a function of temperature [30].

Based on a study held on a stainless steel specimen subjected to thermal cycles [31], it was observed that the result is two types of cracks, interior that occurs in any case, and exterior where the crack initiation is accompanied by oxidation and voids formed due to creep.

Therefore, Thermo-Mechanical Fatigue is when these 2 pre-mentioned forms of fatigue are superimposed, their combination could be in-phase or out of phase. Different factors are considered when the life of a components is to be estimated based on the TMF conditions, these factors include material properties, mechanical deformation and its rate, temperature range and the phase condition. The most famous approach to estimate the number of cycles before the failure of the component is the Manson –Coffin approach [30], based on a correlation between the strain and the number of cycles:

$$\bullet \quad \Delta \epsilon^\beta \cdot N = C \quad \text{Eq.2.5}$$

Where:  $\Delta \epsilon_{\text{total}} = \Delta \epsilon_{\text{thermal}} + \Delta \epsilon_{\text{mechanical}}$  is the total applied strain

- **C,  $\beta$ :** coefficient and exponent of strength and ductility to fatigue, evaluated experimentally.
- **N:** number of cycles

This equation, known as strain controlled, is used for the low cycle fatigue test, however a similar stress controlled equation is used for the high cycle fatigue test, the combination of these 2 equations allows to obtain the well-known Basquin-Manson-Coffin curve shown in figure 52 that will give the number of cycles before the failure.

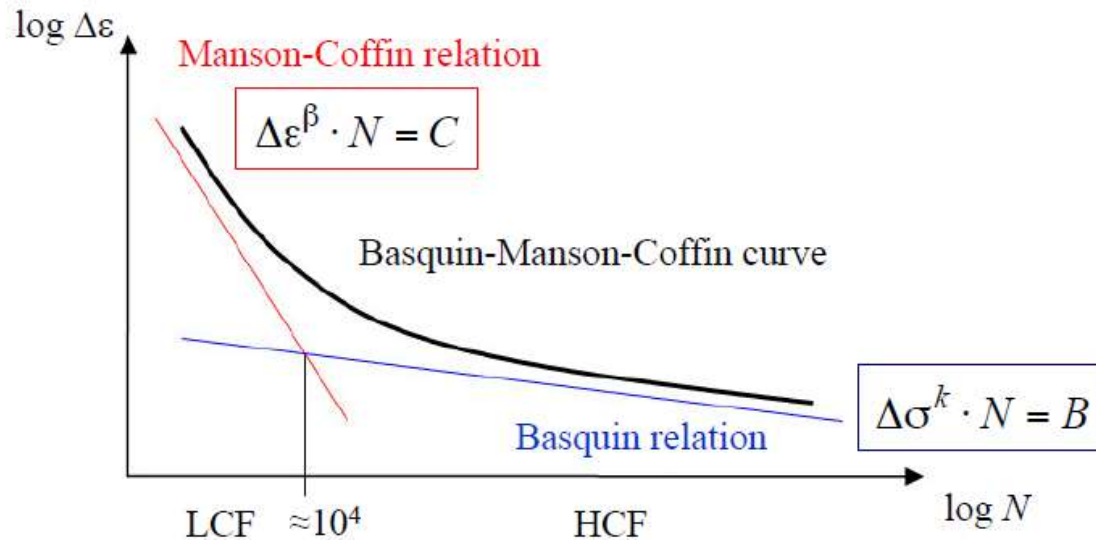


Figure 52 Basquin-Manson-Coffin Curve [30]

In-phase cycles are achieved when the maximum of both the strain and the temperature occur at the same instant, however Out-of-phase case is the contrary, where the maximum of one cycle is super imposed with the minimum of the other as shown in figure 53 .

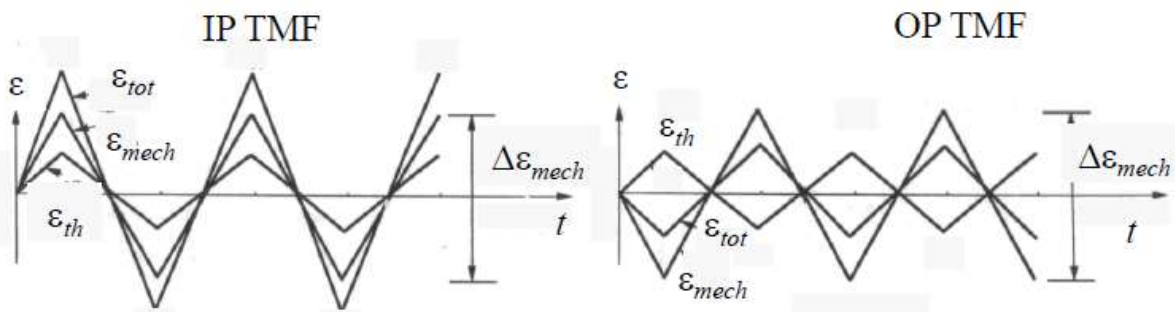


Figure 53 In-phase and Out of Phase TMF cycles [30]

Out-of-Phase condition is considered more critical from the oxidation point of view, because when the oxide layer is formed at high temperature, the corresponding stress will be minimum, then stretching occurs with lower temperature that makes the layer brittle and consequently breaking it exposing new material for the further oxidation.

In the particular case of metallic materials, stainless steels for example, the damage due to the TMF is due to three phenomena:

- 1- Mechanical Fatigue (HCF, LCF)
- 2- Creep
- 3- Oxidation

These three may occur independently, or combined depending on the specific conditions of the application. For example, in the exhaust manifold, these 3 phenomena may be combined because the temperature exceeds 1/3 the melting temperature of the material [30].

### 2.2.1.2. Mechanical Fatigue

Materials respond in a different way when subjected to mechanical fatigue, for example there exist a category of materials that harden cyclically (increase the required stress to reach the applied strain) with the increase number of cycles, this category includes annealed materials in general, or vice versa, a category that softens (thus less stress is required to reach the applied strain) such as heat treated materials by quenching, or plastically deformed materials by drawing belong to this category in general terms [30].

Consequently, damage may occur due to this hysteresis behavior by nucleating a crack that propagates along the crystalline planes resulting in fracture. Other phenomena may also enhance the mechanical damage such as Bauschinger effect, shakedown, or ratcheting [30].

### 2.2.1.3. Creep

Creep is defined as time dependent plastic deformation that occurs under static mechanical stresses and elevated temperatures, it is observed when the temperature exceeds a definite threshold which is 40% [32] melting temperature of the material. The associated failure of creep suffer from rupture failure due to the microstructural consequences described by dislocation movements, cavitation on grain boundary, and microstructure aging [32], that makes creep a limiting factor in the component's life time. In the exhaust manifold, in general, the mechanical fatigue and creep coexist. Figure 54 shows the three stages of creep, the primary creep described by increasing creep resistance i.e. strain hardening, secondary creep is the most important as it is the engineering design parameter for long life applications described by a constant rate, finally the tertiary creep that shows an increase in creep rate resulting in failure.

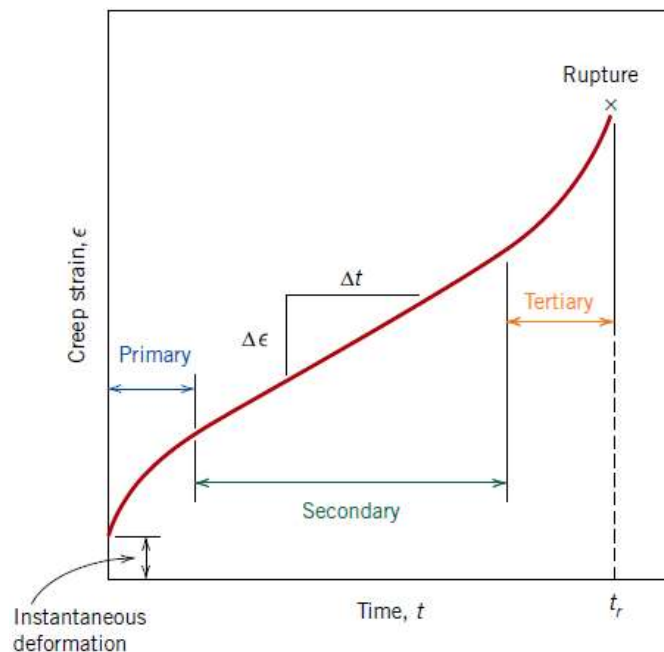


Figure 54 the three stages of creep [32]

Figure 55 shows that creep highly depends on temperature, it is obvious that the higher is the temperature, the lower is the life time.

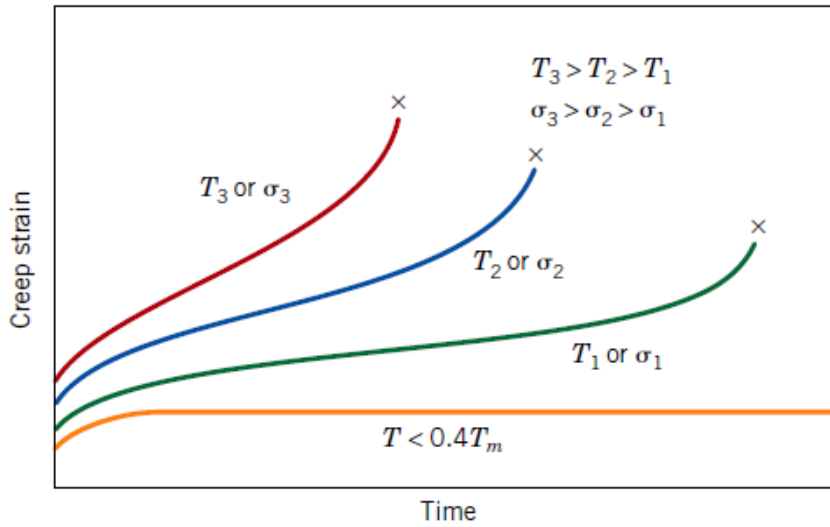


Figure 55 Effect of temperature and stress on the creep behavior [32]

In order to obtain a quantitative measures in terms of creep resistance, experimental approach called the “sag test” shown in figure 56 is applied for the specimen for the desired temperature and time. The results are measured in terms of deflection in [mm]. The lower is the deflection, the higher is the creep resistance of the material.

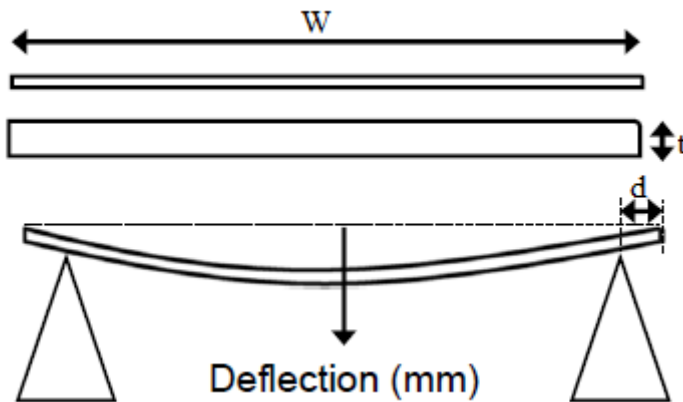


Figure 56 Schematic representation of Sag test [45]

### 2.2.1.4. Oxidation

An oxide layer could be formed on the surface of the metal as a result of its reaction with oxygen. This reaction is influenced by the standard free energy that could be detected from the Ellingham diagram [32], the rate of oxidation described by the Pilling-Bedworth ratio which exceeds two for iron [32] revealing that the oxide cracks off the surface exposing new material as shown in figure 58.

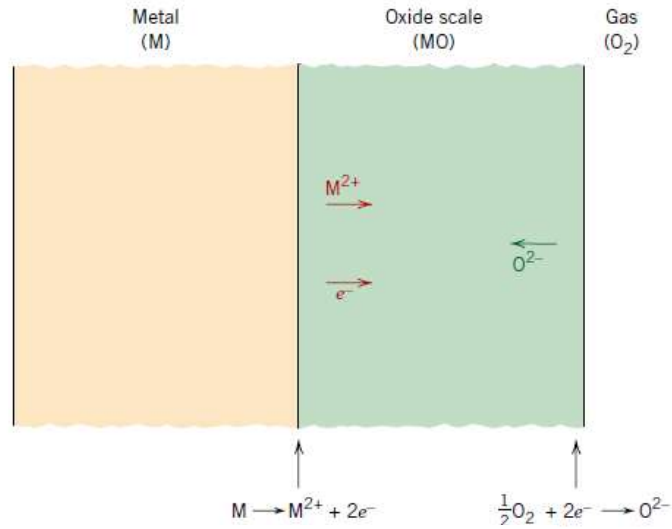


Figure 57 Metal oxidation phenomenon [32]

The general chemical equation of oxidation of metals (M) is:



The first step is the absorption of oxygen into the metal, then it dissolves and forms oxide. Hence, it may happen by oxygen penetrating, or metal being transported to the outer and reacting there. Oxidation reactions are based on diffusion phenomenon. There exist three main types of diffusion shown in figure 59: the vacancy mechanism occurs when an atom jumps into a free site in the adjacent lattice, the interstitial mechanism is the case when an atom pushes an atom to an interstitial site occupying its place, or an interstitial atom moves to another interstitial site. Oxidation damage occurs whenever the temperature is critical for the used steel grade, it is more common with austenitic stainless steels [32], and the in-phase TMF could be dominant.

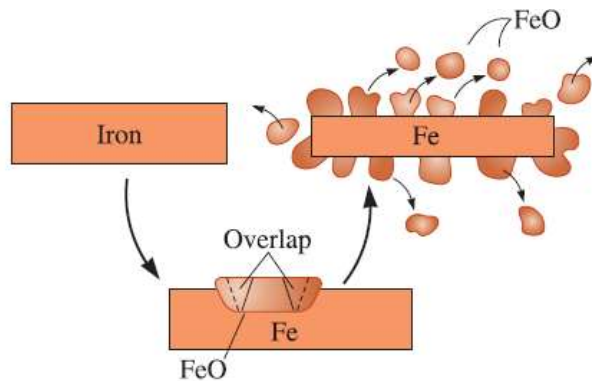


Figure 58 Oxidation of Iron [32]

Even though oxidation is said to be environmental effect, it is temperature dependent, and that was proven by Arrhenius relationship [17] that shows an exponential increase in the oxidation rate as temperature increases. Thus choosing a material that has high oxidation resistant, that depends on the formation of protective oxides including Cr, Si, and Al, is an effective way in minimizing its consequences by avoiding the abnormal oxidation zone.

As a conclusion, for the exhaust manifold as a particular component, the typical working conditions are characterized by thermal cycles featuring temperatures above 900°C for emission demands, and mechanical loads due to bolts, weight, turbochargers, and expansion/compression especially when expansion is hindered by constraints or other components. Hence, the material is a starting point, it should be chosen having high thermal fatigue and oxidation resistance, reduced wall thickness to reduce the weight maintaining in the same time higher conductivity for a faster heat spread and high thermal capacity for a faster light off, and low expansion coefficient to reduces stresses.

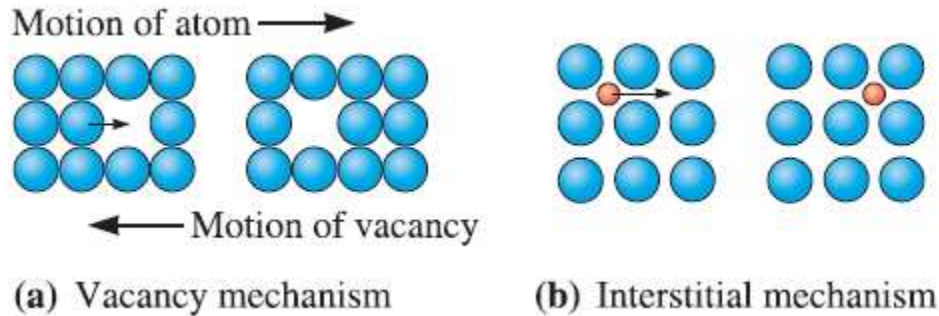
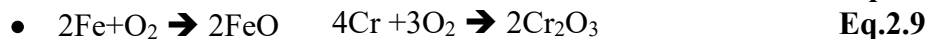
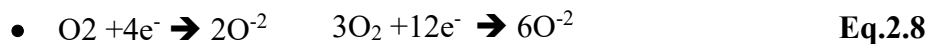


Figure 59 Oxidation: the diffusion mechanisms [6]

#### 2.2.1.4.1. High Temperature Oxidation of Stainless Steels

Consider the particular case of the exhaust manifold, where the temperature is always high and the environment is hot gases containing air, oxygen, CO<sub>2</sub>, steam, hydrocarbons etc... The contact between such hot gases and the stainless steel features the oxidation-reduction reactions that leads for the formation of oxide scales on the surface (for simplicity, consider the f equations 2.7-2.9)



In general, the oxidation rate has a parabolic trend and is described by the inward or outward diffusion phenomena, even though the formed oxide layer could be seen as a protective layer that decreases the oxidation rate, however the imperfections in this layer, such as pores, channels, vacancies or cracks, the oxidation reactions continue with the consequence of alloy depletion combined with oxide spallation and cracks.

Two phenomenon may occur depending on whether the oxide is fragile or adherent. If it is fragile, new material will be exposed and the degradation will occur faster than the case where the oxide is adherent thus preventing the exposure of new material, hence reducing the risk of the component damage. Figure 60 shows the second case where the oxide growth area prevents the passage of other undesired elements, thus protecting the metal.

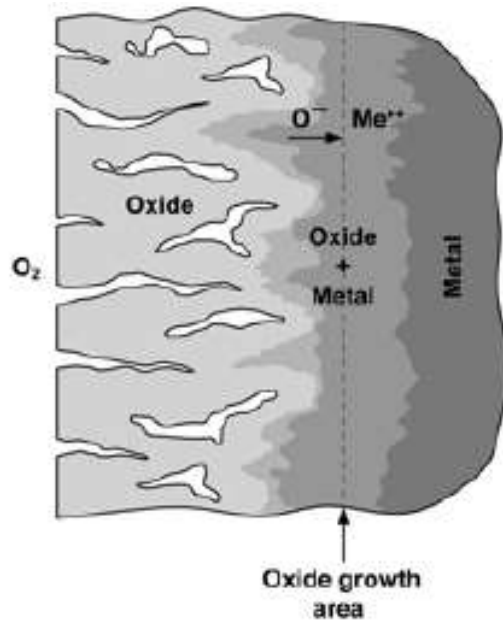


Figure 60 porous  $Fe_2O_3$  layer (900 C, Air, Hk30) [17]

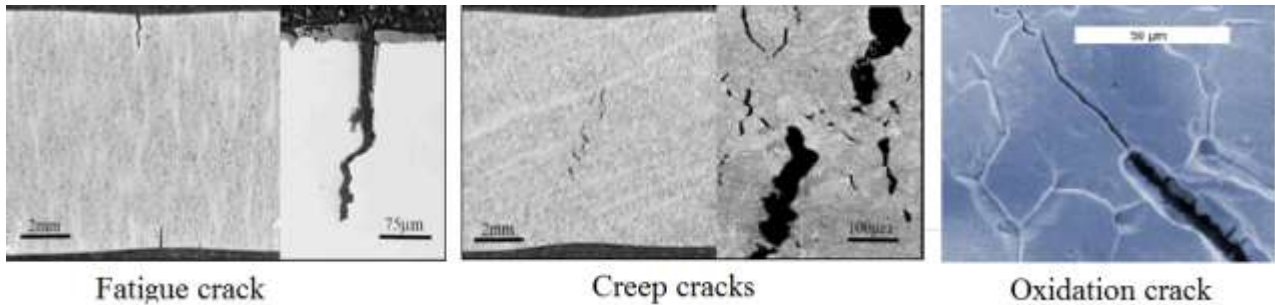


Figure 61 Different form of cracks [30]

## 2.2.2. Corrosion

In this thesis, we are interested in stainless steel among other metals, so we will focus on their corrosion phenomena. Corrosion, an operating degradation phenomenon, is a result of chemical and electrochemical reactions between the main elements (Fe, C, Cr, Ni, etc...) and the aggressive medium at the surface of the metal causing its degradation and ruining its features by the formation of corrosion products.

The corrosion of stainless steel could be classified into 2 categories: The first is electrochemical corrosion, known as wet corrosion, where the presence of an electrolyte enhances a redox reaction [17] in which ions and electrons are involved, such highly corrosive acids are mainly found inside the mufflers and include sulfuric and sulfurous acids derived from sulfur content in the gasoline and fuel additives, the driving habits such as start-stop driving and short journeys leads to condensation of such compounds. The second is chemical corrosion known as dry corrosion, where corrosion occurs due to oxidation of metals by gaseous environment at high temperatures, hence it is mainly related to the operating temperatures.

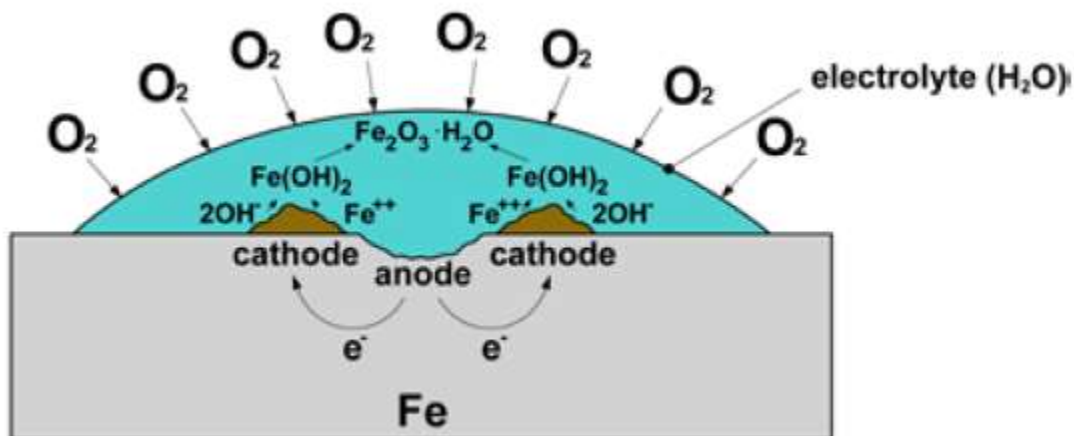


Figure 62 Electrochemical corrosion in a homogeneous metal [17]

Corrosion, as well as vibration, are the only problems that has no absolute solution in the world of mechanical engineering, thus, improvements are carried out for the sake of minimizing such problems as much as possible. In the Automotive exhaust systems, different types of corrosion could be found due to different available conditions such as high temperature, noxious chemical composition, road salt, water condensation in the muffler during cold running, etc...

In terms of location, one should differentiate between generalized corrosion (known as uniform corrosion) and localized corrosion. In the first, attacking occur along the entire surface maintaining a quiet consistent depth, however, only specific areas are involved in the other type. The second family include several types that are fond in the exhaust system such as intergranular corrosion, pitting corrosion, and stress corrosion cracking.

### 2.2.2.1. Intergranular corrosion

Intergranular corrosion, or the so known sensitization phenomenon, is a localized corrosion type as a result of material's microstructure discontinuity due to the formation of carbides and nitrides, mainly chromium carbides, near the grain boundary of stainless steels, as shown in figure 63, when exposed to very high temperatures up to 850°C, such as heat affected zones when the component is subjected to welding. It is characterized by a crack that follows the grain boundary where these carbides settle.

In Austenitic stainless steels, carbon is considered as an undesired impurity due to its high affinity for chromium. Carbon is able to bind with chromium 16 times its weight forming carbides, as well as it diffuses faster than chromium into the austenite capturing the chromium, and the grain boundary's low atomic density is what facilitates the precipitation there[17]. Mainly, this corrosion occurs when the austenitic stainless steel is exposed to temperatures between 400°C and 900°C which is a typical condition in the exhaust system.

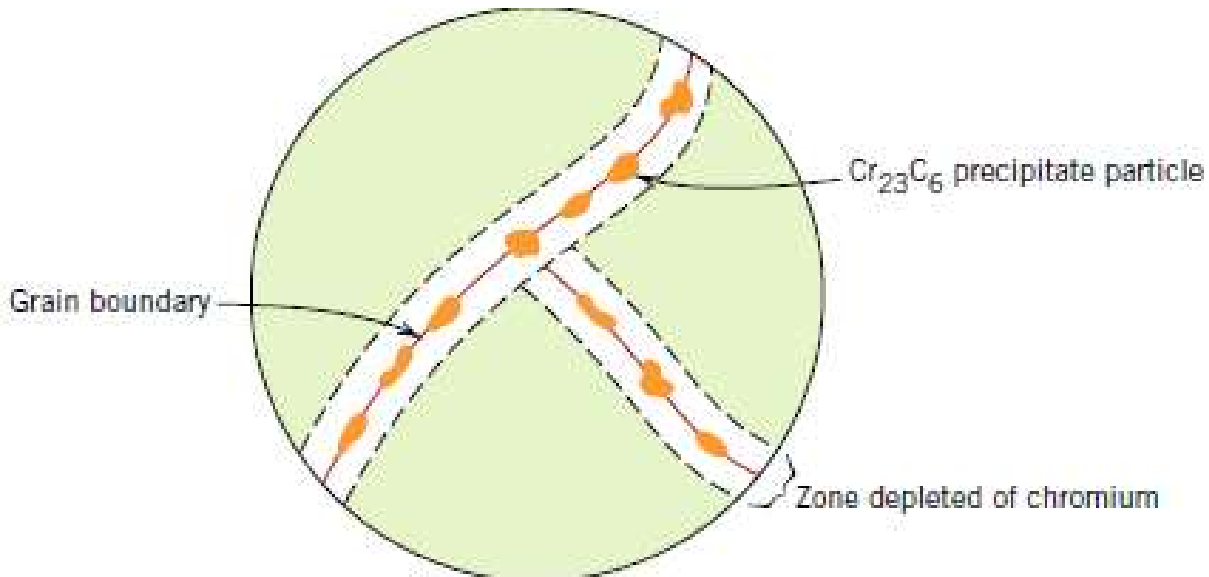


Figure 63 Chromium depletion at grain boundaries [32]

In case of Ferritic Stainless Steels, critical temperatures are lower than those of austenitic, and Cr compound precipitate easily and in shorter time due to its lower solubility of carbon and nitrogen, making Ferritic stainless steel more sensitive to such phenomenon. Figure 64 shows the sensitization curves for both ferritic and austenitic stainless steels [17].

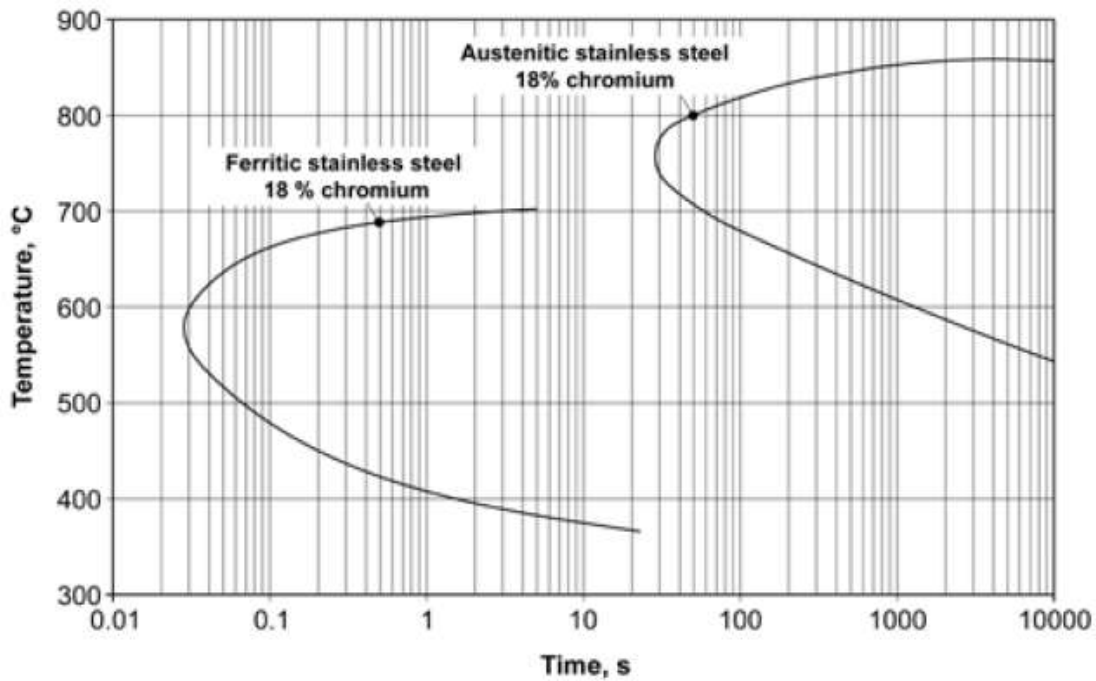


Figure 64 Sensitization curves for ferritic and austenitic stainless steels with the same amount of chromium [17]

Henceforth, it is important to shed the lights on the role of niobium in stabilizing both Ferritic and Austenitic stainless steels, forming carbides and leaving the chromium in the lattice. This would be further discussed in chapter 3.

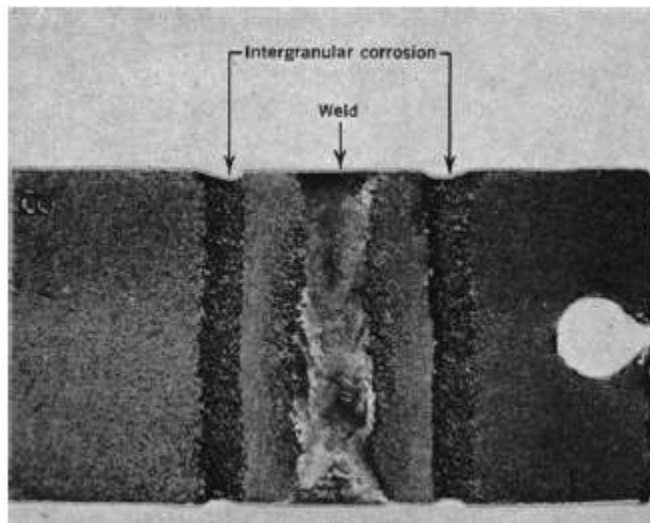


Figure 65 Grooves at sensitized areas due to Integranular corrosion [32]

### 2.2.2.2. Pitting Corrosion

Another type of localized corrosion that happens to stainless steels due to attacking chemically the passive film by neutral or oxidizing environments. This occurs mainly in the rear part (muffler) of the automotive exhaust system that experiences wet corrosion due to the condensation of chloride ion and often low PH values with electrochemical active soot [33]. The consequences of such type of corrosion are penetrating deep holes in the components as shown in figure 66, and the corresponding loss of mass from the resisting section.

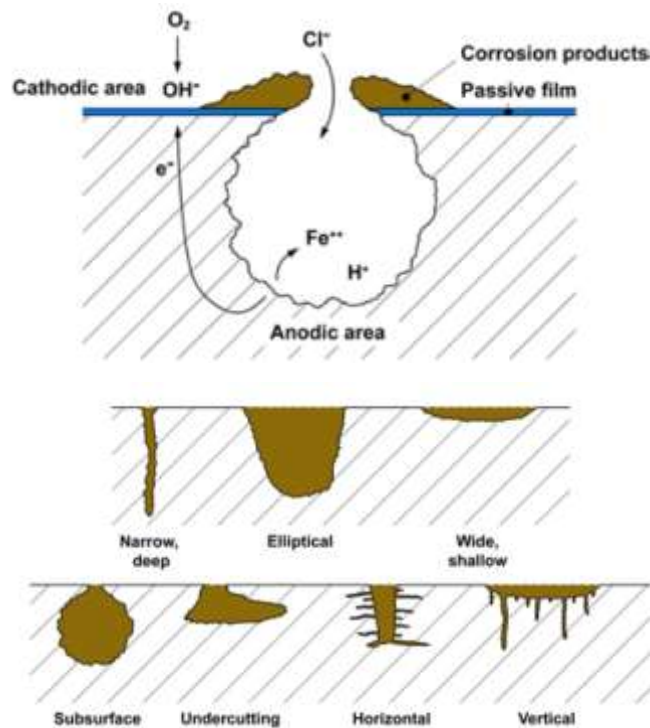


Figure 66 pitting corrosion phenomenon and pits or holes morphologies [17]

Such type of corrosion may hit the parts of the exhaust systems that are exposed to road salt such as the muffler's jacket, pipes and tail pipe.

The ability of stainless steels to resist

Pitting corrosion is measured by the PREN (Pitting Resistance Equivalent Number) index, for which the higher is the PREN index, the more resistive is the stainless steel. It is verified that elements such as Cr, N and Mo increase the resistance to pitting [17].

$$\bullet \text{ PREN} = \% \text{Cr} + 3.3 \cdot \% \text{Mo} + 16 \cdot \% \text{N} \quad \text{Eq.2.10}$$

The condensation of the combustion products produces sulphurous acid, which creates critical PH conditions with the hydrochloric acid [33] and result in wet corrosion due to the chloride ions and deposits of electrochemical active soot particles impacting the inner parts as shown in figure 67. PREN number is not the only indicator, because in this case the loss of mass would give a clearer idea about the behavior of different stainless steels under these conditions. Studies show that stainless steels with low chromium content had the highest mass loss, while

the presence of the alloying elements Molybdenum (Mo) and Nickel (Ni) aided in the fast passivation, thus showed much better results in terms of mass loss [33] as shown in figure 68.

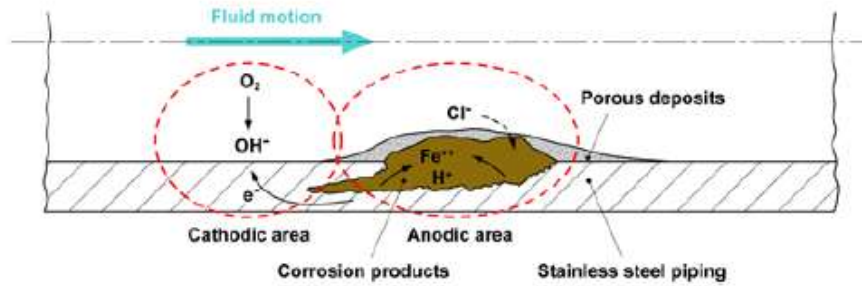


Figure 67 Corrosion under deposit in a pipe [17]

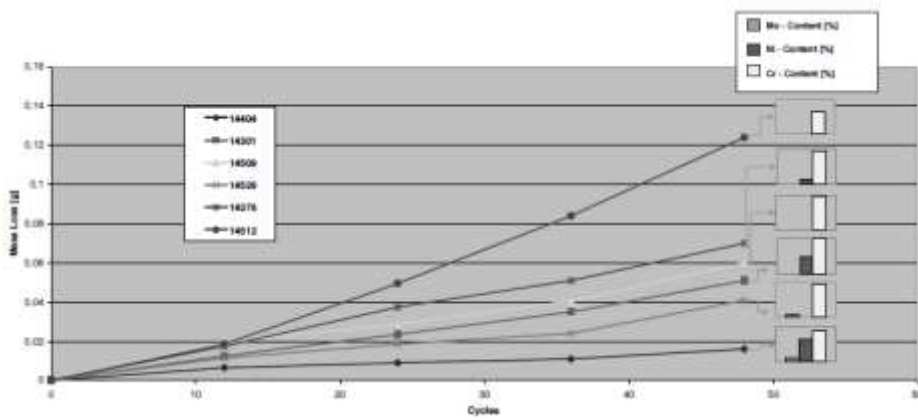


Figure 68 Mass loss as function of cycles for different stainless steel grades [33]

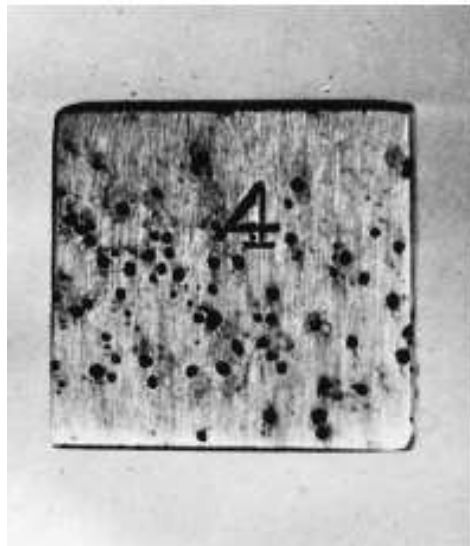


Figure 69 Pitting corrosion on 304 stainless steel plate [32]

### 2.2.2.3. Stress Cracking Corrosion

Stress Cracking Corrosion is a localized damage occurs only under the combined effect of three conditions: specific stainless steel composition, specific environment and a mechanical stress exceeding a specific threshold. It starts with simple crack, then it propagates, finally resulting in component's malfunction.

In the stainless steels where nickel is not an alloying element- Ferritic for example- or when its percentage exceeds 40% [17], stress cracking corrosion is less likely to occur. Figure 70 shows the stress cracking corrosion of an 18-20% chromium content stainless steel and variable nickel amount under the following conditions: aqueous solution with 42% magnesium chloride at 154°C.

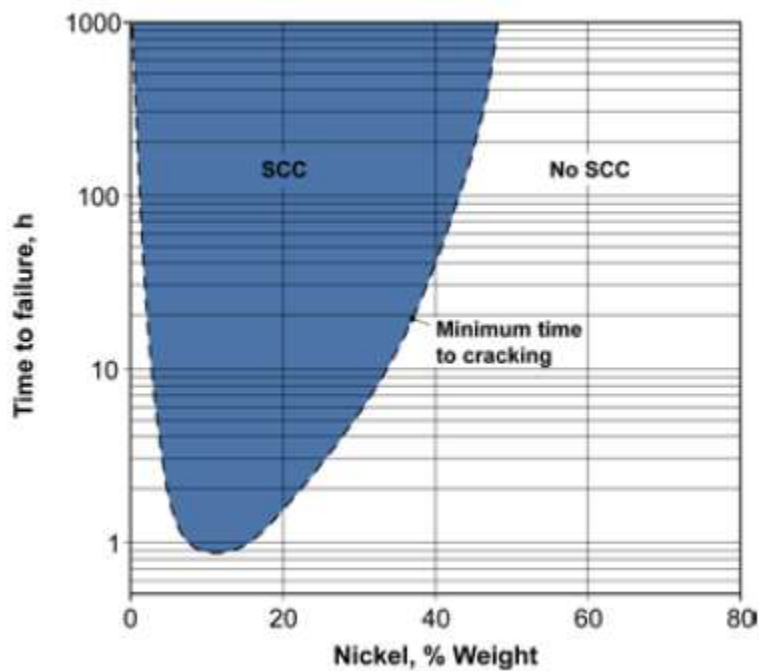


Figure 70 Stress Cracking Corrosion for a 18-20% Cr stainless steel [17]

### 2.2.3.Vibration and Noise

Vibration is becoming more crucial due to the usage of lightweight material, which is considered more sensitive, in order to reduce the total weight of the vehicle so that the stringent requirements on the emitted CO<sub>2</sub> levels could be matched.

The internal combustion engine, being the main source of vibration, transmits its vibration to the rest of the powertrain leading to many problems including the silencer (muffler) breakage in the exhaust system [34]. As mentioned before, the first type of transmitted vibration is the sonic waves propagating from the exhaust ports that are dampened and cancelled in the muffler, otherwise it may cause resonance in the muffler. However, the vibration of the engine torque running at idle or operating conditions i.e. time varying loading, as well as the road ups and downs, can shake the pipes causing damage in addition to lowering the performance of the components during their operating life and lowering comfort level.

A key word when talking about vibration is resonance, which is the purpose of many dynamic studies aiming to avoid such phenomenon. Resonance is a high amplitude response resulting in the damage of the components, it occurs when the component is excited by a loading that has the same natural frequency as the component. Natural frequency is the frequency at which a component will vibrate freely if allowed, each of these frequencies have a corresponding modal shape, in other words, a unique deformation form. Considering a 4 stroke engine of a typical car running below 6000 rpm, studies show that the range of frequencies of our interest is 0-200 Hz where both engine harmonics belong [35].

The transmitted vibrations from the engine to the exhaust system could be classified into longitudinal and bending vibration [36], these vibrations introduce stress into the exhaust system, mainly the pipes, ending up in reducing the fatigue life of the system. Some available techniques excelled in reducing the transmission of vibration, for example, the flexible bellow type joint, shown in figure 71, which is used in transversal engine layout, it is usually located between the exhaust manifold and the catalytic converter, another example is the rubber attachments between the exhaust system and the chassis.



*Figure 71 bellow type joint used in exhaust systems*

### 2.2.3.1. Material Effect on natural Frequencies

A study was carried out to mark the effect of the material on the natural frequency, 3 different materials are tested (grey cast iron, structural steel, and Al-Mg alloys), the result showed that the natural frequencies and the mode shapes show different characteristics as we change the material [37].

In a modal analysis study, the obtained differential equation contains the mass and stiffness matrices, the bending stiffness itself depends on the Young's modulus, and the shear modulus in case of torsional stiffness [38]. The corresponding solution of the system gives the Eigen values. The natural frequencies of the studied system are the square roots of the obtained Eigen values, hence, it is mathematically proven that the mechanical properties of the material change the natural frequencies of the component.

According to the study carried on Euler-Bernoulli's beams [38], it has been proved that Poisson ratio can change the frequencies of the modes and their order as shown in figure 72, as well as the effect of the Young's modulus is plotted in figure 73 where it is obvious that as it increases, the natural frequencies increase while maintaining their order. Figure 74 shows that the relation between the mass density and natural frequency is inversely proportional, in other words, as the mass density increases, the natural frequency decreases.

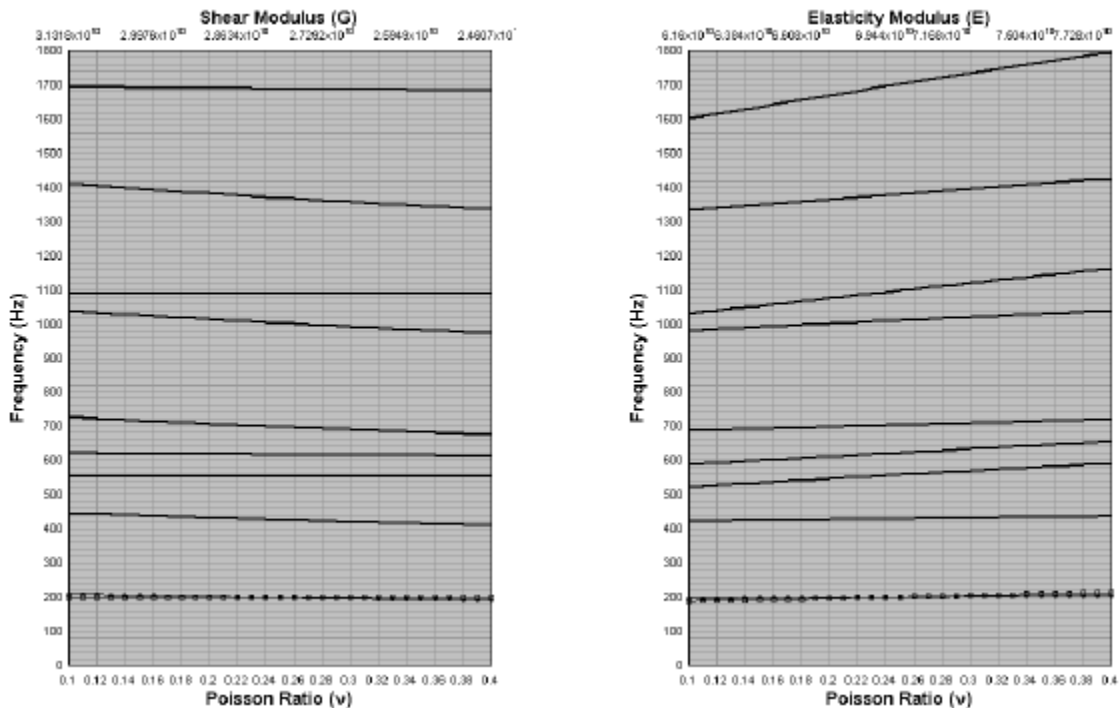


Figure 72 trend of natural frequencies as a function of Poisson ratio for fixed Elastic modulus (a), and fixed shear modulus (b) [38]

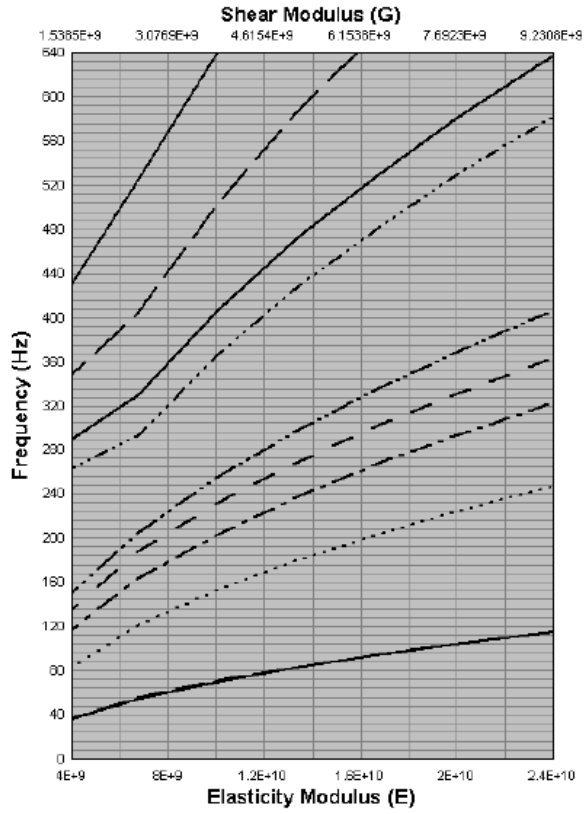


Figure 73 trend of Natural Frequency as a function of Elastic modulus [38]

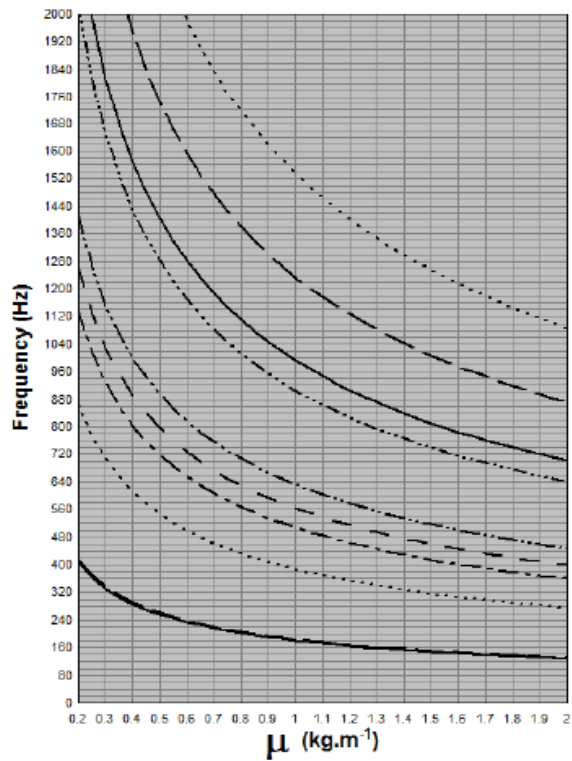


Figure 74 trend of natural frequencies as a function [38]

## 2.2.4. Conclusion

Upon stating the problems of the exhaust systems and the future requirements that are to be fulfilled, it is concluded that the chosen material is of high importance, as it influences the emission quality, as well as providing a reliable system. For the particular application of the exhaust systems, in order to reduce the problems, the material should satisfy the following requirements:

- Low density to improve fuel economy and reduce CO<sub>2</sub> emissions.
- High resistance to different types of corrosion.
- High thermal conductivity for a uniform spread of heat and faster light off.
- Low expansion coefficient to avoid additional stresses.
- High fracture toughness to resist crack propagation.
- High resistance to thermal fatigue.
- High melting point due to the higher temperature gases, and creep.
- High oxidation resistance.
- High Young modulus to withstand the engine's vibration.
- High yield strength to withstand thermal stresses.
- Good weldability, and formability.

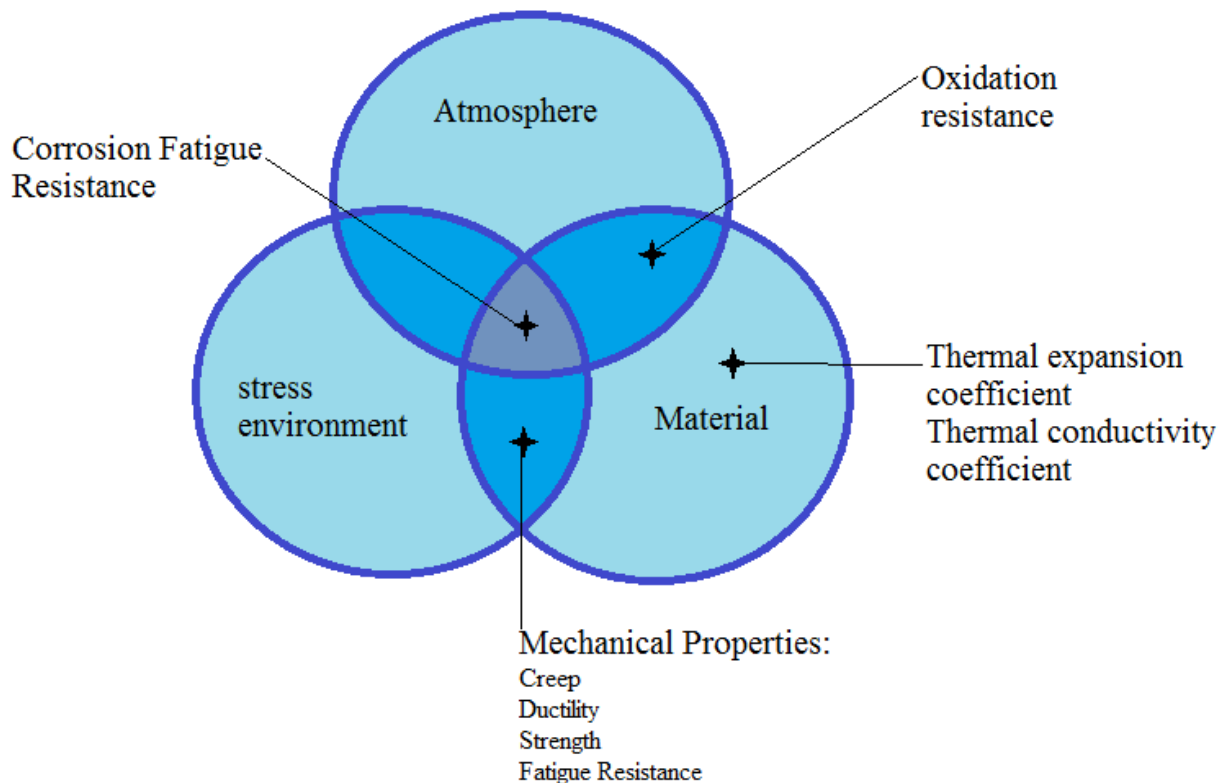


Figure 75 Material Properties for a durable exhaust manifold

# Chapter 3

## Stainless Steel in Exhaust Systems

### Introduction

All over the years, the chosen material for the exhaust system components has been always changing to meet the increased warranty period, up to 10 years, and the new conditions, mainly, the increase in temperature that corresponds to the improvements made in order to increase the efficiency. Among the metals, many have been competing, such as cast iron, mild steel, Nickel based alloys, and stainless steels which has been already used in the automobile sector since 1990 in decorative trims and many functional parts. However, in order to satisfy the stringent rules, nowadays stainless steel has taken the priority, not only by being preferred and used, but also by trying to invest in new stainless steel that is able to fit the next generations whose temperature is going to exceed 1000°C.

In the following chapter it will be proven that, according to several studies, stainless steel has won the competition among the other metals, featuring good resistance to corrosion, oxidation, creep and costs. Particularly, talking about Ferritic and Austenitic stainless steel in this application and highlighting the importance of the role played by Niobium (Nb) as an alloying element that enhances the characteristics of the stainless steel under the conditions presented in the exhaust system. Apart, metallurgical mechanisms that increase the performance of stainless steels have been stated.



Source: AK Steel

*Figure 76 Benefits of Stainless Steels*

### 3.1. Materials Trend: From Cast Iron to Stainless Steel

According to several studies, the benefits of stainless steels over other metals such as Nickel based super alloys, Ni-Cr alloys and low steel [39] will be presented, as well as the comparison with the cast iron [40], the conventional material, will demonstrate why stainless steel will replace the last in the modern and near future.

#### 3.1.1. Stainless steel Advantages in Terms of Oxidation Resistance

Cast iron that was used for exhaust manifolds, such as Ni-resist and D5S grades, showed oxide scale spallation at 700-800°C [41], which made them no longer an available option for the material selection when dealing with elevated temperatures up to 1000°C. Meanwhile, the Ferritic and Austenitic stainless steels showed better behavior in terms of oxidation resistance.

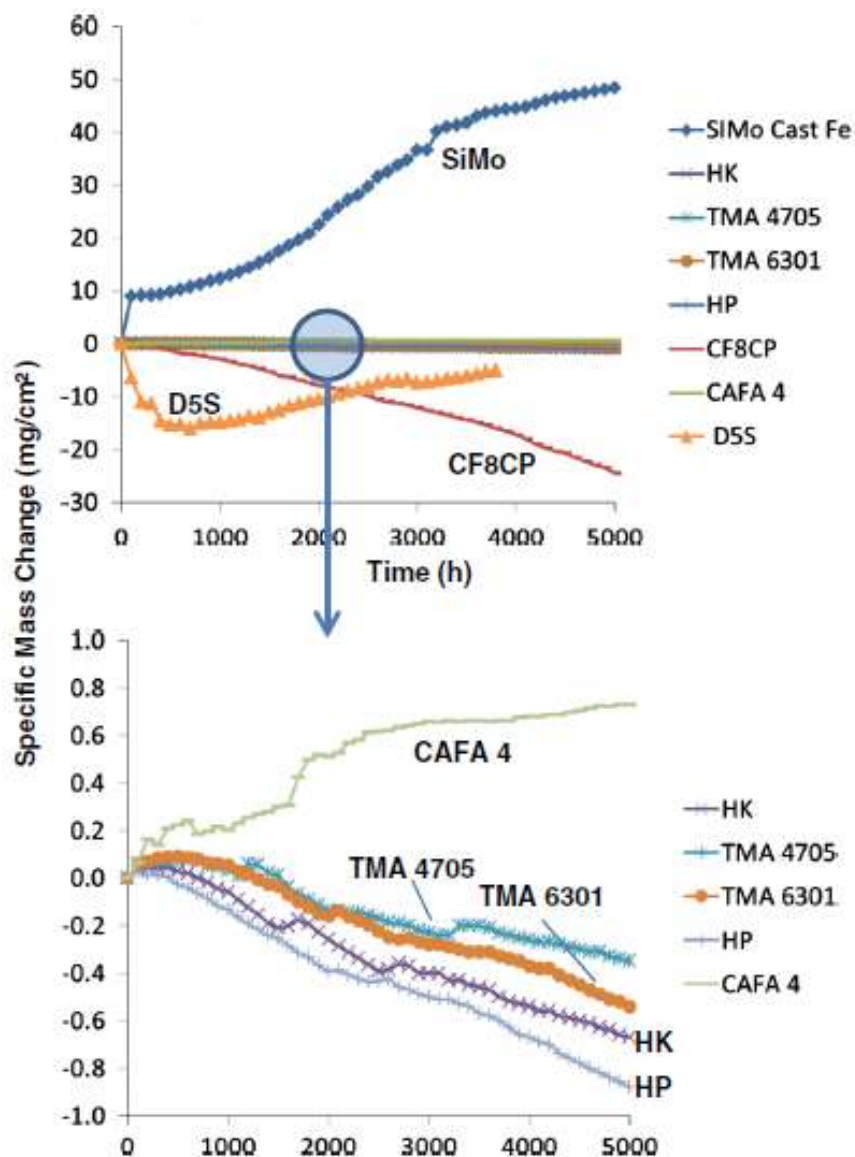


Figure 77 oxidation data at 750°C in air with 10% H<sub>2</sub>O [41]

As revealed in figure 77, SiMo exhibited unusual pattern of oxidation mass change with the increasing temperature, and D5S suffered from oxide scale spallation, whereas a good oxidation resistance with modest mass loss behavior was observed for the stainless steels HK (0.19% Nb) and TMA 4705 (0.38% Nb) [41] alloys.

Figures 78 and 79 [41] show the cross section images comparing D5S and austenitic stainless steel at different temperatures and time, as we observe voids and cracks in cast iron at 650°C, while the CAFA 4 (with 0.94% Nb, 0.05% V and 1.0% W) was the most oxidation resistant [41], even though CF8C-plus showed lower oxidation resistant under the experimental conditions, however it showed better oxidation resistance when tested under real conditions.

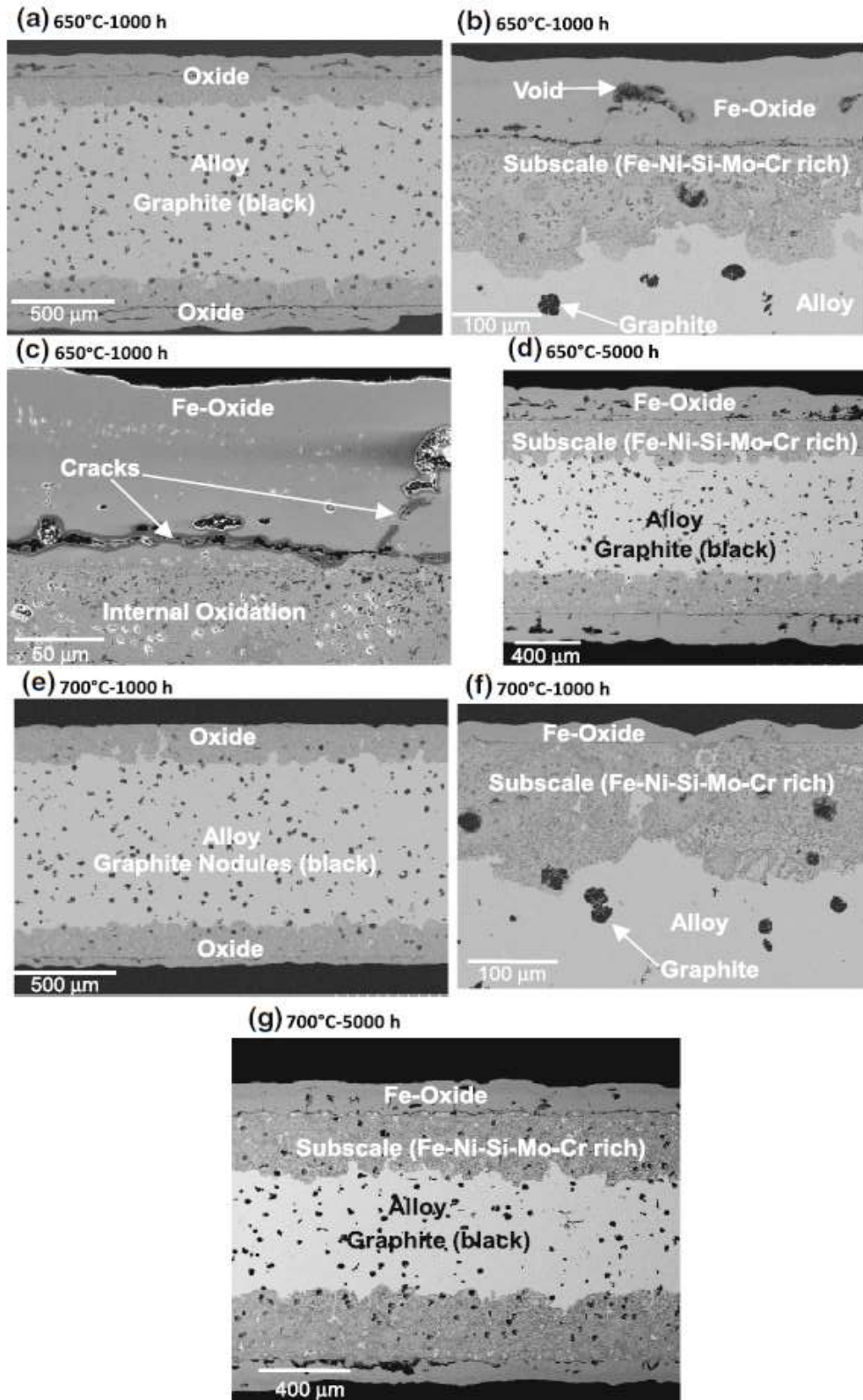
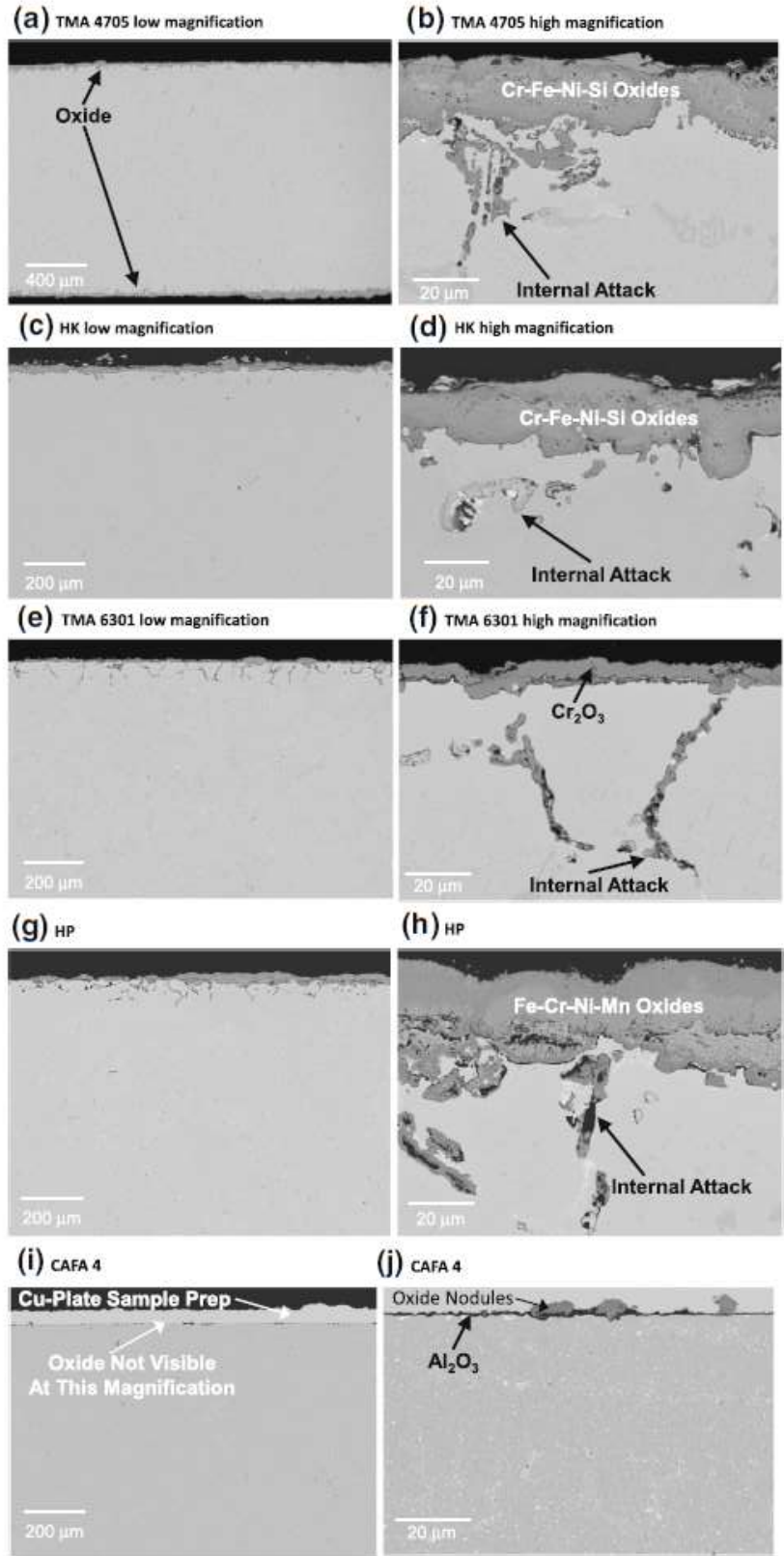


Figure 78 Backscatter SEM cross-section images of D5S cast iron after 1,000 h and 5,000 h in air with 10 % H<sub>2</sub>O. a-c 650 °C/1,000 h; d 650 °C/5,000 h; e, f 700 °C/1,000 h; g 700 °C/5,000 h [41]



**Figure 79** Backscatter SEM cross-section images of austenitic stainless steels after 5,000 h at 800 °C in air with 10 % H<sub>2</sub>O. a, b TMA 4705; c, d HK; e, f TMA 6301; g, h HP; i, j CAFA 4 [41]

### 3.1.2. Stainless Steel Advantages in terms of Fatigue Strength

Both Ni based super alloys and stainless steels provide a satisfying result when compared in terms of fatigue life even though stainless steel has slightly higher expansion coefficient as shown in figure 80. However, the thermal conductivity of Stainless steels is higher than that of Ni-based super alloys at the required temperature, even though the Ni-based super alloys may operate at higher temperatures, their cost is much higher as shown in figure 81, thus giving the privilege of the stainless steels among Ni-based super alloys and Ni-Cr alloys.

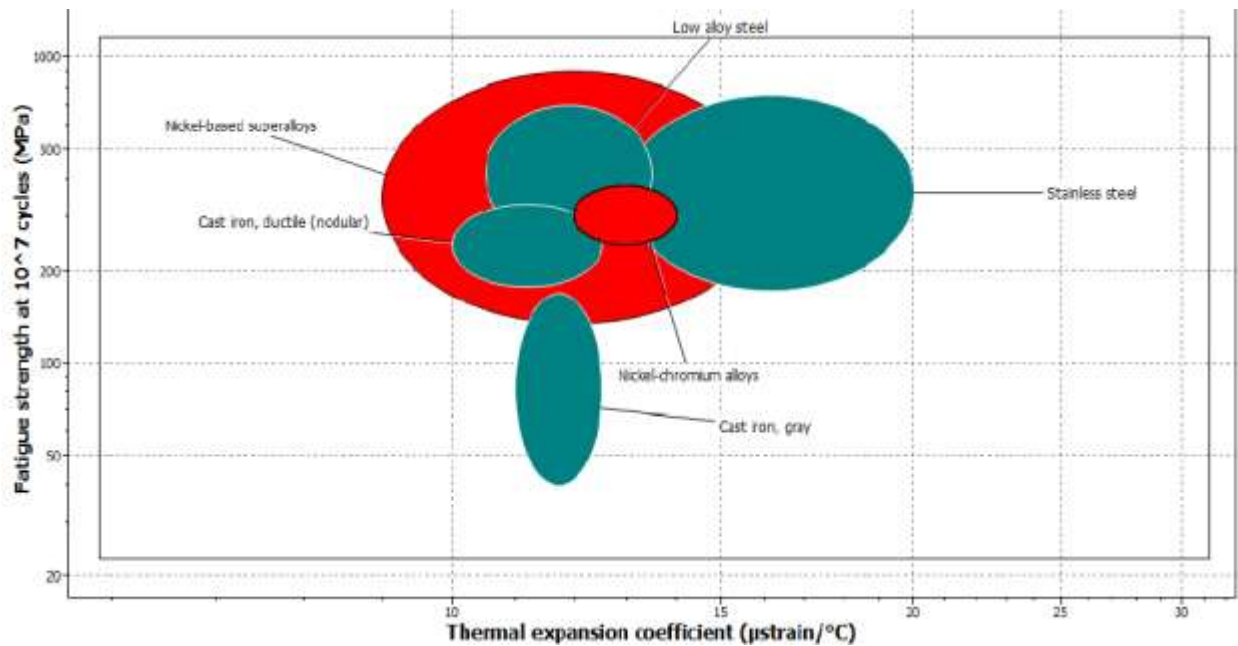


Figure 81 Fatigue life against thermal expansion coefficient for Stainless Steels and Ni based super alloys [39]

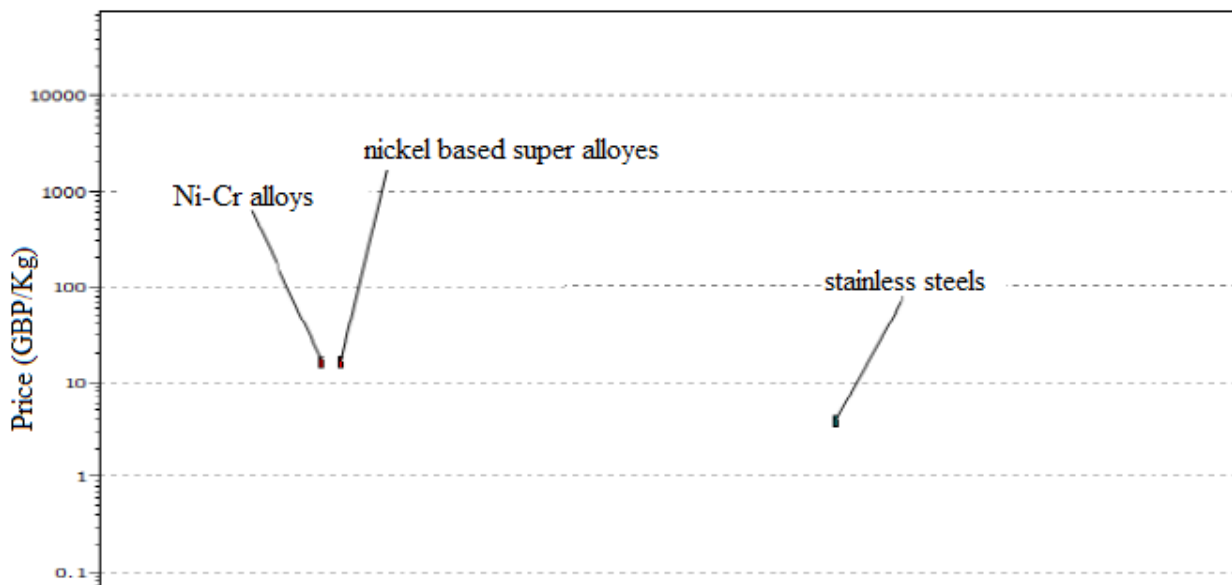


Figure 80 Prices of Stainless steels and Ni based alloys [39]

### 3.1.3. Stainless Steel advantages in Terms of Creep Resistance

Comparing austenitic stainless steels, in particular the CF8C-plus, to the cast iron SiMo and Ni-resist, it is found that the first has superior properties up to 900°C, and excellent creep rupture resistance as shown in figure 82, that demonstrates the strength of CF8C-plus compared to cast iron [42].

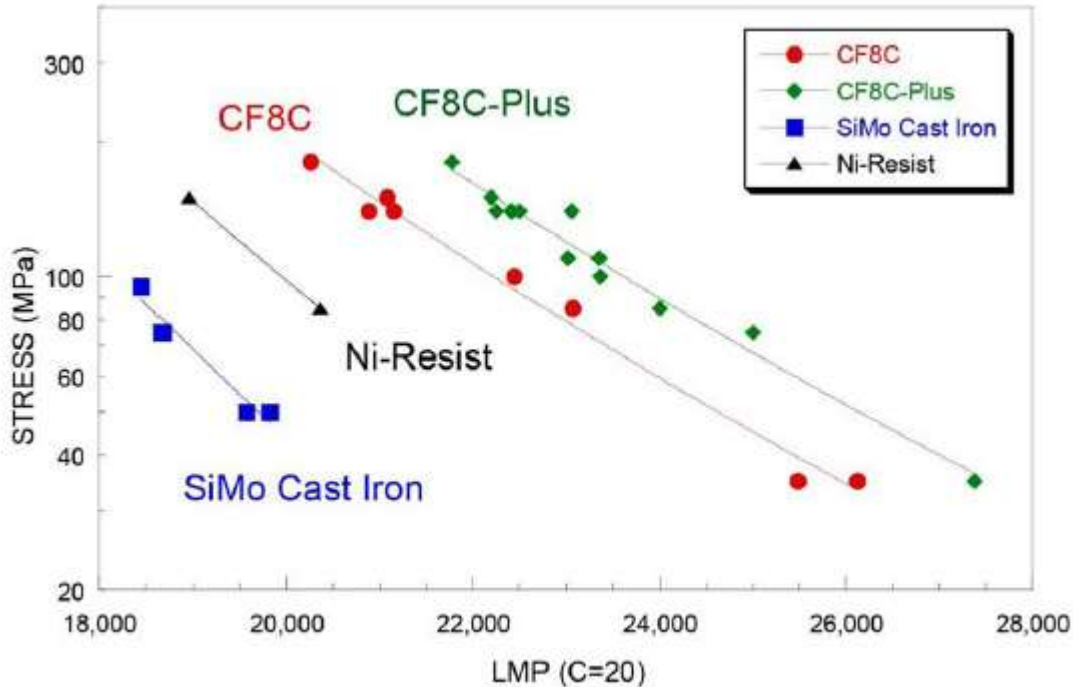


Figure 82 Creep stress versus the Larson Miller for cast iron and CF8C stainless steels [42]

### 3.1.4. Stainless Steel Advantages in Terms of Density

A study that aims at comparing Ni-based super alloys and Ni-Cr to stainless steel [39] for the manufacturing of the exhaust components has revealed that, despite the fact that the competitive alloys achieve the requested young modulus, stainless steel has shown a similar performance providing lower density as shown in figure 83, making it a better choice in terms of density-young modulus basis, while cast iron has been avoided due to its low toughness that cannot withstand the requirements, especially when tested under muffler conditions.

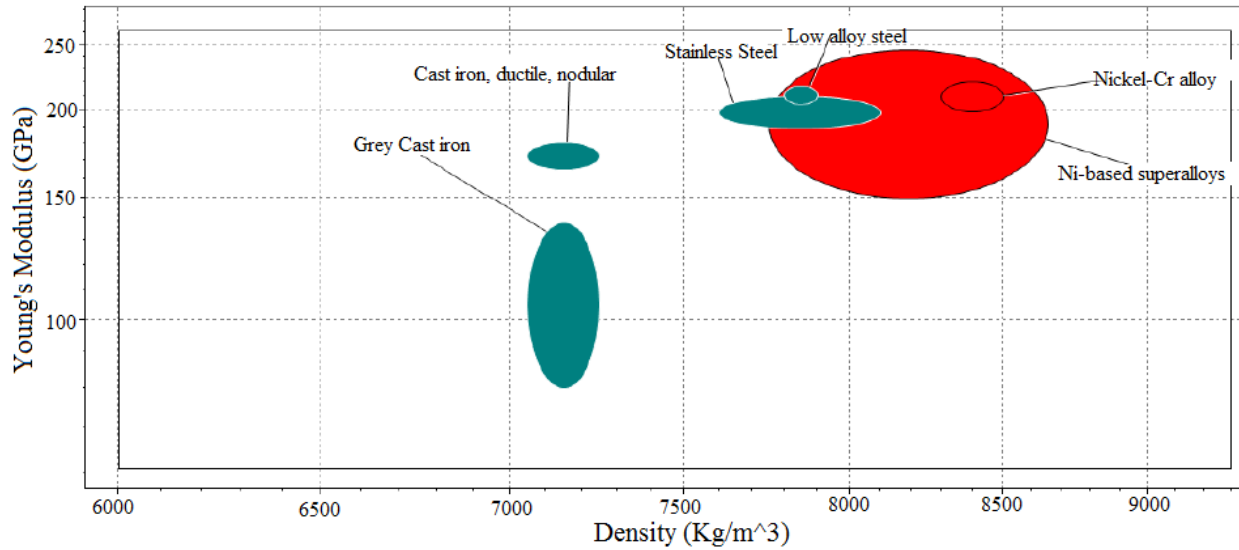


Figure 83 Young modulus Vs. Density for Stainless steels and Ni based super alloys [39]

Ductile cast Iron in general are used due to their low melting point and high fluidity that permit good castability, such as SiMo (effective until 750°C), however either their improved versions such as SiMoCr, SiMoNi, SiMo1000 are used until 835°C [40], above this temperature, the cast iron is replaced with the Ni-resist alloys such as D5S which contains the highest Ni content (up to 37%) that shows satisfying performance around 850°C [40], but also high costs, the reason why Stainless steel has been preferred among others.

In terms of weight reduction, the stainless steel manifold may save up to 50%, where in general terms the stainless steel manifold could be 3 to 4 Kg while that made up of cast iron is about 7 kg.

### 3.1.5. Ferritic Vs. Austenitic Stainless Steel

Efforts have been made in order to develop ferritic stainless steels that can replace the austenitic grades in order to save costs keeping the needed performance and even surpassing the austenitic in terms of thermal oxidation, this is well achieved by adding stabilizing elements, such as Nb, W, and Ti, meanwhile avoiding the volatility of the Ni and Mo additions.

It is important to mention that the new ferritic stainless steel-400-series, showing impressive technical properties, is ready to prove an excellent alternative material to several application used to be “only austenitic”. They were also able reached better weldability and deformability than 304 grade.

#### 3.1.5.1. Ferritic Stainless Steels

Among the different families of stainless steels, Ferritic and Austenitic are considered as competitive for the Exhaust system components. Upon comparing these 2 families, we can say list the benefits of ferritic grades in general terms:

- Some Ferritic grades are cheaper due to the lack of the nickel content.
- Lower thermal expansion coefficient, thus better thermal fatigue resistance and less oxidation.
- Higher thermal conductivity, thus faster reach of TWC light-off temperature.
- Ferritics have higher limit drawing ratio “LDR” which makes them suitable for deep drawing applications.
- Better resistance in terms of stress cracking corrosion.

Many Ferritic grades were able to perform well until 900°C. Nonetheless, temperatures will exceed 1000°C so the focus is to improve the high temperature strength and oxidation resistance. For such purposes, the addition of Nb and/or Ti will increase the strength by strengthening the solid solution, and forming stable carbides. This will be better explained later in this chapter, keeping in mind that ferritic stainless steel has got the privilege on the austenitic due to the higher chromium content and lower cost.

#### 3.1.5.2. Austenitic Stainless Steels

The Nickel content in this family enhances its properties, allowing the following benefits to be achieved, knowing that its employment is considered under the conditions where ferritic cannot be used:

- Higher carbon content than ferritic which make it easier to be casted due to the corresponding lower melting temperature.
- Higher temperature strength.
- Lower Cr% content (17-18%) to maintain the phase stability, further increase of Cr content will require increase in the Nickel content associated with its higher price.
- Better performance in pure stretch forming, i.e. Austenitics have higher degree of deformation in terms of dome height.

The Austenitic Stainless steel grade AISI 309, for example, is used for temperatures up to 1000°C, as well as Cfc8-plus (with 0.8% Nb) is developed just for saving costs. Both grades

have added Niobium in order to improve their mechanical properties and increase the carbide formation that was decreased by lowering the Ni content, for instance in Cfc8-plus [40].

Table 11 shows the difference between the thermal conductivity, thermal expansion, density and young's modulus of ferritic and austenitic stainless steels.

Type of Stainless steel	Density [g/cm <sup>3</sup> ]	Thermal conductivity 100°C [W/m. °C]	Thermal Expansion coefficient 0-600°C, 10 <sup>4</sup> /°C	Young's modulus x10 <sup>3</sup> /Nmm <sup>3</sup>
409/410	7.7	28	12	220
430	7.7	26	11.5	220
Stabilized 430Ti, 439	7.7	26	11.5	220
434, 436, 444	7.7	26	11	220
309	7.9	15	16.5-19.5	200
304	7.9	15	18	200

*Table 11 comparison between developed ferritic grades and the basic austenitic grade 304*

The ferritic Stainless steel AISI 444 has corrosion resistance close to that of the Austenitic grade AISI 316, hence it is considered as an alternative to it. In a similar manner, the stabilized grade AISI 441 could be considered as an alternative to the austenitic grade 304. [43]

## 3.2. Benefits of Niobium Alloyed Stainless Steel into the Application of Exhaust System Components

As we have seen yet, Stainless steel is the major material for the automotive exhaust components, featuring the needed qualifications in terms warranty competence in the market, in addition, the Niobium alloyed grades have been suggested for each of the components such as the new ferritic stainless steel AISI 444 for the exhaust manifold that is able to resist the elevated temperatures up to 1000°C, the higher heat conductivity coefficient for a faster reach of the catalytic converter light-off temperature, highlighting the role Niobium in increasing the oxygen storage capacity in the catalytic converter, and the dual stabilized grade AISI 409 for the muffler. In what follows, we will shed the light on the superior role of Niobium in stainless steels, and its impact on the micro-structural level that improves their characteristics including high temperature strength, creep resistance, drawbaility, weldability, and pitting corrosion resistance making them a first choice.

### 3.2.1. Hot End Components

The position of the exhaust manifold and the close coupled catalytic converter in the hot end makes them the primer components that confronts the very high temperatures exhaust gases up to 1050°C, leading to the need of a new stainless steel grades that is able to maintain their mechanical properties at such temperature, featuring good resistance in terms of creep, oxidation corrosion, and high thermal fatigue life. For such purposes, the two candidate new ferritic stainless steels are 1.4521 and 1.4622.

#### 3.2.1.1. Exhaust Manifold

With the increasing trend of the exhaust gas temperature, material evolution demanded the abundance of the cast iron, due to what have been mentioned before, and the improvement of the ferritic and austenitic stainless steels as shown in figure 84 due to their better mechanical properties at elevated temperature. However, the used stainless steels nowadays can resist temperatures until 950°C such as the Niobium alloyed stainless steel AISI 441, so exceeding 1000°C requested the use of much more resisting stainless steel, for

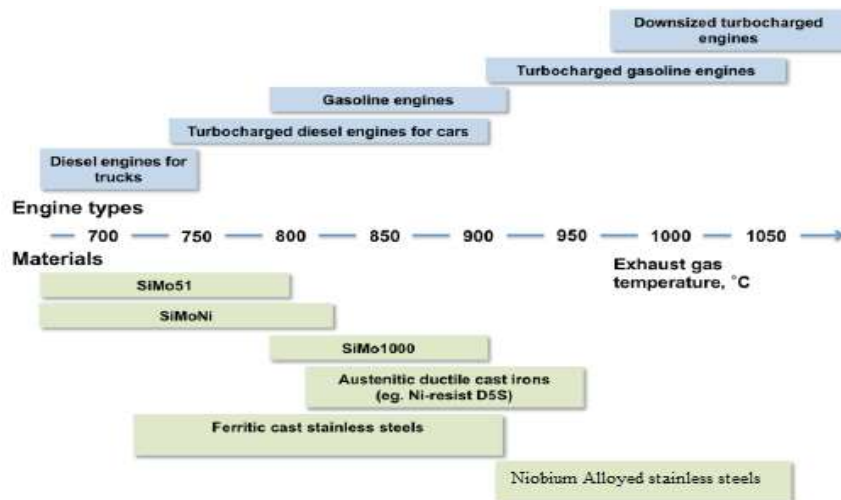


Figure 84 Material Trend evolution for exhaust manifold

which the niobium alloyed stainless steel AISI 444, or En 1.4622, both with added Niobium and Molybdenum could be selected.

For the particular case of exhaust manifolds, Thinner sheet are preferred due to their smaller heat capacity, so high temperature would reach the catalytic converter without great loss resulting in a faster rise in its temperature. Austenitic stainless steels are considered excellent in high temperature applications, however their oxidation scale peels off easily, thus ferritic grades are preferred due to their higher oxidation resistance and lower thermal expansion and the higher thermal conductivity coefficients.

Up to 850°C, some stainless steels are being used for this component such as: AISI 409 (EN 1.4512), a further increase in the temperature up to 950°C where handled by the Niobium addition to the stainless steels, making it possible for the grades AISI 441 (EN 1.4509) and AISI 429 (EN 1.4595) to be used [31].

### 3.2.1.2. Niobium Alloyed Stainless Steel for Exhaust Manifold

#### 3.2.1.2.1. The New Ferritic Grade 1.4521 (AISI 444)

Up to 1000-1050°C, Niobium stabilized stainless steels are emerging to be the solution featuring high strength properties at such elevated temperatures. The new ferritic stainless steel grade AISI 444 (EN 1.4521) whose composition is shown in table 12, showed better mechanical properties, higher creep and fatigue resistance, and improved cyclic oxidation keeping a comparable weldability and formability [44].

Grade	C	Cr	Si	Mn	Mo	Nb
1.4521	0.02	19	0.6	0.3	1.9	0.6

Table 12 Chemical composition of the new ferritic Stainless steel AISI 444

In terms of high temperature strength, the added Molybdenum and Niobium played an effective role in the solid solution hardening, giving the 444 30% higher tensile strength than 1.4509 as shown in figure 85. As well as the higher mechanical strength provided by the added Nb and Mo increased the fatigue limit about 50% at 850°C as shown in figure 86.

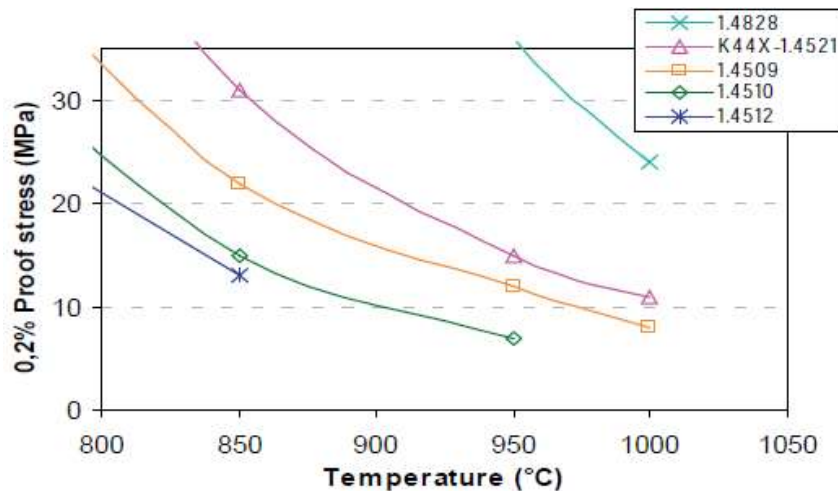


Figure 85 the higher tensile strength of AISI 444 between 750 and 1000 °C [44]

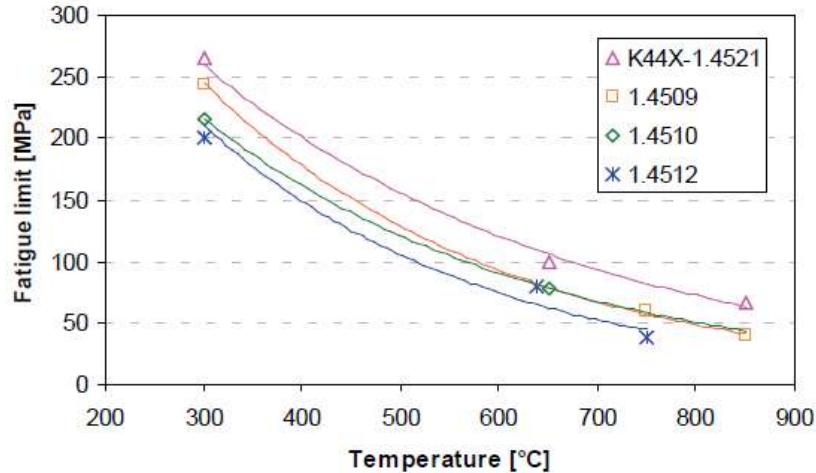


Figure 86 Fatigue limit of AISI 444 at 2 million cycles as function of Temperature [44]

Compared to 1.4509, the new AISI 444 showed 25% less mass gain at 950°C, and it showed parabolic trend when temperature is up to 1000°C while the 1.4509 showed rapid acceleration, which means that AISI 444 has higher oxidation resistance as demonstrated in figure 87.

The fact that Niobium is able to bind with Fe forming Fe-Nb precipitation can explain the better creep resistance of the new AISI 444 that showed the lowest deflection at all temperatures among the tested austenitic and ferritic grades as shown in figure 88.

In terms of thermal fatigue, 4444 showed superior performance over AISI 441 (1.4509), where the first has up to 40% longer life time as demonstrated in figure 89.

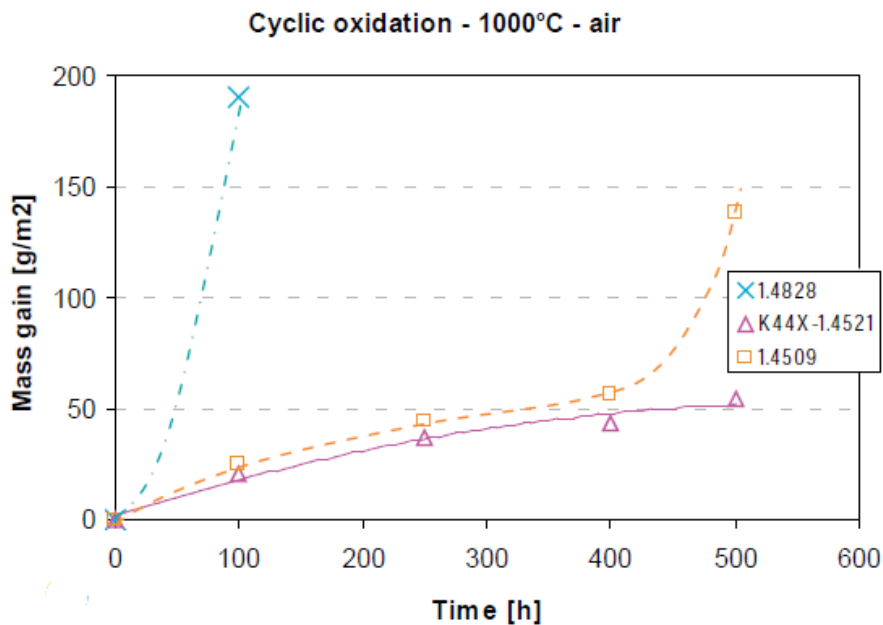


Figure 87 Cyclic oxidation at 1000 °C of AISI 444 and 1.4509 [44]

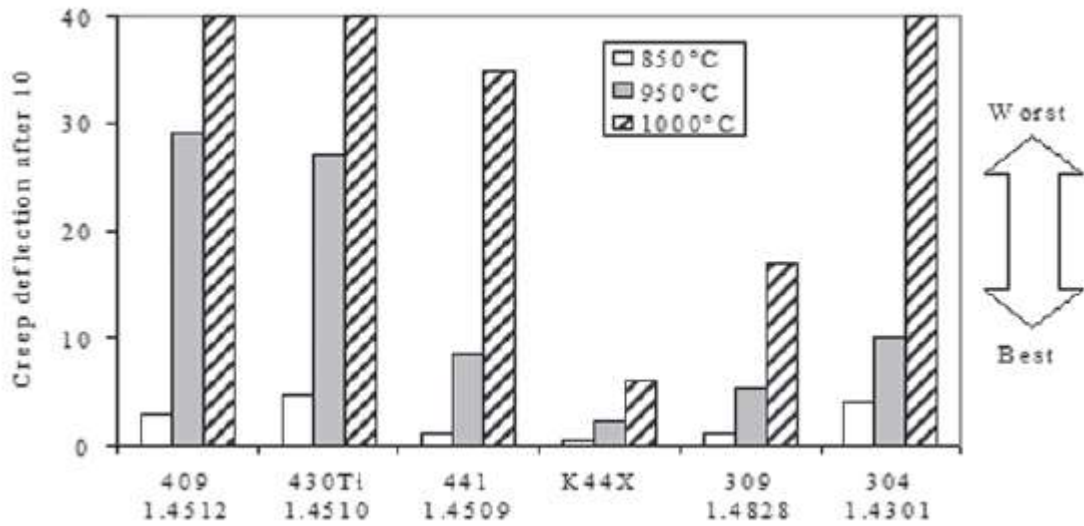


Figure 88 deflection of different Stainless steel grades at different temperatures [44]

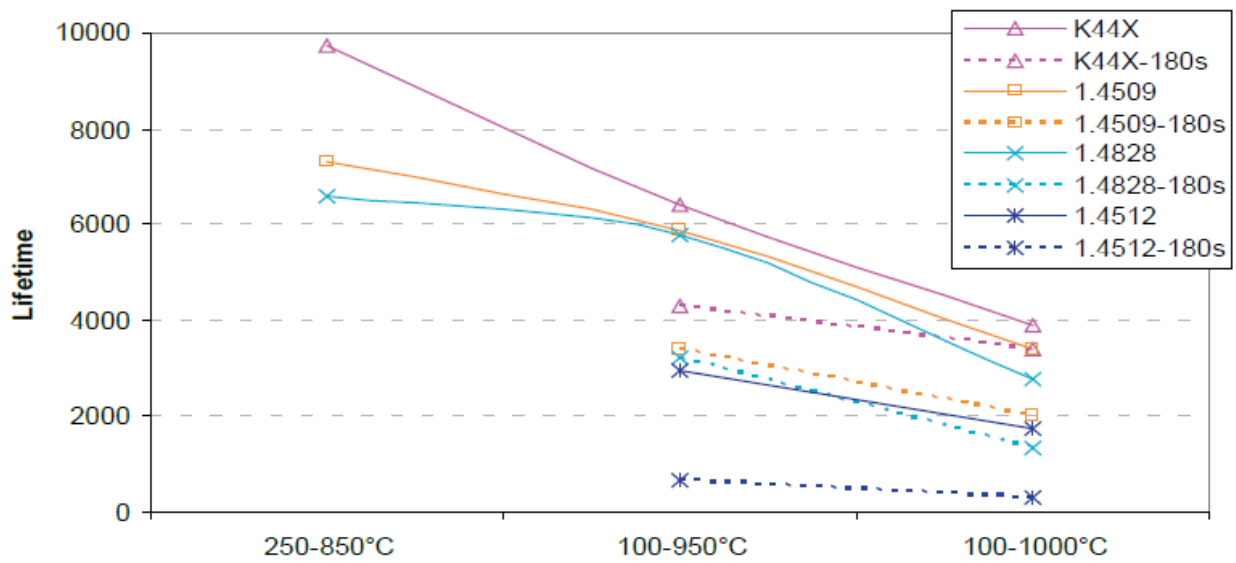


Figure 89 Lifetime of different stainless steel grades up to 1000°C [44]

Figure 90 illustrates the superior resistance measured in PRE to localized corrosion of the grade AISI 444 compared to several different austenitic and ferritic grades which showed inferior performance.

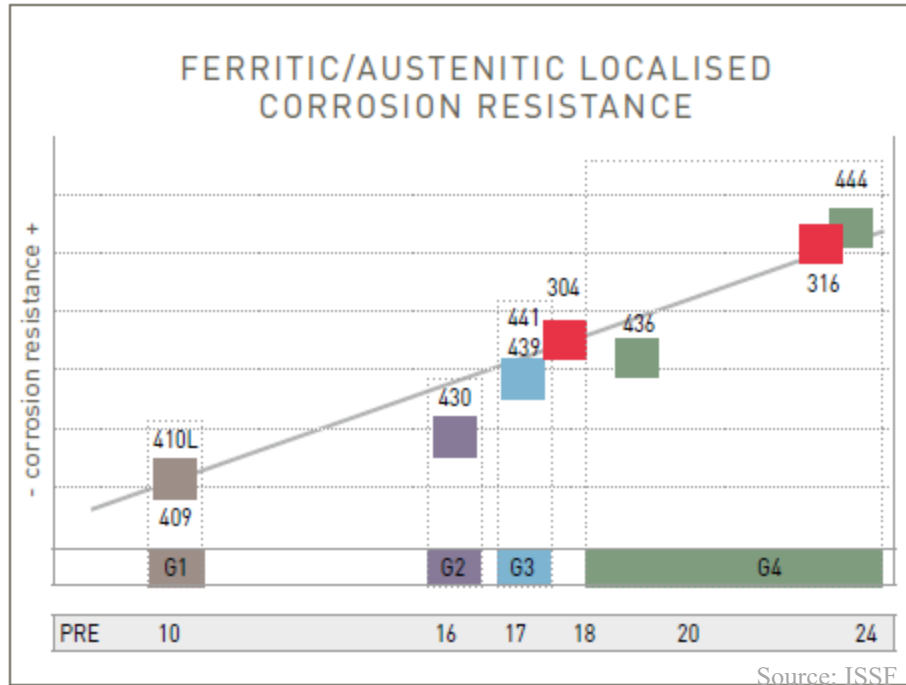


Figure 90 Corrosion resistance of AISI 444 compared to other Ferritic and Austenitic Grades [60]

### 3.2.1.2.2. The New High Nb Ferritic Grade 1.4622

Another new dual stabilized ferritic stainless steel whose chemical composition is shown in table 13 has shown a good performance in temperatures up to 1050°C, as well as high formability (see chapter 4). Such grade with 21% Cr has a high corrosion resistance, comparable to that of the austenitic grades. The performance achieved in terms of keeping good mechanical properties at high temperatures is related to higher dissolution temperature of the laves phase Fe<sub>2</sub>Nb (known as η phase) that increases the onset of grain growth consequently [45]. This

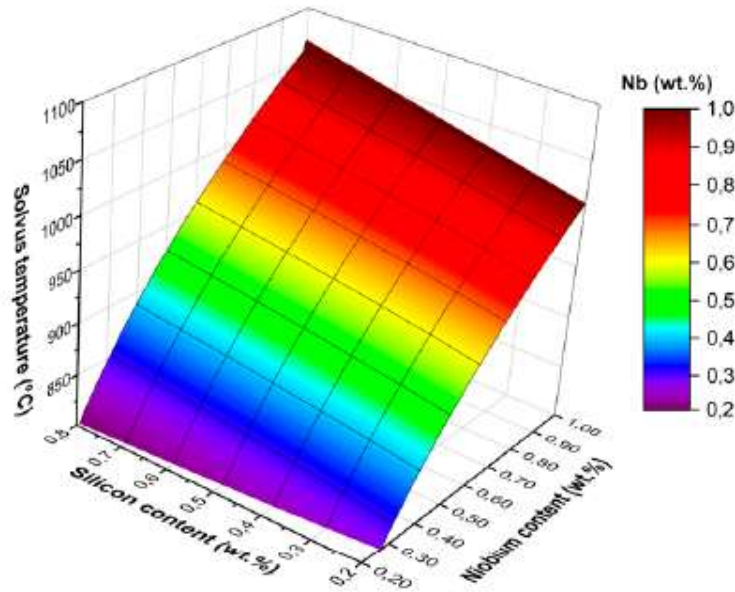


Figure 91 η-phase solvus temperature as function of Nb content [45]

improvement is found to be increasing with the increase of Nb content as shown in figure 91, where the highest solvus temperature is associated with the higher Nb content.

Grade	C	N	Cr	Ti	Mo	Nb	Si	Mn
1.4622	0.02	0.02	20.8	0.17	0.03	0.36	0.48	0.4
High Nb	0.02	0.02	21	0.2	0.02	0.8	0.8	0.32

Table 13 Chemical composition -by mass%- of 1.4622 and High Nb Stainless steels

Even though the increase in the solvus temperature could be achieved by adding Si as shown in figure 91, however an increase by 0.4 wt.% Si results in 30°C higher solvus temperature, whereas the same fraction, if added as Nb instead, would result in up to 150°C higher temperature. On the other hand, Mo is much lower in 1.4622 than in 1.421, because upon comparing the effect of Mo on the solvus temperature, the 2% presented in 1.4521 got no significant increase.

For dual stabilized stainless steels, the Ti content should be no more than 0.2% [45] limiting its role to capturing C and N forming carbides and avoiding the Cr depletion, while higher amount of the Nb is added to further form carbides, and form the  $\eta$ -phase associated with the increased creep resistance.

In terms of creep resistance, the creep size that dominates in the hot end is called “Coble creep” i.e. low stresses and high temperatures. This type of creep is highly dependent on the grain size, and it is inversely proportional to its cubic [45], it is controlled by grain boundary diffusion where the  $\eta$ -laves provide the needed pinning effect, thus preventing grains from sliding even with those of finer size. The  $\eta$ -laves phase advantages are translated to their precipitation hardening effect. Even though these precipitates could be found both on the grain boundaries and inside the matrix, the need of controlling their nucleation by choosing the appropriate annealing temperature and holding time is a must.  $\eta$ -laves precipitate during pre- annealing (in a 2 step reduction process discussed in chapter 4) as well as during cooling, then these precipitates are meant to be dissolved during pre-annealing to obtain a full recrystallization. Hence, full recrystallization and dissolved precipitates are obtained at an optimal pre-annealing temperature 1150°C, then it will precipitate again after recrystallization featuring the creep resistance.

Nonetheless, a compromise is to be considered in terms of the grains size. On one hand, the larger grain size (associated with the increase in the pre-annealing temperature to dissolve the  $\eta$ -laves) increases the creep strength, while on the other hand, the finer grain size is advantageous in terms of formability, and high temperature strength. So, the temperature for the final annealing has to be lower and carefully selected, it was shown that 1120°C is an optimal choice to obtain a finer grain [45].

In order to mark the effect of Nb on the creep resistance, a comparison is made between the 1.4622 and a similar composition with higher Nb content (labeled as High-Nb stainless steel) whose composition is shown in table 13. In order to be able also to compare the two candidate

steels for the hot end, 1.4521 (AISI 444) is also tested. The results of the sag test are shown in figure 92 [45], where the high-Nb stainless steel showed the lowest deflection (in [mm])

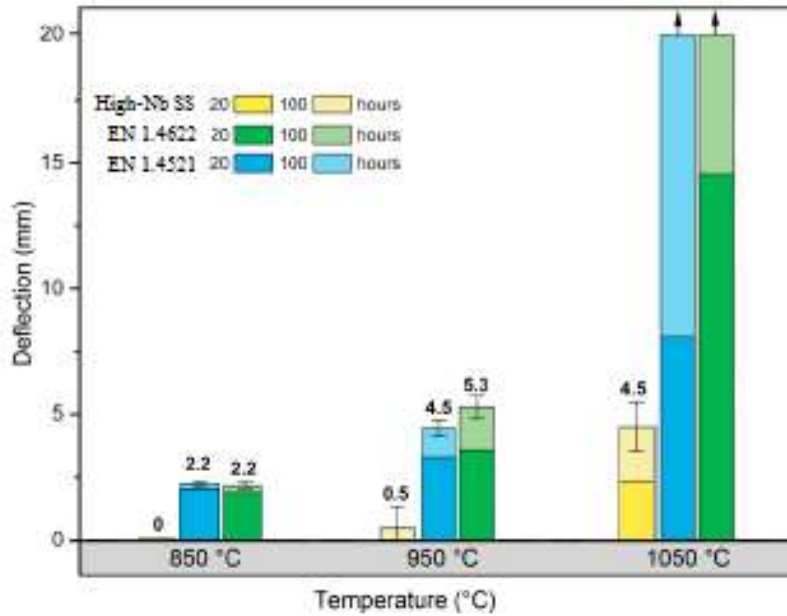


Figure 92 creep resistance of hot end candidate steels [45]

compared to both grades 1.4622 and 1.4521 at the target temperature 1050°C.

It is also beneficial to mention that this grade has a high pitting corrosion resistance, higher than that of the austenitic grade 304, but inferior to the previously mentioned 1.4521 (AISI 444) as shown in the figure 93, however both grades showed much higher PRE number [46].

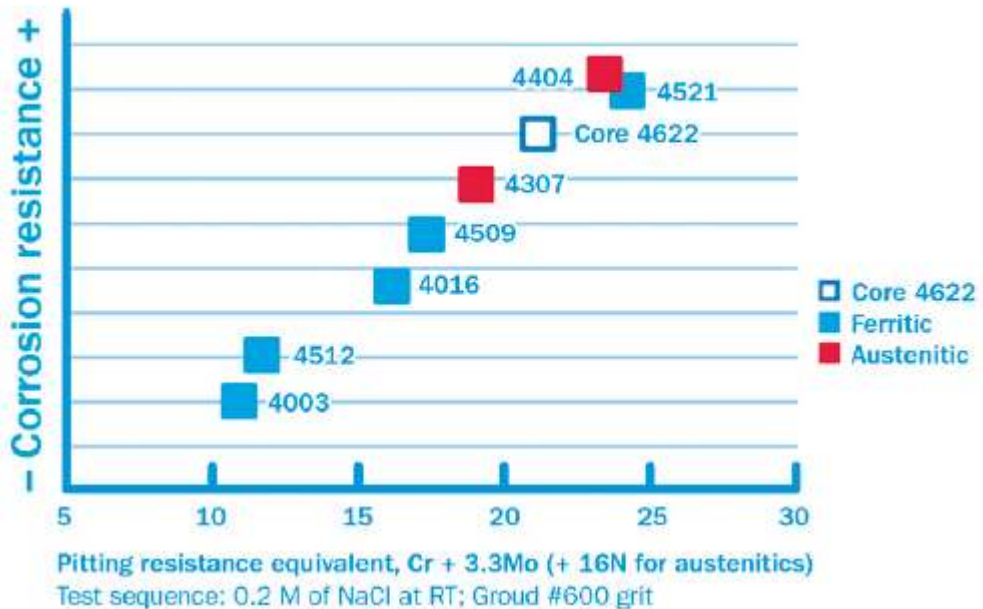


Figure 93 Pitting corrosion resistance of the grades 1.4622 and 1.4521 compared to other stainless steels [46]

### 3.2.1.2. Catalytic Converter

The metallic honeycomb substrate of the catalytic converter shown in figure 40 is preferred at high temperatures as it is placed close to the exhaust manifold in close coupled layout.

Ferritic stainless steel foils are chosen for the honeycomb core, and sheets are chosen for the shell due to their good thermal shock properties and small heat capacity. For the shell, some the recommended grades are: SUS 439L, SUH 409L, SUS 430, SUS 432L, SUS 441L, and SUS 436LM for their ductility, strength and corrosion resistance [47], whereas for the substrate, SUS 441L, SUS 432L, SUS 436L, SUS 439L.

However, when closed coupled, the exhaust gas will directly reach it after the exhaust manifold, hence the AISI 444 or 1.4622 stainless steels are recommended for the same features they provided for the exhaust manifold, with exhaust gas reaching with temperature up to 1000-1050°C.

### 3.2.1.3. Flexible Joint

As explained bin Chapter 2, the flexible joint (or flexible below) shown in figure 71 is a necessary component that reduces the vibration and their impact on the exhaust system. The chosen material should show high ductility and bendability, for this, the recommended stainless steel grades are: SUS 304, SUS316Ti, SUH 409L, SUS 439L and SUS430 [47].

## 3.2.2. Effect of Niobium on High temperature Strength

Knowing that Molybdenum is effective in increasing the high temperature strength as the associated proof stress increases linearly with Mo, it was found that Niobium has a similar effect,

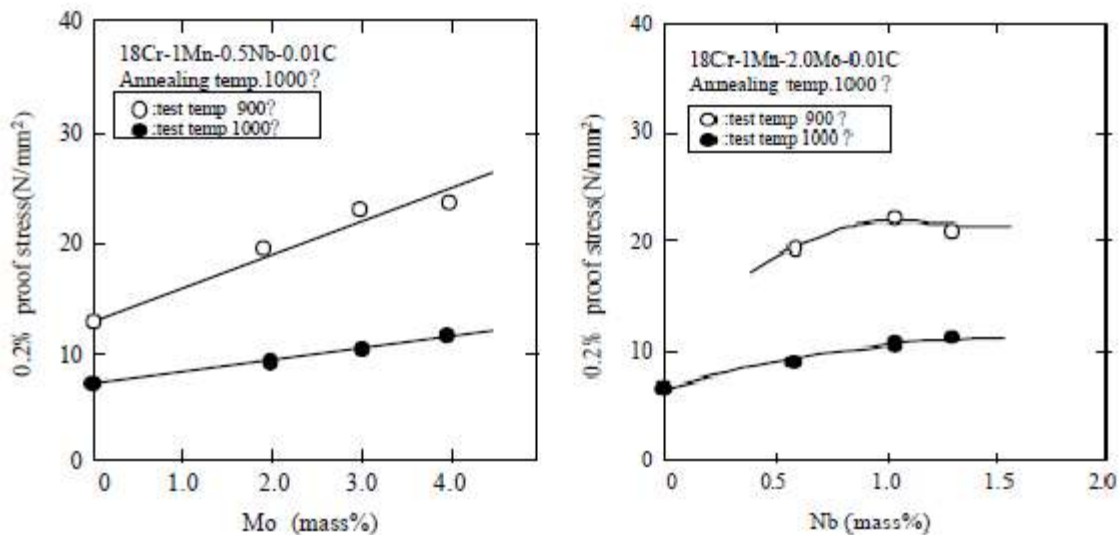


Figure 94 comparison between the effect of Mo and Nb on high temperature strength at 900 and 1000°C [48]

however, Niobium keeps a linear trend up to 0.8% then it tend to flatter. In order to evaluate which one is more efficient from alloying percentage point of view, Niobium is considered more effective, and this is well demonstrated in figure 94 [48].

### 3.2.2.1. Niobium Role as a Stabilizing Element

Due to the fact that the solubility of carbon in ferrite is much lower than that in austenite, stabilization was found in order to maintain a fully ferritic structure at all temperatures. Ti was the first stabilizing element in this domain due to its higher affinity to C and N than Cr, however increasing the Ti content was not beneficial at high temperatures as it starts to precipitate at 850°C, as well as high concentrations of Ti compromise the steel casting and the surface quality. For such reasons Niobium was introduced as a better stabilizing element that may be added with Ti in order to remove the C and N from the high temperature solid solution thus eliminating  $\text{Cr}_{23}(\text{C}, \text{N})_6$  at grain boundaries, where  $(\text{Ti}, \text{Nb})\text{C}$  was found to precipitate at higher temperatures (up to 1150 °C) as shown in figure 95. Thus, hindering the formation of Cr carbides, leaving Chromium in the steel lattice instead of depleting it.

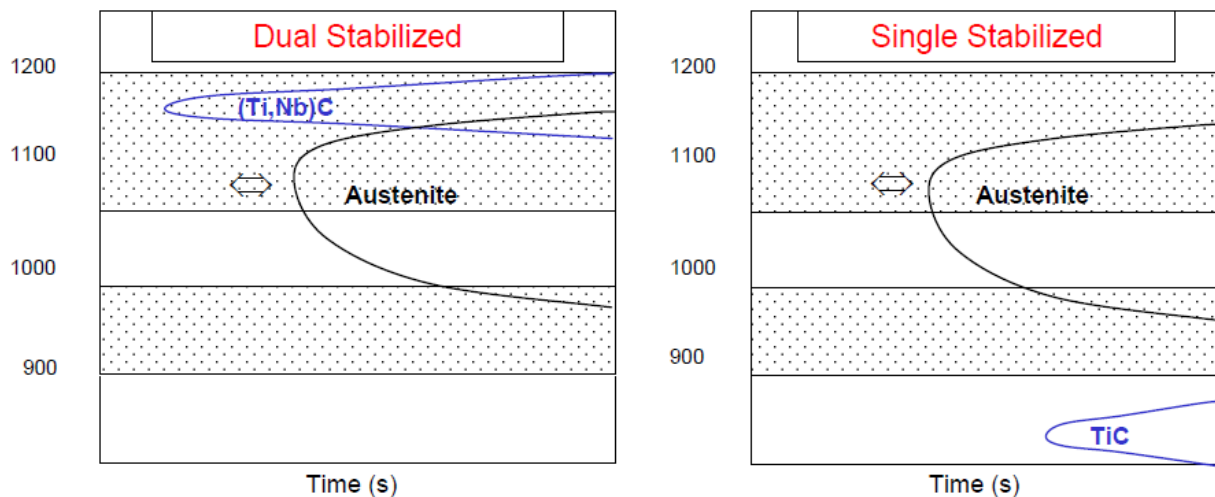


Figure 95 Niobium effect in Stabilization of T409 stainless steels [49]

Consider the non-stabilized stainless steels with 16-18% Cr content, these grades show grain coarsening at high temperature, and possible martensitic transformation in the austenized areas and intergranular carbides precipitation, resulting in brittle microstructure especially under welding conditions.

The amount of the stabilizing elements, Nb and Ti, should be 6 to 8 times the Carbon + Nitrogen content for an effective results.

The major benefits of using Nb as a stabilizing element, especially in dual stabilized grade such as AISI 409 Ti-Nb, are the improved surface quality, better formability and weldability, improved thermal fatigue resistance, better resistance to dry (high temperature corrosion) and wet corrosion. These results are interpreted as a consequence of the excess of Nb solute remaining in the matrix after precipitation reactions took place. [49]

### 3.2.2.2. Niobium Role in Improving High Temperature Strength

High temperature strength could be improved by solid solution strengthening, precipitation hardening and grain refinement. These three mechanism are established by adding Niobium as a stabilizing element, especially in the case of ferritic stainless steels.

Titanium stabilizing effect in AISI 409 was satisfying until temperatures exceeded 800°C in the exhaust system application, these higher temperatures demanded the dual stabilization by Niobium and Titanium instead. Niobium addition made it possible to resist temperatures up to 950°C i.e. 150°C more with acceptable mechanical properties of AISI 441, providing that both grades with niobium, AISI 441 and AISI 444, were able to perform at higher temperatures where other grades was not able to resist as shown in figure 96.

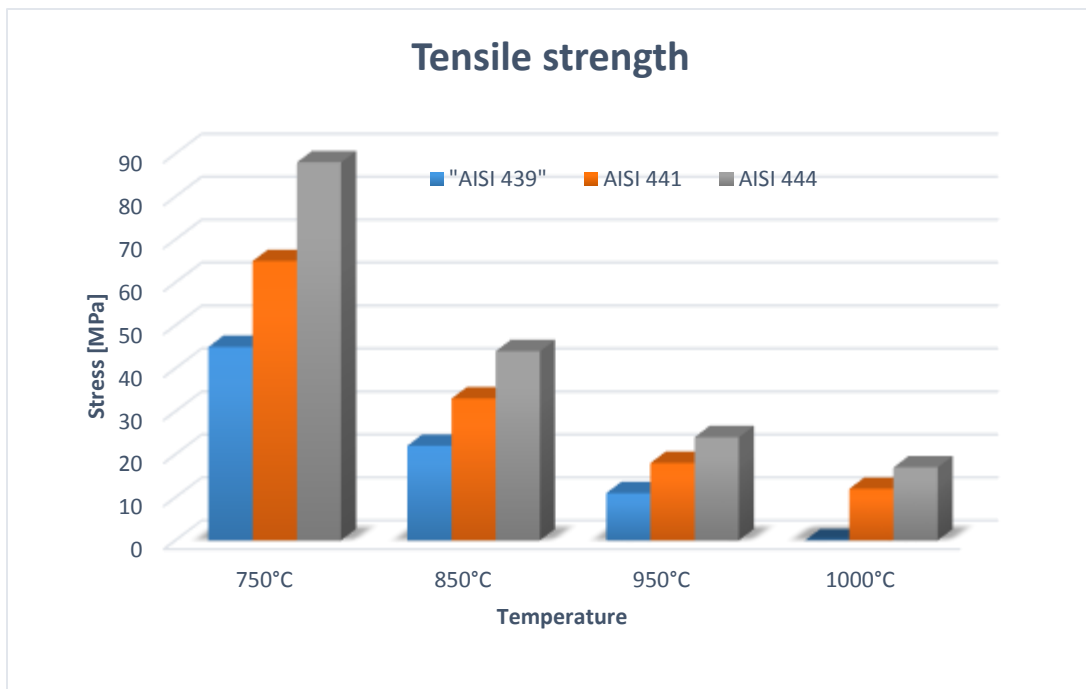


Figure 96 Tensile strength as function of temperature of AISI 439, 441, and 444

Aiming at comparing the effect of different alloying elements on the high temperature strength, Nb, Si, Ti, Mo, W, Hf, and Ta are tested and compared. The results shown in figure 97 demonstrated that Niobium additions are the best in increasing the high temperature (950°C) yield strength (0.2% proof strength) among the other candidates [49]. The result revealed that for a defined yield strength, some elements are not even able to be adopted, as well as among those who were able to increase the yield strength to the needed level, they must be added in a higher weight percent reaching almost double or triple that achieved by Nb.

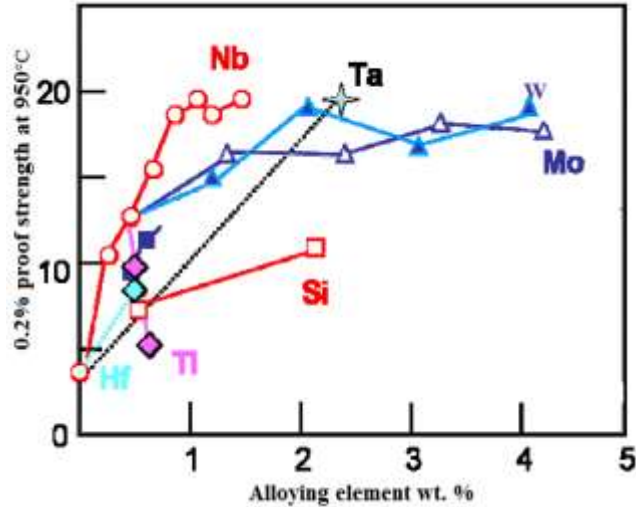


Figure 97 Effect of different alloying elements on yield strength [49]

### 3.2.2.3. Niobium in Increasing Creep Resistance

Niobium carbides, mainly NbC, is of primer importance when it comes to creep resistance. The role that Niobium plays in solid solution strengthening through the formation of fine Nb(C, N) and Fe<sub>2</sub>Nb can achieve also the precipitation hardening effect. This is well demonstrated in a study tested the difference between 15CrNbTi and 15Cr0.5MoNbTi [50], where despite the advantages that Mo added at high temperatures, the precipitates formed by Nb, shown in figure 98, both the rod and the ellipsoidal Fe<sub>2</sub>Nb shapes (which is considered better than rod shape), improved the creep resistance and increased the fatigue life due to their pinning effect.

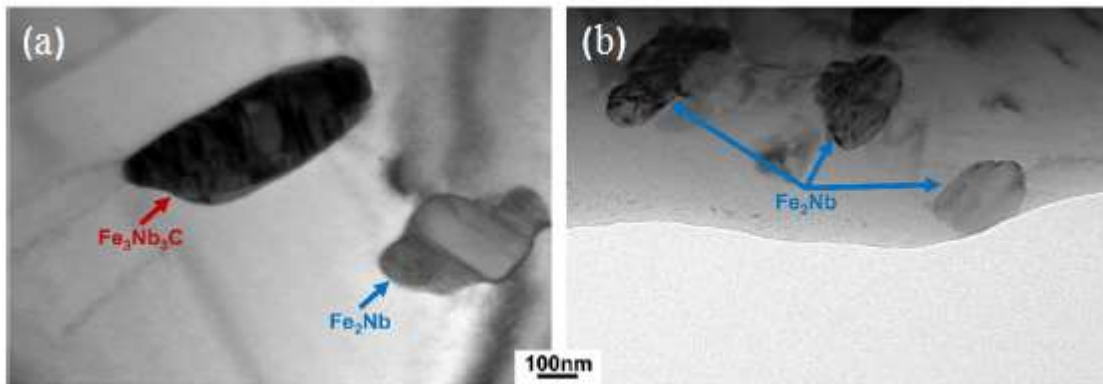


Figure 98 Bright field images of the precipitates in fractured specimens for (a) 15CrNbTi and (b) 15Cr0.5MoNbTi in simulated exhaust gas [50]

In a more general terms, comparing the stress-strain diagrams of stabilized and non-stabilized stainless steels [51], the result indicated that the temperature associated with a steady state creep is shifted for the stabilized grades as shown in the figure 99.

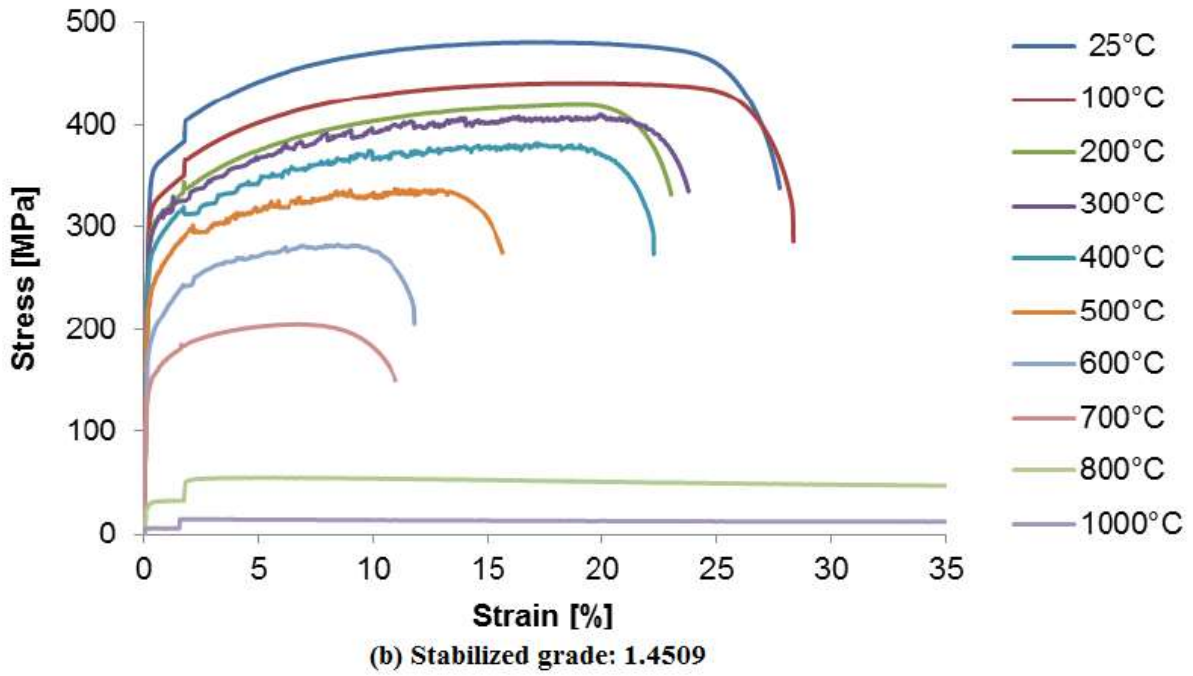
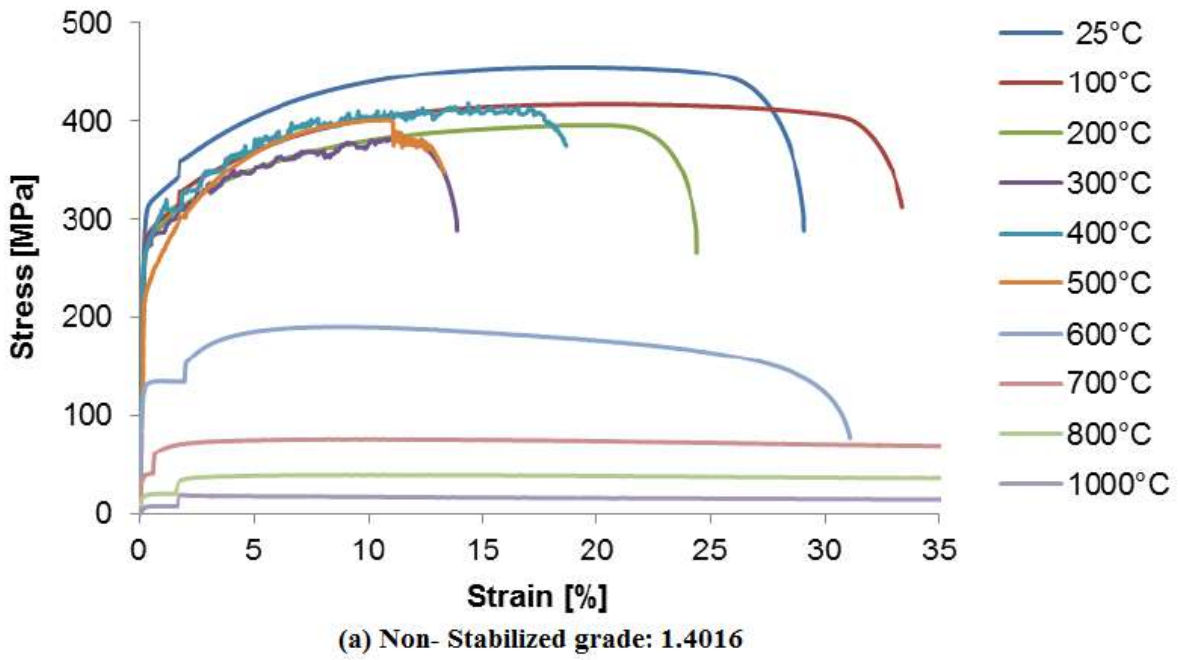
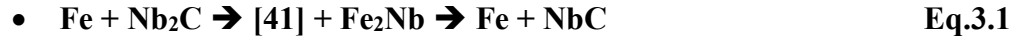


Figure 99 Stress-strain diagrams of non-stabilized and stabilized grades at different temperatures [51]

### 3.2.2.4. Niobium Role in Mitigating Lüders Deformation at High Temperature

For a better formability of Ferritic stainless steels, Lüders deformation is an undesired mechanism. A study testing the effect of Niobium stabilization on such deformation revealed that annealing at high temperatures (about 1000°C) has promoted the formation of the Fe<sub>2</sub>Nb laves type releasing a free Carbon atoms, according to the following reaction 2.1, starting from Niobium precipitates type Nb<sub>2</sub>C [53]:



Hence, with the increased annealing temperatures, Nb<sub>2</sub>C tends to form Fe<sub>2</sub>Nb laves with the carbon being distributed around it. Further annealing at higher temperatures around 1050-1100°C enhanced the Carbon distribution homogeneously, leaving only Niobium precipitates of the type NbC and Nb(C, N) that hindered the Lüders deformation as shown in figure 100 [53], in addition, the brittle sigma precipitation doesn't take place. As well as, these formed particles provided the pinning effect that hindered the grain growth. It is important to mention that, among the precipitates, the Fe<sub>2</sub>Nb was found to have a higher coarsening rate at high temperature than that of NbC, which makes the MX (Nb(C, N)) precipitates preferable [54].

Apart, a uniform  $\gamma$ -fiber texture is obtained, which could be translated into better formability performance.

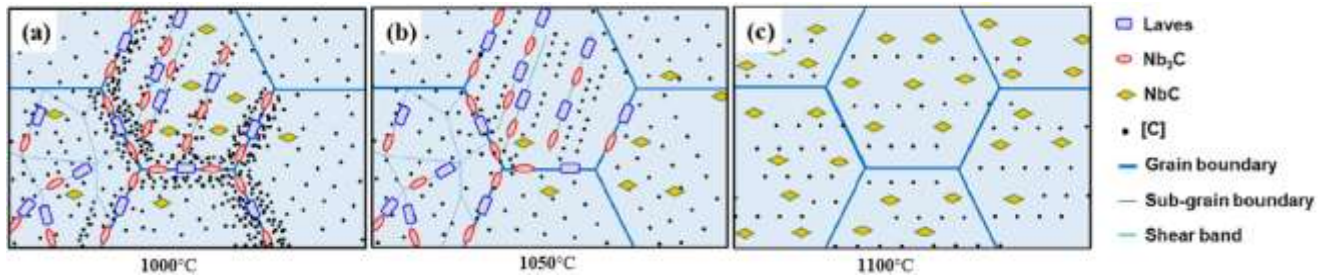


Figure 100 Laves phase Transformation at (a) 1000°C, (b) 1050°C, and (c) 1100°C [53]

Furthermore, two levels of Niobium, 0.5% and 1% are tested to evaluate the associated increase in the proof strength as function of the annealing temperature, it was found higher proof stress is achieved at higher annealing temperature, and that the higher amount of Niobium in the solid solution increases with the corresponding higher annealing temperature. Consequently, the proof stress is higher for the 1% Nb stainless steel due to the effect of Niobium in solid solution hardening as shown in figure 101 [48].

The percentage of Nb in the solid solution could be estimated by the equation 3.2 [55]:

$$\bullet \Delta\text{Nb} = \% \text{Nb} - 7.7 \times 0.74 (\% \text{C}) \quad \text{Eq. 3.2}$$

In addition, above 1050°C no molybdenum is detected as precipitate, however, Niobium precipitates exist, and they also improved the high temperature strength.

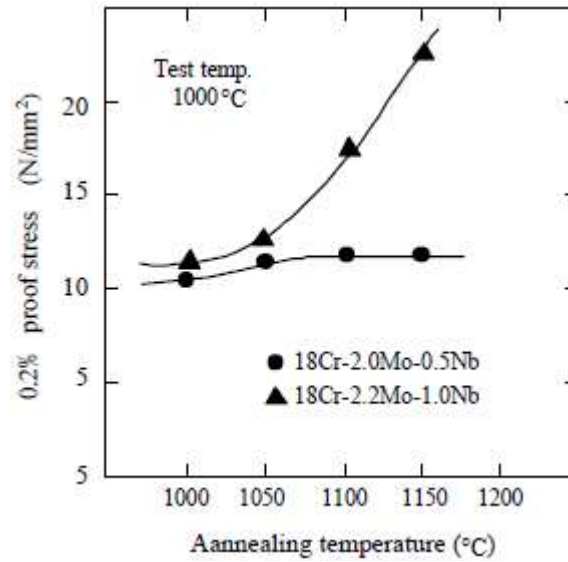


Figure 101 Effect of Niobium and annealing temperature on the proof stress [48]

### 3.2.3. Cold End Components

The components that belong to the cold end fails because of corrosion, suffering mainly from pitting corrosion due to the condensation of the very corrosive agents. Thus the need to improve their corrosion resistance is derived from the increasing warranty period (up to 10 years) for the competitiveness in the market.

#### 3.2.3.1. Muffler

The temperature of the muffler is not as high as the components belonging to the hot end making it easier to employ already existing grades that satisfy the requirements in terms of corrosion. Among the available grades that have good strength and corrosion resistance, is the ferritic grade SUH409L that was designed for the external part of the exhaust automotive system silencers which are not exposed to severe corrosive conditions [43], as well as SUS436L and SUS436J1L with the reduction of the added molybdenum for economic reasons, and SUS 441, i.e. Niobium stabilized grade [47].

Encountering the pitting corrosion that is mostly appearing in the muffler, the developed YUS190 (with added Niobium, similar to AISI 444 in composition) shows a behavior similar to the austenitic grade SUS304 as shown in figure 102, thus providing the needed resistance with saving advantages.

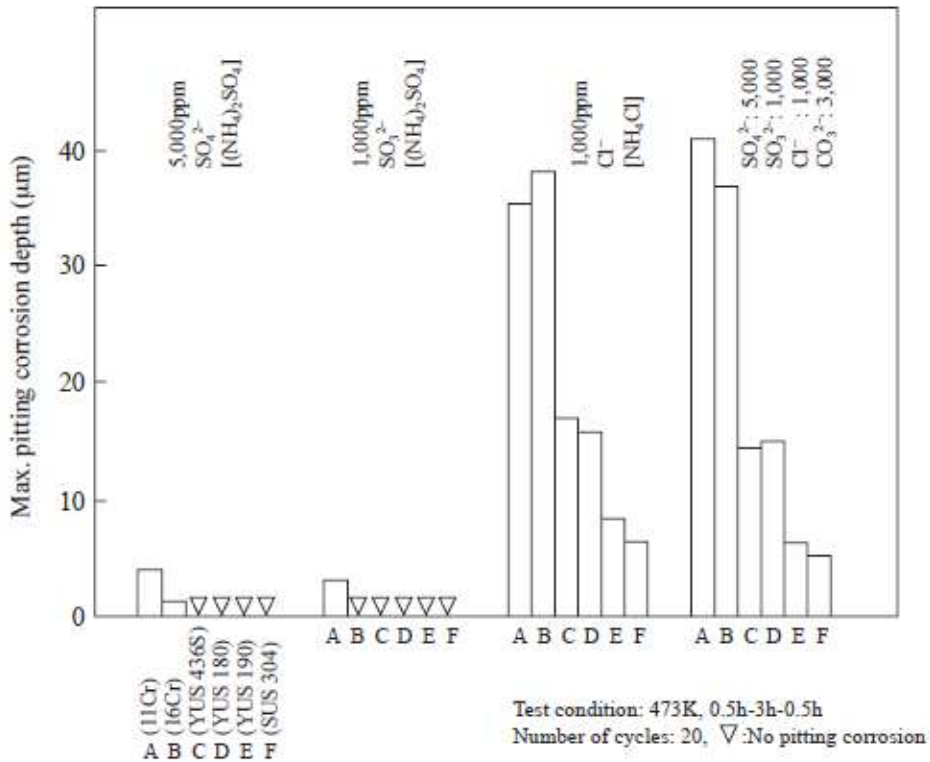


Figure 102 resistance to pitting corrosion of different stainless steels [57]

### 3.2.3.1.1. Niobium Addition for Muffler's Stainless Steel

According to a study that tested the effect of niobium on the corrosion resistance [56], it was observed that the increasing resistance against corrosion corresponds to the increase of the Niobium content from 0 to 0.15% in the 409 Ti-Nb, as well as the fatigue life increased as shown in figure 103.

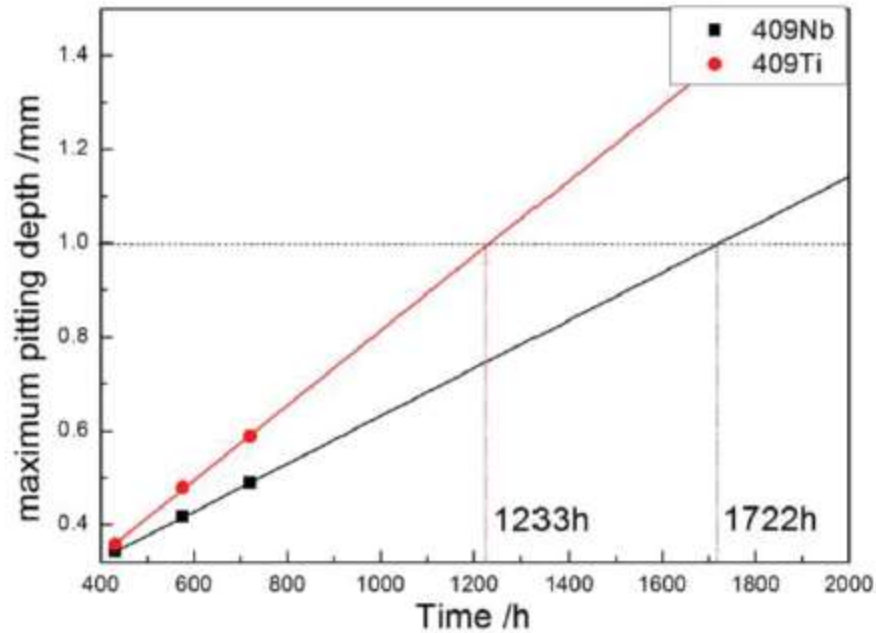


Figure 103 Life prediction of 409Ti-Nb and 409Ti [52]

The Niobium addition to the 409Ti grade resulted in an increase in the high temperature mechanical properties [56] as shown in the figure 104, this increase is due to the Nb (C, N) precipitation that takes place in the steel. Even though at 800°C both grades are almost similar, however, the muffler belongs to the cold end, where the temperature will not reach that limit, giving the privilege to the Nb alloyed grade over the other.

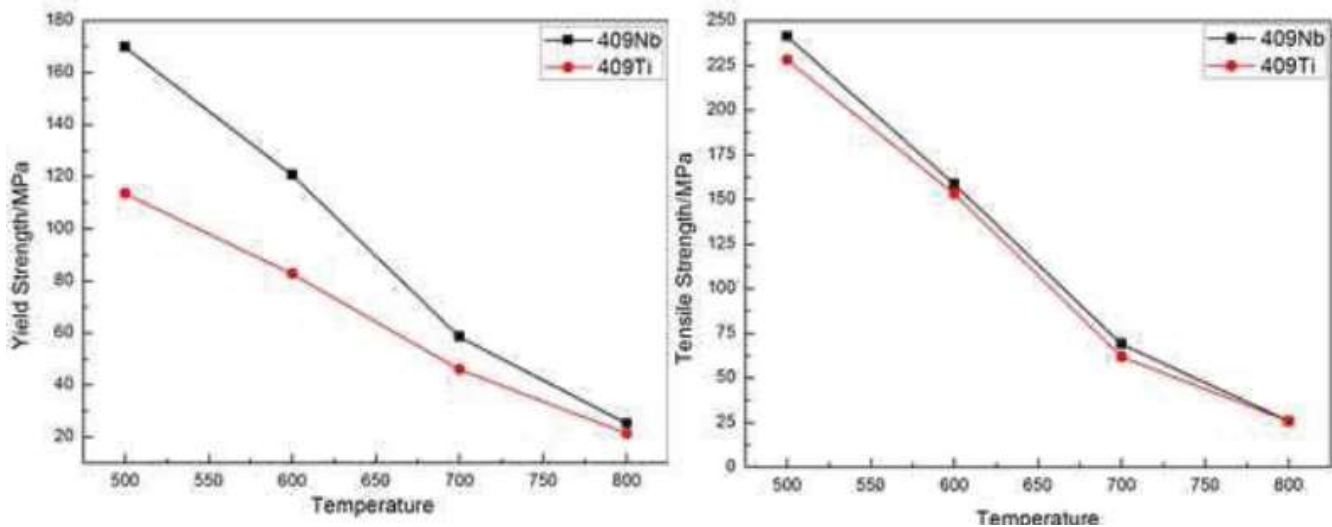


Figure 104 Yield and Tensile strength of 409Ti and 409 Ti-Nb at different functions.[52]

In a test aiming at increasing the Niobium content to 0.31%, it was found that the 409Ti-Nb 0.31% performs the best in high temperature fatigue [56] compared to 0.15% and 0% Nb as shown in figure 105, where N is the number of cycles.

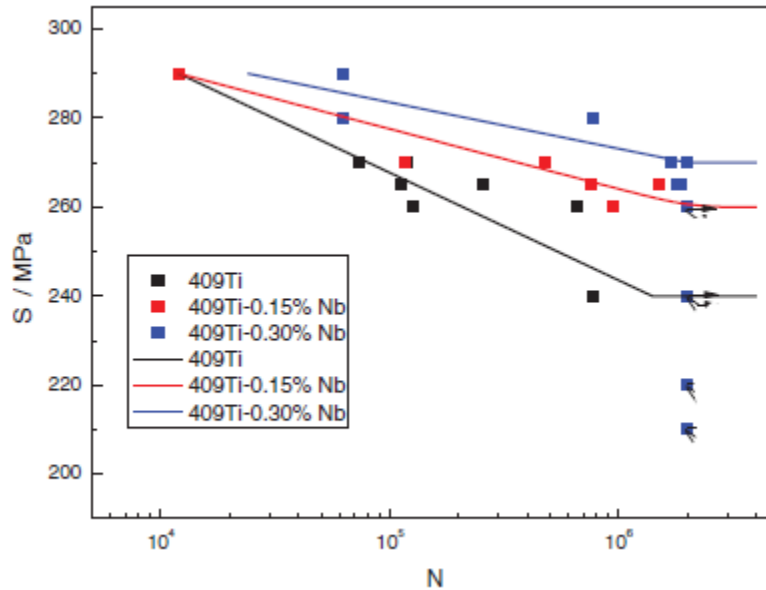


Figure 105 fatigue life comparison for 0.31%, 0.15% and 0% Nb [52]

### 3.2.3.2. Tail End Pipe

Considering this part as an external-visible part that is exposed to eyes, the chosen material must have also good appearance in addition to the corrosion resistance. Since the temperature is the lowest at this point, high purity ferritic and austenitic grades as used such as SUS409L, SUS 430 and SUS436, and SUS 304 [57].

In other words, when the tail pipe is not below the car, 304 grade is preferred due to its bright look after polishing, however, the ferritic grades are an alternative when the appearance is not of primer importance, i.e. the tail pipe is not visible.

### 3.2.4. Niobium against Corrosion

#### 3.2.4.1. Niobium against Pitting Corrosion

In chapter 2, the direct relation between the chemical composition and the pitting resistance is stated in terms of the PREN number. However, the comparison of different grades containing Niobium in the grade AISI 441 and AISI 444 (with Molybdenum) shows increased pitting corrosion resistance compared to the grade AISI 409 that has been used before, as the PREN number increased up to almost 18 and above 25 for the grades AISI441 and AISI 444 respectively, while it was below 12 for AISI 409 [43].

However, a study aiming at testing the effect of Niobium has considered the grade AISI 409 in three different chemical compositions, the first if Niobium free, the second is alloyed with 0.15 wt.% Nb, and the third with 0.3 wt.% Nb [50]. The result in terms of pitting depth revealed that AISI 409 Ti-Nb has better corrosion resistance than the AISI 409 Ti (Nb free), and that the increasing Nb content is associated with decreasing pitting depth measured in [mm] as shown in figure 106.

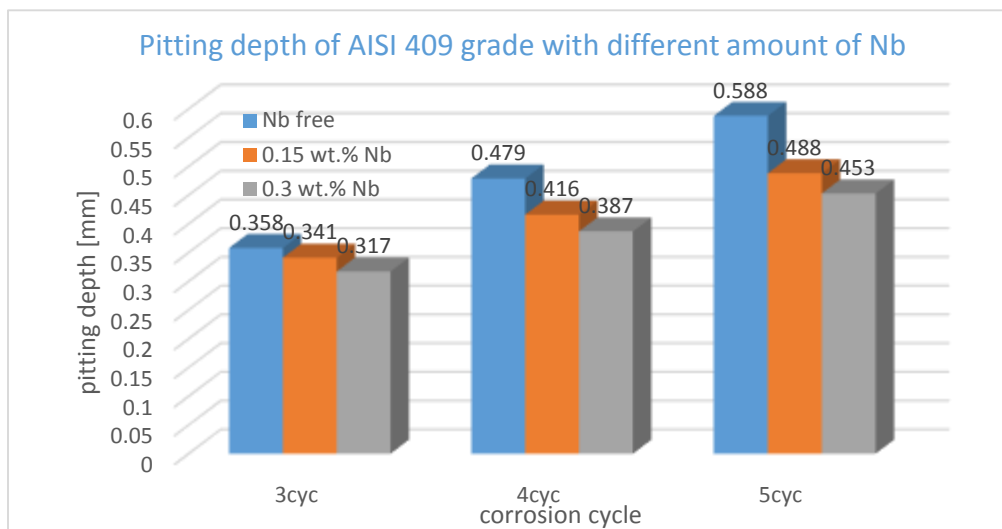


Figure 106 pitting depth trend as function of Niobium content in Ferritic stainless steel

For the same studied sample, a failure threshold is considered to be at 1[mm] pitting depth, and the life time is measure accordingly. The results showed that the higher Nb containing sample i.e. 0.3 wt.% AISI 409 Ti-Nb has the longest life reaching 1874 h compared to 1233 h for Nb free AISI 409 Ti. Thus, 40% longer lifetime as demonstrated in figure 107. In particular, the range up to 600°C -containing the cold end components- could see that AISI 409Ti-Nb a material of choice, featuring such characteristics for the muffler.

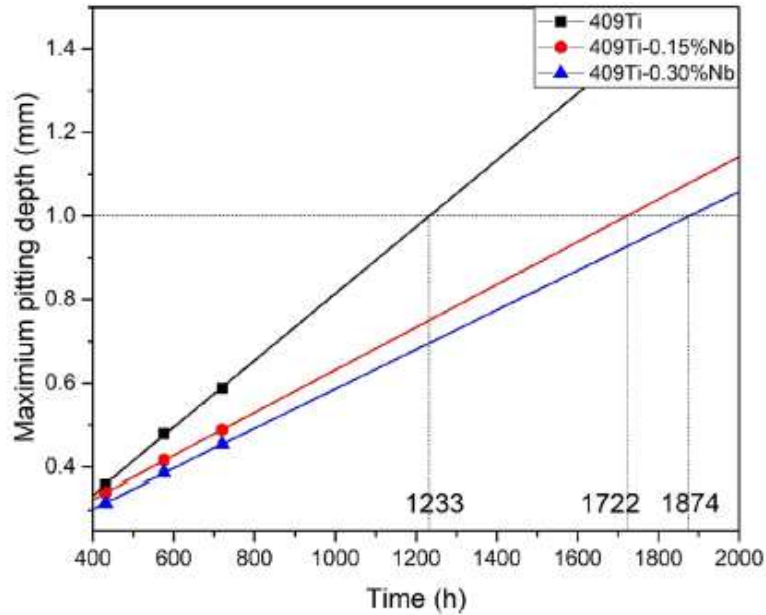


Figure 107 Niobium effect in improving lifetime [52]

Yet, the improvements that have been mentioned in terms of pitting corrosion in Ferritic stainless steels could also be proven for the Austenitic grades, a study carried on the Austenitic Fe25Ni15Cr grade [58] with addition of niobium showed that higher pitting corrosion resistance is observed in Niobium containing Austenitic stainless steel translated as higher positive potential as shown in the figure 108.

This increase in pitting corrosion due to the addition of Niobium in Austenitic stainless steels is interpreted as the result of the increasing disorders due to higher Niobium level in the matrix, as Niobium may form Niobium oxides that helps in protecting the surface, such protection is rated to be higher than that offered by Cr oxides [58].

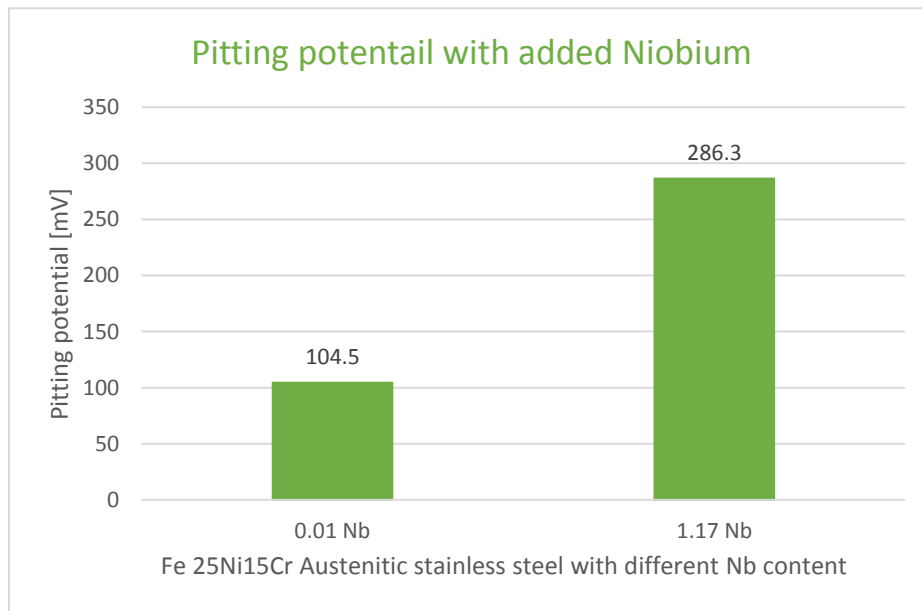


Figure 108 Effect of Niobium in increasing the resistance to pitting corrosion in Austenitic stainless steel

### 3.2.4.2. Niobium Role in refining inclusions

Inclusions are regarded as an initiation point for pitting, as a cavity may form and propagate through the inclusion dissolution, thus the larger is the inclusion size, the quicker the crack propagates decreasing the fatigue life. Niobium has a significant effect on the inclusion size, where the inclusions found in AISI 409 Ti-Nb are  $(\text{Nb, Ti})(\text{C, N})$  are identified to have irregular shape with an average size  $0.61 \mu\text{m}^2$  and  $0.62 \mu\text{m}^2$ , when compared to Niobium free AISI 409 Ti whose inclusions are TiN tetragonal shape with an average size  $4.09 \mu\text{m}^2$  [50] as shown in figures 109 and 110.

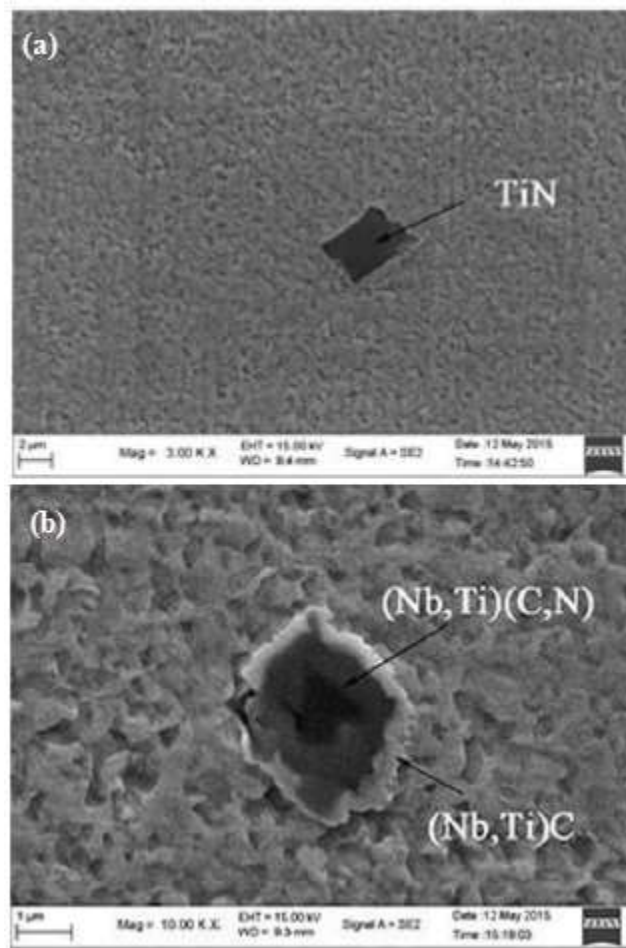


Figure 109 Niobium effect on inclusion shapes [52]

Hence, Niobium has a significant effect in refining the inclusion by reducing its average size. This effect has advantages in terms reducing pitting and lowering the discontinuities on the passive  $\text{Cr}_2\text{O}_3$  film.

In correspondence with the decreased average size of the inclusions in the Niobium alloyed stainless steel shown in the figure 110, a direct partial effect on increasing the fatigue life could be realized, where the refining of inclusions increased the number of cycles associated with a definite stress level as shown in figure 111.

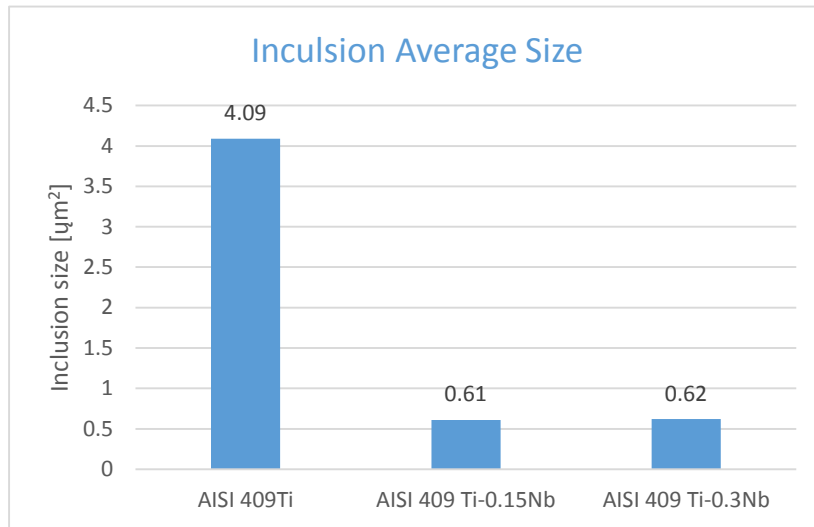


Figure 110 Effect of Nb on inclusion average size

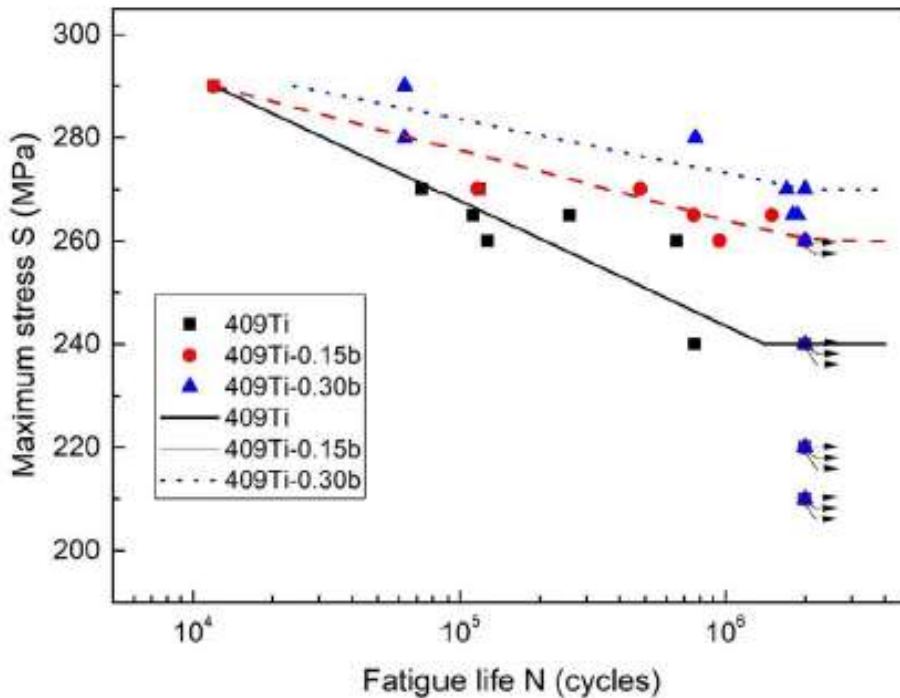


Figure 111 Niobium effect in increasing fatigue life [52]

# Chapter 4

## Manufacturing processes

### Introduction

Yet, we have discussed the problems that each component in the exhaust system suffers from, finding for each a suitable Niobium alloyed stainless steel, as well as shedding the light on Niobium as an individual alloying element. However, taking into consideration the complex design of the components that is done in order to obtain a good performance, attention should be drawn to the manufacturing processes, such as deep drawing and welding. In the following, the aspects of formability and weldability will be discussed, with the focus on the advantages of Niobium in each process, mainly in terms of texture, fibers, and intergranular corrosion with a special focus on the heat affected zone (HAZ).

Figure 112 shows some automotive exhaust components made up by forming processes (source ISSF).

### 4.1. Formability

Formability is the process in which a stainless steel sheet is subjected to tensile or compressive loads using stretching and deep drawing deformations. The difference between deep drawing and stretching is that, during stretching, the sides are fixed by the setup. Austenitic stainless steels show better behavior than Ferritic in this phenomenon, as they tend to neck at a higher dome height [60]. The behavior of stainless steels in terms of forming is indicated by the Forming Limiting Curve (FLC) that combines both, stretching at the right and deep drawing at the left, specifying for each grade the maximum deformation below failure and a safe area (below the curve) in which it could be formed and still maintain the performance. On the Y-axis, the major strain is measured, while the X-axis indicates the minor strain.



Grade 1.4509/441, manifold, Faurecia



Grade 1.4512/409, silencer, Faurecia, S. Korea



Grade 1.4509/441, catalytic converter, Faurecia

source: ISSF, the ferritic solution

Figure 112 different stamped automotive exhaust components [60]

The FLD provides more precise results for the correct dimensioning of raw material through revealing the performance of the material in the deep drawing process. Figure 113 shows the different zones of the Forming Limit Diagram (FLD), while figure 114 shows the FLD of different stainless steel grades.

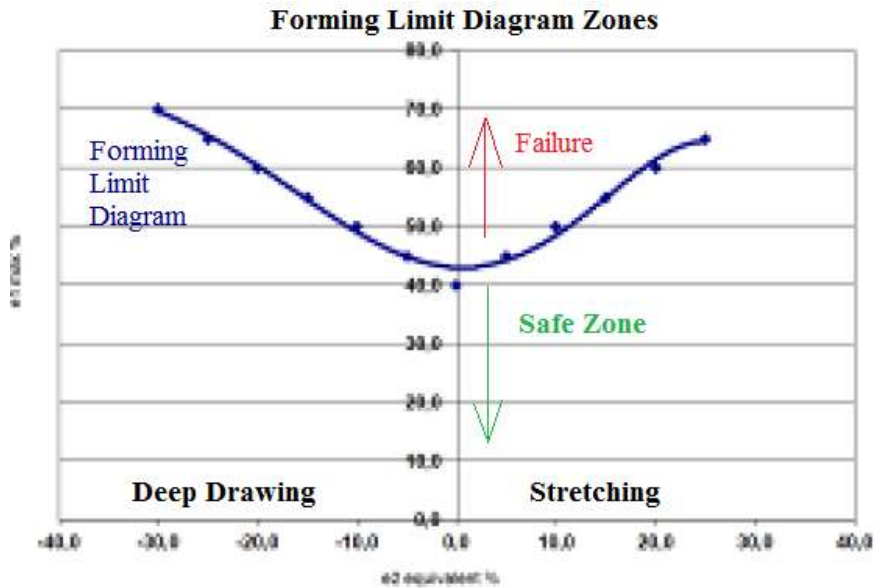


Figure 113 Forming Limit Diagram zones [59]

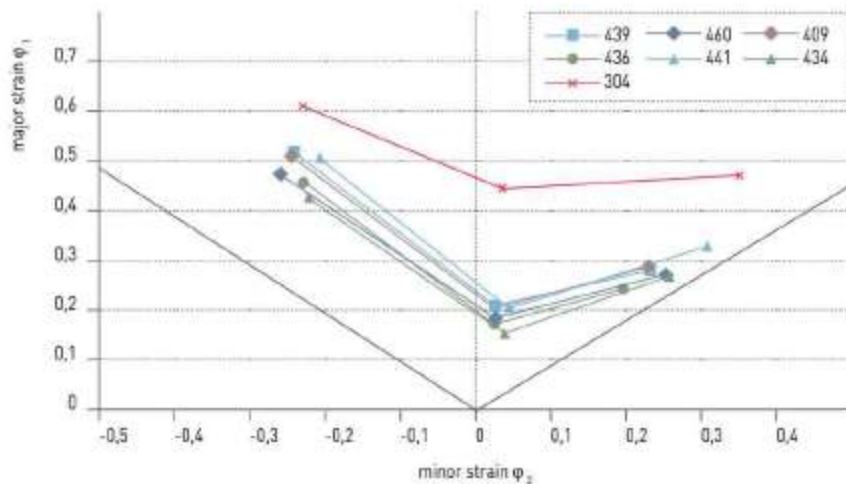


Figure 114 FLD of different stainless steel grades [60]

Some of the defects associated with forming processes are “ridging” and “roping”, described by lines or ridges on the surface of the object parallel to the pressing direction. It is important to highlight here that the addition of stabilizing elements in the case of ferritic stainless steel will be able to improve the performance to an extent where these stabilized ferritics are replacing the austenitic grades.

Another way to enhance the forming processes is lubricating the blank and the tools in order to avoid the sticking phenomenon. Lubricants used are special oils with high pressure resistance and viscosity that are easily removable after the process.

#### 4.1.1. Deep Drawing Process

Deep drawing is the process in which a punch presses a sheet into a die cavity resulting in a hollowed object the desired shape as shown in figure 115. A deep drawing operation of good

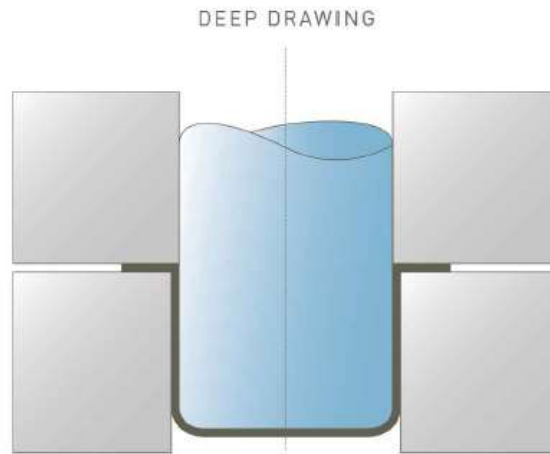


Figure 115 scheme of the deep drawing operation [60]

quality is that which features no fractures, excellent surface appearance and minimal material consumption. The idea is to obtain the desired shape while maintaining the thickness of the sheet, i.e. the material flow should occur from the width and not from the thickness.

Swift test is a deep drawing test indicator, which is stamping a sheet to form a cylindrical cup, then the Limiting Drawing Ratio (LDR) is determined in order to have a quantitative idea about the performance of certain material in deep drawing, LDR is defined as the ratio between the maximum diameter of the blank and the diameter of the cylinder that could be drawn from the blank in one step without fracture [59]. Even though Austenitic stainless steels are said to have better drawing capacity in absolute terms, however the stabilized ferritic grades also show excellent behavior, and in some cases they are considered better than Austenitics as shown in



Figure 116 LDR comparison between different stainless steel grades [60]

figure 116, where the green bars stand for ferritic grades, while the red stands for the austenitic grade 304[60].

#### 4.1.2. Anisotropic Coefficients

In order to indicate the performance of the stainless steel that undergoes deep drawing, the Lankford coefficient (known as the R-value) is evaluated at different angles, it indicates the capacity of the material to deform from the width while maintaining the thickness, then the average is calculated, it is the so known average anisotropic coefficient  $\bar{r}$  that presents the resistance to deformation in the thickness of the sheet, while the planar anisotropic coefficient evaluates the variation of the  $\bar{r}$ -value along the transversal and longitudinal rolling directions indicating the tendency to form earing. These coefficients are calculated according to the following equations [60, 61, 62]:

$$\bar{r} = (r_0 + r_{30} + 2r_{45} + r_{60} + r_{90})/6 \quad \text{Eq.4.1}$$

$$\text{or } \bar{r} = (r_0 + 2r_{45} + r_{90})/4 \quad \text{Eq.4.2}$$

$$\Delta r = (r_0 - 2r_{45} + r_{90})/2 \quad \text{Eq.4.3}$$

Where the index indicates the orientation of the tensile axis with respect to the rolling direction.

The grade is considered better as the average anisotropic coefficient increases, and the planar decreases. These properties are achieved by a texture which favors a strong intensity of  $\gamma$ -fiber after recrystallization.

#### 4.1.3. Crystallographic Texture

During the thermo-mechanical processes, i.e. rolling and annealing, the microstructure evolves and changes. Getting deeper in the grains, the intensity of the so-known  $\gamma$ -fiber and  $\alpha$ -fiber varies. However, these changes should be controlled in a way such that the  $\gamma$ -fiber intensity is maximized because it increases the average anisotropic coefficient, and consequently

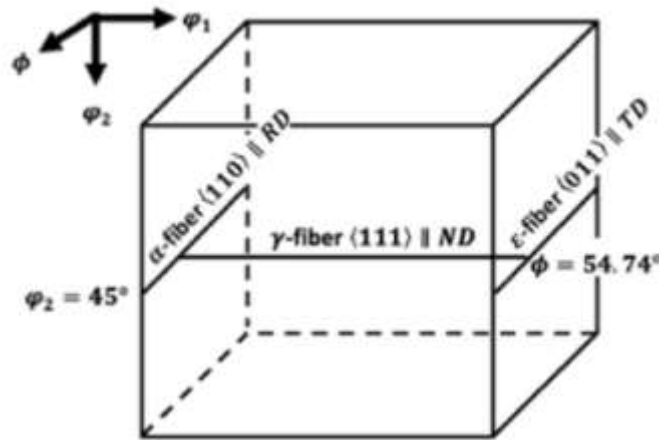


Figure 117 Euler representation of fibers orientation in the lattice

the deep drawing behavior, whereas the  $\alpha$ -fiber should be minimized as it is considered undesired.

The representation of the crystallographic structure is done by the Euler angles ( $\Phi_1$ ,  $\Phi$ ,  $\Phi_2$ ) as shown in figure 117 and 118, where RD, TD, and ND stands for rolling direction, Transverse Direction and Normal direction respectively [63]. The experimental methods used in order to describe the crystallographic texture are: electron microscopy scanning (SEM) to study the texture formation, Orientation Distribution Function (ODF) to analyze the preferred orientation (ODF in general are presented at  $\Phi_2=45^\circ$  section), Electron Backscatter Diffraction (EBSD) Pole Figures in order to characterize the anisotropy.

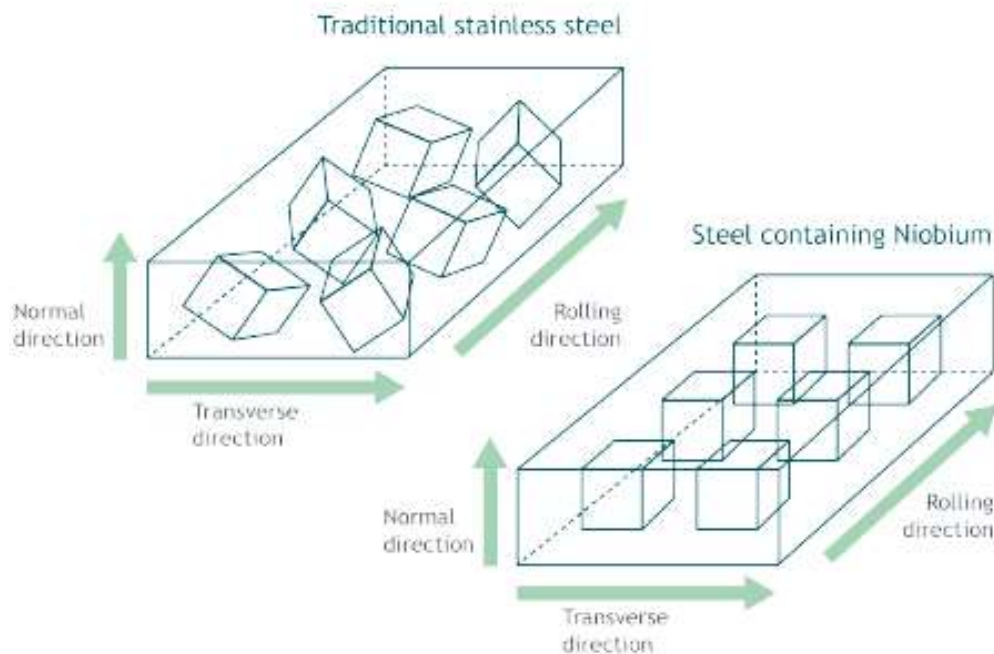


Figure 118 effect of Niobium in improving the crystalline structure [15]

The chemical composition has a significant effect on the deep drawing performance, as it was observed that the grades with lower C and N has a homogeneous solidification mechanism, highly developed  $\gamma$ -fiber after final annealing, hence a higher deep drawing performance[63].

## 4.2. Niobium Role in Improving Formability and Deep Drawing

### 4.2.1. Effect on Formability and deep drawing

After the first cold rolling, the  $\alpha$ -fiber and the  $\gamma$ -fibers increased, noting that the  $\alpha$ -fiber was less intense at the surface than in the central region, while  $\gamma$ -fibers were more developed, as they increase with the reduction in the grain size. However, after the intermediate annealing and the second cold rolling, the  $\alpha$ -fibers were reduced, and the  $\gamma$ -fibers were better developed in both regions with having strong intensity. Due to the higher  $\gamma$ -fibers, higher average anisotropy coefficient  $\bar{R}$  are achieved, which indicated better performance in formability.

After the second cold rolling and the final annealing, the  $\gamma$ -fibers percentage increased to 59% and weak  $\Theta$ -fibers which are found at low rates (7%), with an associated  $\bar{R}$  value 1.92.  $\gamma$  to  $\Theta$  ratio is a good indicator of deep drawing, with better performance resulting from higher  $\gamma$ , lower  $\Theta$ , higher  $\bar{r}$ , and minimum planar anisotropy  $\Delta r$  [64].

#### 4.2.1.1. Niobium Role in promoting $\gamma$ -fibers

Niobium addition as a second stabilizing element for the steel AISI 409 showed a significant effect on the texture and micro-structure for a studied hot rolled sheet, where it was observed that for the dual stabilized steel, the micro-structure is more homogeneous (figure 119 (a)) but less crystalized compared to the Ti stabilized grade (figure 119 (b)) [55].

The reduction of the nucleation and speed of growth during recrystallization accompanying the Niobium stabilized grade during the hot rolling is interpreted as a delay in the onset due to the pinning effect introduced by niobium, and its higher precipitate amount in the solid solution

Upon analyzing the cross section of hot rolled sheets for both steels, it was found that the  $\alpha$ -fibers were more intense in the Ti-Nb dual stabilized steels (see fig. 120) [55] while  $\gamma$ -fibers were poorly developed. However, for cold rolled sheets (60% reduction), even though the

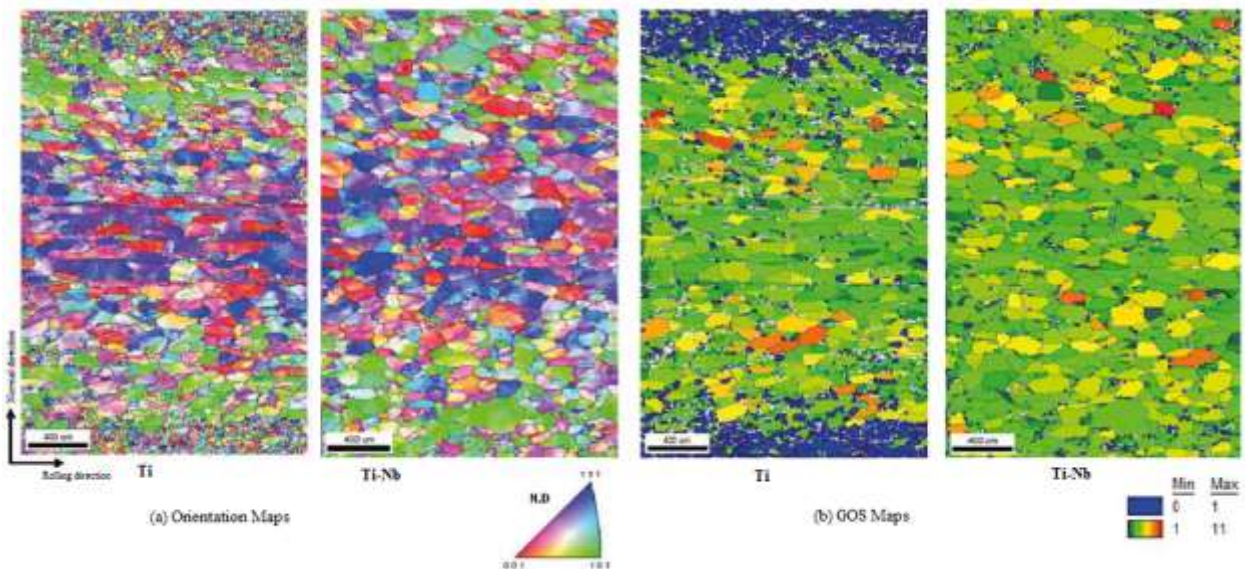


Figure 119 Niobium effect on Homogeneity and recrystallization [55]

$\alpha$ -fibers were stronger than  $\gamma$ -fibers at all regions, The Ti-Nb dual stabilized grade showed more intense  $\gamma$ -fibers as shown in figure 120, where (a) and (b) are respectively the center and the surface of Ti stabilized grade, and (c) and (d) are respectively the center and the surface of dual stabilized grade.

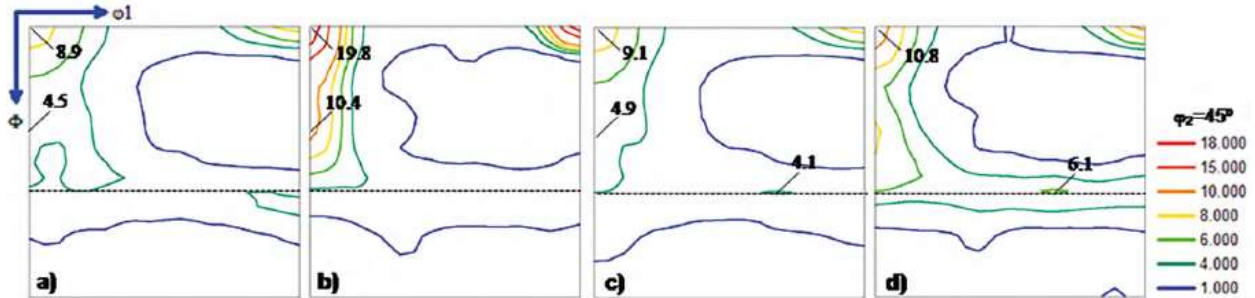


Figure 120  $\alpha$  and  $\gamma$  fibers in cold rolled sheets with single (a) and (b) and double stabilization (c) and (d) [55]

After annealing, the dual stabilized grade showed an increase from 0.4 to 0.56 of  $\gamma$ -fibers by volumetric fraction [55], this increase signifies the better anisotropy coefficients that improves the deep drawing application (explained later in the next chapter).

Apart, being a stabilized grade, Niobium's effect was shown to increase the texture intensity in the hot band because it retards recrystallization, however the increased reduction and temperature counteracted this. However, in the cold bands, the produced  $\alpha$ -fibers will recrystallize as  $\gamma$ -fibers. Hence, a precise stabilization ensures the desired strong  $\gamma$ -fibers [61].

#### 4.2.2.2. Effect of Niobium on Improving Formability

Formability of stainless steels is described by the anisotropy average coefficient  $\bar{R}$  and the planar average coefficient  $\Delta r$ . By definition, the average normal anisotropy coefficient  $\bar{R}$  value measures the resistance to deformation in the thickness of the sheet, while the planar anisotropy coefficient  $\Delta r$  measures the variation of R along the longitudinal and transverse rolling directions that indicates the tendency to form an earing. For a better formability performance, higher  $\bar{R}$  with lower  $\Delta r$  are desired.

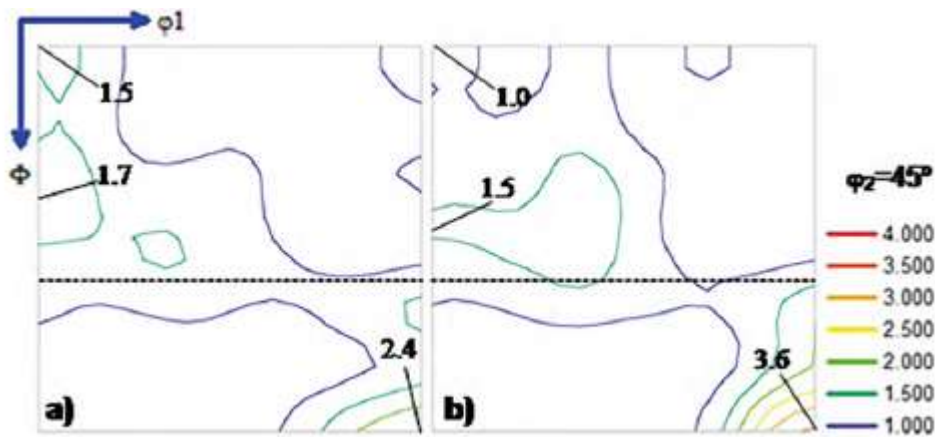


Figure 121 ODF sections of hot rolled sheets (a) Ti stabilized, (b) Ti-Nb stabilized [55]

Comparing these values for a Ti stabilized stainless steel and Ti-Nb stabilized stainless steel, the result indicated higher  $\bar{R}$  value due to the addition of Nb and lower  $\Delta r$  as shown in the figure 122.

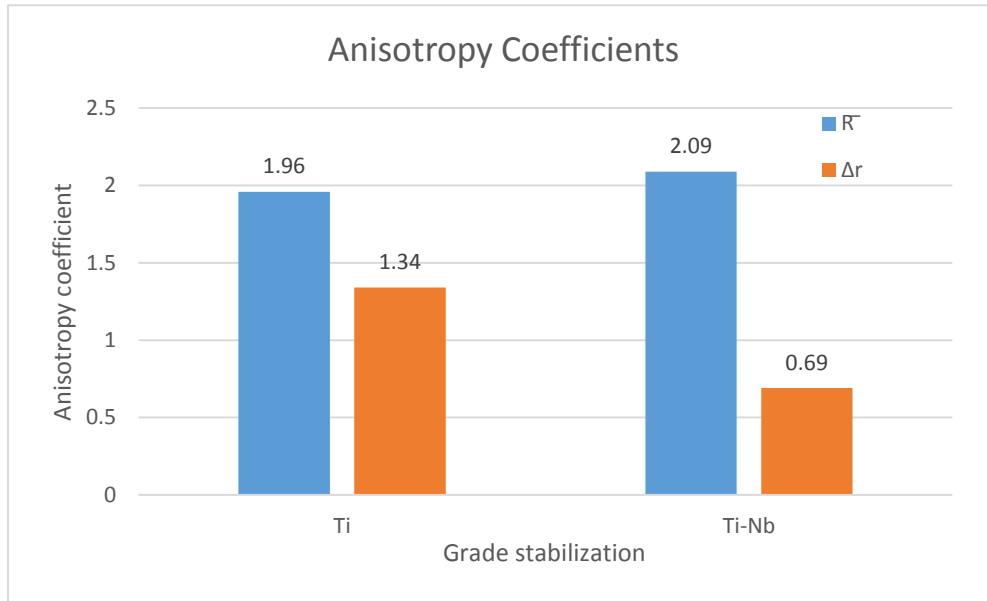


Figure 122 Anisotropy coefficients of single and dual stabilized grades

The higher  $\bar{R}$  value allows a better performance in deep drawing applications, the Niobium dual stabilized steels thus reached higher stamping depth compared to the single stabilized. The results of swift test are shown in figure 123 for (a) Ti stabilized and (b) Ti-Nb stabilized [55].

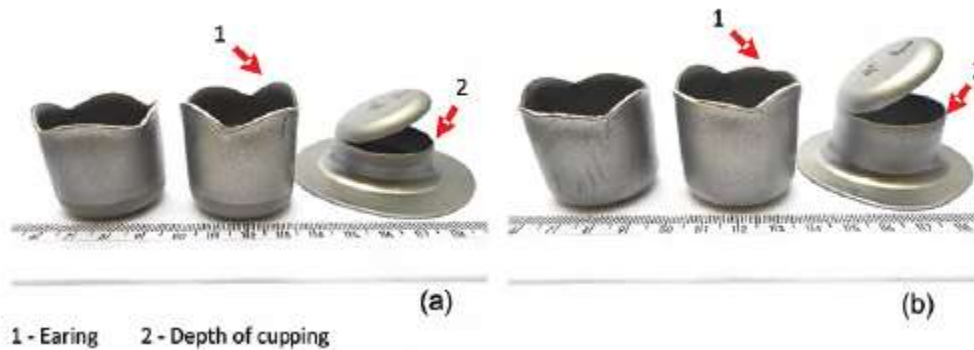


Figure 123 Swift test comparison for single (a) and dual (b) stabilized grades [55]

In order to demonstrate the effect of added Niobium on formability, a single stabilized ferritic 409 grade is compared to the double stabilized version with Nb that was found surpassing, as it allowed more severe depths to be reached [49] as shown in figure 124

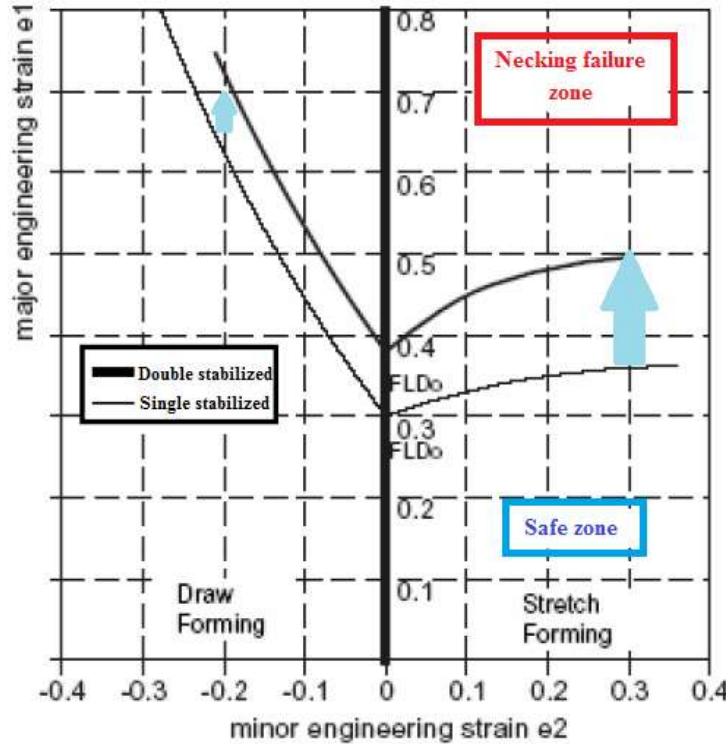


Figure 124 LDR improvement by the addition of Niobium [49]

Another Ferritic stainless steel has also been tested in order to mark the variation of the average anisotropic coefficient that describes the deep drawing performance as a function of added niobium, a low carbon ferritic stainless steel with 16.5% Cr has been tested with different levels of niobium, and the result showed that the addition of Niobium increased the average  $r$ -value at all levels, however, it has an optimum, for this studied case- around 0.5 mass % as shown in figure 125 [48].

The observed deterioration for the higher amounts of niobium is related to the associated increase in the transition temperature which makes formability more difficult.

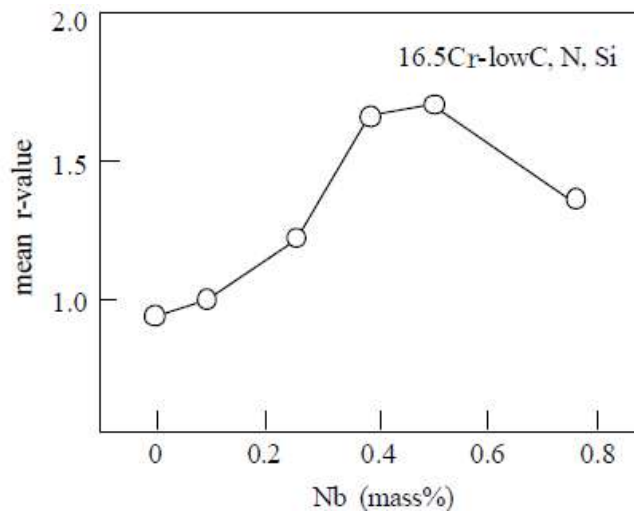


Figure 125 Effect of Niobium on the mean anisotropic coefficient [48]

#### 4.2.2. Formability of the Ferritic Grades 1.4622 and 1.4521

Such grade, being Ni-Mo free making it cost efficient, and high chromium content to have a competitive resistance to austenitics, has also featured low tendency to ridging. Figure 126 shows the  $\gamma$ -fiber increased intensity in the 1.4622 grade after reduction that makes it suitable for deep drawing operations [61].

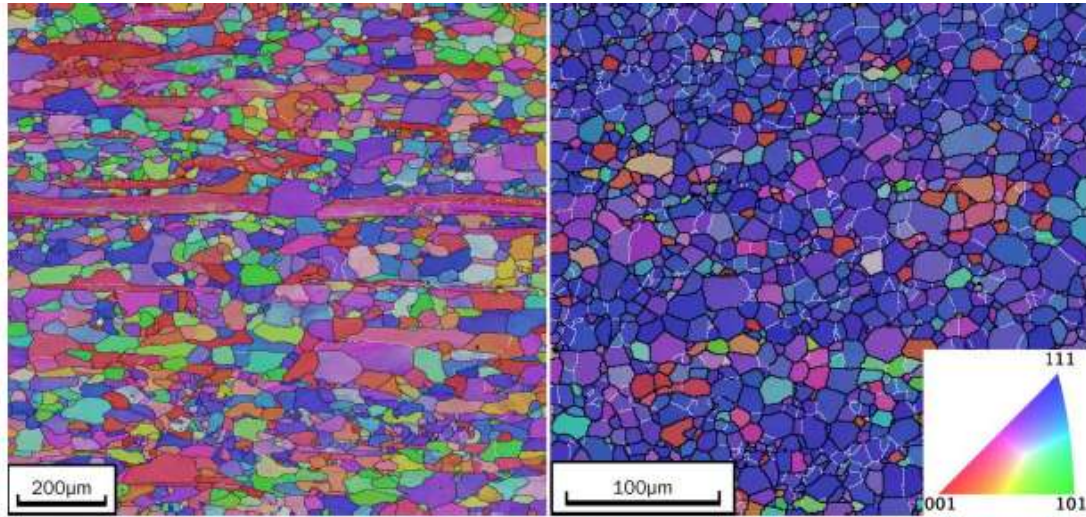


Figure 126 optimized microstructure of 1.4622 with high  $\gamma$ -fiber intensity [61]

Compared to other similar grades, such as the grade 1.4509 (AISI 441 that is used up to 950°C) it has been shown that 1.4622 has higher  $\bar{r}$ , lower  $\Delta r$  (varying from 0.2 to 0.3), and similar LDR to 1.4509 which is higher than that of 1.4521 as shown in the figure 127 [61,62]. Nonetheless, the formability of the grade 1.4521 could be improved by the addition of Tungsten [62] (see chapter 5).

In addition, the EN 1.4622 has showed the least ridging index among other ferritic stainless steels considered as competitors shown in figure 127[61].

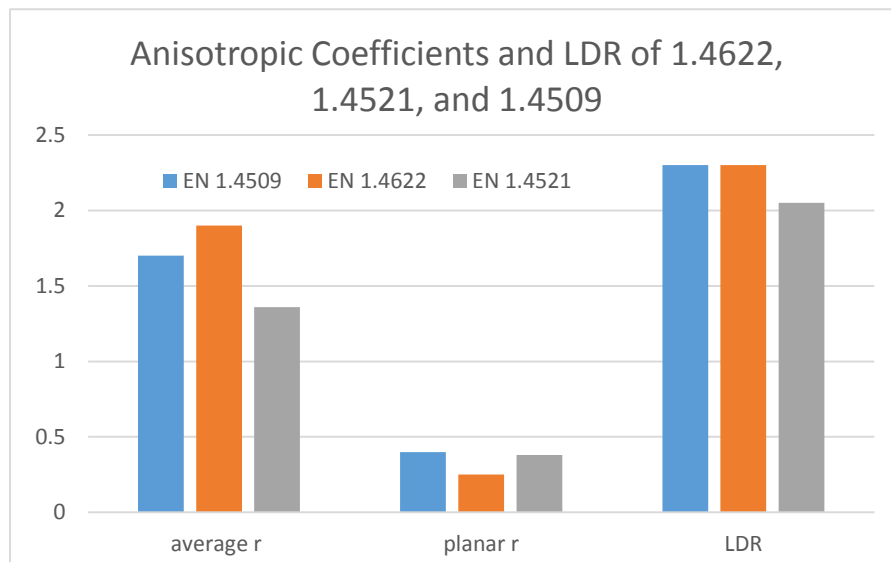


Figure 127 Anisotropic coefficients of EN 1.4622 and EN 1.4509

### 4.2.3. Formability of the Ferritic Grade AISI 409

Consider the evolution of the AISI 409 grade from standard 409 to single stabilized grade by Titanium that suffered from surface defects, to the dual stabilization by Nb and Ti. The formability of the dual stabilized Grade was superior, it was able to reach higher depth compared to non- and single stabilization. These results are verified by plotting the associated LDR shown in figure 128 [49].

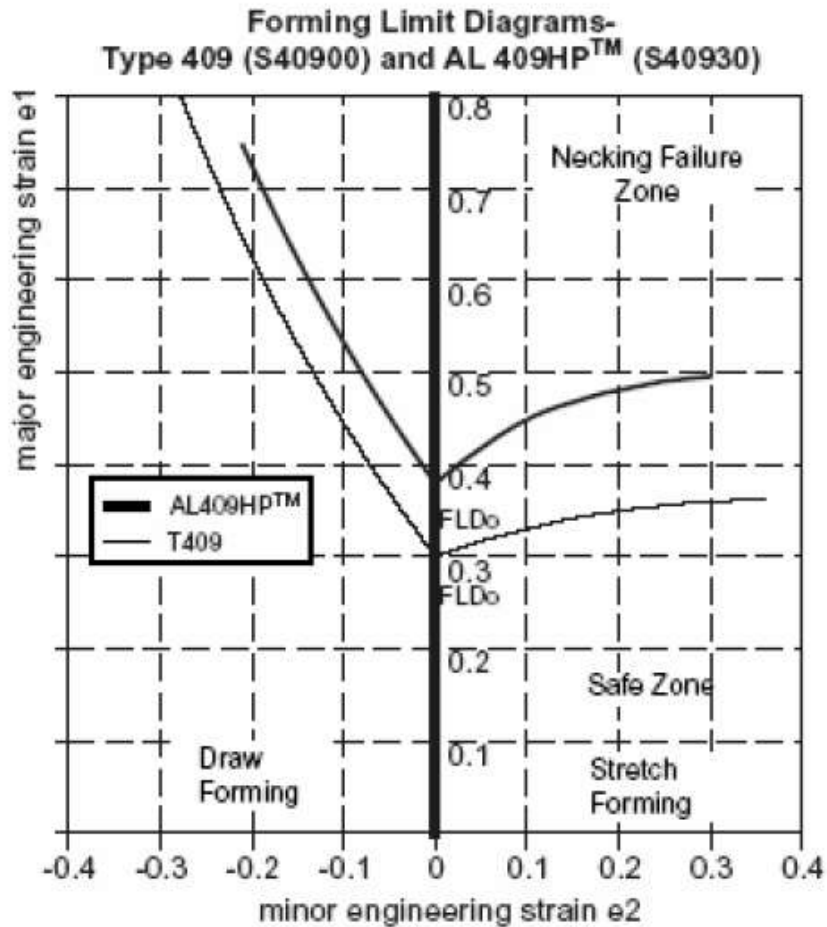
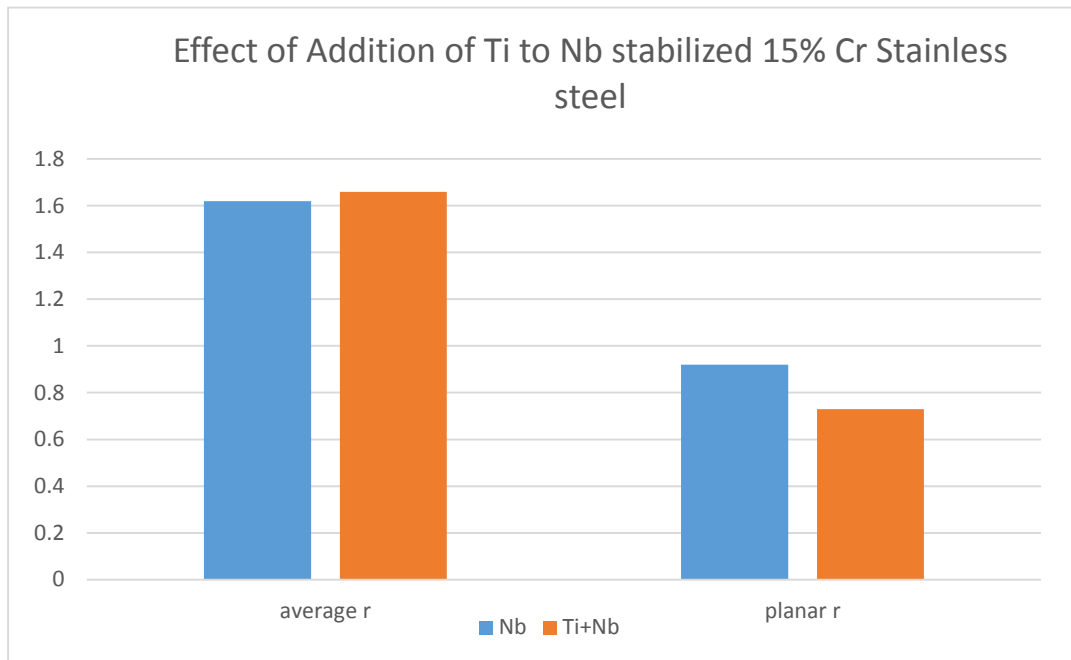


Figure 128 Effect of Dual Stabilization on the LDR of AISI 409 [49]

Nonetheless, a study that tested the addition of Ti on a single stabilized Nb 15% Cr has showed a similar result, i.e. dual stabilization showed higher average anisotropic coefficient and lower planar anisotropic coefficient as shown in figure 129. This improvement in terms of formability could be address to the role of Ti in keeping higher amount of Niobium in the solid solution and hindering the second precipitates, because TiC are more stable than NbC [65].



*Figure 129 Effect of Ti addition on Nb stabilized Stainless steel*

### 4.3. Weldability

#### Introduction

Welding is considered one of the most common joining methods due to its efficient and cost saving characteristics, it is the process during which the joining occurs by melting and re-solidification of the base and filler material. The structural integrity of steel structures not only depends upon the strength of the steel but also the strength of the welded joints. This is why the weldability of steel is always an important consideration. For a good choice of welding and welding characteristics, one should consider the chemical composition of the stainless steel, its metallurgical structure and physical properties. In addition, the phenomenon of intergranular corrosion (explained in chapter 2) that is common at the heat affected zone is less prone for ferritic grades especially the stabilized ones. In other words, the advantages of alloying with niobium is translated to the higher intergranular corrosion resistance in the case of the stabilized stainless steels that are considered as “virtually immune to intergranular corrosion”.



Grade 304 & 441, diesel  
particle filter, E Class  
Mercedes, Faurecia

source: ISSF, The Ferritic Solution

*Figure 130 Welded automotive exhaust component [60]*

Different welding techniques could be applied to stainless steels such as arc welding, Gas Tungsten Arc Welding (known as GTAW or TIG) which does not involve the usage of filler metal, but providing the necessary heat by the un-consumable TIG electrode so that the base metals are melt and then solidified as one part, the Gas Metal Arc Welding (known as GMAW or MIG) where the electrode is consumable, and laser welding are the most used in the automotive industry.

To maintain the corrosion resistance at the welded area, the used filler metal should show a chemical composition compatibility with the base metal, as well as, the use of protective gases such as Argon (Ar) or Helium (He) is necessary to avoid the loss of chromium due to the high temperature. A mixture of the inert gases with hydrogen is not suitable in the case of ferritic stainless steels due to the induced embrittlement in the joint [60].

Nonetheless, the stabilized grades may show some grain coarsening at the welded area to the high temperature, hence it is important to minimize the heat input of welding as much as possible.

Pickling by special designed pastes for welding or fluonitric acids, or mechanical descaling are applied after welding to remove the discoloration effect. Then, passivation and decontamination are held to help reforming the passive layer and remove the residues.

In what concerns the Shield gas, hydrogen containing mixes must not be used with ferritic, martensitic or duplex grades. Nitrogen could be added to nitrogen containing austenitic and duplex grades.

In what concerns the welding parameters, the heat input should be minimized to minimize distortion and avoid stress cracking. Heat Input is calculated as the product of the current (Amperage) and the Voltage (Volts) multiplied by 60 and divided by the travel speed. Lower heat input is achieved by lowering the voltage and amperage, and increasing the travel speed [66].

The amperage and voltage are adjusted on the basis of arc stability, desired penetration, spatter, undercut and dilution.

## 4.3.1 Weldability of Ferritic and Austenitic Grades

### 4.3.1.1. Ferritic Grades

- Semi ferritic grades (0.04% C, 17% Cr) are sensitive to embrittlement by grain coarsening above 1150°C, poor toughness and ductility, sensitive to intergranular corrosion. [67]
- Stabilized Ferritic Grades with Ti, Nb: sensitive to embrittlement by grain coarsening above 1150°C, satisfactory ductility and improved toughness, more resistant to intergranular corrosion.
- They show better resistance to stress corrosion due to their lower thermal expansion coefficient.
- Problems related to embrittlement, stress corrosion, and shrinkage cracks could be encountered by preheating up to 200-400°C [68].
- 750-800°C stress relieving gives an optimum strength and corrosion resistance. If the grade is stabilized by Ti this relieving process could be omitted [68].

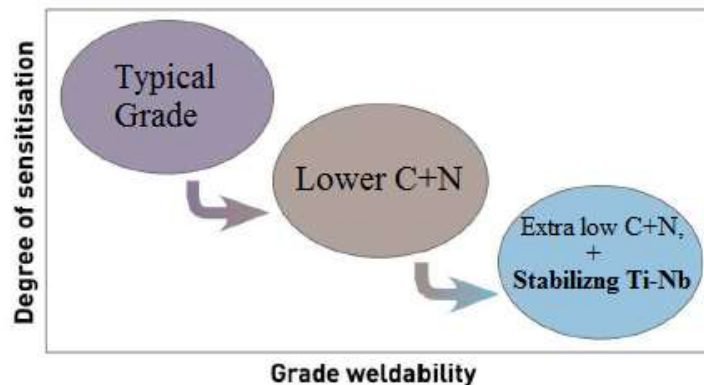
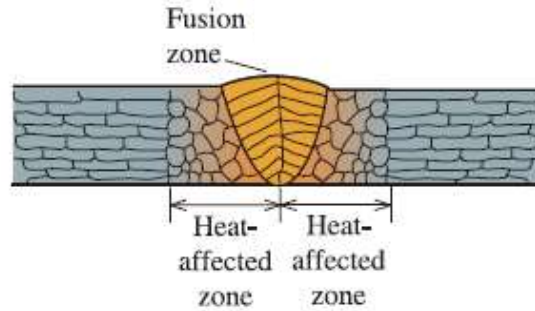


Figure 131 Stabilization effect on increasing weldability

### 4.3.1.2. Austenitic Grades

- Insensitive to hot cracking, good resistance to intergranular corrosion for low carbon and stabilized steels, excellent toughness and ductility, embrittlement may occur. [67]
- Even though the heating and cooling associated with the welding process does not affect the microstructure significantly, secondary phases may occur, such as ferrite which has beneficial consequences such as prevention of hot cracks, and detrimental consequences such as selective attacks in certain corrosive media [68].

- The thermal expansion coefficient and the heat conductivity coefficients that are higher in this family compared to ferritic may result in contraction and welding stresses. However, stress relieving could be carried out at 850-950 C or 400-500 C. choosing the temperature range should be based on avoiding carbide formation [68].



*Figure 132 Welding different zones [32]*

### 4.3.2. Stainless Steel Welding Techniques

Different welding techniques could be applied, depending on the grade and the thickness, figure 133 represent all the techniques, with specifying the recommended grade and thickness for each [67].

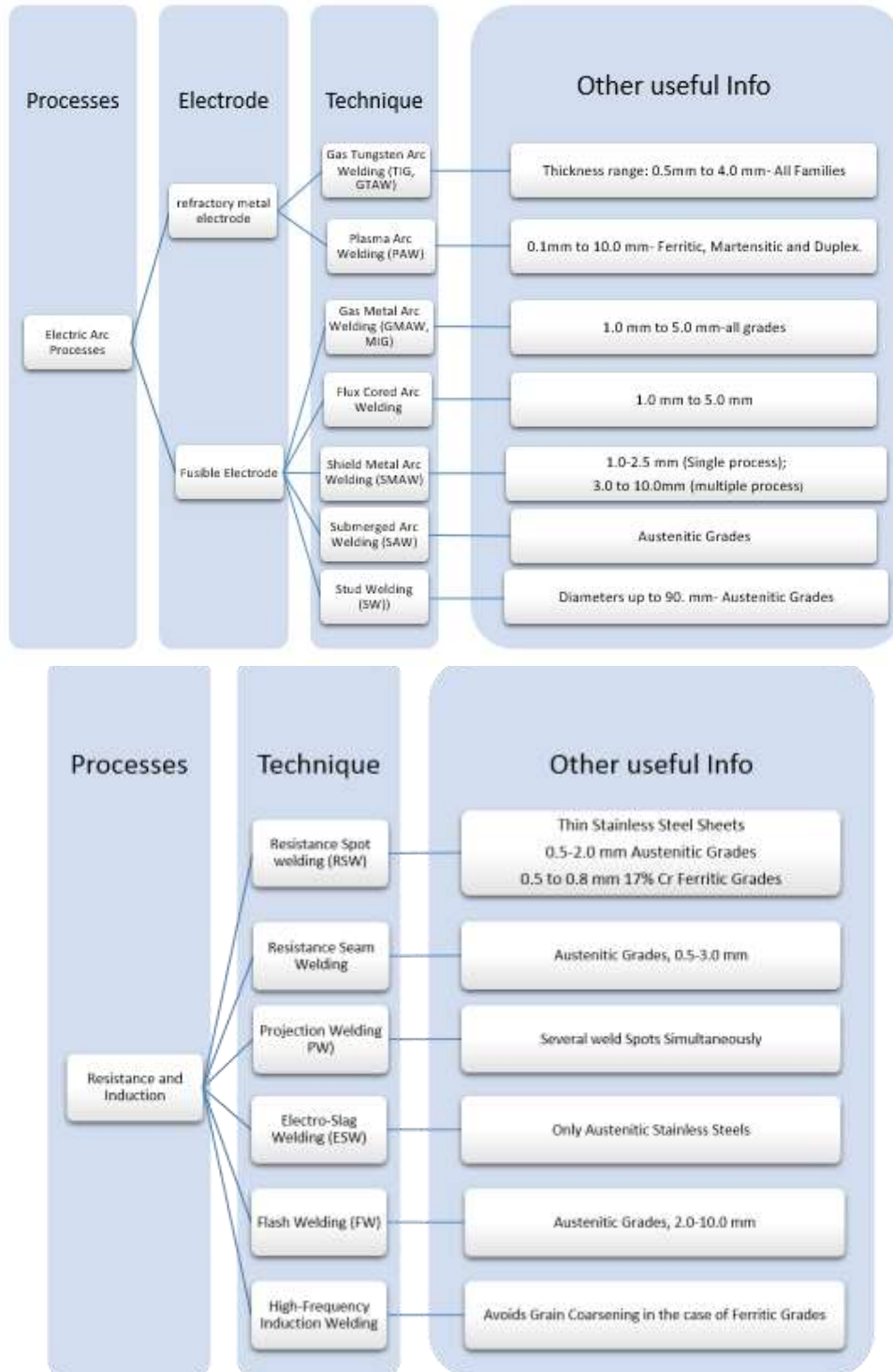


Figure 133 Stainless Steel Welding Techniques

#### 4.3.2.1. TIG – GTAW Electric Arc Welding Technique

Tungsten Inert Gas (TIG) or known as GTAW (Gas Tungsten Arc Welding) or WIG (Wolfram Inert Gas) shown in figure 134 is a welding process in which an electric arc supplies the energy needed for melting the metal by a Tungsten or Tungsten alloy (mainly 2% thoriated Tungsten) non-consumable electrode. Filler metal may employed in the form of bare rods or automatic wire. The inert gas (Argon (Ar), Helium (He), or Hydrogen in some cases) protects from the atmosphere and maintain stable arc.

Its advantages could be summarized in the following:

- Narrow fusion zone due to the concentrated heat source.
- Stable arc, small size welding pool, simplified cleaning operations because of oxidation residues eliminations due to the absence of flux.
- Excellent metallurgical quality, precise control of penetration and weld shapes.
- Pore-free welds.
- The common work piece thickness ranges from 0.5 to 4.0 mm, which is common range in exhaust components.
- Ability to weld complex shapes with wide ranges [69].
- Recommended Shield Gas\*: Ar, Ar+H<sub>2</sub> mixes, Ar + He mixes, Ar + H<sub>2</sub>+ He, Ar+ N<sub>2</sub>.

*\*for more info please check ref [67]*

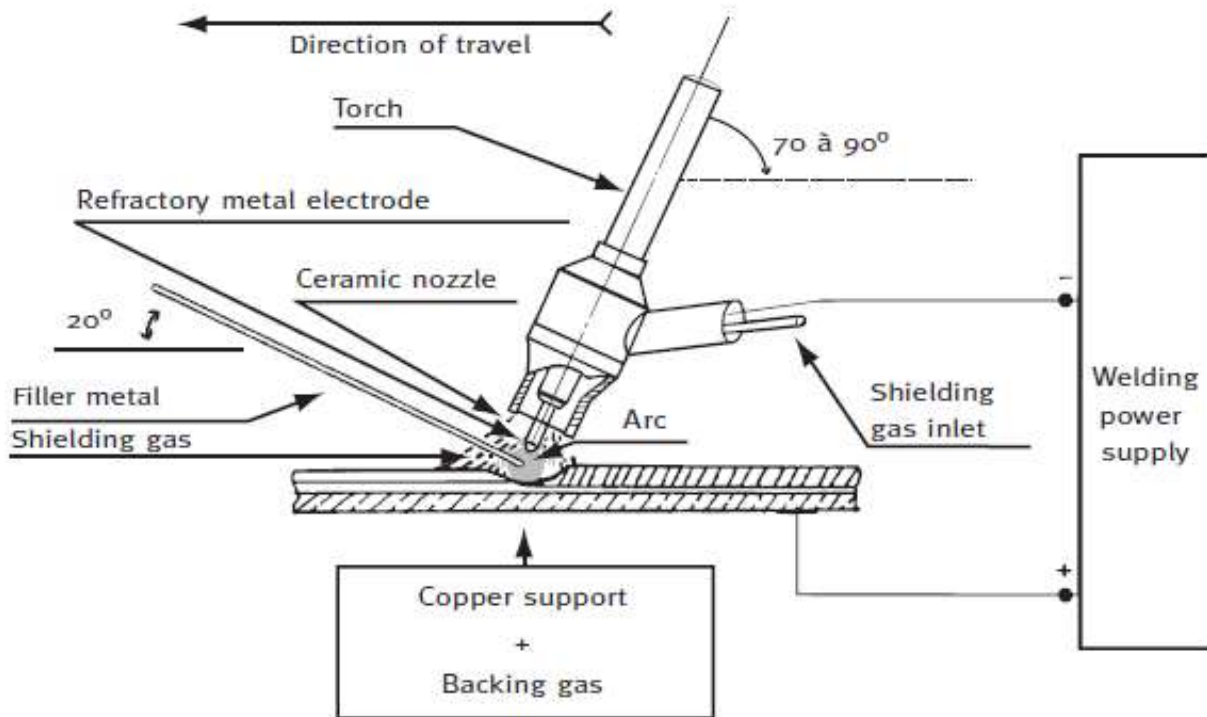


Figure 134 Schematic Representation of TIG welding process [67]

#### 4.3.2.2 MIG-GMAW Electric Arc Welding Process

MIG (Metal Arc Welding) known also as GMAW (Gas Metal Arc Welding) shown in figure 135 is a welding process in which the heat is provided by an arc between an automatic continuously fed metal wire consumable electrode and the piece. It is characterized by high temperature arc that results in a rapid melting of the electrode. Such Technique also requires shielding gas to prevent oxidation, Argon with 2% oxygen is used for stable arc, and same result could be obtained with Argon and 3% Carbon dioxide. [67]

Recommended shield Gas\*: Ar + 2% O<sub>2</sub>, Ar + 3% CO<sub>2</sub>, Ar + CO<sub>2</sub> + H<sub>2</sub> mixes, He + Ar+ CO<sub>2</sub>;

*\*for more info please check ref [67]*

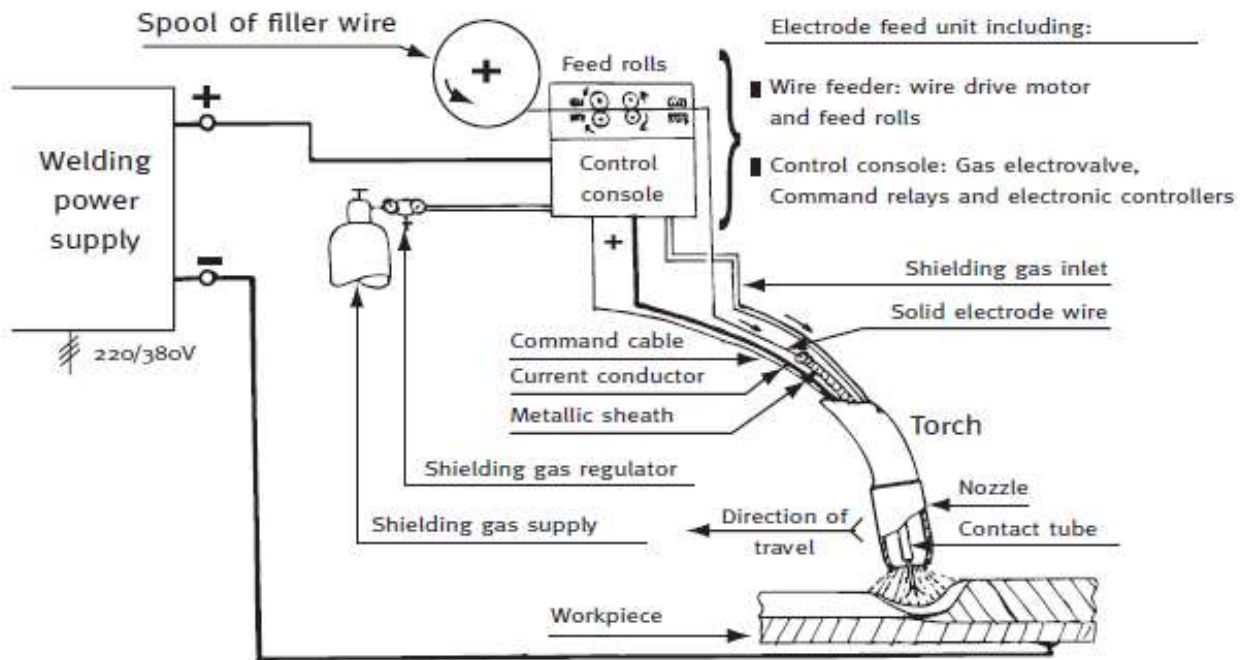


Figure 135 Schematic representation of MIG welding process [67]

### 4.3.3. Choosing the Filler Material

Choosing the right filler material is very important when welding stainless steel to stainless steel, or dissimilar metals. Nonetheless, the ability to tailor the mechanical and properties and corrosion resistance increases the complexity of choosing the filler material. Several electrodes could be used, knowing that the decision is made based on considering the cost, service conditions and properties of the base materials.

The composition of the welded zone has to be as homogeneous as possible as the base metal, the filler metal should contain a similar content of the main alloying elements such as Cr, Mo, and Nb to ensure good corrosion resistance and high temperature strength.

Some guidelines could be followed in choosing the filler material [66]:

- 1- If both base metals are the same, use the base metal alloy as a guide, choose a similar filler. For example 316L to 316L → choose 316L filler.
- 2- If dissimilar materials, choose a filler that matches the highly alloyed material. For example, 304L and 316L → choose 316L.
- 3- Use over-alloyed grades when welding dissimilar materials.

In the case of dissimilar, attention should be drawn to the metallurgy of the weld metal. Schaeffler Diagram (figure 20) is a useful tool that allows the estimation of the weld metals by calculating the Chromium and Nickel equivalents, then finding the appropriate filler material [68].

- 1- Determine the position of the two materials, and draw a straight line between them.
- 2- Plot the position of the proposed filler material.
- 3- Draw a straight line from the position of the filler material to the center point of the line joining the two base materials.
- 4- 20 to 40% away along the filler material position will be the result of 20-40% dilution of the filler metal in the base metal.
- 5- If the structure achieved is suitable, than the proposed filler material could be used.

Figure 136 shows an example of dissimilar welding that is followed by the proposed steps. The base metals are EN 1.0401(A) and EN 1.4301 (B) using a filler material having the equivalence point (D). The obtained structure is austenite with 10% ferrite noted as point (E) [68].

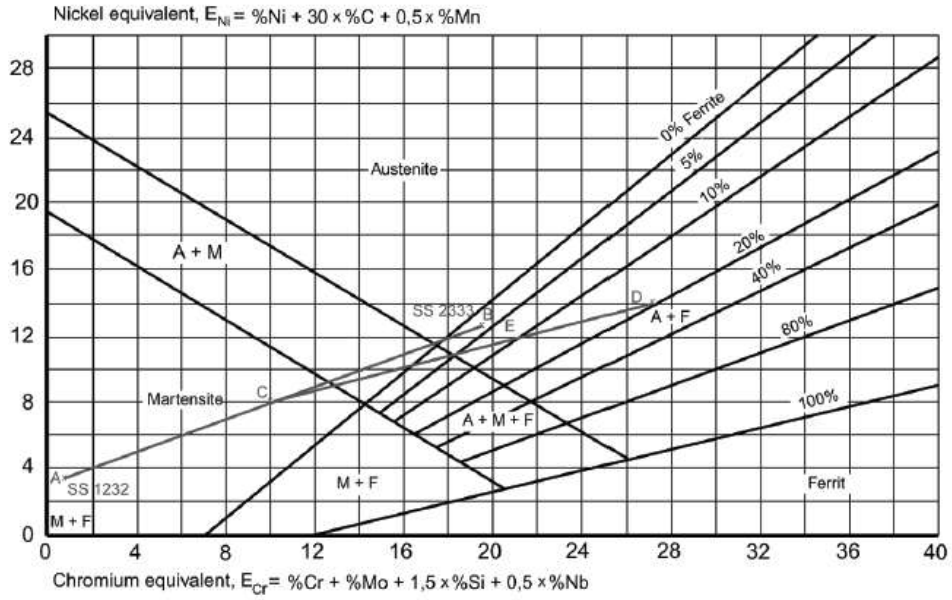


Figure 136 filler material compatibility check by Schaeffler diagram [68]

#### 4.3.4. Niobium against Intergranular Corrosion

As mentioned many times before, Niobium stabilizing effect inhibits the formation of chromium carbides that precipitate in the grain boundaries (figure 63), especially in the heat affected zone (HAZ) after the steel is subjected to welding, consequently, keeping the chromium in the steel instead of depleting it. As a result, intergranular corrosion, which is a typical problem in the welded zones is inhibited.

Consider 2 different ferritic stainless steels, the AISI 441 dual stabilized by Ti and Nb (0.343wt.% Nb), and AISI 409 with only Ti, the microstructure of that alloyed with niobium shows a defined grain boundaries that are not visible in the AISI 409 Ti as shown in figure 137 [70].

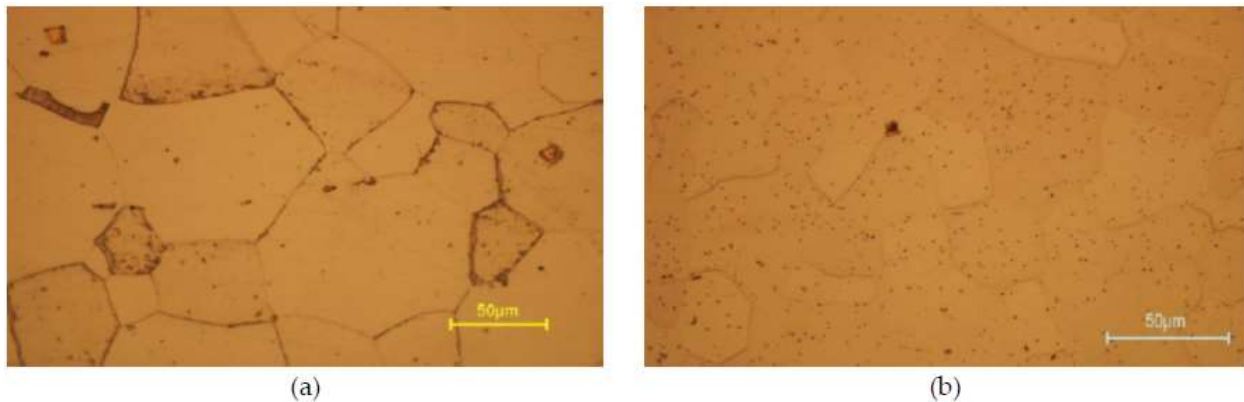


Figure 137 Microstructure of (a) AISI 441 Ti-Nb and (b) AISI 409 Ti [70]

After subjecting these two materials to welding, it was observed that in the case of the grade containing Niobium, no grain growth occurs in the heat affected zone (HAZ), however the lack of niobium in the AISI 409 stabilized with Ti showed significant grain growth as shown in figure 138 that is associated with intergranular corrosion.

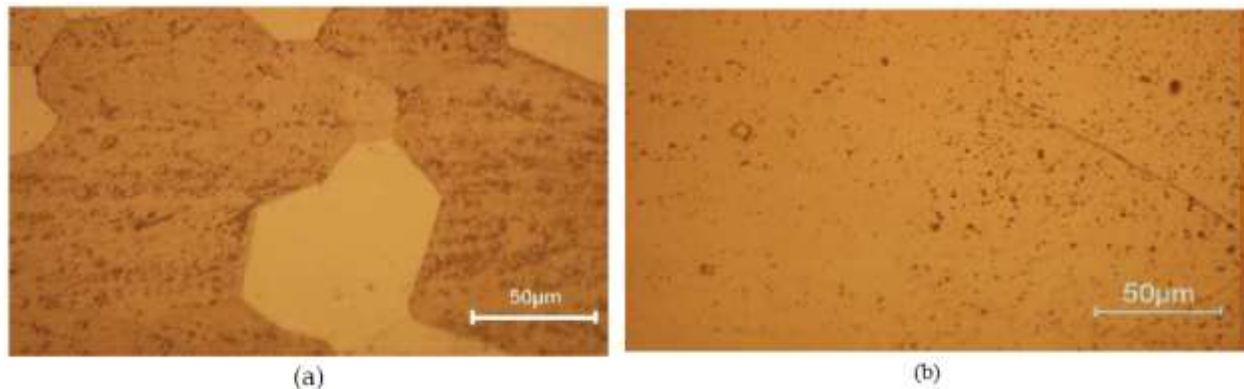


Figure 138 HAZ in (a) Nb-Ti stabilized AISI 441, and (b) Ti alloyed AISI 409 [70]

After welding, the specimens are subjected to corrosive environment, the result revealed a loss of material at the grain boundaries in the single stabilized stainless steel, while a higher resistance to intergranular corrosion accompanied the addition of Niobium that showed no structural incompatibilities. Figure 138 shows the difference between the macrostructure of (a) Nb-Ti stabilized HAZ and Ti stabilized HAZ after subjecting them to corrosion [70].

In a similar manner, the effect of niobium was much more evident at microstructural level after the corrosion test, where defects are detected at the grain boundaries in the alloy that lack the addition of Niobium, as shown in figure 139.

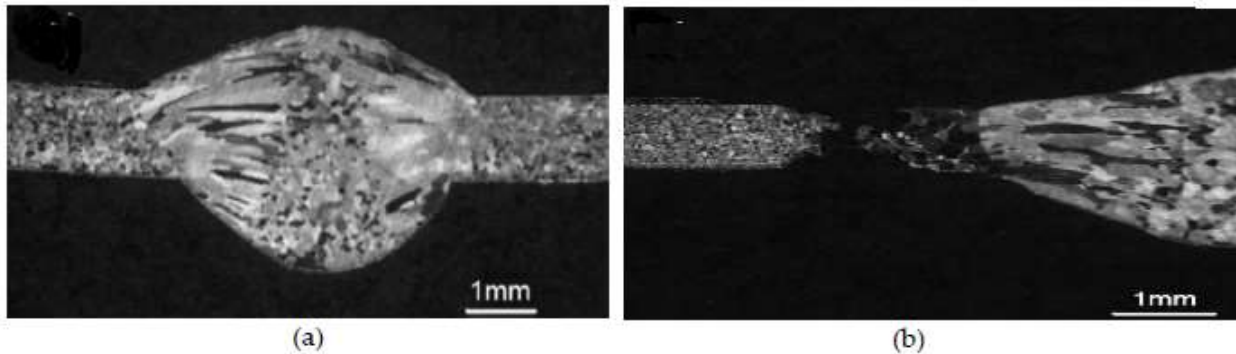


Figure 139 Effect of Nb stabilization at the grain boundaries at the HAZ at macro-structural level [70]

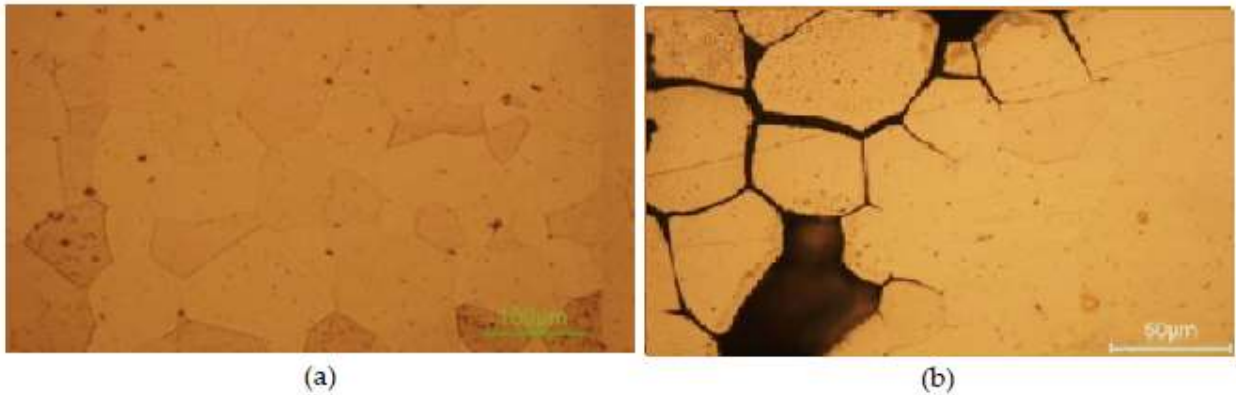


Figure 140 Effect of Niobium on microstructural level at HAZ [70]

The effect of Niobium addition on the thermal fatigue life in the HAZ is tested, and the results demonstrated 2 main issues, one is said to be not beneficial which is the degradation of the solid solution strengthening explained by coarsening of the laves phase that is increasing with the increase of niobium, which in turn reduced the thermal fatigue life. However, the second issue is beneficial, and it overcame the pre mentioned disadvantage, the pinning effect that hinders the grain growth resulted in smaller grain size of fine (Nb, Ti) (C, N) that in turn increased the thermal fatigue life, even though more precipitates were formed with increasing the niobium content, however their volume fraction did not change because of their smaller size. As a net result, Niobium's effect was found to increase the thermal fatigue life in the HAZ [71].

#### 4.3.5. Niobium Role in Improving Weldability

The properties after welding using TIG (GTA) Tungsten Inert Gas (Gas Arc Welding) was analyzed for the Niobium added to Ti stabilized grade. This addition resulted in increased toughness with respect to the single stabilized grade, as well as it retained good weld toughness in the thicker material [49]. It is important to notice that the hardness is higher in the heat affected zone for the alloys stabilized with Nb and Ti rather than single stabilization by Ti as shown in figure 141 [70].

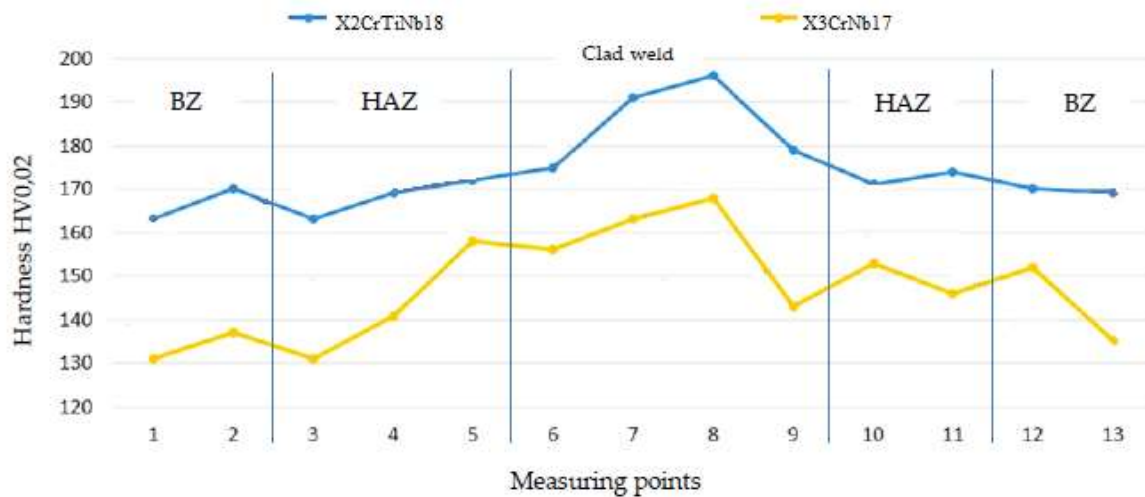


Figure 141 Hardness distribution in the welded zone [70]

#### 4.3.6. Weldability of the Grades 1.4622

The stabilization of this grade features the benefits of Niobium that are already discussed above, it has low risk of sensitization, and less distortion than the austenitic grades. Conventional welding methods could be employed, using an austenitic filler 316L [46].

The shielding gases could be Argon, Helium, or a mixture of both with a maximum of 26% oxygen to improve the arc stability, with no added nitrogen and hydrogen. It is also important to reinforce the minimization of the input heat in order to reduce the grain growth.

#### 4.3.7. Weldability of the Grade AISI 444

It is important to mention that the used filler material should match the chemical composition of the base metal, a metal cored filler is also a good choice as it allows the addition of elements as powder mixture in the core. The AISI 409 stainless steel containing 12% Cr, 0.2% Ti makes up the external foil, while Cr, Mo, Nb and additional Ti could be adjusted in the powder in order to obtain the desired composition. It is important to relate the difference in the composition with respect to the base metal to the losses during the process, because some elements suffer from vaporization or reaction during chemical transfer in the arc [72]. The contents of the stabilizing elements used with this ferritic grade (AISI 444) to stabilize the molten zone could be theoretically calculated as [72]:

$$\%Nb = 0.2 + 7 (\%C + \%N) \quad \text{EQ. 5.1}$$

$$\%Ti = 0.15 + 4 (\%C + \%N) \quad \text{EQ. 5.2}$$

$$0.2 + 4 (\%C + \%N) < \%Nb + \%Ti < 0.8 \quad \text{EQ. 5.3}$$

In order to address the best filler material that result in a good properties of the welded zone, 7 different filler wires, whose composition in wt.% is shown in table 14, with the same Cr and Mo contents of the base metal with different amounts of Ti and Nb were tested [73].

Element	C	Si	Mn	N	Cr	Mo	Ti	Nb
Filler 1	0.01	0.6	0.3	0.01	19	1.9	<0.1	0
Filler 2	0.01	0.6	0.3	0.01	19	1.9	0.45	0
Filler 3	0.01	0.6	0.3	0.01	19	1.9	<0.1	0.5
Filler 4	0.01	0.6	0.3	0.01	19	1.9	<0.1	0.8
Filler 5	0.01	0.6	0.3	0.01	19	1.9	0.2	0
Filler 6	0.01	0.6	0.3	0.01	19	1.9	0.1	0.4
Filler 7	0.01	0.6	0.3	0.01	19	1.9	0.3	0.3

Table 14 Chemical composition in wt.% of the tested filler wires for the AISI 444

Ti has high affinity to oxygen which makes it sensitive to oxidation, this is why almost double the desired quantity should be added in the filler wire to obtain the final desired amount in the welded zone, however, Niobium has almost a ratio 1 to 1, so it is added assuming no losses.

The benefits of Ti are summed up in the formation of refractory compounds in the molten steel and to enhance the equiaxed grain formation in the fusion zone, however, the addition of Ti in the filler wire had detrimental effect on the arc stability, where the higher content of Ti is associated with less regular welding lines.

Niobium, on the other hand, has a ratio 1 to 1, which means the amount in the filler wire is the same as that in the deposit, it is added to improve the high temperature mechanical properties, however, it had no effect on the shape and the grain structure of the fusion zone.

Among the 7 tested filler metals, the best was the filler 7 with 0.3 wt.% Ti and 0.3 wt.% Nb, it is important to mention that the desired Ti content is 0.15%, but 0.3% Ti in the wire is added to account for the losses, Figure 142 shows the difference between the filler 1 (with no Nb), filler 6 (with added Nb) and filler 7 which was chosen as the best.

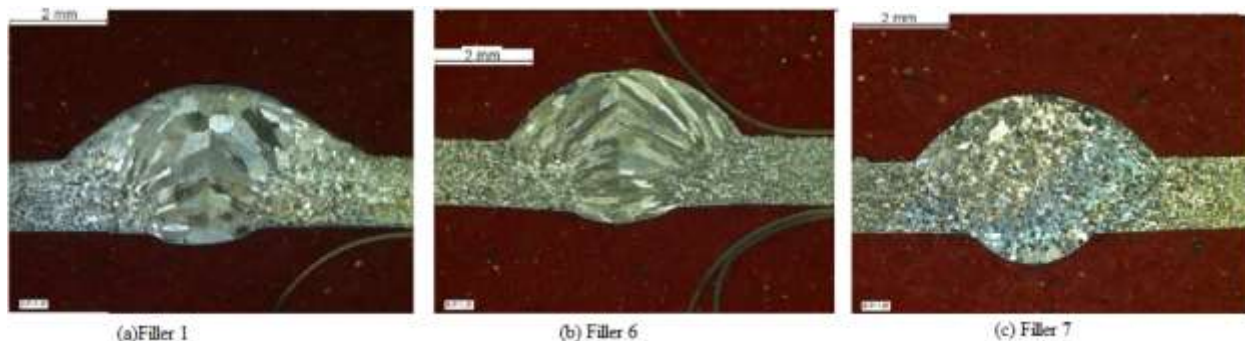


Figure 142 Grain structure of fusion zone obtained with the filler metals 1, 6, and 7 in the pulsed mode [73]

#### 4.3.8. Weldability of the Dual Stabilized AISI 409

The addition of Niobium on the single stabilized Ti-409 showed no adverse effect in terms of welding using the TIG method, where this addition was found to be beneficial in increase in the toughness of the welded area. The dual stabilized grade with 0.28% Nb 0.1% Ti has a higher toughness compared to the 0.25% Ti single stabilized grade [49].

#### 4.4. Post-Welding Cleaning

The heat resulting from the welding is able to deplete the chromium at the surface and lead to corrosion, hence, cleaning gains its importance in order to ensure an optimum corrosion resistance, where the protective chrome oxide layer should be reformed at the surface.

Different cleaning methods could be used, such as electrolyte polishing, pickling, grinding, mechanical polishing, brushing, and sand blasting [66].

# Chapter 5

## Metallurgical Mechanism in Increasing the Performance

### 5. Introduction

Apart from alloying with Niobium, many metallurgical mechanisms are beneficial in further increasing the performance of stainless steels, such as alloying elements for a defined target, cold rolling, two step cold rolling with intermediate annealing, warm rolling and other would be discussed here.

### 5.1. Alloying

In addition to the elements mentioned in details before, Chromium and Niobium, Several other alloying elements have been proven to enhance the performance of the stainless steels, in particular the austenitic and ferritic grades. Some of the elements are beneficial in terms of creep resistance such as Nitrogen, others increase the oxidation resistance such as Silicon, and many others with diverse improvements.

#### 5.1.1. Molybdenum (Mo)

Added by 2 to 4 wt.% in stainless steel can improve the resistance to pitting corrosion, as well as increasing the solid solution hardening, resulting in improved thermal fatigue life.[58] however, attention should be drawn to its drawbacks in terms of promoting the brittle sigma phase that reduces the toughness, in particular under the cyclic condition of the exhaust manifold [54].

#### 5.1.2. Tungsten (W)

One of the best methods in increasing the high temperature strengthening is adding Tungsten as an alloying element. W is highly soluble in the  $\alpha$ -Fe and it has a relatively large atomic radius resulting in solid solution strengthening. Figure 143 shows the effect upon increasing the mass content of W with respect to the W free ferritic stainless steel [54], the study suggested an optimum addition of 2% of W.

Another advantage associated with the addition of Tungsten is the increase of the thermal fatigue life in the heat affected zone (HAZ), in which the combination with Niobium in ferritic stainless steel with 15% Cr content resulted in a better performance than the sole Nb sample [71], where the alloyed with 0.5% Nb fractured after 380 cycles, while the W-0.5 %Nb resisted until 650 cycles, with an optimum of W-0.4%Nb who fractured after 680 cycle. These benefits could be attributed to the increase of solute W in the matrix

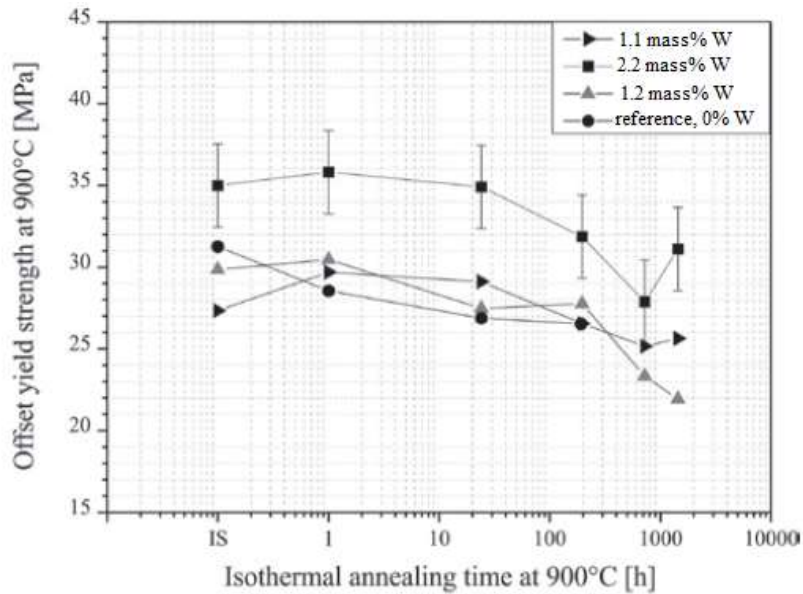


Figure 143 Tungsten in increasing the offset yield strength [54]

As well as, the stabilizing effect of W on the laves phase at high temperature is observed, increasing their dissolution temperature and decreasing their size as shown in figure 144, it is also remarkable that the precipitate type  $M_6C$  has disappeared due to the addition of W which is also attributed to the higher temperature dissolution of the laves.

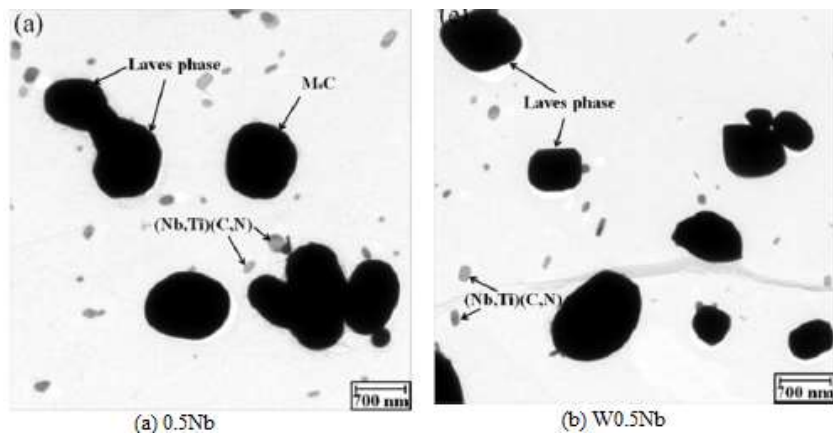


Figure 144 Effect of W on the laves phase size (a) with Nb (b) with W and Nb [71]

Another remarkable benefit that could be achieved through the addition of Tungsten up to certain extent is the higher formability of the ferritic grade 1.4521, where the AISI grade alloyed with 1.2wt.% tungsten has shown better anisotropic coefficients than both grades: Tungsten free and 0.58wt.% grades as shown in the figure 145.

This improvement is interpreted as a result of the better texture developed by the addition of Tungsten, in other words, it favored the presence of  $\gamma$ -fibers and resulted in finer recrystallized grains [62].

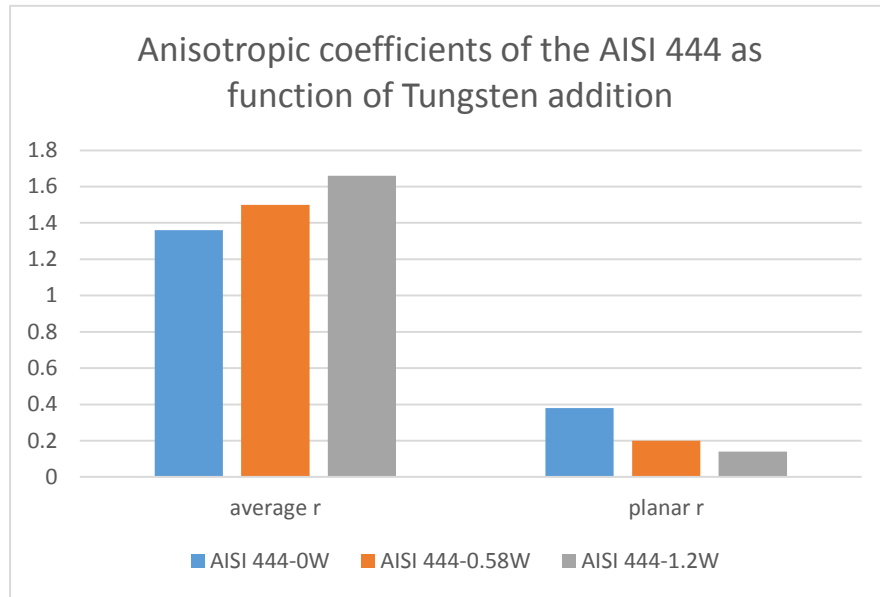


Figure 145 Improvement in the deep drawing performance of AISI 444 by the addition of tungsten

### 5.1.3. Vanadium (V)

The effect of increasing the vanadium content in an austenitic stainless steel, already alloyed with Nb, showed a further increase in the resistance to pitting corrosion from 286.3mV to 360.1 mV for 0.2 and 1.01% V respectively [58].

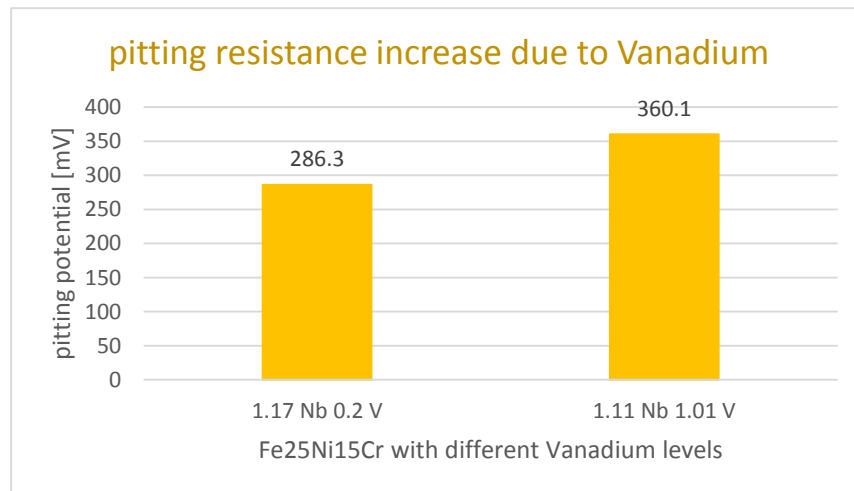


Figure 146 Pitting resistance increase with the addition of Vanadium

### 5.1.4. Nitrogen (N)

Nitrogen addition is effective in increasing the strength, however if added in increased amounts it would result in hot ductility problems [74]. In general, Nitrogen is added to Austenitic stainless steels to increase the tensile strength by solid solution hardening, even though when nitrogen in the matrix is reduced due to the formation of nitrides, these nitrides are beneficial in

terms of increasing creep strength, and in particular, Niobium carbonitride precipitate is a strengthening factor [75].

In order to mark the effect of nitrogen addition on the creep resistance, a test carried out on 4 different austenitic stainless steels with 0.07, 0.11, 0.14, and 0.22 wt.% of nitrogen respectively. The results shown an increase in creep rupture strength, decreased steady state creep, and increased rupture life for a defined applied stress levels as shown in the figures 147, 148, and 149 [76].

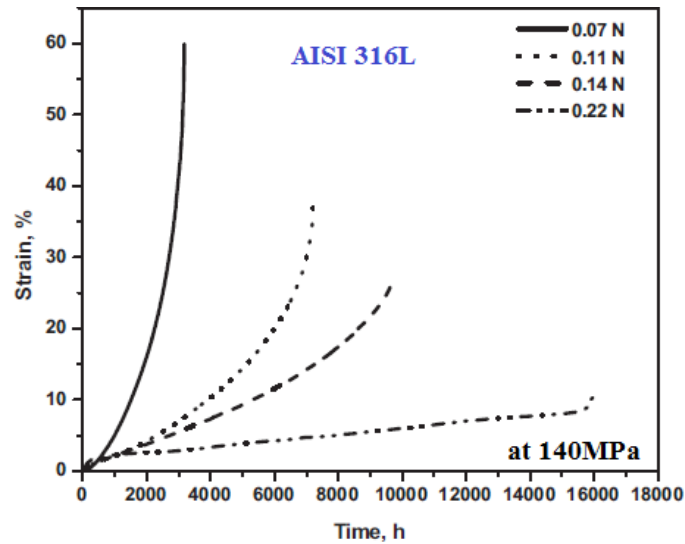


Figure 147 Creep curve flattening by increasing the nitrogen content [76]

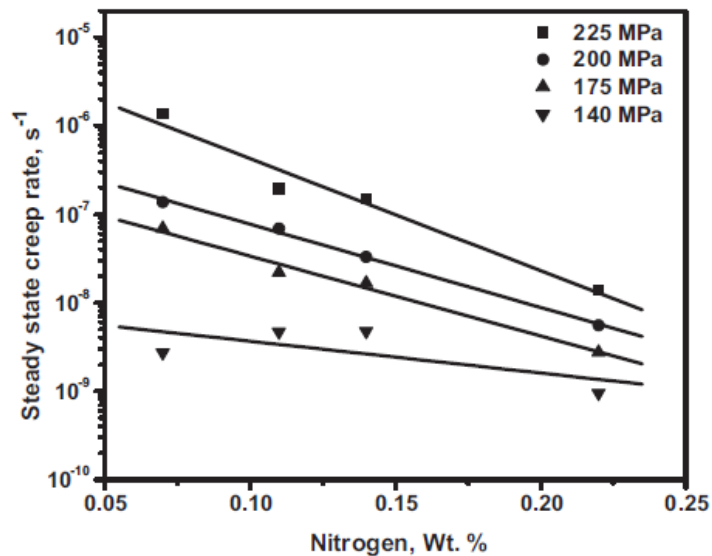


Figure 148 Nitrogen influence on steady state creep[76]

This improvements are attributed to the solid solution hardening by nitrogen, decrease in the stacking fault energy (from 26.41 mJ/m<sup>2</sup> to 15.04 mJ/m<sup>2</sup> with the increasing nitrogen content from 0.07 to 0.22 wt.%), and matrix precipitation of carbonitrides. As well as, an increase in Vickers hardness by 37 HV, and 20 GPa increase in Young's modulus are observed when the nitrogen content is increased from 0.07 to 0.22wt.%.

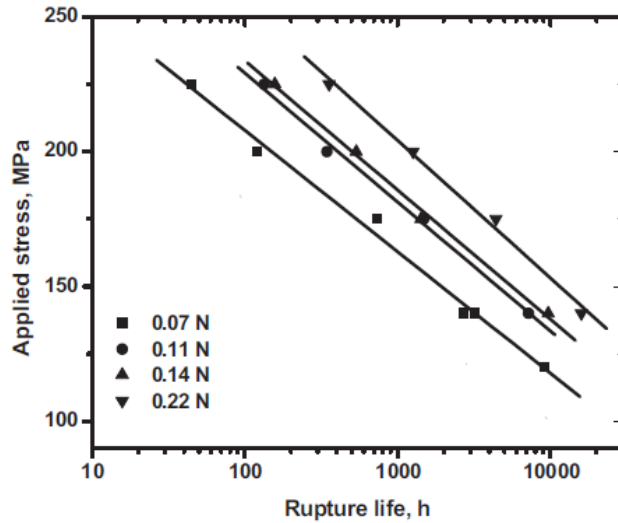


Figure 149 Effect of increasing nitrogen content on rupture [76]

In terms of intergranular and surface cracks, the increase in nitrogen content from 0.07 to 0.22wt.% resulted in significant improvements as shown in figure 150 [76]

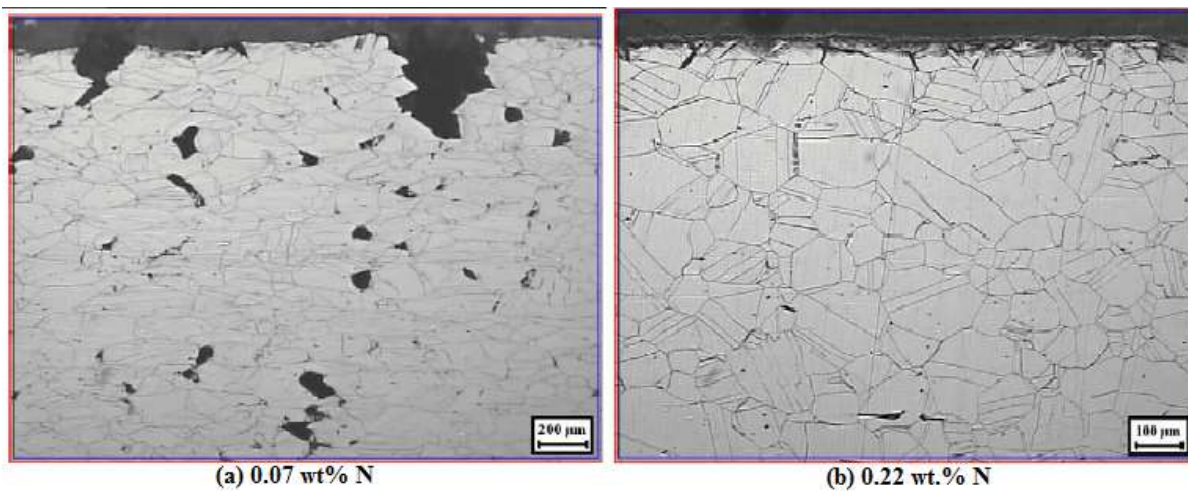


Figure 150 Life Influence of nitrogen on surface cracks [76]

### 5.1.5. Silicon (Si)

Silicon addition is well known in increasing the oxidation resistance of stainless steels by facilitating the formation of the initial chromia layer or by forming silica particles beneath the chromia layer which make the chromia layer more adherent to the substrate, where its performance is enhanced at high temperatures (above 700°C) [75]. Adjusting the Silicon content with the chromium results in increase in the oxidation resistance without drawbacks in terms of creep. On the other hand, some drawbacks in terms of weldability and toughness are recorded, leading to its limitation.

## 5.2. Two Step Reduction

Two step reduction is a process made up of 2 cold rolling reductions with an intermediate and final annealing processes. In order to visualize the effect of two step cold rolling, the results are recorded after each sub process. After receiving an initial specimen of Nb stabilized ferritic stainless steel with 0.35% Nb, 50% cold rolling reduction is carried out, followed by annealing at 800°C for 24s, then a second cold rolling reduction by 80%, and a final annealing at 880°C [64].

### Effect of Two Step Cold Rolling on Hardness

After the first reduction step, the grains tend to join and flatten along with the rolling direction, then grains undergo recrystallization during the intermediate annealing step. Similarly for the first step, grains tend to further elongate and join along the rolling direction with the second cold rolling step, and fully recrystallized after the last annealing as shown in figure 151. The mean grain size has been reduced from 50 $\mu$ m to 10  $\mu$ m. The associated improvement in terms of hardness is shown in figure 152.

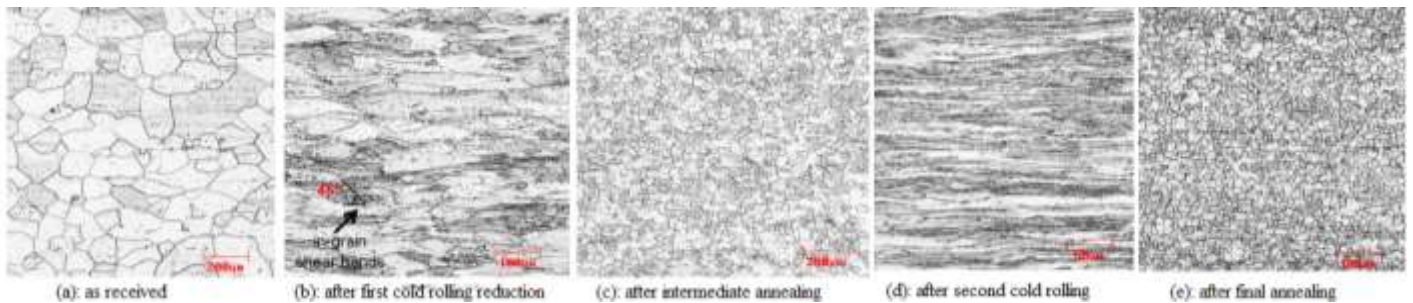


Figure 151 Microstructure after 2 step cold rolling [64]

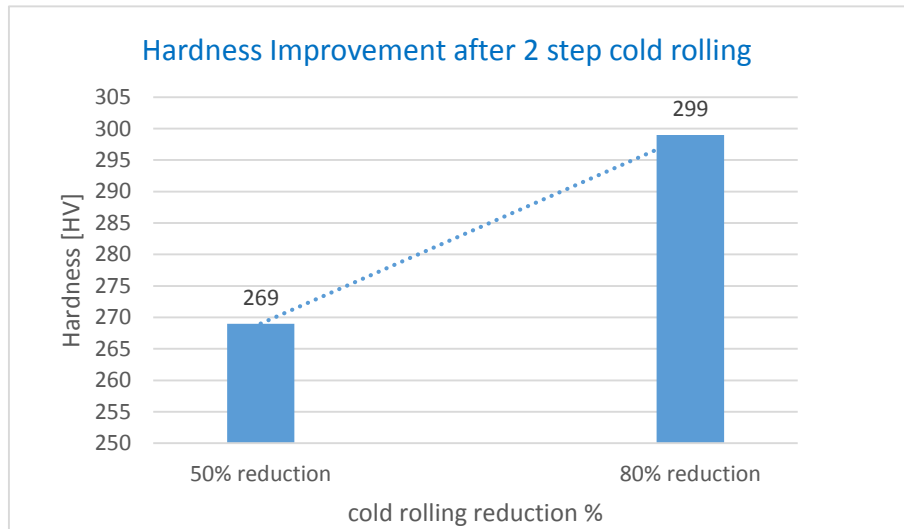


Figure 152 two-step cold rolling effect on hardness

### 5.3. Warm Rolling

In a study aiming at highlighting the effect of the rolling temperature on the microstructure, two initially identical Niobium stabilized Ferritic stainless steels specimens are subjected to conventional hot rolling ( Finisher delivery Temperature 850- 930°C) and Warm rolling (Finisher delivery Temperature 620-740°C) reaching 80% thickness reduction [77]. Warm Rolling benefits are in terms of weakening the  $\alpha$ -fibers and intensifying the  $\gamma$ -fibers, resulting in an almost uniform  $\gamma$ -fiber recrystallization texture after final annealing, In contrast to

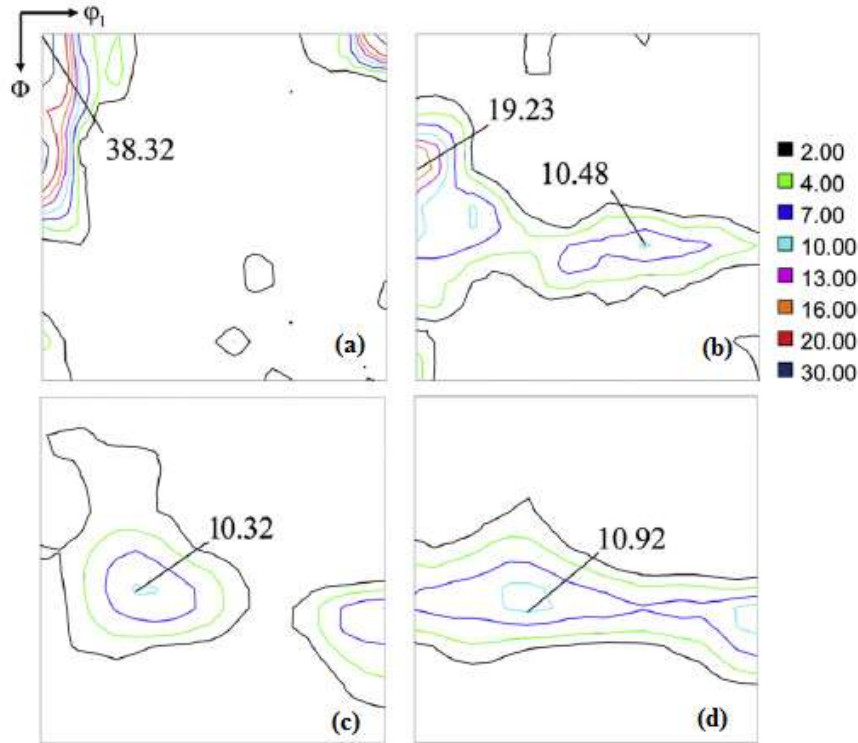


Figure 153 Texture of conventional (a and c) and warm rolled (b and d) specimens [77]

the non-uniform texture obtained in the conventional specimen as shown in figure 153, where (c) and (d) are the final results after the final annealing, with . As well as, the warm rolled surface was found to be smoother with lower roughness coefficient.

Translating these benefits in terms of improvements, the more uniform  $\gamma$ -fiber results in higher average anisotropy coefficient, and lower planar anisotropy coefficient, Thus better formability and deep drawing performance. On the other hand, the lower surface roughness reduces the surface ridging. The results are plotted in figure 154.

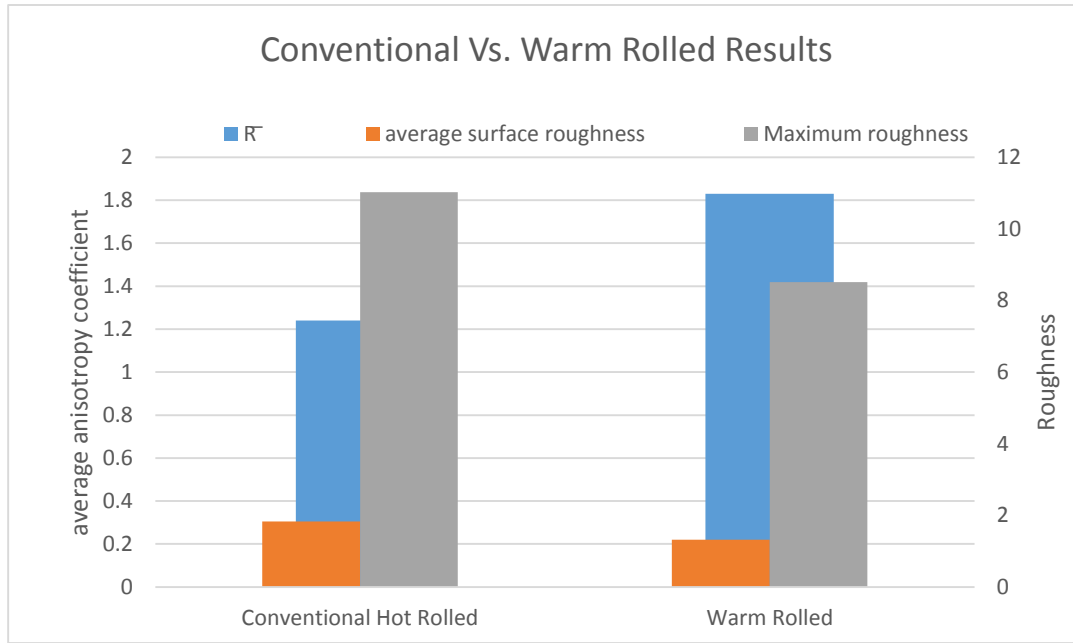


Figure 154 Roughness and Formability improvements by warm rolling

## 5.4. Shear Bands

In another study that also compared two Nb-stabilized ferritic stainless steels rolled at different finisher temperature, 970 and 750 °C respectively was able to discuss the improvements of warm rolling. It was found that the lower finisher temperature introduced shear bands that in turn resulted in  $\gamma$ -fiber that improved the formability and deep drawing by increasing the average anisotropy coefficient by 25% and decreasing the surface roughness by 40% [78].

Shear bands are thin and plate-like structures at 20-35° with the rolling direction. The formed shear bands during warm rolling caused fragmentation of the microstructure that enhanced the nucleation of the recrystallized grains in grain interiors and grain boundaries and modified the structure. These shear bands are not observed during hot rolling due to the rapid recovery at higher temperatures.

After the final annealing, the microstructure of the warm rolled was found to be more homogeneous with smaller grain size, hence, the decrease in the rolling temperature accelerated the recrystallization during annealing, as well as higher hardness value by 80 HV after recrystallization due to the entangled dislocations of higher density in the case of warm rolled.

Table 15 summarizes the results, showing the improvements achieved by shear bands due to warm rolling.

	Hot Rolled [970 °C]	Warm Rolled [750 °C]
Average grain size [μm]	29	24
Average Anisotropy Coefficient	1.63	2.0
Average surface Roughness[μm]	1.94	1.33
Maximum Surface Roughness [μm]	6.0	4.24

Table 15 Comparison between hot and warm rolled results in terms of formability, grain size and roughness

## 5.5. Precipitations in Increasing Creep Resistance

During the service life of stainless steels different precipitates occur, such as  $M_{23}C_6$ , MX, Z phase, and intermetallic phases such as laves and G-phase.

### 5.5.1. MX Carbides

This secondary carbide formed upon the addition of Nb, and/or Ti is observed as beneficial precipitate due to its hardening effect, and its effect in binding the carbon atoms preventing the chromium rich precipitation at grain boundaries thereby hindering the sensitization and inhibiting the grain growth [79].

### 5.5.2. Z-phase

Z phase is observed in austenitic stainless steels with high niobium and nitrogen content, it is observed as NbCrN precipitate. This phase has advantages in terms of improving the mechanical properties, they are highly stable up to 700°C then they show slow increase in size. They contribute to the increase in creep strength [79].

## 5.6. Shot Peening

Shot peening is a surface modification technique based on inducing compressive stress into the surface of the stainless steels, resulting in increased density of the grain boundary due to the cold deformation, a similar effect as grain refining in facilitating the diffusion of Chromium, thus resulting in improved oxidation resistance [75]. This technique has also showed advantages in terms of fatigue life, hardness and closing of pores.

The recorded mass gain on a shot peened surface was lower than other untreated surfaces, for instance, a test carried out on 304H showed that the thin oxide layers formed are less likely to spall, this is said to be the result of the induced stresses.

## 5.7. Post Weld Heat Treatment (PWHT)

Post weld heat treatment (PWHT) is a heat treatment carried out on weldments in order to eliminate the high temperature embrittlement, tempering of martensite and hydrogen degasing. Its effect on the microstructural evolution has been studied, and it is found to be mainly beneficial in improving the toughness without scarifying the tensile strength and hardness. [69]

The hardness in the heat affect zone has remarkably increased after PWHT at 500°C and it exceeded the hardness of the welded zone (WZ), this increase in the hardness is addressed to be a result of the formed precipitates (such as NbC) and laves phases. Further increase in the temperature resulted in a homogeneous hardness between HAZ and WZ [69], while PWHT at 700°C showed the lower hardness due to grain coarsening. Nonetheless, the latest showed optimum tensile properties, as shown in figure 155. This increase is a result of the stabilizing elements and their associated laves that has ordered structure which exhibits good oxidation resistance, and excellent mechanical properties at high temperatures.

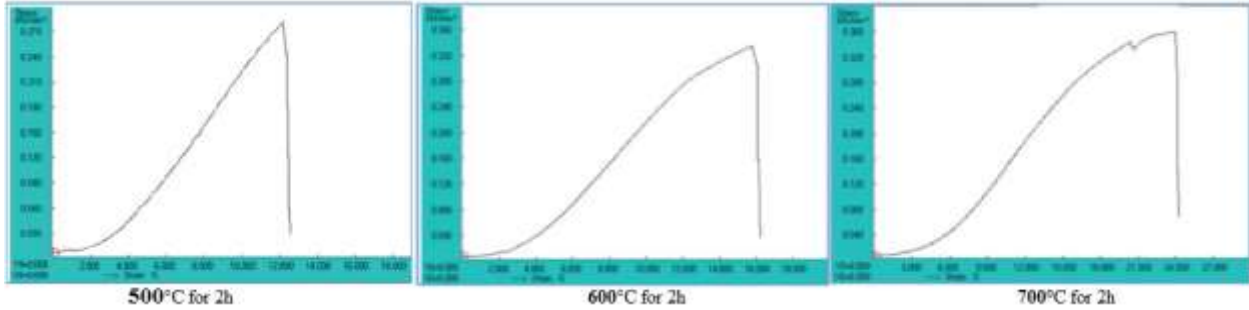


Figure 155 Stress-Strain diagrams of TIG weldments after different PWHT temperatures [69]

## 5.8. Titanium for a Finer Grain in the Welding Zone

The addition of Ti, and consequently its precipitation in the form of stable Titanium nitride in the molten zone, is considered as the nucleation site of the equi-axed fine grains during solidification which improves the fatigue behavior [72].

A study aimed at proposing the best filler material for AISI 444 suggested the addition of Ti up to 0.45% in the AISI 409 metal core wire, as it was found that the increase in the Ti content refined the grain and resulted in equi-axed grains. The results shown in figure 156 highlighted that the increased Ti is beneficial, but 0.12% Ti are not enough [72].

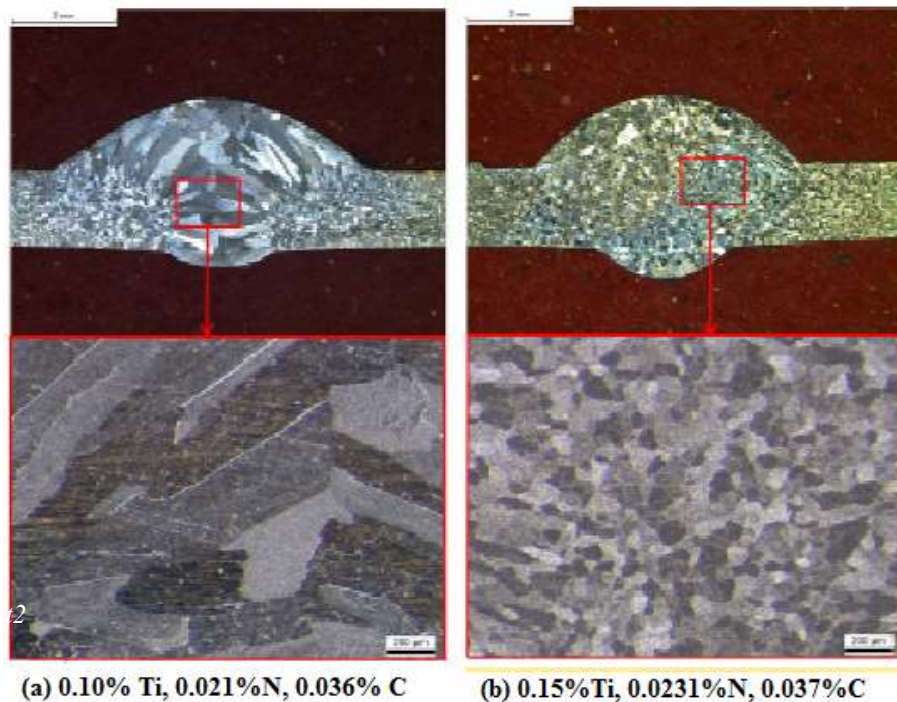


Figure 156 Molten zone macro and micrographs showing the effect of Ti in refining the grain size [72]

# Conclusion

The stringent emission regulations associated with the ecological and economic competition in the automotive sector have forced the OEMs to adopt a continuous improvement approach in optimizing the energy efficiency of the vehicle, which demanded a faster reach of the light-off temperature of the catalytic converter (to be able to decrease the emissions), and the usage of a lighter material. The result of the increased efficiency is a higher exhaust gas temperatures up to 1000-1050°C, where the conventional cast iron exhaust system components in the hot end are not efficient anymore, and inventing a new material that is able to withstand these high temperature while keeping a good mechanical properties is a must, as well as the increase in the warranty period up to 10 years demanded a material that has superior corrosion resistance. Henceforth, cast iron has evolved to thin sheets of stainless steels, in particular, ferritic stainless steel grades are the most promising as they are found to be lighter, cheaper, and more resistant to the service conditions of the automotive exhaust systems

Niobium alloyed stainless steels excelled in satisfying the needed requirements, as the addition of niobium to ferritic stainless steel provided the desired high temperature strength, high resistance to creep and oxidation, as well as increased the pitting corrosion resistance for a longer warranty period, all with lighter components which contributed to weight saving and consequently less CO<sub>2</sub> emissions. Up to now, the most used grade is the DIN. 1.4509 which shows good performance, however, for temperatures exceeding 1000°C, the grades used in the hot end are 1.4521 and 1.4622 both with niobium content, and among those proposed for the cold end is the dual-stabilized 1.4512. In addition the added niobium resulted in better formability and weldability, making the niobium alloyed ferritic stainless steels suitable for the automotive exhaust application.

The Improvements achieved upon adding Niobium could be interpreted as a result of the solid solution strengthening, pinning effect, and refining the grain size that are effective in increasing the high temperature performance, formation of precipitates and laves that increased the resistance to creep, fatigue, and increased the thermal fatigue life. Niobium stabilization effect improves the drawbaility through enhancing the  $\gamma$ -fibers and lowering the  $\alpha$ -fibers and  $\theta$ -fibers in the texture. As well as, its higher affinity to carbon was able to inhibit the intergranular corrosion by forming NbC instead of Cr carbides, mainly in the heat affected zone, resulting in a stainless steel that is virtually immune to sensitization. In addition, Niobium has also showed its effectiveness in increasing the oxygen storage capacity in the catalytic converter.

Although the future of the automotive sector is running towards electrification and the elimination of the Internal Combustion Engine (ICE) and its corresponding exhaust system in order to achieve zero emissions, Niobium technology has already paved its way in the electric mobility, where niobium technology could be implemented in the energy generation of batteries as an alternative to Li-Ion batteries, fuel cells and super capacitors, in addition to other roles of Niobium in the body in white, brakes, chassis, wheels and engine parts.

# Future Trends

Transportation represents almost a quarter of the greenhouse gas emissions, and it is the main cause of air pollution in the cities. As the emission regulations are becoming more and more stringent and firmly on the path towards zero, the only solution on a long term vision is Hybridization and electrification, in other words, low and zero emission vehicles. Phased in from 2020, in 2021 the European fleet wide average emission target for new cars is 95 g.CO<sub>2</sub>/Km. [ac.europa.eu].

Regulation EU 2019/631 sets new EU fleet-wide CO<sub>2</sub> emission targets for the next 5 and 10 years in terms of percentage reduction from the 2021 starting points:

- 2025 and on : 15% reduction for cars and Light Duty Vehicles (LDV)
- 2030 and on: 37.5% reduction for cars and 31% reduction for LDV.

Thus, the market share of hybrid electric vehicles (HEV) and battery electric vehicles is expected to jump in the upcoming years. In 2019, the EU share was 4% HEV, 1% Plug-in Hybrid (PHEV), and about 2% battery electric vehicles (BEV). [www.theicct.org]

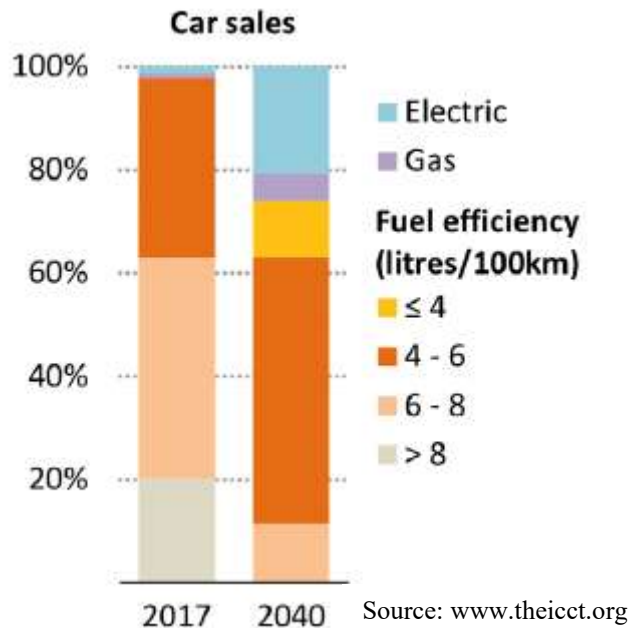


Figure 157 evolution of car share from 2017 to 2040 [29]

Apart from the Niobium-alloyed stainless steels that are used in the exhaust systems in order to withstand the increasing temperature, Niobium technology has also paved it way in the batteries and fuel cells for the electric vehicle.

# References

1. Roudier, Serge, et al. "Best Available Techniques (BAT) reference document for iron and steel production: Industrial emissions directive 2010/75/EU: integrated pollution prevention and control". No. JRC69967. Joint Research Centre (Seville site), 2013.
2. Green J. and Batchelor J. following a visit to BHP NZ Steel "The Manufacture of Steel".
3. Ministry of steel govt. of India "Recommended guidelines for iron and steel sector, Steel melting shop", Doc. No. SG/39.
4. Ahindra Ghosh, Amit Chatterjee, 2008, "Iron Making and Steelmaking: Theory and Practice"
5. "Guidance on Making Ferroniobium Additions During Ladle Steelmaking, Optimizing Niobium Recover" 2018, available online at [www.CBMM.com](http://www.CBMM.com)
6. Donald R. Askeland, Pradeep P. Fulay, Wendelin J. Wright, 2010, "The science and engineering of materials" sixth edition.
7. Singh, B. Bhav, et al. "Effect of hot rolling on mechanical properties and ballistic performance of high nitrogen steel." *Procedia engineering* 173 (2017): 926-933.
8. Li, Xiao, et al. "Effect of Cold Rolling on Microstructure and Mechanical Properties of AISI 304N Stainless Steel." *IOP Conference Series: Earth and Environmental Science*. Vol. 252. No. 2. IOP Publishing, 2019.
9. ASM international Subjective Guide, Materials Park, Ohio, "Heat treating".
10. Spínola, Carlos G., et al. "Real-time supervision of annealing process in stainless steel production lines." *Journal of Metallurgical Engineering (ME) Volume 3.1* (2014).
11. Bornmyr, A., and Björn Holmberg "Handbook for the pickling and cleaning of stainless steel." *AvestaPolarit Welding AB* (1995).
12. Euro Inox, the European stainless steel development association, materials and application series, volume 4. "Pickling and passivation Stainless steel".
13. Euro Inox, materials and application series volume 6, "The mechanical finishing of decorative stainless steel surfaces".
14. Krajnik P., Hashimoto F. (2018) Finishing. In: Chatti S., Laperrière L., Reinhart G., Tolio T., The International Academy for Production (eds) CIRP Encyclopedia of Production Engineering. Springer, Berlin, Heidelberg. [https://doi.org/10.1007/978-3-642-35950-7\\_16717-1](https://doi.org/10.1007/978-3-642-35950-7_16717-1)
15. "Niobium in Automotive Exhaust Systems", available online at [www.Niobiumtech.com](http://www.Niobiumtech.com)
16. Marco Boniardi and Andrea Casaroli, Gruppo Lucefin, Research and Development, Politecnico di Milano, "Steel Metallurgy Volume I".
17. Marco Boniardi and Andrea Casaroli, Gruppo Lucefin, Research and Development, Politecnico di Milano, "Stainless Steels".
18. G. Krauss "Steels—Processing, Structure, and performance", 2015, Second Edition.

19. Charles, J., et al. "The ferritic stainless family: the appropriate answer to nickel volatility?" *Revue de métallurgie* 106.3 (2009): 124-139.
20. Hiramatsu, Naoto. "Niobium in ferritic and martensitic stainless steels." *Proceedings of the International Symposium Niobium 2001*. 2001.
21. Michael F. McGUIRE ASM International®, 2008, "Stainless Steels for Design Engineers"
22. Padilha, Angelo Fernando, Izabel Fernanda Machado, and Ronald Lesley Plaut. "Microstructures and mechanical properties of Fe–15% Cr–15% Ni austenitic stainless steels containing different levels of niobium additions submitted to various processing stages." *Journal of Materials Processing Technology* 170.1-2 (2005): 89-96.
23. "GRWA performance: History of Exhaust systems" (Available online) <https://www.grwaautomotive.com/History-of-exhaust-system-id3647392.html>
24. "GRWA performance: How exhaust systems work" (Available online) <https://www.grwaautomotive.com/How-exhaust-system-works-id3289002.html>
25. Hall, D. 2006 "Automotive engineering" (Available online) <http://ebookcentral.proquest.com>
26. Millo F. 2019, Politecnico di Torino, "Engine Emission Control"
27. Leman, A. M., et al. "Advanced Catalytic Converter in Gasoline Engine Emission Control: A Review." *MATEC Web of Conferences*. Vol. 87. EDP Sciences, 2017.
28. Potente, Daniel. "General design principles for an automotive muffler." *Proceedings of ACOUSTICS*. 2005.
29. Spessa E. 2019, Politecnico di Torino, "Design of Engine Control System".
30. Deleprete C. 2019, Politecnico di Torino, Department of Mechanical and Aerospace Engineering "Powertrain component design".
31. Chinouilh, G., P. O. Santacreu, and J. M. Herbelin. "Thermal fatigue design of stainless steel exhaust manifolds". No. 2007-01-0564. SAE Technical Paper, 2007.
32. William D. Callister, Jr., David G. Rethwisch. Eighth Edition, "Material Science and Engineering, An Introduction".
33. Hoffmann, C., and P. Gümpel. "Pitting corrosion in the wet section of the automotive exhaust systems." *Journal of Achievements in Materials and Manufacturing Engineering* 34.2 (2009): 115-121.
34. Renugadevi, R., V. Rajkumar, and A. Rajesh Kannan. "Modelling and Analysis of Damping Effect in Exhaust System Using Ansys." *International Journal of Aerospace and Mechanical Engineering* 3.5 (2016).
35. Wall, Johan. "Dynamics study of an automobile exhaust system". Diss. Blekinge Institute of Technology, 2003.

36. Anekar, Nitinkumar, and S. Nimbalkar. "Vibration and noise in reactive muffler: A study." *AMET Conference*. 2015.
37. Kumar, Ashwani, et al. "Free vibration and material mechanical properties influence based frequency and mode shape analysis of transmission gearbox casing." *Procedia Engineering* 97 (2014): 1097-1106.
38. Altıntaş, Gökhan. "Effect of material properties on vibrations of nonsymmetrical axially loaded thin-walled Euler-Bernoulli beams." *Mathematical and Computational Applications* 15.1 (2010): 96-107.
39. Kelly, Orhororo Ejiroghene, and Gobir Abdulsamad. "Engineering material selection for automotive exhaust systems using CES software." *International Journal of Engineering Technologies* 3.2 (2017): 50-60.
40. Ekström, Madeleine. "Oxidation and corrosion fatigue aspects of cast exhaust manifolds". Diss. KTH Royal Institute of Technology, 2015.
41. Brady, Michael P., et al. "Long-term oxidation of candidate cast iron and stainless steel exhaust system alloys from 650 to 800° C in air with water vapor." *Oxidation of metals* 82.5 (2014): 359-381.
42. Maziasz, Philip J. "Development of creep-resistant and oxidation-resistant austenitic stainless steels for high temperature applications." *JOM* 70.1 (2018): 66-75.
43. Charles, J., et al. "The ferritic stainless family: the appropriate answer to nickel volatility?" *Revue de métallurgie* 106.3 (2009): 124-139.
44. Faivre, Laurent, Pierre-Olivier Santacreu, and Antoine Acher. "A new ferritic stainless steel with improved thermo-mechanical fatigue resistance for exhaust parts." *Materials at High Temperatures* 30.1 (2013): 36-42.
45. Juuti, Timo, et al. "New Ferritic Stainless Steel for Service Temperatures up to 1050° C Utilizing Intermetallic Phase Transformation." *Metals* 9.6 (2019): 664.
46. OUTOKUMPU steels, "Stainless Steel Grade to meet your needs" *Introducing Core 4622 Supra 316 plus*, outokumpu.com.
47. Rajadurai, S., et al. "Materials for automotive exhaust system." *International Journal of Recent Development in Engineering and Technology* 2.3 (2014): 82-89.
48. Hiramatsu, Naoto. "Niobium in ferritic and martensitic stainless steels." *Proceedings of the International Symposium Niobium 2001*. 2001.
49. DeArdo, A. J., M. Hua, and C. I. Garcia. "NIOBIUM-BEARING FERRITIC STAINLESS STEELS IN THE NORTH AMERICAN MARKET."
50. Liu, Tianlong, et al. "Fatigue–creep behavior of two ferritic stainless steels in simulated automotive exhaust gas and argon." *Journal of Materials Science* 55.8 (2020): 3684-3699.

51. Manninen, Timo, and Jukka Säynäjäkangas. "Mechanical properties of ferritic stainless steels at elevated temperature." *Proceedings of the Fourth International Experts Seminar on Stainless Steel in Structures*. 2012.
52. Li, Mingxuan, et al. "Effect of Nb on the Performance of 409 Stainless Steel for Automotive Exhaust Systems." *steel research international* 89.7 (2018): 1700558.
53. Lu, Hui-Hu, et al. "High-temperature Laves precipitation and its effects on recrystallisation behaviour and Lüders deformation in super ferritic stainless steels." *Materials & Design* 188 (2020): 108477.
54. Nabiran, N., S. Weber, and W. Theisen. "Ferritic stainless steels for high-temperature applications: stabilization of the microstructure by solid state precipitation of MX carbonitrides." *High Temperature Materials and Processes* 32.6 (2013): 563-572.
55. Costa, Ricardo José Gonçalves, et al. "Comparative study of microstructure, texture, and formability between 11CrTi and 11CrTi+ Nb ASTM 409 ferritic stainless steel." *Materials Research* 20.6 (2017): 1593-1599.
56. Çelik, G. Aktaş, et al. "Characterization of the high temperature oxidation behavior of iron based alloys used as exhaust manifolds." *MATEC Web of Conferences*. Vol. 188. EDP Sciences, 2018.
57. Inoue, Yoshiharu, and Masao Kikuchi. "Present and future trends of stainless steel for automotive exhaust system." *High-temperature* 950 (2003): 750.
58. Prifiharni, Siska, et al. "The hardness, microstructure, and pitting resistance of austenitic stainless steel Fe25Ni15Cr with the addition of tungsten, niobium, and vanadium." *AIP Conference Proceedings*. Vol. 1964. No. 1. AIP Publishing LLC, 2018.
59. South, Hélio José Batista Alves-Aperam, and America Tarcísio Reis de Oliveira-Aperam. "Comparative investigation of deep drawing formability in austenitic (AISI 321) and in ferritic (DIN 1.4509) stainless steel sheets."
60. International Stainless Steel Forum ISSF, the essential guide to Ferritic Stainless Steels, "The Ferritic Solution, Properties, Advantages, Applications".
61. Kodukula, Suresh. (2017). Development of new high-performance cost-efficient high-Cr stainless steel grade for sheet forming applications.
62. Liu, Houlong, et al. "Structure–Mechanical Property–Formability Relationships for 444-Type W-Containing Ferritic Stainless Steels." *Journal of Materials Engineering and Performance* 30.1 (2021): 467-478.
63. Galindo, A. Núñez, et al. "Evolution of crystalline orientations in the production of ferritic stainless steel." *IOP Conference Series: Materials Science and Engineering*. Vol. 891. No. 1. IOP Publishing, 2020.

64. Rodrigues, Daniella Gomes, et al. "*The effect of grain size and initial texture on microstructure, texture, and formability of Nb stabilized ferritic stainless steel manufactured by two-step cold rolling.*" *Journal of Materials Research and Technology* 8.5 (2019): 4151-4162.
65. Shu, Jun, et al. "*Effect of Ti addition on forming limit diagrams of Nb-bearing ferritic stainless steel.*" *Journal of Materials Processing Technology* 212.1 (2012): 59-65.
66. ESAB welding, Knowledge center, "*Welding Guidelines for Stainless Steel and Nickel Alloys*", available online at: <https://www.esab.it/it/en/education/blog/exaton-welding-guidelines.cfm>
67. Pierre-Jean Cunat, The European Stainless Steel Development Association Euro Inox, Second Edition, 2007 (Materials and Applications Series, Volume 3) "*The Welding of Stainless Steels*".
68. Weman, K.. Second Edition, 2011 "*Welding Processes Handbook*".
69. Mandal, P. K., et al. "*Influence of Ta+ Nb Addition on Microstructure and Mechanical Properties of Ferritic Stainless Steel TIG Weldments.*" *Fatigue, Durability, and Fracture Mechanics*. Springer, Singapore, 2021. 83-95.
70. Żuk, Marcin, et al. "*The effect of niobium and titanium in base metal and filler metal on intergranular corrosion of stainless steels.*" *Welding Technology Review* 91.6 (2019): 30-38.
71. Oh, Daehee, et al. "*Effects of alloying elements on the thermal fatigue properties of the 15 wt% Cr ferritic stainless steel weld HAZ.*" *Materials Science and Engineering: A* 555 (2012): 44-51.
72. Villaret, Vincent, et al. "*Weldability of new ferritic stainless steel for exhaust manifold application.*" *Advanced Materials Research*. Vol. 445. Trans Tech Publications Ltd, 2012.
73. Villaret, Vincent, et al. "*Influence of filler wire composition on weld microstructures of a 444 ferritic stainless steel grade.*" *Journal of Materials Processing Technology* 213.9 (2013): 1538-1547.
74. Karjalainen, L. P., et al. "*Some strengthening methods for austenitic stainless steels.*" *steel research international* 79.6 (2008): 404-412.
75. Simms, Henry George. "*Oxidation behaviour of austenitic stainless steels at high temperature in supercritical plant.*" Diss. University of Birmingham, 2011.
76. Mathew, M. D., K. Laha, and V. Ganesan. "*Improving creep strength of 316L stainless steel by alloying with nitrogen.*" *Materials Science and Engineering: A* 535 (2012): 76-83.
77. Gao, Fei, et al. "*Texture evolution and formability under different hot rolling conditions in ultra purified 17% Cr ferritic stainless steels.*" *Materials Characterization* 75 (2013): 93-100.

78. Zhang, Chi, Zhenyu Liu, and Guodong Wang. "*Effects of hot rolled shear bands on formability and surface ridging of an ultra purified 21% Cr ferritic stainless steel.*" *Journal of Materials Processing Technology* 211.6 (2011): 1051-1059.
79. Wojciech Borek, Tomasz Tanski, Zbigniew Brytan, *Austenitic Stainless Steels: New Aspects*, 2017.
80. "Automotive Basics" [https://www.youtube.com/watch?v=W6dIsC\\_eGBI](https://www.youtube.com/watch?v=W6dIsC_eGBI).